IDENTIFICATION OF NOVEL LOCI AND ALLELES FOR DROUGHT AND HEAT STRESS TOLERANCE IN WHEAT

Jessica Schmidt

A thesis submitted to The University of Adelaide in fulfilment of the requirements for the degree of Doctor of Philosophy

Faculty of Sciences
School of Agriculture, Food and Wine
The University of Adelaide

September 2019

Table of contents

Abstract

Wheat is one of the most important food sources worldwide contributing to around 20 % of the total calories and proteins in the human diet. However, many wheat growing regions of the world are affected by drought and heatwave events every year, threatening global food security. Whereas responses to drought and heat stress have been studied extensively in wheat, the combination of both environmental stresses has just recently become a matter of research. To ensure future food productivity, the genetic improvement of crops for combined drought and heat stress tolerance and the development of high-throughput phenotyping methods are required.

With the aim to identify novel loci for drought and heat stress tolerance at early grain-filling, which then could be used in future wheat breeding, a worldwide collection of 315 diverse wheat genotypes was analysed using genome-wide association (Chapter 2). Experiments were carried out in a semi-controlled facility over two successive years, subjecting plants to either drought or combined drought and heat treatments. We identified a total of 452 quantitative trait loci (QTL) for flag leaf water potential, spike length, spike number, aboveground biomass, harvest index, screenings (i.e., percentage of small seeds), single seed weight, seed number and seed weight under drought, for the heat response under drought and under combined drought and heat stress. 134 of the QTL for seed weight were independent from flowering time and several QTL were novel with favourable alleles widespread in Asian landraces. A target QTL on the short arm of chromosome 6A was validated under semi-controlled field conditions using near-isogenic lines (NILs). The allele donated by the non-Australian parent contributed to higher seed weight, thousand kernel weight and seed number under drought and heat stress, being consistent with allelic effects observed in the genome-wide association study.

NILs targeting a region on chromosome 6B, which had been identified during the genome-wide association studies, were phenotyped in a gravimetric platform with precision irrigation to assess the QTL effect on plant water use, photosynthesis-related traits and yield components (Chapter 3). Plants were grown in pots and exposed to either drought or combined drought and heat stress three days after anthesis, similar to the treatment applied in the genome-wide association studies. Allelic effects on seed weight, single seed weight and seed number under drought and combined drought and heat stress were consistent with previous results. An

increase in yield was also associated with thicker leaves, a higher photosynthetic capacity as well as a better acclimation to different water availabilities and a higher water use efficiency. Using gene expression analysis, we could narrow down the target region to a total of 41 candidate genes. The majority of these genes have not been previously characterized under drought or heat stress and might serve as candidate genes for crop improvement in dry and hot climates. Further analysis regarding their involvement in the observed changes in physiology and yield components is required.

Manual threshing and phenotyping of the spikes from the genome-wide association studies was work- and time-intensive and is often affected by human errors. We, therefore, decided to develop a method that was more accurate and faster for measuring wheat seed set components under different abiotic stresses using computed tomography (Chapter 4). The X-ray computed tomographic analysis was carried out on 291 spikes of wheat plants which had been exposed to either drought or combined drought and heat stress during the second year of genome-wide association study. An algorithm was developed and evaluated comparing actual measurements of seed weight and seed number per spike to the virtual measurements. Results demonstrated that our computed tomography pipeline could evaluate these traits with an accuracy of 0.70-0.99. Subsequently, the algorithm was used to acquire further grain set characteristics such as seed weight along the spike, single seed weight, seed size, seed shape and seed surface area, enabling a detailed analysis of the performance of genotypically very diverse wheat accessions under both stress regimes.

In conclusion, this study has contributed to the genetic dissection of combined drought and heat stress as well as the implementation of a more accurate and faster phenotyping platform for the evaluation of yield components. Markers have been developed for two target loci offering potential for marker-assisted selection in wheat breeding programs.

Declaration

I certify that this work contains no material which has been accepted for the award of any other degree or diploma in my name, in any university or other tertiary institution and, to the best of my knowledge and belief, contains no material previously published or written by another person, except where due reference has been made in the text. In addition, I certify that no part of this work will, in the future, be used in a submission in my name, for any other degree or diploma in any university or other tertiary institution without the prior approval of the University of Adelaide and where applicable, any partner institution responsible for the joint-award of this degree.

I acknowledge that copyright of published works contained within this thesis resides with the copyright holder(s) of those works.

I also give permission for the digital version of my thesis to be made available on the web, via the University's digital research repository, the Library Search and also through web search engines, unless permission has been granted by the University to restrict access for a period of time.

I acknowledge the support I have received for my research through the provision of an Australian Government Research Training Program Scholarship.

Signature **Date**

30/09/2019

Acknowledgements

First of all, I would like to thank my supervisors, Dr. Delphine Fleury, Dr. Penny Tricker and Dr. Melissa Garcia for joining me in this journey and for all their support – both personally and professionally. I also have to apologize for taking away their victory by constantly winning the best costume prize in our yearly bowling competition.

I acknowledge the University of Adelaide and the Australian Research Council for offering me this opportunity and providing financial support.

I am grateful for my Indian mum and partner in crime Priyanka Kalambettu for all her help in my experiments, her motivation and for feeding me with delicious food. She shared both my frustration (when things went utterly wrong) and joy (when things finally worked out).

I would like to extend my gratitude to Dr. James Edwards for his advice and for giving me insights into his work as a breeder as well as to Paul Eckermann, Yuriy Onyskiv, Martha Van Os, Larissa Chirkova, Alex Kovalchuk and Hui Zhou for all their technical support.

I particularly would like to thank Dr. Trevor Garnett and Dr. Stefan Gerth for giving me chance to visit the Fraunhofer Institute and not only acquire knowledge about new technologies but also to get to know such a great group of people, including Joelle Claussen, Norbert Wörlein (alias the 'Thermomix-Mann') and Dr. Anja Eggert.

I also would like to thank all my PhD colleagues, Vahid Rahimi-Eichi, Caterina Selva, Abdeljalil El Habti, Margaret Wambui Kirika, Pauline Thomelin, Alberto Casartelli and Allan Kouidri for being part of this journey and for all the great conversations during lunch.

I am grateful for all the people at the Australian Plant Genomics Centre and ARC Wheat Hub as well as Matteo Riboni, Mathieu Beas and Amelie Jeanneau.

Least but not last, I would like to acknowledge my partner Jose Luis Fernandez Lopez, who supported me in every situation and never doubted of my success. His patience and optimism gave me strength to accomplish this journey.

Abbreviations

$-\log_{10}(p)$	Negative logarithmic function with base 10 of p-value
2D	Two-dimensional
3D	Three-dimensional
ACRF	Australian cancer research foundation
adj	Predicted mean value adjusted for days to anthesis
BC1F4	Fourth generation of a backcross population
BC1F5	Fifth generation of a backcross population
BC1F6	Sixth generation of a backcross population
BM	Above-ground biomass
BMS	Building management system
bp	Base pair
Chr	Chromosome
CIMMYT	International maize and wheat improvement center
cM	Centimorgan
CRISPR-Cas9	Clustered regularly interspaced short palindromic repeats and associated protein 9
D	Drought
DAA	Days after anthesis
DH	Combined drought and heat stress
DNAse	Deoxyribonuclease
DTA	Days to anthesis
e-	Electron
EZRT	Development center X-Ray technology
FDR	False discovery rate
FPKM	Fragments per kilobase of transcript sequence per millions base pairs sequenced
g_{BM}	Gram above-ground biomass at maturity
g_{DM}	Gramm leaf dry mass
GAPIT	Genomic association and prediction integrated tool
GC content	Guanine-cytosine content
GO	Gene ontology
GWAS	Genome-wide association study
H^2	Heritability estimate
HI	Harvest index
HISAT	Hierarchical indexing for spliced alignment of transcripts
ID	Identity name
INRA	Institut national de la recherche agronomique
IWGSC	International wheat genome sequencing consortium
J	Electron transport capacity

KASP	Kompetitive allele specific polymerase chain reaction
KEGG	Kyoto encyclopedia of genes and genomes
LED	Light emitting diode
log_2	Fold-change in gene expression
LWP	Leaf water potential
Max	Maximum value
Mbp	Mega base pairs
Min	Minimum value
MTA	Marker-trait association
NCBI	National center for biotechnology information
NIL	Near-isogenic line
non-adj	Predicted mean value without adjusting for Days to anthesis
PH	Plant height
Ppd	Photoperiod genes
Q20	Percentage of bases whose correct base recognition rates are greater than 99 % in total bases
Q30	Percentage of bases whose correct base recognition rates are greater than 99.9 % in total bases
QTL	Quantitative trait loci
R^2	Correlation coefficient
RefSeq v1.0	Chinese spring reference sequence v1.0
Rht	Reduced plant height genes
RIN	RNA integrity number
SCR	Screenings
SCRp	Screenings per plant
SCRt	Screenings per primary tiller
SN	Seed number
SNP	Single nucleotide polymorphism
SNp	Seed number per plant
SNt	Seed number per primary tiller
SPAD	Chlorophyll index
SPL	Spike length
SPN	Spike number
SSW	Single seed weight
SSWp	Single seed weight per plant
SSWt	Single seed weight per primary tiller
SW	Seed weight
SWp	Seed weight per plant
SWt	Seed weight per primary tiller
tGBS	Targeted genotyping by sequencing
TKW	Thousand kernel weight

Tukey’s HSD test	Tukey's honest significant difference test
Vcmax	Photosynthetic capacity
Vrn	Vernalisation genes
WSN	Wireless sensor network
WUE	Water use efficiency

Publications arising from this thesis

1. **Schmidt, J.**, Tricker, P. J., Eckermann, P., Kalambettu, P., Garcia, M., & Fleury, D. (2019). Novel alleles for combined drought and heat stress tolerance in wheat. *Frontiers in Plant Science*, doi: 10.3389/fpls.2019.01800.

2. **Schmidt, J.**, Claussen, J., Wörlein, N., Eggert, A., Fleury, D., Garnett, T., & Gerth, S. (2020). Drought and heat stress tolerance screening in wheat using computed tomography. *Plant Methods,* 16.

3. **Schmidt, J.**, Garcia, M., Brien, C., Kalambettu, P., Garnett, T., Fleury, D., & Tricker, P. J. (2020). Transcripts of wheat at a target locus on chromosome 6B associated with increased yield, water use and photosynthetic capacity under combined drought and heat stress. *Manuscript*.

4. Tricker, P. J., ElHabti, A., **Schmidt, J.**, & Fleury, D. (2018). The physiological and genetic basis of combined drought and heat tolerance in wheat. *Journal of Experimental Botany*, 69, 3195-3210.

Chapter 1

Introduction and literature review

1.1 Introduction

Since its first cultivation 10,000 years ago, wheat has become one the main providers of calories for humankind. Bread wheat (*Triticum aestivum* L.) is the most widely distributed and cultivated cereal owing to its high nutritional value and easiness of storage and transport (Feuillet et al. 2008, Shiferaw et al. 2013). Its annual production reaches 730.2 million tonnes worldwide, with Australia accounting for 17.3 million tonnes in 2018-2019. Australian wheat production occurs mainly across the southern and eastern regions of Western Australia, New South Wales, Queensland and South Australia. South Australia is the second largest wheat producer in Australia, contributing approximately 17.5 % of national wheat production (ABARES 2019, FAO 2019a). The optimal sowing time for Australia's wheat is between April and June, however the timepoint is always a compromise. Early sowing allows full usage of the growing season but increases the chance of frost damage and diseases, whereas late sowing increases the risk of drought and heat stress during anthesis and grain filling (GRDC 2011).

Drought is defined as the reduction in accessible water in soil limiting productivity, while heat stress is a function of the intensity, duration and rate of the increase in temperature (Passioura 1996, Wahid et al., 2007). Drought and heat are considered the two major abiotic stresses constraining wheat productivity worldwide, reducing grain yields up to 69 % and 81 %, respectively (Pradhan et al. 2012). Both stresses are more likely to occur simultaneously rather than separately in most wheat producing regions of the world. Particularly semi-arid and Mediterranean-type regions such as South Europe, North Africa and southern Australia are regularly affected by combined drought and heat stress (Borghi et al. 1990, Toreti et al. 2019). The southern Australian weather is characterized by warm to hot, dry summers and mild, wet winters. During summer, average maximum temperatures range between 23 and 36 °C with a total of 50 to 60 millimetres of rainfall. Periods of rainfall are followed by periods of water scarcity causing cyclic drought events (Izanloo et al. 2008, Australian Bureau of Meteorology 2019a). Extreme drought and heat events are predicted to become more frequent with annual temperatures steadily rising. Mean surface temperatures in Australia have been 1.1-1.4 °C above average since 2013, and 2018 was Australia's third-warmest year on record with a mean temperature of 1.1 °C above average and national rainfalls 11 % below average (Trnka et al. 2014, Australian Bureau of Meteorology 2019b, FAO 2019b).

As aridity and temperature increases, yield losses will be even more exacerbated raising serious concerns about the possibility of meeting the world's growing food demand (Rosenzweig and Parry 1994). The production of wheat varieties that are high yielding and stable under different

environmental stresses is required. This implies the analysis of traits contributing to yield despite water limitations and high temperatures, as well as the identification of the genomic regions associated with these adaptive traits (Reynolds et al. 2001, Tilman et al. 2011). Novel molecular and phenotyping technological advances have been made in recent years and promise to accelerate breeding processes to enable breeders and researchers to meet the projected demand for wheat (Ben-Ari and Lavi 2012, Tardieu et al. 2017). The following literature review summarises the current knowledge about the impact of combined drought and heat stress on yield components, potential tolerance mechanisms, molecular and phenotypic achievements in breeding so far and the genetic basis of drought and heat stress tolerance.

1.2 Impact of drought and heat stress on yield traits

Responses to drought and heat stress have been studied extensively in wheat, whereas the combination of both environmental stresses has only recently become a matter of research. Overall, the combination of drought and heat stress has a negative, additive impact on yield traits as well as plant phenology, morphology and physiology including growth, chlorophyll content and leaf photosynthesis. However, the ways in which drought and heat stress constrain these traits might be quite different or even antagonistic (Machado and Paulsen 2001, Perdomo et al. 2015, Qaseem et al. 2019b). As growth and photosynthesis are constrained by both drought and heat, fewer assimilates are available for grain filling leading to a reduction in grain size, grain weight, grain number and, ultimately, grain yield (Gupta et al. 2011, Sanchez-Bragado 2014, Dodig et al. 2016). The impact of a certain stress varies according to its severity and duration as well as to the developmental stage and the genotype of the plant (Porter and Gawith 1999, Abbad et al. 2004). Grain yield is more sensitive to early (i.e., meiosis or anthesis) than to late stress (i.e., grain filling), and as stress intensity increases or is prolonged, physiological changes are more severe and additional components become affected (van Ginkel et al. 1999, Calhoun et al. 1994, Foulkes et al. 2002).

When drought and heat stress occur during meiosis or anthesis, the number of grains per spike is significantly reduced due to an increased abortion of young kernels. Individual grain weight, in contrast, is hardly affected due to the distribution of assimilates among fewer grains. Drought and heat stress during grain filling, as it occurs in Mediterranean climate, are usually thought not to affect grain number but individual grain weight due to a reduced grain filling capacity (Dias and Lidon 2009, Rajala et al. 2009, Weldearegay et al. 2012, Fabian et al. 2019).

However, recent studies also observed a reduction in grain number under combined drought and heat stress during early grain filling (Prasad et al. 2011; Pradhan et al. 2012, Qaseem et al. 2018). A decrease in seed number during grain filling might be due to the impediment of remobilisation of water-soluble carbohydrates leading to an increase in smaller, shrivelled seeds. In comparison to drought, grain filling duration and thus individual grain weight are more sensitive to heat stress, whereas drought has a greater effect on grain number (Prasad et al. 2011).

1.3 Mechanisms of resistance to drought and heat stress in plants

The ability of plants to resist drought and heat stress and maintain high yield depends on physiological, biochemical, molecular and genetic adaptations (Redondo-Gomez 2013). These adaptations allow plants to either (i) escape, (ii) avoid or (iii) tolerate stress. Stress escape refers to the ability of a plant to fulfil its life cycle by altering its vegetative and reproductive growth, whereas stress avoidance in terms of drought and heat stress includes the maintenance of a high cell turgor and cooler canopies, preventing the proliferation of the stress. Mechanisms to tolerate stress allow the plant to maintain, at least partially, its functionality despite the presence of an internal stress (e.g., decreased cell turgor) such as through the accumulation of molecular protectants which prevent cell damage (Levitt 1980a, Levitt 1980b).

While some resistance mechanisms are specific to either drought or heat stress, others such as early flowering, flag-leaf persistence and the initiation of the reactive oxygen species scavenging system are common responses under both stresses. However, plant responses to one stress might be altered by the level of the other stress (Machado and Paulsen 2001). A greater understanding of the mechanisms conferring combined drought and heat stress tolerance will be crucial for researchers and breeders to identify promising traits and loci for future wheat improvement (Tricker et al. 2018). Resistance mechanisms associated with drought, heat or the combination of both stresses in wheat have been listed in Table 1. Mechanisms which seem especially important in order to cope with the stress combination will be explained in more detail.

Table 1. Mechanisms of drought and heat stress resistance in wheat.

Resistance mechanism			
Category	***Trait***	***Type of stress associated with***	***Reference***
Morphology	Reduced leaf area	Drought	Sirault (2007), Izanloo et al. (2008)
	Increased leaf area	Heat	Qaseem et al. (2019b)
	Decreased leaf area	Drought	Machado and Paulsen (2001)
	Thicker leaves	Drought	Izanloo et al. (2008)
	Greater leaf waxiness	Drought	Izanloo et al. (2008)
	Increased leaf glaucousness	Drought	Richards et al. (1986)
	Greater leaf shading	Drought	Sirault (2007)
	Greater leaf rolling	Drought	Sirault (2007), Izanloo et al. (2008), Edwards (2012)
	Presence of awns	Drought	Blum (1985)
	Increased early vigour	Drought	Richards et al. (2001)
	Decreased tiller number	Drought	Richards et al. (2001), Izanloo et al. (2008)
	Increased root biomass	Drought, heat	Manschadi et al. 2008, Gupta et al. (2013)
	Deeper rooting	Drought	Kirkegaard et al. (2007), Li et al. (2019a)
	Shallower root systems	Heat	Pinto and Reynolds (2015)
	Reduced stomatal density	Drought	Dunn et al. (2019)
Plant life cycle	Early flowering	Drought, heat, combined drought & heat	Worland (1996), Foulkes et al. (2007), Qaseem et al. (2019b)
	Extending the duration of stem elongation	Drought	Araus et al. (2002)
Plant water relations	Improved water use efficiency	Drought	Batool et al. (2019), Dunn et al. (2019)
	More efficient water use	Drought	Blum (2009)
	Greater transpiration efficiency	Drought	Richards et al. (2001)
	Lowered transpiration rate	Drought	Machado and Paulsen (2001), Izanloo et al. (2008)
	Increased transpiration	Heat	Sharma et al. (2015)
	Osmoregulation	Drought, heat, combined drought & heat	Morgan (1983), Machado and Paulsen (2001), Wang et al. (2010)
	Accumulation of osmoprotectants (e.g., proline, glycinebetaine, soluble sugars)	Drought, heat, combined drought & heat	Ashraf and Foodlad (2007), Wahid et al. (2007), Gupta et al. (2013), Batool et al. (2019), Qaseem et al. (2019b)
Canopy temperature	Canopy temperature depression	Drought, heat	Fischer et al. (1998), Li et al. (2019a)
Photosynthetic adaptions	Flag leaf persistence	Drought, heat, combined drought & heat	Foulkes et al. (2007), Pradhan et al. (2012), Sharma et al. (2015)

Table 1. Continued.

Resistance mechanism			
Category	***Trait***	***Type of stress associated with***	***Reference***
Photosynthetic adaptions	Increased chlorophyll fluorescence (i.e., increased photosynthetic capacity)	Drought, heat, combined drought & heat	Araus et al. (2002), Izanloo et al. (2008), Pradhan et al. (2012), Perdomo et al. (2015)
	Higher stomatal conductance	Heat	Fischer et al. (1998), Sharma et al. (2015)
	Increased photosynthetic rate	Drought, heat, combined drought & heat	Fischer et al. (1998), Wang et al. (2010), Sharma et al. (2015)
Water soluble carbohydrates	Accumulation of water-soluble carbohydrates in stem, sheaths and leaves	Drought, heat, combined drought & heat	Blum (1998), Dodig et al. (2016), Dreccer et al. (2009), Qaseem et al. (2019b)
	Increased remobilization of water-soluble carbohydrates from stem to grains	Drought, heat, combined drought & heat	Palta et al. (1994), Dreccer et al. (2009), Dodig et al. (2016)
	Increased stem length as water-soluble carbohydrate storage	Drought	Blum (1998)
Protection of membranes and proteins	Higher expression of heat shock proteins	Drought, heat, combined drought & heat	Wahid et al. (2007), Grigorova et al. (2011)
	Initiation of reactive oxygen species scavenging system	Drought, heat, combined drought & heat	Price and Hendry (1991), Wang et al. (2010)
	Increased photorespiration	Drought, heat	Aliyev (2012)
Stress signalling	Increased abscisic acid concentration	Drought, heat	Quarrie and Jones (1979), Wahid et al. (2007), Wang et al. (2015)
	Increased cytokinin concentration	Drought	Peleg et al. (2011)
	Decreased ethylene concentration	Drought, heat	Yang et al. (2006), Hays et al. 2007
	Up-regulation of phosphatidic acid and phosphatidylinositol genes	Drought, heat, combined drought & heat	Aprile et al. (2013)

a. Accelerated plant development allows plants to escape drought and heat stress

Early flowering enables plants to avoid high temperatures and water restrictions, especially during the development of floral primordia. The mechanism triggering flowering time and life-cycle duration relies on a complex genetic control with about twenty-five loci involved. The allelic variation at these loci enhances the wide adaption of wheat worldwide (Worland 1996, Snape et al. 2001, Yan et al. 2004). The genetic control of the life-cycle duration can be divided

into three groups of genes: i) vernalization (*Vrn* genes), ii) photoperiod (*Ppd* genes) and iii) development rate or 'earliness per se' (*Eps* genes). The control of the two former gene groups depends on the environment, whereas *Eps* genes determine flowering time independently from photoperiod and vernalization (Laurie 1997, Snape et al. 2001).

The vernalization pathway is mainly regulated by three *Vrn-1* orthologous genes (*Vrn-A1, Vrn-B1* and *Vrn-D1* located on chromosomes 5A, 5B, and 5D, respectively) and a *Vrn-1* repressor gene named *Vrn-2* (Yan et al. 2004, Loukoianov et al. 2005). In wheat adapted to cooler climates such as in Northern Europe (i.e., winter wheat), *Vrn-1* is repressed by *Vrn-2,* preventing the transition to flowering during winter and protecting thus the floral meristem against frost (Snape et al. 2001, Yan et al. 2004, Loukoianov et al. 2005). In contrast, the growth habit of wheat adapted to warmer climates (i.e., spring wheat) is linked to the occurrence of a mutation in one of the *Vrn-1* genes, enabling a faster reproductive development (Yan et al. 2004, Dubcovsky et al. 2007). Alleles at the *Vrn-A1*, *Vrn-B1*, and *Vrn-D1* loci are dominant for the spring growth habit. Winter wheat is therefore homozygous for all three recessive alleles at *VRN-1* (Yan et al. 2004). In dry and hot climates, vernalization-sensitive types are disadvantageous due to their disability to reach anthesis at all, or a delay in flowering time causing an exposure to terminal drought and heat stress. Studies from Rollins et al. (2013) showed that the earlier flowering spring types outperformed vernalization-sensitive types in regard to yield by up to 52.2 % in the dry and hot weather conditions of Syria.

Apart from vernalization, plants regulate and adjust their life cycle in response to day length (i.e., photoperiod). The main genes controlling the photoperiod response in wheat are the *Ppd-1* genes including *Ppd-A1*, *Ppd-B1* and *Ppd-D1* on the short arm of chromosomes 2A, 2B and 2D, respectively (Snape et al. 2001). Most modern European and Australian varieties are photoperiod insensitive, carrying a *Ppd-D1a* allele. The allele in European varieties derived from the Japanese variety Akakomugi and was first introduced by an Italian breeder to accelerate flowering time in order to avoid the local dry and hot summers. In Australia, the allele became common after the release of cultivars containing CIMMYT germplasm in 1973. (Worland 1996, Eagles et al. 2009). In dry and hot conditions, photoperiod-insensitive varieties flowered 4-10 days earlier and showed a yield advantage of around 35 % in comparison to sensitive varieties (Worland 1996).

Due to their strong pleiotropic effect on yield, *Vrn* and *Ppd* genes often coincide with yield loci in the field, making it hard to identify loci regulating yield and yield-related traits independently of development (Arjona et al. 2018, Mason et al. 2018, Garcia et al. 2019, Qaseem et al. 2019a). Breeding for drought and heat stress adaptation has been largely based

on stress escape through manipulation of development, but not on tolerance mechanisms so far (Farooq et al. 2014). To identify tolerance-associated loci independent from plant development, a controlled pot system in which plants can be treated individually according to their flowering time has proven successful in wheat. Qaseem et al. (2018) identified a total of nine novel, yield-regulating loci under well-watered, heat and combined drought and heat stress which might have been masked otherwise by the confounding effects of plant phenology.

b. Alterations of transpiration coupled with increased water uptake and osmotic adjustment are responsible for cooler canopies and increased water content under drought and heat stress

Drought reduces cell water content, cell turgor and plant metabolism. Heat stress exacerbates the impact of drought by accelerating the depletion of soil water due to an elevated rate of evapotranspiration (Levitt 1980a, Levitt 1980b). The main mechanism to maintain cell turgor and to allow metabolism to continue under drought is the reduction of water loss by lowering the transpiration rate (Turner 1986). A lower transpiration rate and thus an improved water use efficiency, i.e., low rate of water use while maintaining biomass production, is correlated with the degree of stomatal closure. Stomatal closure, in turn, is regulated by the amount of the phytohormone abscisic acid in leaves (Quarrie and Jones 1979, Wahid et al. 2007, Redondo-Gomez 2013). A positive association between reduced water loss, lower transpiration rate and grain weight under drought stress has been found in bread wheat by Izanloo et al. (2008). Accessions which transpired less had a yield advantage of up to 46.2 % in comparison to those transpiring more.

The closure of the stomata limits, however, transpirational cooling. As a result, drought stressed plants display higher leaf and canopy temperatures than well-watered plants, aggravating the heat stress effect on canopy temperature (Ludlow and Muchow 1990, Izanloo et al. 2008, Pinto and Reynolds 2015). To prevent high canopy temperatures without causing cell dehydration, an increased water uptake has shown to be of advantage. Studies from Reynolds (2007) reported that plants which can extract more of the available water in soil, maintained cooler canopies and higher photosynthetic rates. The morphology and physiology of roots play a key role. Plants that developed a deeper root system under drought, or concentrated their roots at the soil surface under heat stress, increased their water uptake by 35 %. Additional water from soil during early grain-filling can contribute to an increase in wheat yield by as much as 628 kg ha^{-1} (Pinto and Reynolds 2015, Li et al. 2019a).

Another important component to prevent cell dehydration and to maintain the turgor pressure is the lowering of the plant water potential. In water-restricted environments, plant water potential correlates positively with cell dehydration and turgor loss, being an indicator of the level of stress of the plants (Jones and Turner 1978). The water potential of plants can be lowered by the accumulation of solutes, a process known as osmotic adjustment (Redondo-Gomez 2013). The synthesis and accumulation of osmotically active solutes such as ions (particularly potassium), amino acids (e.g., proline) and soluble carbohydrates (e.g., sugars), enable plants to create a more negative leaf water potential and to maintain cell turgor. The maintenance of the cell turgor, in turn, allows turgor-dependent processes such as plant growth by cell expansion and stomatal opening, and hence photosynthesis, to continue (Redondo-Gomez 2013). Higher osmotic adjustment improves tiller survival, reduces leaf senescence and increases the mobilization of pre-anthesis stored assimilates to the grains, contributing to grain filling and resulting in an increased harvest index (Ludlow and Muchow 1990). Morgan (1983) observed that higher osmoregulating plants were more tolerant to drought and showed higher yields than those with lower osmoregulation ability and Qaseem et al. (2019b) reported a positive correlation between proline accumulation and yield under drought and heat stress in wheat.

c. Maintenance of photosynthesis under drought and heat stress is associated with higher yields

Flag leaf photosynthesis is responsible for ~30 % of assimilates used in grain filling and correlates positively with grain yield (Throne 1965, Abbad et al. 2004). Photosynthetic activity is restricted under drought and heat stress. Under drought, the principal limitation to photosynthesis is stomatal closure in order to avoid cell dehydration, resulting in a lower internal CO_2 concentration (Levitt 1980b). In contrast, the decline of the photosynthetic activity under heat stress is associated with an accelerated senescence (i.e., decline in chlorophyll content and increase in proteolytic activity) as well as with a loss of the enzymatic activity of ribulose-1,5-bisphosphate carboxylase/oxygenase and of thylakoid membrane integrity (Al-Khatib and Paulsen 1984, Allakhverdiev et al. 2008). With prolonged stress exposure, photosynthetic activity is further inhibited by the formation of reactive oxygen species, causing damage to the membranes, proteins and chlorophyll molecules of the photosynthetic apparatus (Price and Hendry 1991, Redondo-Gomez 2013, Allakhverdiev et al. 2008).

Studies of Gratani et al. (1998) showed that flag leaf photosynthesis correlates positively with chlorophyll content. Chlorophyll content and photosynthetic activity can be maintained over a longer period by delaying the onset and rate of flag-leaf senescence (Richards 2000, Hao et al.

2012). In cereal breeding, delayed flag leaf senescence (i.e., flag leaf persistence or stay green) has been considered as a reliable trait for stress tolerance (Blum 1998). Foulkes et al. (2007) reported that flag-leaf persistence was positively correlated to grain yield and that the onset of flag leaf senescence was significantly delayed in drought tolerant wheat plants in comparison to drought sensitive genotypes. Reynolds et al. (2000) observed the same correlation under heat stress.

1.4 High-throughput phenotyping for drought and heat stress tolerance

Evaluation of morphological, physiological and seed traits are important to improve our understanding of complex quantitative traits such as yield and stress tolerance and to identify desirable genotypes related to stress tolerance (Tester and Langridge 2010). Conventional phenotyping methods relying on manual measurements are, however, often time-consuming, inaccurate and destructive. Increased phenotyping throughput and accuracy are therefore required (Furbank and Tester 2011).

Novel technologies including non-invasive imaging/sensing techniques, robotics and high-performance computing have been developed and recently applied to crops in glasshouses and fields (Tardieu et al. 2017, Sytar et al. 2018)**.** Automated phenotyping platforms in glasshouses using hyperspectral, red-green-blue and fluorescence imaging are able to provide a wide range of information about single plant performance over time, including plant health (plant senescence, nutrient and water content), plant growth (shoot area, plant height and width) and plant physiology (transpiration, water use efficiency). In addition, programmable room temperature and watering to weight of plants enables precise control and analysis of abiotic stresses such as drought and heat stress (Parent et al. 2015, Ge et al. 2016, Muraya et al. 2017, Chen et al. 2019). Other techniques for small-scale experiments include X-ray computed tomography. Computed tomography has been successfully applied in evaluation of seed morphology, root growth and lately of yield traits in wheat and rice (Gregory et al. 2003, Duan et al. 2011, Hughes et al. 2017, Hughes et al. 2019).

Ground (phenomobiles, phenotowers) and aerial (drones, manned aircrafts) are high-throughput imaging platforms can be used in field trials and enable the assessment of plant performance in whole plots in relation to environmental conditions and treatments (Ahamed et al. 2012, Bai et al. 2016, Holman et al. 2016, Shakoor et al. 2017, Walter et al. 2019). These

platforms allow to predict phenotypic traits like plant height, ground cover, above-ground biomass, vegetation indices and growth rates (Bai et al. 2016, Holman et al. 2016, Jimenez-Berni et al. 2018). In dry and hot climates, high-throughput digital phenotyping accurately predicted canopy cover and colour-based traits such as disease assessment when compared to visual scores with an image acquisition speed of 7,400 plots per hour. The digital scores showed similar or even greater heritability than visual scores, indicating that digital scores were more accurate in the assessment of the traits (Walter et al. 2019).

Even though these novel technologies are faster, more precise and enable whole lifecycle measurements, plant phenomics research struggles with large data sets, complex data analysis, environmental fluctuations in the field and applicability in breeding programs (Furbank and Tester 2011, Bai et al. 2016, Tardieu et al. 2017). First attempts using high-throughput image platforms in breeding programs have been made (Bai et al. 2016, Haghighattalab et al. 2016, Walter et al. 2019), but remain an exception. To identify genotypes with the ability to adapt to changing environments through high-throughput phenotyping and to accelerate breeding, the most recent advances in information technology must be employed and collaborative and coordinated work between statisticians, plant researchers and breeders is required (Furbank and Tester 2011, Tardieu et al. 2017).

1.5 Breeding for tolerance to combined drought and heat stress

For thousands of years, humans selected plant types they valued (e.g., plants which showed a higher productivity, or which were easier to harvest), a process called ‘domestication’. Nevertheless, the mechanisms underlying the variation of plant characteristics were not clear until Mendel’s laws of inheritance and the discovery of the genome, leading the way to conventional and molecular plant breeding. Significant improvement in wheat production through exploitation of major genes for traits like photoperiod insensitivity, dwarfness and plant resistance to biotic stresses has been achieved since the initiation of the ‘Green Revolution’ in the 1960s (Gupta et al. 2012, Voss-Fels et al. 2019). However, the selection and cultivation of so called ‘elite crops’ through domestication and breeding has often been associated with a loss of genetic diversity in modern wheat cultivars (‘genetic bottleneck’) and has been speculated to limit further crop improvement and to make crops more vulnerable to abiotic and biotic stresses (Roussel et al. 2004, Fu and Somers 2009, Kahiluoto et al. 2019). Other studies argue about the existence of a long-term genetic bottleneck and doubt that a short-

term reduction in genetic diversity would negatively affect the climate resilience of wheat (van de Wouw et al. 2010, Snowdon et al. 2019). Whether or whether not a genetic bottleneck in wheat exists, the genetic diversity in modern wheat cultivars can be enhanced by the introgression of loci and alleles from landraces and wild relatives (Reif et al. 2005, Feuillet et al. 2008), ensuring the potential for further yield improvement through breeding.

Modern plant breeding comprises conventional and molecular plant breeding. Both, conventional and molecular plant breeding rely largely on hybridization and selection. Hybridization refers to the process of crossing genetically different plants to bring together different loci and alleles associated with desirable traits. After the hybridization process, the most desirable recombinants are selected. The selection process in conventional breeding is based on phenotyping only and remains the most widely applied approach due to its accessibility to most small- to mid-scale breeding programs, lower costs and simple performance (Acquaah 2012). However, conventional breeding methods result in a global wheat yield gain of 0.5-0.9 % per annuum (i.e., 1.0-6.4 g m^{-2} yr^{-1}), while a total yield increase of 50 % in the next 20 years is required in order to meet the predicted global food demand, meaning an increase of ~2.5 % annually (i.e., ~12 g m^{-2} yr^{-1}). Conventional breeding strategies would require on average 70 years to reach this aim and are no longer sufficient (Lopes et al. 2012, Sukumaran et al. 2015). The integration of molecular techniques can potentially increase the efficiency and effectiveness in the identification of favourable genetic diversity (Araus et al. 2002).

One approach in molecular plant breeding is the use of molecular markers. Techniques relying on molecular markers as a tag for genomic regions controlling traits of interest are marker-assisted and genomic selection. While in marker-assisted selection favourable individuals are selected based on a small number of known marker-trait associations, genomic selection uses the information from markers distributed across the whole genome to predict the breeding value of individual accessions and make selections. Genomic selection is based on previously estimated marker effects in populations that have been both genotyped and phenotyped (Meuwissen et al. 2001, Heffner et al. 2009). With the use of molecular markers, the performance of individuals can be scored at an earlier stage, reducing the number of individuals which have to be assessed in the field. Further, molecular markers facilitate the assessment of traits which are difficult to select phenotypically, subject to high environmental error, or time-intensive to score (Collard et al. 2005, Ben-Ari and Lavi 2012). Nevertheless, to be able to score individuals at a molecular level, genomic regions controlling important traits have first to be identified and validated or, in case of genomic selection, the development of accurate

prediction models is required (Heffner et al. 2009, Ben-Ari and Lavi 2012). Both genomic and marker-assisted selection are now routinely used in wheat breeding for simpler traits such as flowering time, disease resistance, grain quality and plant height and more recently for multigenic traits like yield (Gupta et al. 2010, Zhao et al. 2014, Norman et al. 2018).

Other approaches in molecular breeding are not based on hybridization but on the creation of novel genetic diversity. One way this can be achieved is through genetic engineering that might include the insertion of whole genes from one organism to another (transgenic) resulting in genetically modified organisms (GMO). An alternative approach is gene editing that alters gene sequences by insertion or deletion of DNA base pairs. Gene editing can either be induced randomly by chemical and X-ray mutagenesis, or targeted using methods such as clustered regularly interspaced short palindromic repeats and CRISPR-associated protein 9 (CRISPR-Cas9) (Acquaah 2012, Farooq et al. 2018). GMO and CRISPR-Cas9 are however, politically controversial and legally restricted in their cultivation and sale, particularly in Europe (Mwadzingeni et al. 2017, Araus et al. 2019, Mallapaty 2019). Drought or heat resistant wheat accessions have been generated using GMO and mutagenesis with yield improvements of 6-13 % and first drought-responsive transcription factor genes have been edited using CRISPR-Cas9 (Mullarkey and Jones 2000, Khan et al. 2001, reviewed in Araus et al. 2019, Kim et al. 2018). However, most have been tested only in the glasshouse and not field conditions and no transgenic or gene-edited wheat has been approved for commercial cultivation to date (Araus et al. 2019). Besides, the identification of quantitative variability and the genetic engineering of many crops of economic interest such as wheat remains challenging due to the large size of their genome (Kim et al. 2018).

1.6 New molecular technologies to capture the genomic complexity of wheat

Bread wheat is a hexaploid, carrying three closely related or homoeologous genomes (AA, BB and DD), which derived from hybridization of distinct species. Each of these homoeologous genomes consists of seven pairs of chromosomes, resulting in a total of 42 chromosomes with an estimated genome size of around 17 Gb (Feuillet et al. 2008, Brenchley et al. 2012).

Wheat evolved from wild grasses in the Middle East, where the first wheat species were probably cultivated 10,000 years ago (Feuillet et al. 2008). These wheats were low-yielding with a diploid genome consisting of seven chromosomes. The first polyploidization happened

when a diploid wheat species related to *T. urartu*, providing the AA genome crossed with an unknown species containing the BB genome. This tetraploid progeny (AABB) evolved into its own species, known as emmer wheat (*T. turgidum*). Owing to the combination of both genomes, emmer wheat was more vigorous, higher yielding and more broadly adapted to different environments in comparison to its ancestors, making it probably more attractive for early domestication. The second hybridization event between the tetraploid emmer wheat (AABB) and diploid goat grass (DD, *Aegilops tauschii*) resulted into today's bread wheat (Feuillet et al. 2008, Brenchley et al. 2012).

Until recently, the development of highly saturated genetic and physical maps and the identification of genes was challenging due to the large size and nature of the bread wheat genome (Paux et al. 2010, IWGSC 2018). Difficulties arose particularly from the high content of repetitive DNA. The wheat genome contains approximately 80 % repeats, primarily transposons, which are hypothesized to contribute to its highly dynamic character, i.e., changes in local gene order and pseudogene formation; and its enormous genome size (Brenchley et al. 2012). New, cost-effective, high-throughput sequencing techniques such as Illumina sequencing enabled the development of thousands of SNP markers leading to the construction of consensus maps (Wang et al. 2014) and later on to a high-quality reference genome sequence of the bread wheat cultivar Chinese Spring (RefSeq v1.0 (IWGSC 2018). With an estimated coverage of 94 % of the genome and containing ~108 thousand high-confidence genes and ~4 million molecular markers, the RefSeq v1.0 is a powerful tool to explore genes and gene networks underlying traits of agronomic importance (IWGSC 2018).

Platforms like the Diversity Among Wheat geNomes platform (DAWN) integrating the RefSeq v1.0 with whole genome shotgun and exome data from other wheat varieties can provide further insights into global genome compositions and genetic diversity and enable a faster and easier way to identify haplotypes and to select parental material for crossing in breeding (Watson-Haigh et al. 2018). Nevertheless, the RefSeq v1.0 is exclusively based on the reference genome of Chinese Spring and genomic variations within other varieties might remain unobserved (IWGSC 2018). New initiatives such as the 10+ genome project (http://www.10wheatgenomes.com/) focus on the assembly of several reference genomes to create a 'pan genome', which will allow the comparison of multiple wheat genomes and a detailed overview of common and unique variations within species.

1.7 Quantitative trait loci for drought and heat stress tolerance

The relationship between phenotype and genotype for quantitative traits is difficult to detect directly owing to their multigenic control, low-heritability and high genotype by environment interaction. A genomic region controlling a quantitative trait is named a quantitative trait locus (QTL) (Kearsey 1998, van Ooijen 1999). The identification of QTL facilitates our genetic understanding of complex traits and identified QTL can be used for selection in plant breeding (Gupta et al. 2017).

Several genetic studies identified QTL in wheat under dry and hot field conditions (e.g., Hafsi et al. 2000, Kirigwi et al. 2007, Maccaferri et al. 2008, Bennett et al. 2012, Qaseem et al. 2019a) corresponding to the mega-environments 1 and 4 defined by Gbegbelegbe et al. (2016), but only a few studies imposed combined drought and heat stress under controlled conditions (Aprile et al. 2013, Qaseem et al. 2018) (Table 2). The identification of QTL in field conditions can be problematic due to environmental fluctuations and factors which can additionally influence the yield outcome such as diseases, wind, radiation and soil conditions. Identified QTL might therefore not be actually, or at least not exclusively, associated with drought and heat stress (Izanloo et al. 2008). Issues can also arise from the strong flowering time impact on yield in dry and hot conditions masking the effect of other QTL of interest (Gupta et al. 2010). In addition, the majority of the conducted studies reporting large single gene effects on yield under stress (e.g., Kirigwi et al. 2007, Golabadi et al. 2011, Kadam et al. 2012) remain at a primarily descriptive stage lacking large scale field-based evaluation, validation in other genetic backgrounds and the genetic and physiological dissection of these QTL.

The analysis and mapping of QTL is performed by associating genotypic with phenotypic variation for a certain quantitative trait. The most common methods for QTL mapping are linkage analysis and association mapping (Zhu et al. 2008). While linkage analysis uses bi-parental populations which derive from a cross between two phenotypically diverse parents (e.g., drought-sensitive and drought-tolerant parent), association mapping explores genetic variations in a large set of diverse germplasm. The fraction of genetic diversity that is captured is therefore lower in linkage analysis compared to association mapping (Zhu et al. 2008, Hamblin et al. 2011).

Table 2. QTL identified in wheat under combined and single drought or heat stress (updated version of Table 1 from Tricker et al. 2018). Dry and hot field conditions are defined based on the CIMMYT mega-environments 1 and 4 (Gbegbelegbe et al. 2016). [a] means field conditions; [b] controlled conditions; [c] semi-controlled conditions; * trials in Italy, Tunisia and Morocco with maximum temperature at grain filling ≤26.1°C; NDVI: Near Differential Vegetative Index; WSC: water soluble carbohydrates.

Combined dry and hot conditions

Trait	Chromosome	Reference
Grain yield	1AL, 1B, 1D, 2AL, 2BL, 2D, 3AL, 3B, 3D, 4AL, 4BL, 5A, 6AS, 6BS, 6BL, 6DS, 7A, 7BS, 7DS	Kirigwi et al. (2007)[a], Maccaferri et al. (2008)[a]*, Pinto et al. (2010)[a], Golabadi et al. (2011)[a], Bennett et al. (2012)[a], Ain et al. (2015)[a], Merchuk-Ovnat et al. (2016)[a], Tahmasebi et al. (2017)[a], Li et al. (2019b)[c]
Biological yield	1AL, 4BL, 4DS, 6BL	Ain et al. (2015)[a]
Thousand grain weight	1BL, 1DL, 2AL, 2BL, 2DL, 3AL, 3BL, 4AL, 4B, 4D, 5AL, 5BL, 5DL, 6AL, 6BS, 6DL, 7A, 7B, 7D	Pinto et al. (2010)[a], Golabadi et al. (2011)[a], Bennett et al. (2012)[a], Ain et al. (2015)[a], Tahmasebi et al. (2017)[a], Garcia et al. (2019)[a], Khalid et al. (2019)[a], Li et al. (2019b)[c]
Kernel weight index (large grains$^{-\text{all grains}}$)	1A, 2B, 6A	Pinto et al. (2010)[a]
Grain weight spike^{-1}	2A, 2B, 4A, 5A, 5B, 6A, 6D, 7B, 7D	Golabadi et al. (2011)[a], Zhang et al. (2018)[a]
Grain number m^{-2}	1B, 2A, 3B, 3D, 4AL, 6B, 7A, 7B	Kirigwi et al. (2007)[a], Pinto et al. (2010)[a], Bennett et al. (2012)[a], Liu et al. (2019)[a]
Grain number spike^{-1}	1AL, 1DL, 2AS, 2BS, 2DL, 4AL, 5AL, 5BL, 6AS, 6BL, 7A, 7B	Golabadi et al. (2011)[a], Tahmasebi et al. (2017)[a], Qaseem et al. (2018)[b], Li et al. (2019b)[c]
Harvest index	1B, 2A, 2B, 3BL, 4A, 5A, 5B, 6A, 6BL, 7A, 7B, 7D	Peleg et al. (2009)[c], Golabadi et al. (2011)[a], Ain et al. (2015)[a], Qaseem et al. (2018)[b], Qaseem et al. (2019a)[a]
Spike weight	1B, 6A	Golabadi et al. (2011)[a]
Spike number plot^{-1}	4B	Garcia et al. (2019)[a]
Spike number plant^{-1}	1AL, 1B, 2AL, 2BS, 2BL, 2DL, 3B, 3D, 4AL, 4B, 5AL, 5B, 6DS, 7B, 7D	Kirigwi et al. (2007)[a], Golabadi et al. (2011)[a], Ain et al. (2015)[a], Qaseem et al. (2018)[b], Li et al. (2019)[c], Qaseem et al. (2019a)[a]
Spike weight	2A, 4A, 7A, 7B	Peleg et al. (2009)[c]
Spike harvest index	2B, 3B	Golabadi et al. (2011)[a]
Spikelet number spike^{-1}	1A, 1B, 2B, 3D, 4B, 5A, 7A, 7B, 7D	Tahmasebi et al. (2017)[a], , Zhang et al. (2018)[a], Qaseem et al. (2019a)[a]
Biomass	2A, 2BS, 3B, 4AL, 4B, 5A, 5B, 5D, 7AS, 7B, 7D	Kirigwi et al. (2007)[a], Peleg et al. (2009)[c], Merchuk-Ovnat et al. (2016)[a], Qaseem et al. (2018)[b], Garcia et al. (2019)[a], Qaseem et al. (2019a)[a]
Plant height	1A, 1B, 2AL, 2BS, 2BL, 3AL, 3BS, 4AL, 4B, 4D, 5AS, 5BL, 6AL, 7AS, 7B, 7D	Maccaferri et al. (2008)[a]*, Pinto et al. (2010)[a], Ain et al. (2015)[a], Tahmasebi et al. (2017)[a], Garcia et al. (2019)[a], Qaseem et al. (2019a)[a]

Table 2. Continued.

Combined dry and hot conditions

Trait	Chromosome	Reference
Shoot length	2B, 3B, 4A, 4B, 6B, 7A, 7B	Peleg et al. (2009)[c]
Peduncle length	2A, 3A, 3B, 5A, 7A	Bennett et al. (2012)[a], Qaseem et al. (2018)[b]
Peduncle extrusion	3A, 5A, 7A	Qaseem et al. (2018)[b]
Spike length	2A, 4B, 4D, 5A, 6B, 7A, 7B, 7D	Qaseem et al. (2018)[b], Garcia et al. (2019)[a], Khalid et al. (2019)[a], Qaseem et al. (2019a)[a]
Awn length	2A, 3A, 7A	Qaseem et al. (2018)[b]
Flag leaf length	7B, 7D	Qaseem et al. (2019a)[a]
Flag leaf width	1A, 2B, 2D, 3B, 4A, 4B, 6A, 7B, 7D	Bennett et al. (2012)[a], Qaseem et al. (2019a)[a]
Leaf area	5A, 5B, 7A, 7B, 7D	Qaseem et al. (2018)[b], Qaseem et al. (2019a)[a]
Days to heading	1A, 1BS, 1D, 2AS, 2BS, 2BL, 3A, 3BL, 4AL, 4B, 4D, 5A, 5D, 6A, 6D, 7AS, 7BS, 7DL	Kirigwi et al. (2007)[a], Maccaferri et al. (2008)[a]*, Peleg et al. (2009)[c], Pinto et al. (2010)[a], Ain et al. (2015)[a], Merchuk-Ovnat et al. (2016)[a], Ogbonnaya et al. (2017)[a], Tahmasebi et al. (2017)[a], Liu et al. (2019)[a]
Days to anthesis	2A, 7A	Qaseem et al. (2018)[b]
Days to maturity	1A, 1BS, 1D, 2A, 2BS, 4B, 5A, 5D, 7A, 7B, 7DL	Pinto et al. (2010)[a], Ain et al. (2015)[a], Tahmasebi et al. (2017)[a], Qaseem et al. (2018)[b], Qaseem et al. (2019a)[a]
Days from heading to maturity	1B, 2B, 4A, 4B, 5A, 5B, 7A, 7B	Peleg et al. (2009)[c]
NDVI at the vegetative stage	1B, 3B, 4A, 5A, 5D, 7A	Pinto et al. (2010)[a], Bennett et al. (2012)[a], Liu et al. (2019)[a]
NDVI at the grain filling stage	1B, 1D, 2A, 2B, 4A, 4B, 5A, 6A, 6B, 7A, 7B	Pinto et al. (2010)[a]
WSC plant^{-1}	1A, 1B, 1D, 2D, 4A	Ovenden et al (2017)[a]
Stem WSC	1A, 1B, 3A, 3B, 4A, 6D	Pinto et al. (2010)[a], Bennett et al. (2012)[a]
Grain fill rate	4AL	Kirigwi et al. (2007)[a]
Grain fill duration	4AL	Kirigwi et al. (2007)[a]
Canopy temperature at the vegetative stage	1B, 2B, 3B, 4A, 4B, 6B, 6D, 7A	Pinto et al. (2010)[a], Tahmasebi et al. (2017)[a], Liu et al. (2019)[a]
Canopy temperature at the grain filling stage	1A, 1B, 2B, 3B, 4A, 5A, 6B, 6D, 7A	Pinto et al. (2010)[a], Liu et al. (2019)[a]
Canopy temperature depression	1A, 2A, 2B, 3A, 3B, 4A, 4B, 5A, 5B, 6A, 6B, 7A, 7B	Diab et al. (2008)[a]
Flag leaf rolling	1A, 2A, 2B, 4B, 5A, 5B, 6B, 7A, 7D	Peleg et al. (2009)[c], Tahmasebi et al. (2017)[a]
Early vigour	2B, 2D, 3B, 4A	Bennett et al. (2012)[a]
Early ground cover	6AS	Mondal et al. (2017)[a]
Chlorophyll content	1A, 1B, 3A, 4A, 4B, 4D, 5A, 5B, 6A, 6B, 7A	Diab et al. (2008)[a], Peleg et al. (2009)[c], Bennett et al. (2012)[a]
Chlorophyll fluorescence	1A, 1B, 2A, 2B, 3A, 3B, 4A, 4B, 5A, 5B, 6A, 6B, 7A, 7B	Diab et al. (2008)[a]

Table 2. Continued.

Combined dry and hot conditions

Trait	Chromosome	Reference
Carbon isotope discrimination	1B, 2A, 2B, 3A, 3B, 4A, 4B, 5A, 5B, 6B, 7A, 7B	Diab et al. (2008)[a], Peleg et al. (2009)[c]
Photosynthetically active radiation	1A, 1B, 2B, 3A, 3B, 4A, 4B, 5A, 5B, 6A, 6B, 7A, 7B	Diab et al. (2008)[a]
Stomatal density	4AS, 5AS, 7AL	Shahinnia et al. (2016)[a]
Stomatal index	2BL, 7BL	Shahinnia et al. (2016)[a]
Stomatal aperture area	7AL	Shahinnia et al. (2016)[a]
Stomatal aperture length	2BS, 2BL, 7AL	Shahinnia et al. (2016)[a]
Guard cell length	1AS, 3BL, 7AL	Shahinnia et al. (2016)[a]
Guard cell area	1BL, 4BL, 5AL, 5DL	Shahinnia et al. (2016)[a]
Guard cell length	1AS, 3BL, 7AL	Shahinnia et al. (2016)[a]
Transpiration efficiency	1A, 1B, 2B, 3A, 3B, 4A, 4B, 5A, 5B, 6A, 6B, 7A, 7B	Diab et al. (2008)[a]
Leaf relative water content	1B, 2B, 3A, 3B, 4A, 4B, 5A, 5B, 6A, 6B	Diab et al. (2008)[a]
Water index	1A, 1B, 2A, 2B, 2D, 3A, 3B, 4A, 4B, 5A, 5B, 5D, 6A, 6B, 7A, 7B	Diab et al. (2008)[a], Zhang et al. (2018)[a]
Leaf osmotic potential	2A, 2B, 3A, 3B, 4B, 5A, 5B, 6B	Peleg et al. (2009)[c]
Osmotic adjustment	1A, 3A, 3B, 4A, 7A	Diab et al. (2008)[a]
Metabolites (mQTL)	2B, 4A, 5A, 7A, 7D	Hill et al. (2015)[a]
Expression of stress-related genes (eQTL)	6BL	Aprile et al. (2013)[b]
Superoxide dismutase concentration	7B	Khalid et al. (2019)[a]

Drought stress

Trait	Chromosome	Reference
Grain yield	2AL, 2BS, 2BL, 2D, 3D, 3DL, 4AL, 4BS, 4DL, 5AS, 5BS, 5DL, 6AS, 6BS, 6BL, 6DS, 6DL, 7AL, 7BL, 7D	Quarrie et al. (2005)[a], Czyczylo-Mysza et al. (2011)[c], Kadam et al. (2012)[b], Tahmasebi et al. (2017)[a], Li et al. (2019b)[a]
Grain weight spike^{-1}	1B, 1DS, 3DL	Xu et al. (2017)[a], Lehnert et al. (2019)[b]
Thousand grain weight	1B, 1D, 2AL, 2B, 2DL, 3AL, 3BL, 3D, 4A, 4D, 5AL, 5BL, 6A, 6BS, 6DL, 7A, 7B, 7DS	Quarrie et al. (2005)[a], Dashti et al. (2007)[b], Yang et al. (2007)[a], Tahmasebi et al. (2017)[a], Xu et al. (2017)[a], Li et al. (2019b)[a]
Grain number m^{-2}	1B, 5B, 7D	Tahmasebi et al. (2017)[a]
Grain number spike^{-1}	1AL, 1DS, 2AS, 2AL, 2BS, 2BL, 2D, 3A, 3B, 4A, 4BL, 5AL, 5BL, 5DL, 6A, 6BL, 6DL, 7A, 7B	Quarrie et al. (2005)[a], Czyczylo-Mysza et al. (2011)[c], Xu et al. (2017)[a], Lehnert et al. (2019)[b], Li et al. (2019b)[a]
Harvest index	1B, 2D, 3BL, 3DL, 4BS, 5A, 7B, 7D	Kadam et al. (2012)[b], Xu et al. (2017)[a], Qaseem et al. (2018)[b], Lehnert et al. (2019)[b]

Table 2. Continued.

Drought stress

Trait	Chromosome	Reference
Spike number plant^{-1}	1A, 2A, 2B, 2DS, 4AL, 4B, 5AL, 5DL, 6A, 7AL, 7B	Quarrie et al. (2005)[a], Xu et al. (2017)[a], Qaseem et al. (2018)[b], Li et al. (2019b)[a]
Spikelet compactness	6A, 7A	Xu et al. (2017)[a]
Spikelet number spike^{-1}	1A, 1DS, 2AS, 2B, 2DS, 3DL, 4AL, 5AS, 5BS, 5DS, 6AS, 7AS, 7D	Tahmasebi et al. (2017)[a], Xu e tal. (2017)[a], Li et al. (2019b)[a]
Sterile spikelet number spike^{-1}	7A	Xu e tal. (2017)[a]
Fertile spikelet spike-^{1}	2A	Xu e tal. (2017)[a]
Biomass	1B, 3B, 4AL, 5A	Xu et al. (2017)[a], Qaseem et al. (2018)[b], Lehnert et al. (2019)[b]
Shoot biomass	4B	Kadam et al. (2012)[b]
Root biomass	2D, 3AS, 3BL, 3DS, 3DL, 4BS	Kadam et al. (2012)[b], Lehnert et al. (2019)[b]
Plant height	1BL, 2A, 2BS, 2BL, 2DS, 2DL, 3AL, 3BL, 4AS, 4AL, 4BL, 4DS, 4DL, 5AS, 5BL, 5DS, 5DL, 6AS, 6BS, 6BL, 6DS, 6DL, 7DL	Tahmasebi et al. (2017)[a], Xu et al. (2017)[a], Qaseem et al. (2018)[b], Li et al. (2019b)[a]
Peduncle length	3B, 7D	Dashti et al. (2007)[b], Qaseem et al. (2018)[b]
Peduncle extrusion	2A, 7A	Qaseem et al. (2018)[b]
Coleoptile length	6AS	Spielmeyer et al. (2007)[b]
Spike length	1BL, 2B, 2DS, 4AL, 4BL, 5AL, 5BS, 7A, 7B, 7D	Xu et al. (2017)[a], Qaseem et al. (2018)[b], Li et al. (2019b)[a]
Awn length	5A, 6A, 7B, 7D	Qaseem et al. (2018)[b]
Root length	2D, 4B, 5D, 6B	Kadam et al. (2012)[b]
Flag leaf width	2BS	Edae et al. (2014)[a]
Leaf area	5A, 6A, 7B, 7D	Qaseem et al. (2018)[b]
Growth rate	5BL	Parent et al. (2015)[b]
Relative growth rate	4AL	Parent et al. (2015)[b]
Inflexion point in growth curves	7DS	Parent et al. (2015)[b]
Leaf expansion rate	5BL	Parent et al. (2015)[b]
Inflexion point in leaf expansion curves	5BL	Parent et al. (2015)[b]
Days to heading	1D, 2A, 4B, 7D	Tahmasebi et al. (2017)[a], Qaseem et al. (2018)[b]
Days to anthesis	2A, 2D, 7A	Kadam et al. (2012)[b], Qaseem et al. (2018)[b]
Days to maturity	5A, 7A	Qaseem et al. (2018)[b]
Stem WSC at the flowering stage	1A, 1D, 2D, 4A, 4B, 7B	Yang et al. (2007)[a]
Stem WSC at the grain filling stage	4A	Yang et al. (2007)[a]

Table 2. Continued.

Drought stress

Trait	Chromosome	Reference
Stem WSC at the maturity stage	6B	Yang et al. (2007)[a]
Accumulation efficiency of stem WSC	1A, 2A, 5A, 7B	Yang et al. (2007)[a]
Remobilization efficiency of stem WSC	7A	Yang et al. (2007)[a]
Grain filling efficiency	2A, 4B, 5A,	Yang et al. (2007)[a]
Flag leaf rolling	4B, 5A	Tahmasebi et al. (2017)[a]
Chlorophyll content	1B, 2B, 5B, 7A, 7B	Tahmasebi et al. (2017)[a], Xu et al. (2017)[a]
Flag leaf persistence	2D, 3B, 4B, 5A, 6A	Verma et al. (2004)[a], Yang et al. (2016)[a]
Net photosynthetic rate	6B	Xu et al. (2017)[a]
Chlorophyll fluorescence	1B, 2A, 2D, 3A, 3B, 3D, 4A, 4B, 4D, 5A, 5B, 6A, 6B, 7A, 7B, 7D	Czyczylo-Mysza et al. (2011)[c]
Stomatal conductance	5A	Xu et al. (2017)[a]
Stomatal density	5BS	Shahinnia et al. (2016)[b]
Stomatal index	5BS, 6DL	Shahinnia et al. (2016)[b]
Stomatal aperture length	2BL, 4BS, 7AS, 7DL	Shahinnia et al. (2016)[b]
Guard cell area	1BL, 5BS	Shahinnia et al. (2016)[b]
Guard cell length	1BL, 4BS, 7AS	Shahinnia et al. (2016)[b]
Transpiration rate	3Al, 4BL, 6D	Parent et al. (2015)[b], Xu et al. (2017)[a]
Water use efficiency	2AL, 4D	Parent et al. (2015)[b], Xu et al. (2017)[a]

Heat stress

Trait	Chromosome	Reference
Grain yield	1AL, 1BL, 1D, 2BS, 2BL, 3AL, 3BS, 3BL, 3D, 4A, 4B, 4DL, 5A, 5B, 6AS, 6BS, 6BL, 6DS, 7AS, 7AL, 7BS, 7BL	Quarrie et al. (2005)[a], Maccaferri et al. (2008)[a]*, Pinto et al. (2010)[a], Golabadi et al. (2011)[a], Bennett et al. (2012)[a], Paliwal et al. (2012)[a], Merchuk-Ovnat et al. (2016)[a], Ogbonnaya et al. (2017)[a], Li et al. (2019b)[c]
Grain weight spike^{-1}	2A, 2B, 3A, 3BS, 4A, 5A, 5B, 6A, 6D, 7A, 7B, 7D	Golabadi et al. (2011)[a], Shirdelmoghanloo et al. (2016)[b], Ogbonnaya et al. (2017)[a]
Thousand grain weight	1A, 2A, 2B, 2DS, 2DL, 3AS, 3BS, 3D, 4A, 4B, 4D, 5A, 5BL, 5DL, 6A, 6BS, 6DL, 7A, 7B, 7D	Quarrie et al. (2005)[a], Pinto et al. (2010)[a], Golabadi et al. (2011)[a], Bennett et al. (2012)[a], Ogbonnaya et al. (2017)[a], Tahmasebi et al. (2017)[a], Sukumaran et al (2018)[a], Li et al. (2019b)[c]
Single grain weight	2D, 3BS, 5B, 6A	Shirdelmoghanloo et al. (2016)[b]
Kernel weight index (large grains$^{-\text{all grains}}$)	1A, 1D, 2B, 3B, 4B, 5A, 5B, 6A, 6B, 6D	Pinto et al. (2010)[a]
Grain number m^{-2}	1A, 1B, 1D, 2B, 3BS, 3BL, 3D, 4A, 4B, 4D, 5A, 5B, 6A, 6B, 6D, 7A	Pinto et al. (2010)[a], Bennett et al. (2012)[a], Sukumaran et al (2015)[a], Sukumaran et al (2018)[a]

Table 2. Continued.

Heat stress

Trait	Chromosome	Reference
Grain number spike^{-1}	1AL, 1B, 2A, 2BL, 3BS, 3DS, 4AL, 4BS, 4BL, 4DS, 5AL, 5BL, 5D, 6A, 6DL, 7B, 7D	Quarrie et al. (2005)[a], Golabadi et al. (2011)[a], Ogbonnaya et al. (2017)[a], Tahmasebi et al (2017)[a], Li et al. (2019)[c]
Threshing index	1A, 1B, 5B	Ogbonnaya et al. (2017)[a]
Harvest index	1B, 1D, 2B, 3B, 4A, 5A, 5B, 6A, 6B, 7B	Peleg et al. (2009)[c], Sukumaran et al (2015)[a]
Spike weight	2A, 2B, 3A, 3B, 3D, 4B, 5A, 5B, 6A, 6B, 7A, 7B	Valluru et al (2017)[a,b]
Spike number m^{-2}	1A, 1B, 3A, 3B, 4B, 5A, 5B, 7B, 7D	Golabadi et al. (2011)[a], Ogbonnaya et al. (2017)[a]
Spike number plant^{-1}	2BL, 3A, 3B, 3D, 4B, 5AL, 6AL, 7AS, 7DL	Quarrie et al. (2005)[a], Qaseem et al. (2018)[b], Li et al. (2019)[c]
Spike weight	1B, 2B, 2D, 3D, 4A, 5D, 6A, 7B	Peleg et al. (2009)[c], Golabadi et al. (2011)[a], Ogbonnaya et al. (2017)[a]
Spike harvest index	2B, 5B, 7A, 7B	Golabadi et al. (2011)[a]
Spikelet compactness	1A	Tahmasebi et al. (2017)[a]
Spikelet number spike^{-1}	1A, 1B, 1D, 2B, 3D, 4A, 4B, 5A, 5B, 6A, 6B, 6D, 7A, 7B	Ogbonnaya et al. (2017)[a], Tahmasebi et al. (2017)[a], Zhang et al. (2018)[a], Qaseem et al. (2019a)[a]
Biomass	1BL, 2BS, 3B, 3D, 6A, 7AS, 7BS	Sukumaran et al (2015)[a], Merchuk-Ovnat et al. (2016)[a], Qaseem et al. (2018)[b], Qaseem et al. (2019a)[a]
Shoot biomass	3BS, 4A, 6B	Shirdelmoghanloo et al. (2016)[b]
Plant height	1A, 1B, 2A, 2B, 2D, 3A, 3B, 3D, 4A, 4B, 4D, 5A, 5B, 6A, 6B, 6D, 7A, 7B, 7D	Maccaferri et al. (2008)[a]*, Pinto et al. (2010)[a], Ogbonnaya et al. (2017)[a], Tahmasebi et al. (2017)[a], Sukumaran et al (2018)[a], Khalid et al. (2019a)[a]
Shoot length	1B, 2A, 2B, 3A, 3B, 4A, 4B, 5D, 7A, 7B, 7D	Peleg et al. (2009)[c], Ogbonnaya et al. (2017)[a], Maulana et al. (2018)[b]
Peduncle length	1A, 1B, 2B, 3A, 3B, 5A, 5B, 7A	Ogbonnaya et al. (2017)[a], Qaseem et al. (2018)[b]
Peduncle extrusion	1B, 2B, 3B, 7D	Qaseem et al. (2018)[b]
Spike length	5A, 7A, 7D	Qaseem et al. (2018)[b], Khalid et al. (2019)[a], Qaseem et al. (2019a)[a]
Awn length	2A, 7D	Qaseem et al. (2018)[b]
Flag leaf length	2A, 3A, 3B, 5B, 7D	Mason et al. (2010)[b], Qaseem et al. (2019a)[a]
Flag leaf width	1D, 2B, 3BL, 6A, 6D, 7A, 7B	Mason et al. (2010)b, Bennett et al. (2012)[a], Qaseem et al. (2019a)[a]
Number of leaves plant^{-1}	3A, 3B, 4B, 5A, 5B, 7B	Maulana et al. (2018)[b]
Leaf area	1B, 3D, 5A, 5B, 6A, 7B	Qaseem et al. (2018)[b], Qaseem et al. (2019a)[a]
Wax score	1B, 2A, 2B, 2D, 3A, 3B, 5A, 6A, 6B, 7B	Mason et al. (2010)[b], Ogbonnaya et al. (2017)[a]

Table 2. Continued.

Heat stress

Trait	Chromosome	Reference
Days to heading	1BL, 1D, 2A, 2BS, 3B, 3A, 4A, 4B, 4D, 5A, 6A, 6D, 7AS, 7BS, 7D	Maccaferri et al. (2008)[a]*, Peleg et al. (2009)[c], Pinto et al. (2010)[a], Merchuk-Ovnat et al. (2016)[a], Ogbonnaya et al. (2017)[a], Liu et al. (2019)[a]
Days to anthesis	1B, 1D, 2B, 3A, 3B, 3D, 4A, 4B, 4D, 5A, 5B, 6A, 7A	Mason et al. (2010)[b], Pinto et al. (2010)[a], Sukumaran et al (2015)[a], Qaseem et al. (2018)[b], Sukumaran et al (2018)[a]
Days to maturity	1B, 1D, 2A, 2B, 3B, 4A, 4B, 4D, 5A, 5B, 5D, 6A, 6B, 6D, 7A, 7B, 7DS	Pinto et al. (2010)[a], Bennett et al. (2012)[a], Paliwal et al. (2012)[a], Sukumaran et al (2015)[a], Ogbonnaya et al. (2017)[a], Sukumaran et al (2018)[a]
Near Differential Vegetative Index at the vegetative stage	1B, 1D, 2B, 2D, 3A, 3B, 4A, 4B, 4D, 5A, 5B, 6A, 6B, 6D, 7A	Pinto et al. (2010)[a], Bennett et al. (2012)[a], Sukumaran et al (2015)[a], Sukumaran et al (2018)[a]
Near Differential Vegetative Index at the grain filling stage	1A, 1B, 3A, 4A, 4B, 5A, 5B, 6A, 6B, 7B	Pinto et al. (2010)[a], Sukumaran et al (2015)[a]
Stem WSC	1A, 1B, 2D, 3A, 3BL, 5A, 5B, 6A	Pinto et al. (2010)[a], Bennett et al. (2012)[a]
Grain filling duration	1B, 1D, 2A, 2B, 2D, 3BS, 5A, 6A, 6B, 6D	Mason et al. (2010)[b], Shirdelmoghanloo et al. (2016)[b], Ogbonnaya et al. (2017)[a]
Canopy temperature at the vegetative stage	1A, 1B, 1D, 2B, 3A, 3BL, 4A, 4B, 5B, 6B, 7A	Pinto et al. (2010)[a], Bennett et al. (2012)[a]
Canopy temperature at the grain filling stage	1A, 1B, 1D, 2B, 3BS, 3BL, 4A, 4D, 5A, 5D, 6A, 7A, 7B	Pinto et al. (2010)[a], Bennett et al. (2012)[a], Sukumaran et al (2015)[a]
Canopy temperature depression	7BL	Paliwal et al. (2012)[a]
Flag leaf rolling	1A, 2A, 2B, 2D, 3D, 4B, 5A, 5B, 6A, 6B, 7A, 7B	Peleg et al. (2009)[c], Ogbonnaya et al. (2017)[a], Tahmasebi et al. (2017)[a]
Early vigour	2B, 2D, 3BL	Bennett et al. (2012)[a]
Chlorophyll content	1A, 1B, 1D, 2B, 2D, 3A, 3BS, 4A, 4A, 4B, 4D, 5A, 5B, 6A, 6D, 7A, 7B, 7D	Peleg et al. (2009)[c], Pinto et al. (2010)[a], Bennett et al. (2012)[a], Tahmasebi et al. (2017)[a], Maulana et al. (2018)[b]
Flag leaf persistence	1B, 1D, 2A, 3A, 3BS, 6A, 6B, 7A,	Vijayalakshmi et al. (2010)[b], Talukder et al. (2014)[b], Shirdelmoghanloo et al. (2016)[b]
Chlorophyll loss rate	3BS, 6BL	Shirdelmoghanloo et al. (2016)[b]
Chlorophyll fluorescence	7A	Vijayalakshmi et al. (2010)[b]
Carbon isotope discrimination	1A, 2A, 4A, 5B, 6A, 6B, 7B	Peleg et al. (2009)[c]
Water index	1A, 1B, 2D, 3A, 3B, 5A, 5D, 6B, 7A	Zhang et al. (2018)[a]
Leaf osmotic potential	2A, 3A, 3B, 5A, 5B, 6A, 6B	Peleg et al. (2009)
Plasma membrane damage	1D, 2B, 7A	Talukder et al. (2014)[b]
Thylakoid membrane damage	1D, 6A, 7A	Talukder et al. (2014)[b]

Table 2. Continued.

Heat stress

Trait	Chromosome	Reference
Superoxide dismutase concentration	7B	Khalid et al. (2019)[a]
Spike ethylene (phytohormone) concentration	1A, 1B, 1D, 3B, 5B, 7B	Valluru et al (2017)[a,b]

1.8 QTL mapping using genome-wide association

According to the focus of the study, association mapping can be categorized into candidate-gene association mapping or genome-wide association studies (GWAS). Candidate-gene association mapping focuses on polymorphisms in selected candidate genes and associates those with phenotypic variations, whereas GWAS relates polymorphisms across the whole genome to the observed phenotypic variations (Zhu et al. 2008).

Overall, GWAS offers three main advantages (Zhu et al. 2008, Hamblin et al. 2011):

i) It captures a wider genetic diversity than linkage analysis.

ii) It increases mapping resolution by using historic meiotic recombinations.

iii) The use of diversity panels reduces research time and costs because no crossing is required for the development of mapping populations.

The power and accuracy of QTL mapping using GWAS depend on population size, marker density, population structure and the genetic architecture of the trait (Hamblin et al. 2011). Large numbers of markers and accessions are required due to the increased number of recombination breaks and the low frequency of some of the alleles within the population (Hamblin et al. 2011). Rare alleles and complex traits, i.e. traits which are controlled by several loci with mostly very small effects, are often a problem in GWAS because of a lack of statistical power between phenotypic and genetic variations (Hamblin et al. 2011, Muqaddasi et al.2017). Besides, population structure and unequal relatedness among individuals in a given population can confound results and lead to false-positive associations. Both population structure and relatedness have therefore to be accounted for in GWAS analysis and different statistical methods have been developed (Zhang et al. 2010). It is, however, important to acknowledge

that GWAS and linkage analysis are equally affected by a series of other limitations such as genotyping errors, number of biological replicates and genotype by environment interactions. To ensure the identification of stable and reliable QTL in both linkage analysis and association mapping, the repetition of trials and the focus on specific target environments are required (Millet et al. 2016).

GWAS for a number of traits including grain yield have been performed in various crops such as barley, sorghum, maize, rice and durum wheat (Maccaferri et al. 2008, Millet et al. 2016, Pantalião et al. 2016, Tavakol et al. 2016, Xia et al. 2018); and also recently in hexaploid wheat (Sukumaran et al. 2015, Wang et al. 2017, Qaseem et al. 2018, Qaseem et al. 2019a). GWAS in bread wheat targeting combined drought and heat stress identified QTL for yield on chromosomes 1A, 2A, 2B, 2D, 3A, 3B, 4A, 5A, 6A, 6B, 6D, 7A, 7B, 7D so far (Ain et al. 2015, Qaseem et al. 2018, Garcia et al. 2019, Li et al. 2019b, Qaseem et al. 2019a). Given that a large number of QTL might be mapped in diverse populations, GWAS has great potential for mining novel alleles that could be implemented in marker-assisted selection (Zhu et al. 2008).

1.9 Research aims

The primary aim of this study was to identify and validate novel loci and alleles in bread wheat which are associated with the tolerance to combined drought and heat stress at the critical period of early grain filling. Identified loci and alleles could potentially be used in marker-assisted selection in future plant breeding programs. Genome-wide association studies (Chapter 2) were conducted under semi-controlled conditions over two years using a panel of 315 diverse wheat genotypes and measuring 16 grain yield related and physiological traits, which have been hypothesized to be relevant in dry and hot climates (Tricker et al. 2018). Two target QTL on chromosome 6A and 6B associated with yield-related traits under drought and heat stress were subsequently validated in semi-controlled field conditions and in an automated platform at the Plant Accelerator (Adelaide) using near-isogenic lines (Chapter 3, Appendix A). To dissect the tolerance mechanisms associated with the selected target QTL under drought and heat stress, the allelic effects on water consumption, water use efficiency and photosynthesis-related parameters were also studied. Gene expression analysis was performed to identify potential candidate genes. To accelerate and automate the analysis of wheat grain yield per spike, an X-ray system that can be used in future experiments was developed for the prediction of nine seed traits (Chapter 4).

References

Abbad, H., El Jaafari, S., Bort, J., & Araus, J. (2004). Comparison of flag leaf and ear photosynthesis with biomass and grain yield of durum wheat under various water conditions and genotypes. *Agronomie*, 24, 9-28.

Acquaah, G. (2012). *Principles of Plant Genetics and Breeding*. Second edition. Maryland: Wiley-Blackwell.

Ahamed, T., Tian, L., Jiang, Y., Zhao, B., Liu, H., & Ting, K.C. (2012). Tower remote-sensing system for monitoring energy crops; image acquisition and geometric corrections. *Biosystems Engineering*, 112, 93-107.

Ain, Q., Rasheed, A., Anwar, A., Mahmood, T., Imtiaz, M., Mahmood, T., Xia, X., He, Z., & Quraishi, U. M. (2015). Genome-wide association for grain yield under rainfed conditions in historical wheat cultivars from Pakistan. *Frontiers in Plant Science*, 6, 743.

Al-Khatib, K., & Paulsen, G. M. (1984). Mode of high temperature injury to wheat during grain development. *Physiologia Plantarum*, 61, 363-368.

Aliyev, J. A. (2012). Photosynthesis, photorespiration and productivity of wheat and soybean genotype. *Physiologia Plantarum*, 145, 369-383.

Allakhverdiev, S. I., Kreslavski, V. D., Klimov, V. V., Los, D. A., Carpentier, R., & Mohanty, P. (2008). Heat stress: an overview of molecular responses in photosynthesis. *Photosynthesis Research*, 98, 541-550.

Aprile, A., Havlickova, L., Panna, R., Mare, C., Borrelli, G. M., Marone, D., Perrotta, C., Rampino, P., De Bellis, L., Curn, V., Mastrangelo, A. M., Rizza, F., & Cattivelli, L. (2013). Different stress responsive strategies to drought and heat in two durum wheat cultivars with contrasting water use efficiency. *BMC Genomics*, 14, 821-838.

Araus, J. L., Slafer, G. A., Reynolds, M. P., & Royo, C. (2002). Plant breeding and drought in C3 cereals: what should we breed for? *Annals of Botany*, 89, 925-940.

Araus, J. L, Serret, M. D., & Lopes, M. S. (2019). Transgenic solutions to increase yield and stability in wheat: shining hope or flash in the pan? *Journal of Experimental Botany*, 70, 1419-1424.

Arjona, J. M., Royo, C., Dreisigacker, S., Ammar, K., & Villegas, D. (2018). Effect of *Ppd-A1* and *Ppd-B1* allelic variants on grain number and thousand kernel weight of durum wheat and their impact on final grain yield. *Frontiers in Plant Science*, 9, 888.

Ashraf, M., & Foolad, M. R. (2007). Roles of glycine betaine and proline in improving plant abiotic stress resistance. *Environmental and Experimental Botany*, *59*, 206-216.

Australian Bureau of Agricultural and Resource Economics and Sciences (ABARES) (2019). *Australian crop report: June edition.* Retrieved from http://www.agriculture.gov.au/abares/research-topics/agricultural-commodities/australi an-crop-report/overview, 15.07.2019

Australian Bureau of Meteorology (2019a). *Climate Data Online.* Retrieved from http://www.bom.gov.au/climate/data/, 15.07.2019

Australian Bureau of Meteorology (2019b). *Annual climate statement 2018*. Retrieved from http://www.bom.gov.au/climate/current/annual/aus/, 15.07.2019

Bai, G., Ge, Y., Hussain, W., Baenziger, P. S., & Graef, G. (2016). A multi-sensor system for high throughput field phenotyping in soybean and wheat breeding. *Computers and Electronics in Agriculture*, 128, 181-192.

Batool, A., Aisha, N., Cheng, Z., Lv, G., Ashraf, M., Afzal, M., Xiong, J., Wang, J., & Xiong, Y. (2019). Physiological and biochemical responses of two spring wheat genotypes to non-hydraulic root-to-shoot signalling of partial and full root-zone drought stress. *Plant Physiology and Biochemistry*, 139, 11-20.

Ben-Ari, G., & Lavi, U. (2012). Marker assisted selection in plants. In: *Plant biotechnology and agriculture prospects for 21st century* (Altman, A., Hasegawa, P. M., eds), pp. 163-184. San Diego: Academic Press.

Bennett, D., Reynolds, M., Mullan, D., Izanloo, A., Kuchel, H., Langridge, P., & Schnurbusch, T. (2012). Detection of two major grain yield QTL in bread wheat (*Triticum aestivum* L.) under heat, drought and high yield potential environments. *Theoretical and Applied Genetics,* 125, 473-1485.

Blum, A. (1985). Photosynthesis and transpiration in leaves and ears of wheat and barley varieties. *Journal of Experimental Botany,* 36, 432-440.

Blum, A. (1998). Improving wheat grain filling under stress by stem reserve mobilisation. *Euphytica,* 100, 77-83.

Blum, A. (2005). Drought resistance, water-use efficiency, and yield potential are they compatible, dissonant, or mutually exclusive? *Australian Journal of Agricultural Research*, 56, 1159-1168.

Blum, A. (2009). Effective use of water (EUW) and not water-use efficiency (WUE) is the target of crop yield improvement under drought stress. *Field Crops Research,* 112, 119-123.

Borghi, B., Corbellini, M., Gavuzzi, P., Boggini, G., & Ouassou, A. (1990). Breeding for heat and drought tolerance in bread wheat by means of field and laboratory screening procedures. *Bulletin de la Société Botanique de France*, 137, 37-46.

Brenchley, R., Spannagl, M., Pfeifer, M., Barker, G. L. A., D'Amore, R., Allen, A. M., McKenzie, N., Kramer, M., Kerhornou, A., Bolser, D., Kay, S., Waite, D., Trick, M., Bancroft, I., Gu, Y., Huo, N., Luo, M.-C., Sehgal, S., Gill, B., Kianian, S., Anderson, O., Kersey, P., Dvorak, J., McCombie, W. R., Hall, A., Mayer, K. F. X., Edwards, K. J. M., Bevan, W., & Hall, N. (2012). Analysis of the bread wheat genome using whole-genome shotgun sequencing. *Nature,* 491, 705-710.

Calhoun, D. S., Gebeyehu, G., Miranda, A., Rajaram, S., & van Ginkel, M. (1994). Choosing Evaluation Environments to Increase Wheat Grain Yield under Drought Conditions. *Crop Science,* 34, 673-678.

Chen, S., Guo, Y., Sirault, X., Stefanova, K., Saradadevi, R., Turner, N. C., Nelson, M. N., Furbank, R. T., Siddique, K. H. M., & Cowling, W. A. (2019). Nondestructive phenomic tools for the prediction of heat and drought tolerance at anthesis in Brassica species. *Plant Phenomics*, doi: 10.34133/2019/3264872.

Collard, B. C. Y., Jahufer, M. Z. Z., Brouwer, J. B., & Pang, E. C. R. (2005). An introduction to markers, quantitative trait loci (QTL) mapping, and marker-assisted selection for crop improvement: The basic concepts. *Euphytica*, 142, 169-196.

Czyczylo-Mysza, I., Marcinska, I., Skrzypek, E., Chrupek, M., Grzesiak, S., Hura, T., Stojałowski, S., Myskow, B., Milczarski, P., & Quarrie, S. (2011). Mapping QTLs for yield components and chlorophyll a fluorescence parameters in wheat under three levels of water availability. *Plant Genetic Resources*, 9, 291-295.

Dashti, H., Yazdi-Samadi, B., Ghannadha, M., Naghavi, M. R., & Quarri, S. (2007). QTL analysis for drought resistance in wheat using doubled haploid lines. *International Journal of Agriculture and Biology*, 9, 98-101.

Diab, A. A., Kantety, R. V., Ozturk, N. Z., Benscher, D., Nachit, M. M., & Sorrells, M. E. (2008). Drought - inducible genes and differentially expressed sequence tags associated with components of drought tolerance in durum wheat. *Scientific Research and Essay*, 3, 9-26.

Dias, A. S., & Lidon, F. C. (2009). Evaluation of grain filling rate and duration in bread and durum wheat, under heat stress after anthesis. *Journal of Agronomy and Crop Science*, 195, 137-147.

Dodig, D., Savic, J., Kandic, V., Zoric, M., Radovic, B. V., Popovic, A., & Quarrie, S. (2016). Responses of wheat plants under post-anthesis stress induced by defoliation: I. Contribution of agro-physiological traits to grain yield. *Experimental Agriculture*, 52, 203-223.

Dreccer, M. F., Van Herwaarden, A. F., & Chapman, S. C. (2009). Grain number and grain weight in wheat lines contrasting for stem water soluble carbohydrate concentration. *Field Crops Research*, 112, 43-54.

Duan, L., Yang, W., Huang, C., & Liu, Q. (2011). A novel machine-vision-based facility for the automatic evaluation of yield-related traits in rice. *Plant Methods,* 7, 44-57.

Dubcovsky, J., Loukoianov, A., & Bonafede, M. D. (2007). Regulation of flowering time in wheat. *Developments in Plant Breeding,* 12, 659-665.

Dunn, J., Hunt, L., Afsharinafar, M., Al Meselmani, M., Mitchell, A., Howells, R., Wallington, E., Fleming, A. J., & Gray, J. E. (2019). Reduced stomatal density in bread wheat leads to increased water-use efficiency. *Journal of Experimental Botany*, doi: 10.1093/jxb/erz248.

Eagles, H. A., Cane, K., & Vallance, N. (2009). The flow of alleles of important photoperiod and vernalisation genes through Australian wheat. *Crop & Pasture Science*, 60, 646-657.

Edae, E. A, Byrne, P. F., Haley, S. D., Lopes, M. S., & Reynolds, M. P. (2014). Genome-wide association mapping of yield and yield components of spring wheat under contrasting moisture regimes. *Theoretical and Applied Genetics,* 127, 791-807.

Edwards, J. (2012). *A Genetic Analysis of Drought Related Traits in Hexaploid Wheat.* Adelaide: PhD Thesis. The University of Adelaide.

Fabian, A., Safran, E., Szabo-Eitel, G., Barnabas, B., & Jager, K. (2019). Stigma functionality and fertility are reduced by heat and drought co-stress in wheat. *Frontiers in Plant Science*, 10, 244.

Farooq, M., Hussain, M., & Siddique, K. H. M. (2014). Drought stress in wheat during flowering and grain-filling periods. *Critical Reviews in Plant Sciences*, 33, 331-349.

Farooq, R., Hussain, K., Nazir, S., Javed, M. R., & Masood, N. (2018). Crispr/cas9; a robust technology for producing genetically engineered plants. *Cellular and Molecular Biology*, 64, 31-38.

Feuillet, C., Langridge, P., & Waugh, R. (2008). Cereal breeding takes a walk on the wild side. *Trends in genetics,* 24, 24-32.

Fischer, R. A., Rees, D., Sayre, K. D., Lu, Z. M., & Condon, A. G. (1998). Wheat yield progress associated with higher stomatal conductance and photosynthetic rate, and cooler canopies. *Crop Science*, 38, 1467-1475.

Food and Agriculture Organization of the United Nations (FAO) (2019a). *World Food Situation.* Retrieved from http://www.fao.org/worldfoodsituation/csdb/en/, 15/07/2019

Food and Agriculture Organization of the United Nations (FAO) (2019b). *FAOSTAT - Temperature change.* Retrieved from http://www.fao.org/faostat/en/#data/ET, 15/07/2019

Foulkes, M. J., & Sylvester-Bradley, R. (2002). The ability of wheat cultivars to withstand drought in UK conditions: Formation of grain yield. *The Journal of Agricultural Science,* 138, 153-169.

Foulkes, M. J., Sylvester-Bradley, R., Weightman, R., & Snape, J. W. (2007). Identifying physiological traits associated with improved drought resistance in winter wheat. *Field Crops Research,* 103, 11-24.

Fu, Y. B., & Somers, D. J. (2009). Genome-wide reduction of genetic diversity in wheat breeding. *Crop Science*, 49, 161-168.

Furbank, R. T., & Tester, M. (2011). Phenomics – technologies to relive the phenotyping bottleneck. *Trends in Plant Science,* 16, 1360-1385.

Garcia, M., Eckermann, P., Haefele, S., Satija, S., Sznajder, B., Timmins, A., Baumann, U. Petra Wolters, P., Mather, D. E., & Fleury, D. (2019). Genome-wide association mapping of grain yield in a diverse collection of spring wheat (*Triticum aestivum* L.) evaluated in southern Australia. *PLoS ONE*, 14, 2.

Gbegbelegbe, S., Cammarano, D., Asseng, S., Robertson, R., Chung, U., Adam, M., Abdalla, O., Payne, T., Reynolds, M., Sonder, K., Shiferaw, B., & Nelson, G. (2016). Baseline simulation for global wheat production with CIMMYT mega-environment specific cultivars. *Field Crops Research*, 202, 122-135.

Ge, Y., Bai, G., Stoerger, V., & Schnable, J. C. (2016). Temporal dynamics of maize plant growth, water use, and leaf water content using automated high throughput RGB and hyperspectral imaging. *Computers and Electronics in Agriculture*, 127, 625-632.

Golabadi, M., Arzani, A., Mirmohammadi Maibody, S. A., Sayed Tabatabaei, B. E., & Mohammadi, S. A. (2011). Identification of microsatellite markers linked with yield components under drought stress at terminal growth stages in durum wheat. *Euphytica*, 177, 207-221.

Grains Research & Development Corporation (GRDC) (2011). *Time of sowing - Impact on yield and quality of wheat.* Retrieved from https://grdc.com.au/__data/assets/pdf_file/0019/100738/grdcfstimeofsowingsouthpdf.pdf.pdf, 13.06.2019

Gratani, L., Pesoli, P., & Crescente, M. (1998). Relationship between photosynthetic activity and chlorophyll content in an isolated Quercus ilex L. tree during the year. *Photosynthetica,* 35, 445-451.

Gregory, P. J., Hutchison, D. J., Read, D. B., Jenneson, P. M., Gilboy, W. B., & Morton, E. (2003). Non-invasive imaging of roots with high resolution X-ray micro-tomography. *Plant and Soil,* 255, 351-359.

Grigorova, B., Vaseva, I., Demirevska, K., & Feller, U. (2011). Combined drought and heat stress in wheat: changes in some heat shock proteins. *Biologia Plantarum*, 55, 105-111.

Gupta, P. K., Langridge, P., & Mir, R. R. (2010). Marker-assisted wheat breeding: present status and future possibilities. *Molecular Breeding*, 26,145-161.

Gupta, A. K., Kaur, K., & Kaur, N. (2011). Stem Reserve Mobilization and Sink Activity in Wheat under Drought Conditions. *American Journal of Plant Sciences*, 2, 70-77.

Gupta, P. K., Balyan, H. S., Gahlaut, V., & Kulwal, P. L. (2012). Phenotyping, genetic dissection, and breeding for drought and heat tolerance in common wheat: status and prospects. In*: Plant breeding reviews* (Janick, J., ed), pp. 85-168. New Jersey: Wiley-Blackwell.

Gupta, N.K., Agarwal, S., Agarwal, V.P., Nathawat, N. S., Gupta, S., & Singh, G. (2013). Effect of short-term heat stress on growth, physiology and antioxidative defence system in wheat seedlings. *Acta Physiologiae Plantarum*, 35, 1837-1842.

Gupta, P. K., Balyan, H. S., & Gahlau, V. (2017). QTL analysis for drought tolerance in wheat: present status and future possibilities. *Agronomy*, 7, 5.

Hafsi, M., Mechmeche, W., Bouamama, L., Djekoune, A., Zaharieva, M., & Monneveux, P. (2000). Flag leaf senescence, as evaluated by numerical image analysis, and its relationship with yield under drought in durum wheat. *Journal of Agronomy and Crop Science,* 185, 275-280.

Haghighattalab, A., González Pérez, L., Mondal, S., Singh, D., Schinstock, D., Rutkoski, J., Ortiz-Monasterio, I., Singh, R. P., Goodin, D., & Poland, J. (2016). Application of unmanned aerial systems for high throughput phenotyping of large wheat breeding nurseries. *Plant Methods,* 12, 35.

Hamblin, M. T., Buckler, E. S., & Jannink, J. L. (2011). Population genetics of genomics-based crop improvement methods. *Trends in Genetics*, 27, 98-106.

Hao, D., Chao, M., Yin, Z., & Yu, D. (2012). Genome-wide association analysis detecting significant single nucleotide polymorphisms for chlorophyll and chlorophyll fluorescence parameters in soybean (*Glycine max*) landraces. *Euphytica, 186*, 919-931.

Hays, D. B., Do, J. H., Mason, R. E., Morgan, G., & Finlayson, S. A. (2007). Heat stress induced ethylene production in developing wheat grains induces kernel abortion and increased maturation in a susceptible cultivar. *Plant Science*, 172, 1113-1123.

Heffner, E. L., Sorrells, M. E., & Jannink, J.-L. (2009). Genomic selection fro crop improvement. *Crop Science*, 49, 1-12.

Hill, C. B., Taylor, J. D., Edwards, J., Mather, D., Langridge, P., Bacic, A., & Roessner, U. (2015). Detection of QTL for metabolic and agronomic traits in wheat with adjustments for variation at genetic loci that affect plant phenology. *Plant Science*, 233, 143-154.

Holman, F. H., Riche, A.B., Michalski, A., Castle, M., Wooster, M. J., & Hawkesford, M. J. (2016). High throughput field phenotyping of wheat plant height and growth rate in field plot trials using UAV based remote sensing. *Remote Sensing*, 8, 1031.

Hughes, N., Askew, K., Scotson, C. P., Williams, K., Sauze, C., Corke, F., Doonan, J. H., & Nibau, C. (2017). Non-destructive, high-content analysis of wheat grain traits using X-ray micro computed tomography. *Plant Methods*, 13, 76.

Hughes, N., Oliveira, H. R., Fradgley, N., Corke, F. M. K., Cockram, J., Doonan, J. H., & Nibau, C. (2019). CT trait analysis reveals morphometric differences between domesticated temperate small grain cereals and their wild relatives. *The Plant Journal* 99, 98-111.

International Wheat Genome Sequencing Consortium (IWGSC) (2018). Shifting the limits in wheat research and breeding using a fully annotated reference genome. *Scienc*e, 361, 7191.

Izanloo, A., Condon, A. G., Langridge, P., Tester, M., & Schnurbusch, T. (2008). Different mechanisms of adaptation to cyclic water stress in two South Australian bread wheat cultivars. *Journal of Experimental Botany,* 59, 3327-3346.

Jimenez-Berni, J. A., Deery, D. M., Rozas-Larraondo, P., Condon, A. G., Rebetzke, G. J., James, R. A., Bovill, M. D., Furbank, R. T., & Sirault, X. R. R. (2018). High throughput determination of plant height, ground cover, and above-ground biomass in wheat with LiDAR. *Frontiers in Plant Science,* 9, 237.

Jones, M. M., & Turner, N. C. (1978). Osmotic adjustment in leaves of sorghum in response to water deficits. *Plant Physiology,* 61, 122-126.

Kadam, S., Singh, K., Shukla, S., Goel, S., Vikram, P., Pawar, V., Gaikwad, K., Khanna-Chopra, R., & Singh, N. (2012). Genomic associations for drought tolerance on the short arm of wheat chromosome 4B. *Functional & Integrative Genomics*, 12, 447-464.

Kahiluoto, H., Kaseva, J., Balek, J., Olesen, J. E., Ruiz-Ramos, M., Gobin, A., Kersebaum, K. C., Takáč, J., Ruget, F., Ferrise, R., Bezak, P., Capellades, G., Dibari, C., Mäkinen, H., Nendel, C., Ventrella, D., Rodríguez, A., Bindi, M., & Trnka, M. (2019). Decline in climate resilience of European wheat. *Proceedings of the National Academy of Sciences of the United States of America*, 116, 123-128.

Kearsey, M. J. (1998). The principles of QTL analysis (a minimal mathematics approach). *Journal of Experimental Botany*, 49, 1619-1623.

Khalid, M., Afzal, F., Gul, A., Amir, R., Subhani, A., Ahmed, Z., Mahmood, Z., Xia, X., Rasheed, A., & He, Z. (2019). Molecular Characterization of 87 functional genes in wheat diversity panel and their association with phenotypes under well-watered and water-limited conditions. *Frontiers in Plant Science*, 10, 717.

Khan, A. J., Hassan, S., Tariq, M., & Khan, T. (2001). Haploidy breeding and mutagenesis for drought tolerance in wheat. *Euphytica*, 120, 409-414.

Kim, D., Alptekin, B., & Budak, H. (2018). CRISPR/Cas9 genome editing in wheat. *Functional & Integrative Genomics,* 18, 31-41.

Kirigwi, F. M., van Ginkel, M., Brown-Guedira, B., Gill, B. S., Paulsen, G. M., & Fritz, A. K. (2007). Markers associated with a QTL for grain yield in wheat under drought. *Molecular Breeding*, 20, 401-413.

Kirkegaard, J. A., Lilley, J. M., Howe, G. N., & Graham, J. M. (2007). Impact of subsoil water use on wheat yield. *Australian Journal of Agricultural Research*, 58, 303-315.

Laurie, D. A. (1997). Comparative genetics of flowering time. *Plant Molecular Biology*, 35, 167-177.

Lehnert, H., Serfling, A., Friedt, W., & Ordon, F. (2018). Genome-wide association studies reveal genomic regions associated with the response of wheat (*Triticum aestivum* L.) to mycorrhizae under drought stress conditions. *Frontiers in Plant Science*, 9, 1728.

Levitt, J. (1980a). *Responses of plants to environmental stresses. Volume I. Chilling, freezing, and high temperature stresses.* Second edition. Sydney: Academic Press.

Levitt, J (1980b). *Responses of plants to environmental stresses. Volume II. Water, radiation, salt, and other stresses.* Second edition. Sydney: Academic Press.

Li, X., Ingvordsen, C. H., Weiss, M., Rebetzke, G. J., Condon, A. G., James, R. A., & Richards, R. A. (2019a). Deeper roots associated with cooler canopies, higher NDVI and greater yield in three wheat populations grown on stored soil water. *Journal of Experimental Botany*, doi: 10.1093/jxb/erz232.

Li, L., Mao, X., Wang, J., Chang, X., Reynolds, M., & Jing, R. (2019b). Genetic dissection of drought and heat-responsive agronomic traits in wheat. *Plant Cell & Environment*, doi: 10.1111/pce.13577.

Liu, C., Sivakumar, S., Etienne, C., Carolina, S., Susanne, D., & Matthew, R. (2019). Genetic dissection of heat and drought stress QTLs in phenology-controlled synthetic-derived recombinant inbred lines in spring wheat. *Molecular Breeding*, 39, 34.

Lopes, M. S., Reynolds, M. P., Manes, Y., Singh, R. P., Crossa, J., & Braun, H. J. (2012). Genetic yield gains and changes in associated traits of CIMMYT spring bread wheat in a "historic" set representing 30 years of breeding. *Crop Science,* 52, 1123-1131.

Loukoianov, A., Yan, L., Blechl, A., Sanchez, A., & Dubcovsky, J. (2005). Regulation of *VRN-1* vernalization genes in normal and transgenic polyploid wheat. *Plant Physiology,* 138, 2364-2373.

Ludlow, M. M., & Muchow, R. C. (1990). A critical evaluation of traits for improving crop yields in water-limited environments. *Advances in agronomy,* 43, 107-153.

Maccaferri, M., Sanguineti, M. C., Corneti, S., Araus Ortega, J. L., Salem, M. B., Bort, J., DeAmbrogio, E., Garcia del Moral, L. F., Demontis, A., El-Ahmed, A., Maalouf, F., Machlab, H., Martos, V., Moragues, M., Motawaj, J., Nachit, M.,Nserallah, N., Ouabbou, H., Royo, C., Slama, A., & Tuberosa, R. (2008). Quantitative trait loci for grain yield and adaptation of durum wheat (*Triticum durum* Desf.) across a wide range of water availability. *Genetics,* 178, 489-511.

Machado, S., & Paulsen, G. M. (2001). Combined effects of drought and high temperature on water relations of wheat and sorghum. *Plant and Soil,* 233, 179-187.

Mallapaty, S. (2019). Australian gene-editing rules adopt 'middle ground'. *Nature*, doi: 10.1038/d41586-019-01282-8.

Manschadi, A. M., Hammer, G. L., Christopher, J. T., & deVoil, P. (2008). Genotypic variation in seedling root architectural traits and implications for drought adaptation in wheat (*Triticum aestivum* L.). *Plant Soil*, 303, 115-129.

Mason, R. E., Mondal, S., Beecher, F. W., Pacheco, A., Jampala, B., Ibrahim, A. M., & Hays, D. B. (2010). QTL associated with heat susceptibility index in wheat (*Triticum aestivum* L.) under short-term reproductive stage heat stress. *Euphytica,* 174, 423-436.

Mason, R. E., Addison, C. K., Babar, A., Acuna, A., Lozada, D., Subramanian, N., Arguello, M. N., Miller, R. G., Brown-Guedira, G., Guedira, M., & Johnson, J. (2018). Diagnostic markers for vernalization and photoperiod loci improve genomic selection for grain yield and spectral reflectance in wheat. *Crop Science*, 58, 242-252.

Maulana, F., Ayalew, H., Anderson, J. D., Kumssa, T. T., Huang, W., & Ma, X. (2018). Genome-wide association mapping of seedling heat tolerance in winter wheat. *Frontiers in Plant Science*, 9, 1272.

Merchuk-Ovnat, L., Fahima, T., Krugman, T., & Saranga, Y. (2016). Ancestral QTL alleles from wild emmer wheat improve grain yield, biomass and photosynthesis across environments in modern wheat. *Plant Science*, 251, 23-34.

Meuwissen, T. H., Hayes, B. J., & Goddard, M. E. (2001). Prediction of total genetic value using genome-wide dense marker maps. *Genetics*, 157, 1819-1829.

Millet, E. J., Welcker, C., Kruijer, W., Negro, S., Coupel-Ledru, A., Nicolas, S. D., Laborde, J., Bauland, C., Praud, S., Ranc, N., Presterl, T., Tuberosa, R., Bedo, Z., Draye, X., Usadel, B., Charcosset, A., Eeuwijk, F. V., & Tardieu, F. (2016). Genome-wide analysis of yield in Europe: allelic effects vary with drought and heat scenarios. *Plant Physiology*, 172, 749-764.

Mondal, B., Singh, A., Yadav, A., Tomar, R. S. S., Vinod, G. P. S., & Prabhu, K. V. (2017). QTL mapping for early ground cover in wheat (*Triticum aestivum* L.) under drought stress. *Current Science*,112, 1266-1271.

Morgan, J. M. (1983). Osmoregulation as a selection criterion for drought tolerance in wheat. *Australian Journal of Agricultural Research,* 34, 607-614.

Mullarkey, M., & Jones, P. (2000). Isolation and analysis of thermotolerant mutants of wheat. *Journal of Experimental Botany*, 51, 139-146.

Muqaddasi, Q. H., Reif, J. C., Li, Z., Basnet, B. R., Dreisigacker, S., & Röder, M. S. (2017). Genome-wide association mapping and genome-wide prediction of anther extrusion in CIMMYT spring wheat. *Euphytica*, 213, 73.

Muraya, M. M., Chu, J., Zhao, Y., Junker, A., Klukas, C., Reif, J. C., & Altmann, T. (2017). Genetic variation of growth dynamics in maize (*Zea mays* L.) revealed through automated non-invasive phenotyping. *The Plant Journal,* 89, 366-380.

Mwadzingeni, L., Figlan, S., Shimelis, H., Mondal, S., & Tsilo, T. J. (2017). Genetic resources and breeding methodologies for improving drought tolerance in wheat. *Journal of Crop Improvement*, 31, 648-672.

Norman, A., Taylor, J., Edwards, J., & Kuchel, H. (2018). Optimising genomic selection in wheat: effect of marker density, population size and population structure on prediction accuracy. *Genes Genomes Genetics*, 8, 2889-2899.

Ogbonnaya, F. C., Rasheed, A., Okechukwu, E. C., Jighly, A., Makdis, F., Wuletaw, T., Hagras, A., Uguru, M. I., & Agbo, C. U. (2017). Genome-wide association study for agronomic and physiological traits in spring wheat evaluated in a range of heat prone environments. *Theoretical and Applied Genetics,* 130, 1819-1835.

Ovenden, B., Milgate, A., Wade, L. J., Rebetzke, G. J., & Holland, J. B. (2017). Genome-wide associations for water-soluble carbohydrate concentration and relative maturity in wheat using SNP and DArT marker arrays. *Genes Genomes Genetics,* 7, 2821-2830.

Paliwal, R., Roder, M. S., Kumar, U., Srivastava, J. P., & Joshi, A. K. (2012). QTL mapping of terminal heat tolerance in hexaploid wheat (*T. aestivum* L.). *Theoretical and Applied Genetics,* 125, 561-575.

Palta, J. A., Kobata, T., Turner, N. C., & Fillery, I. R. (1994). Remobilization of carbon and nitrogen in wheat as influenced by postanthesis water deficits. *Crop Science,* 34, 118-124.

Pantalião, G. F., Narciso, M., Guimarães, C., Castro, A., Colombari, J. M., Breseghello, F., Rodrigues, L., Vianello, R. P., Borba, T. O., & Brondani, C. (2016). Genome wide association study (GWAS) for grain yield in rice cultivated under water deficit. *Genetica,* 144, 651-664.

Parent, B., Shahinnia, F., Maphosa, L., Berger, B., Rabie, H., Chalmers, K., Kovalchuk, A., Langridge, P., & Fleury, D. (2015). Combining field performance with controlled environment plant imaging to identify the genetic control of growth and transpiration underlying yield response to water-deficit stress in wheat. *Journal of Experimental Botany*, 66, 5481-5492.

Passioura, J. B. (1996). Drought and drought tolerance. *Plant Growth Regulation*, 20, 79-83.

Paux, E., Faure, S., Choulet, F., Roger, D., Gauthier, V., Martinant, J. P., Sourdille, P., Balfourier, F., Le Paslier, M. C., & Chauveau, A. (2010). Insertion site-based polymorphism markers open new perspectives for genome saturation and marker-assisted selection in wheat. *Plant Biotechnology Journal*, 8, 196-210.

Peleg, Z. V., Fahima, T., Krugman, Abbo, S., Yakir, D., Korol, A. B., & Saranga, Y. (2009). Genomic dissection of drought resistance in durum wheat x wild emmer wheat recombinant inbreed line population. *Plant, Cell and Environment,* 32, 758-779.

Perdomo, J. A., Conesa, M. A., Medrano, H., Ribas-Carbó, M., & Galmes, J. (2015). Effects of long-term individual and combined water and temperature stress on the growth of rice, wheat and maize: relationship with morphological and physiological acclimation. *Physiologia Plantarum,* 155, 149-165.

Pinto, R. S., Reynolds, M. P., Mathews, K. L., McIntyre, C. L., Olivares-Villegas, J. J., & Chapman, S. C. (2010). Heat and drought adaptive QTL in a wheat population designed to minimize confounding agronomic effects. *Theoretical and Applied Genetics,* 121, 1001-1021.

Pinto, R. S., & Reynolds, M. P. (2015). Common genetic basis for canopy temperature depression under heat and drought stress associated with optimized root distribution in bread wheat. *Theoretical and Applied Genetics*, 128, 575-585.

Porter, J. R., & Gawith, M. (1999). Temperatures and the growth and development of wheat: a review. *European Journal of Agronomy,* 10, 23-36.

Pradhan, G. P., Prasad, P. V., Fritz, A. K., Kirkham, M. B., & Gill, B. S. (2012). Effects of drought and high temperature stress on synthetic hexaploid wheat. *Functional Plant Biology,* 39, 190-198.

Prasad, P. V., Pisipati, S. R., Momcilovic, I., & Ristic, Z. (2011). Independent and combined effects of high temperature and drought stress during grain filling on plant yield and chloroplast EF-Tu expression in spring wheat. *Journal of Agronomy and Crop Science,* 197, 430-441.

Price, A. H., & Hendry, G. A. (1991). Iron-catalysed oxygen radical formation and its possible contribution to drought damage in nine native grasses and three cereals. *Plant, Cell and Environment,* 14, 477-484.

Qaseem, M. F., Qureshi, R., Muqaddasi, Q. H., Shaheen, H., Kousar, R., & Roder, M. S. (2018). Genome-wide association mapping in bread wheat subjected to independent and combined high temperature and drought stress. *PLoS ONE*, 13, 6.

Qaseem, M. F., Qureshi, R., Shaheen, H., & Shafqat, N. (2019a). Genome-wide association analyses for yield and yield-related traits in bread wheat (*Triticum aestivum* L.) under pre-anthesis combined heat and drought stress in field conditions. *PLoS ONE*, 14, 3.

Qaseem, M. F., Qureshi, R., & Shaheen, H. (2019b). Effects of pre-anthesis drought, heat and their combination on the growth, yield and physiology of diverse wheat (*Triticum aestivum* L.) genotypes varying in sensitivity to heat and drought stress. *Scientific reports*, 9, 6955.

Quarrie, S. A., & Jones, H. G. (1979). Genotypic variation in leaf water potential, stomatal conductance and abscisic acid concentration in spring wheat subjected to artificial drought stress. *Annals of Botany*, 44, 323-32.

Quarrie, S. A., Steed, A., Calestani, C., Semikhodskii, A., Lebreton, C., Chinoy, C., Steele, N., Pljevljakusic, D., Waterman, E., Weyen, J., Schondelmaier, J., Habash, D. Z., Farmer, P., Saker, L., Clarkson, D. T., Abugalieva, A., Yessimbekova, M., Turuspekov, Y., Abugalieva, S., Tuberosa, R., Sanguineti, M. C., Hollington, P. A., Aragues, R., Royo, A., & Dodig, D. (2005). A high-density genetic map of hexaploid wheat (*Triticum aestivum* L.) from the cross Chinese Spring x SQ1 and its use to compare QTLs for grain yield across a range of environments. *Theoretical and Applied Genetics*, 110, 865-880.

Rajala, A., Hakala, K., Mäkelä, P., Muurinen, S., & Peltonen-Sainio, P. (2009). Spring wheat response to timing of water deficit through sink and grain filling capacity. *Field Crops Research*, 114, 263-271.

Rana, M., Sood, A., Hussain, W., Kaldate, R., Sharma, T. R., Gill, R., Kumar, S., & Singh, S. (2019). Gene pyramiding and multiple character breeding. In: *Lentils - Potential Resources for Enhancing Genetic Gains* (Singh, M., ed), pp. 83-124. London: Academic Press.

Redondo-Gomez, S. (2013). Abiotic and biotic stress tolerance in plants. In: *Molecular stress physiology of plants* (Rout, G. R., Das, A. B., eds), pp. 1-20. New Delhi: Springer India.

Reif, J. C., Zhang, P., Dreisigacker, S., Warburton, M. L., van Ginkel, M., Hoisington, D., Bohn, M., & Melchinger, A. E. (2005). Wheat genetic diversity trends during domestication and breeding. *Theoretical and Applied Genetics*, 110, 859-864.

Reynolds, M. P., Delgado B, M. I., Gutierrez-Rodriguez, M., & Larque-Saavedra, A. (2000). Photosynthesis of wheat in a warm, irrigated environment I: Genetic diversity and crop productivity. *Field Crops Research,* 66, 37-50.

Reynolds, M. P., Trethowan, R.M., van Ginkel, M., & Rajaram, S. (2001). Application of Physiology in Wheat Breeding. In: *Application of physiology in wheat breeding* (Reynolds, M. P., Ortiz-Monasterio, J. I., McNab, A., eds), pp. 2-10. Obregon: CIMMYT.

Reynolds, M. P., Pierre, C. S., Saad, A. S. I., Vargas, M., & Condon, A. G. (2007). Evaluating potential genetic gains in wheat associated with stress-adaptive trait expression in elite genetic resources under drought and heat stress. *Crop Science*, 47, 172-189.

Richards, R. A., Rawson, H. M., & Johnson, D. A. (1986). Glaucousness in wheat: its development and effect on water-use efficiency, gas exchange and photosynthetic tissue temperatures. *Australian Journal of Plant Physiology,* 13, 465-473.

Richards, R. A. (2000). Selectable traits to increase crop photosynthesis and yield of grain crops. *Journal of Experimental Botany,* 51, 447-458.

Richards, R.A., Condon, A.G., & Rebetzke, G. J. (2001). Traits to improve yield in dry environments. In: *Application of physiology in wheat breeding* (Reynolds, M. P., Ortiz-Monasterio, J. I., McNab, A., eds), pp. 88-100. Mexico: CIMMYT.

Rollins, J. A., Drosse, B., Mulki, M. A., Grando, S., Baum, M., Singh, M., Ceccarelli, S., & von Korff, M. (2013). Variation at the vernalisation genes *Vrn-H1* and *Vrn-H2* determines growth and yield stability in barley (*Hordeum vulgare*) grown under dryland conditions in Syria. *Theoretical and Applied Genetics,* 126, 2803-2824.

Rosenzweig, C., & Parry, M. L. (1994). Potential impact of climate change on world food supply. *Nature,* 367, 133-138.

Roussel, V., Koenig, J., Beckert, M. & Balfourier, F. (2004). Molecular diversity in French bread wheat accessions related to temporal trends and breeding programmes. *Theoretical and Applied Genetics,* 108, 920-930.

Sanchez-Bragado, R., Molero, G., Reynolds, M. P., & Araus, J. L. (2014). Relative contribution of shoot and ear photosynthesis to grain filling in wheat under good agronomical conditions assessed by differential organ δ13C. *Journal of Experimental Botany,* 65, 5401-5413.

Shahinnia, F., Le Roy, J., Laborde, B., Sznajder, B., Kalambettu, P., Mahjourimajd, S., Tilbrook, J., & Fleury, D. (2016). Genetic association of stomatal traits and yield in wheat grown in low rainfall environments. *BMC Plant Biology*, 16, 1-14.

Shakoor, N., Lee, S., & Mockler, T. C. (2017). High throughput phenotyping to accelerate crop breeding and monitoring of diseases in the field. *Current Opininion in Plant Biology*, 38, 184-192.

Sharma, D. K., Andersen, S. B., Ottosen, C.-O., & Rosenqvist, E. (2015). Wheat cultivars selected for high Fv/Fm under heat stress maintain high photosynthesis, total chlorophyll, stomatal conductance, transpiration and dry matter. *Physiologia Plantarum*, 153, 284-29.

Shiferaw, B., Smale, M., Braun, H.-J., Duveiller, E., Reynolds, M., & Muricho, G. (2013). Crops that feed the world 10. Past successes and future challenges to the role played by wheat in global food security. *Food Security*, 5, 291-317.

Shirdelmoghanloo, H., Taylor, J. D., Lohraseb, I., Rabie, H., Brien, C., Timmins, A., Martin, P., Mather, D. E., Emebiri, L., & Collins, N. C. (2016). A QTL on the short arm of wheat (*Triticum aestivum* L.) chromosome 3B affects the stability of grain weight in plants exposed to a brief heat shock early in grain filling. *BMC Plant Biology*, 16, 100.

Sirault, X. R. (2007). *Leaf rolling in wheat.* Canberra: PhD Thesis. The Australian National University.

Snape, J. W., Butterworth, K., Whitechurch, E., & Worland, A. J. (2001). Waiting for fine times: genetics of flowering time in wheat. *Euphytica,* 119, 185-190.

Snowdon, R. J., Stahl, A., Wittkop, B., Friedt, W., Voss-Fels, K., Ordon, F., Frisch, M., Dreisigacker, S., Hearne, S. J., Bett, K. E., Cuthbert, R. D., Bentley, A. R., Melchinger, A. E., Tuberosa, R., Langridge, P., Uauy, C., Sorrells, M. E., Poland, J., & Pozniak, C. J. (2019). Reduced response diversity does not negatively impact wheat climate resilience. *Proceedings of the National Academy of Sciences of the United States of America*, 116, 10623-10624.

Spielmeyer, W., Hyles, J., Joaquim, P., Azanza, F., Bonnett, D., Ellis, M. E., Moore, C., & Richards, R. A. (2007). A QTL on chromosome 6A in bread wheat (*Triticum aestivum*) is associated with longer coleoptiles, greater seedling vigour and final plant height. *Theoretical and Applied Genetics*, 115, 59-66.

Sukumaran, S., Dreisigacker, S., Lopes, M., Chavez, P., & Reynolds, M. P. (2015). Genome-wide association study for grain yield and related traits in an elite spring wheat population grown in temperate irrigated environments. *Theoretical and Applied Genetics,* 128, 353-363.

Sukumaran, S., Reynolds, M. P., & Sansaloni, C. (2018). Genome-wide association analyses identify QTL hotspots for yield and component traits in durum wheat grown under yield potential, drought, and heat stress environments. *Frontiers in Plant Science,* 9, 81.

Sytar, O., Zivcak, M., Olsovska, K., & Brestic, M. (2018). Perspectives in high-throughput phenotyping of qualitative traits at the whole-plant level. In: *Eco-friendly agro-biological techniques for enhancing crop productivity* (Sengar, R. S., Singh, A., eds), pp. 213-243. Singapore: Springer.

Tahmasebi, S., Heidari, B., Pakniyat, H., & McIntyre, C. L. (2017). Mapping QTLs associated with agronomic and physiological traits under terminal drought and heat stress conditions in wheat (*Triticum aestivum* L.). *Genome*, 60, 26-45.

Talukder, K. S., Babar, M. A., Vijayalakshmi, K., Poland, J., Prasad, P. V., Bowden, R., & Fritz, A. (2014). Mapping QTL for the traits associated with heat tolerance in wheat (*Triticum aestivum* L.). *BMC Genetics,* 15, 97.

Tardieu, F., Cabrera-Bosquet, L., Pridmore, T., & Bennett, M. (2017). Plant phenomics, from sensors to knowledge. *Current Biology*, 27, 770-783.

Tavakol, E., Elbadry, N., Tondelli, A., Cattivelli, L., & Rossini, L. (2016). Genetic dissection of heading date and yield under Mediterranean dry climate in barley (*Hordeum vulgare* L.). *Euphytica*, 212, 343-353.

Tester, M., & Langridge, P. (2010). Breeding technologies to increase crop production in a changing world. *Science*, 327, 818-822.

Throne, G. N. (1965). Photosynthesis of ears and flag leaves of wheat and barley. *Annals of Botany*, 29, 317-329.

Tilman, D., Balzer, C., Hill, J., & Befort, B. L. (2011). Global food demand and the sustainable intensification of agriculture. *Proceedings of the National Academy of Sciences of the United States of America,* 108, 20260-20264.

Toreti, A., Cronie, O., & Zampieri, M. (2019). Concurrent climate extremes in the key wheat producing regions of the world. *Scientific reports*, 9, 5493.

Tricker, P. J., ElHabti, A., Schmidt, J., & Fleury, D. (2018). The physiological and genetic basis of combined drought and heat tolerance in wheat. *Journal of Experimental Botany*, 69, 3195-3210.

Trnka, M., Rötter, R. P., Ruiz-Ramos, M., Kersebaum, K. C., Olesen, J. E., Žalud, Z., & Semenov, M. A. (2014). Adverse weather conditions for European wheat production will become more frequent with climate change. *Nature Climate Change*, 4, 637-643.

Turner, N. C. (1986). Adaptation to water deficits: a changing perspective. *Functional Plant Biology,* 13, 175-190.

Valluru, R., Reynolds, M.P., Davies, W.J., & Sukumaran, S. (2017). Phenotypic and genome-wide association analysis of spike ethylene in diverse wheat genotypes under heat stress. *New Phytologist,* 214, 271-283.

van de Wouw, M., van Hintum, T., Kik, C., van Treuren, R., & Visser, B. (2010). Genetic diversity trends in twentieth century crop cultivars: a meta analysis. *Theoretical and Applied Genetics,* 120, 1241-1252.

van Ginkel, M., Calhoun, D. S., Gebeyehu, G., Miranda, A., Tian-you, C., Pargas Lara, R., Trethowan, R. M., Sayre, K., Crossa, J., & Rajaram, S. (1998). Plant traits related to yield of wheat in early, late, or continuous drought conditions. *Euphytica*, 100, 109-121.

van Ooijen, J. W. (1999). LOD significance thresholds for QTL analysis in experimental populations of diploid species. *Heredity*, 83, 613-624.

Verma, V., Foulkes, M. J., Worland, A. J., Sylvester-Bradley, R., Caligari, P. D., & Snape, J. W. (2004). Mapping quantitative trait loci for flag leaf senescence as a yield determinant in winter wheat under optimal and drought-stressed environments. *Euphytica,* 135, 255-263.

Vijayalakshmi, K., Fritz, A. K., Paulsen, G. M., Bai, G., Pandravada, S., & Gill, B. S. (2010). Modeling and mapping QTL for senescence-related traits in winter wheat under high temperature. *Molecular Breeding,* 26, 163-175.

Voss-Fels, K. P., Stahl, A., & Hickey, L. T. (2019). Q&A: modern crop breeding for future food security. *BMC Biology*, 17, 18.

Wahid, A., Gelani, S., Ashraf, M., & Foolad, M. R. (2007). Heat tolerance in plants: An overview. *Environmental and Experimental Botany*, 61, 199-223.

Walter, J., Edwards, J., Cai, J., McDonald, G., Miklavcic, S. J., & Kuchel, H. (2019). High-throughput field imaging and basic image analysis in a wheat breeding programme, *Frontiers in Plant Science*, 10, 449.

Wang, G.-P., Hui, Z., Li, F., Zhao, M.-R., Zhang, J., & Wang, W. (2010). Improvement of heat and drought photosynthetic tolerance in wheat by overaccumulation of glycinebetaine. *Plant Biotechnoly Reports*, 4, 213-222.

Wang, S., Wong, D., Forrest, K., Allen, A., Chao, S., Huang, B. E., Maccaferri, M., Salvi, S., Milner, S. G., Cattivelli, L., Mastrangelo, A. M., Whan, A., Stephen, S., Barker, G., Wieseke, R., Plieske, J., International Wheat Genome Sequencing Consortium, Lillemo, M., Mather, D., Appels, R., Dolferus, R., Brown-Guedira, G., Korol, A., Akhunova, A. R., Feuillet, C., Salse, J., Morgante, M., Pozniak, C., Luo, M.-C., Dvorak, J., Morell, M., Dubcovsky, J., Ganal, M., Tuberosa, R., Lawley, C., Mikoulitch, I., Cavanagh, C., Edwards, K. J., Hayden, M., & Akhunov, E. (2014). Characterization of polyploid wheat genomic diversity using a high-density 90,000 single nucleotide polymorphism array. *Plant Biotechnology Journal,* 12, 787-796.

Wang, X., Vignjevic, M., Liu, F., Jacobsen, S., Jiang, D., & Wollenweber, B. (2015). Drought priming at vegetative growth stages improves tolerance to drought and heat stresses occurring during grain filling in spring wheat. *Plant Growth Regulation*, 75, 677-687.

Wang, S. X., Zhu, Y. L., Zhang, D. X., Shao, H., Liu, P., Hu, J. B., Zhang, H., Zhang, H. P., Chang, C., Lu, J., Xia, X. C., Sun, G. L. & Ma, C. X. (2017). Genome-wide association study for grain yield and related traits in elite wheat varieties and advanced lines using SNP markers. *PLoS ONE,* 12, 11.

Watson-Haigh, N.S., Suchecki, R., Kalashyan, E., Garcia, M., & Baumann, U. (2018). DAWN: A resource for yielding insights into the diversity among wheat genomes. *BMC Genomics*, 19, 941.

Weldearegay, D. F., Yan, F., Jiang, D., & Liu, F. (2012). Independent and combined effects of soil warming and drought stress during anthesis on seed set and grain yield in two spring wheat varieties. *Journal of Agronomy and Crop Science,* 198, 245-253.

Worland, A. J. (1996). The influence of flowering time genes on environmental adaptability in European wheats. *Euphytica,* 89, 49-57.

Xia, J., Zhao, Y., Burks, P., Pauly, M., & Brown, P. J. (2018). A sorghum NAC gene is associated with variation in biomass properties and yield potential. *Plant Direct,* 2, 1-11.

Xu, Y.-F., Li, S.-S., Li, L.-H., Ma, F.-F., Fu, X.-Y., Shi, Z.-L., Xu, H.-X., Ma, P.-T., & An, D.-G. (2017). QTL mapping for yield and photosynthetic related traits under different water regimes in wheat. *Molecular Breeding*, 37, 34.

Yan, L., Loukoianov, A., Blechl, A., Tranquilli, G., Ramakrishna, W., SanMiguel, P., Bennetzen, J. L., Echenique, V., & Dubcovsky, J. (2004). The wheat *Vrn2* gene is a flowering repressor down-regulated by vernalization. *Science,* 303, 1640-1644.

Yang, J., Zhang, J., Liu, K., Wang, Z. & Liu, L. (2006). Abscisic acid and ethylene interact in wheat grains in response to soil drying during grain filling. New Phytologist, 171, 293-303.

Yang, D.-L., Jing, R.-L., Chang, X.-P., & Li, W. (2007). Identification of quantitative trait loci and environmental interactions for accumulation and remobilization of water-soluble carbohydrates in wheat (*Triticum aestivum* L.) stems. *Genetics,* 176, 571-584.

Zhang, Z., Ersoz, E., Lai, C. Q., Todhunter, R. J., Tiwari, H. K., Gore, M. A., Bradbury, P. J., Yu, J., Arnett, D. K., Ordovas, J. M., & Buckler, E. S. (2010). Mixed linear model approach adapted for genome-wide association studies. *Nature Genetics,* 42, 355-360.

Zhang, J., Gizaw, S. A., Bossolini, E., Hegarty, J., Howell, T., Carter, A. H., Akhunov, E., & Dubcovsky, J. (2018). Identification and validation of QTL for grain yield and plant water status under contrasting water treatments in fall-sown spring wheats. *Theoretical and Applied Genetics*, 131, 1741-1759.

Zhao, Y., Mette, M. F., Gowda, M., Longin, C. F. H., & Reif, J. C. (2014). Bridging the gap between marker-assisted and genomic selection of heading time and plant height in hybrid wheat. *Heredity*, 112, 638-645.

Zhu, C., Gore, M., Buckler, E. S., & Yu, J. (2008). Status and Prospects of Association Mapping in Plants. *The plant genome,* 1, 5-20.

Chapter 2

Novel alleles for combined drought and heat stress tolerance in wheat

Statement of Authorship

Title of Paper	Novel alleles for combined drought and heat stress tolerance in wheat
Publication Status	☐ Published ☐ Accepted for Publication ☒ Submitted for Publication ☐ Unpublished and Unsubmitted work written in manuscript style
Publication Details	Schmidt J., Tricker P., Eckermann P., Kalambettu P., Garcia M., & Fleury D. Novel alleles for combined drought and heat stress tolerance in wheat.

Principal Author

Name of Principal Author (Candidate)	Jessica Schmidt
Contribution to the Paper	Designed the experiments with Paul Eckermann and supervisors. Conducted the experiments, performed the statistical analysis and wrote the manuscript.
Overall percentage (%)	70%
Certification:	This paper reports on original research I conducted during the period of my Higher Degree by Research candidature and is not subject to any obligations or contractual agreements with a third party that would constrain its inclusion in this thesis. I am the primary author of this paper.
Signature	Date 09/09/19

Co-Author Contributions

By signing the Statement of Authorship, each author certifies that:

i. the candidate's stated contribution to the publication is accurate (as detailed above);

ii. permission is granted for the candidate in include the publication in the thesis; and

iii. the sum of all co-author contributions is equal to 100% less the candidate's stated contribution.

Name of Co-Author	Penny Tricker
Contribution to the Paper	Conceived the study, supervised the design, performance and data analysis of the experiments and reviewed the manuscript.
Signature	Date 10/9/19

Name of Co-Author	Paul Eckermann
Contribution to the Paper	Designed the experiment in 2016. Gave support in designing the experiments in 2017 and 2018 and the statistical analysis. Reviewed the manuscript.
Signature	Date 10/9/19

Name of Co-Author	Priyanka Kalambettu		
Contribution to the Paper	Helped with the performance of the experiments. Reviewed the manuscript.		
Signature		Date	10/09/19

Name of Co-Author	Melissa Garcia		
Contribution to the Paper	Supervised the design, performance and data analysis of the experiments and reviewed the manuscript. Developed the nested-association mapping population. Will act as the corresponding author.		
Signature		Date	10/09/19

Name of Co-Author	Delphine Fleury		
Contribution to the Paper	Conceived the study, supervised the design, performance and data analysis of the experiments and reviewed the manuscript.		
Signature		Date	23/09/2019

Link to Chapter 2

This chapter aimed to identify quantitative trait loci in bread wheat (*Triticum aestivum*) associated with the combination of two major abiotic stresses, drought and heat. The identification and introgression of novel loci and alleles linked to these stresses are crucial for future crop improvement and to secure future food supply. However, the identification of loci, particularly those for yield, is problematic due to their high genetic × environment interaction and the association with plant phenology. We, therefore, conducted a genome-wide association study in pots under semi-controlled conditions over two years allowing us to treat plants individually according to their flowering time. The findings of this study revealed >150 loci for grain weight under drought and heat stress, of which the majority were not associated with either plant phenology or plant height. Favourable alleles were widespread in Asian and African landraces, providing opportunities for their incorporation into modern varieties through breeding. Two QTL, which were located on chromosome 6A and 6B, were of particular interest and have been validated in this chapter (Chapter 2 – 6A QTL) and Chapter 3 (6B – QTL) using near-isogenic lines. The chapter has been published as follows: Schmidt, J., Tricker, P., Eckermann, P., Kalambettu, P., Garcia, M., & Fleury, D. (2019). Novel alleles for combined drought and heat stress tolerance in wheat. *Frontiers in Plant Science*, doi: 10.3389/fpls.2019.01800.

.

frontiers in Plant Science

ORIGINAL RESEARCH
published: 31 January 2020
doi: 10.3389/fpls.2019.01800

Novel Alleles for Combined Drought and Heat Stress Tolerance in Wheat

Jessica Schmidt, Penny J. Tricker, Paul Eckermann, Priyanka Kalambettu, Melissa Garcia and Delphine Fleury*

School of Agriculture, Food and Wine, The University of Adelaide, Adelaide, SA, Australia

Drought and heat waves commonly co-occur in many wheat-growing regions causing significant crop losses. The identification of stress associated quantitative trait loci, particularly those for yield, is problematic due to their association with plant phenology and the high genetic × environment interaction. Here we studied a panel of 315 diverse, spring type accessions of bread wheat (*Triticum aestivum*) in pots in a semi-controlled environment under combined drought and heat stress over 2 years. Importantly, we treated individual plants according to their flowering time. We found 134 out of the 145 identified loci for grain weight that were not associated with either plant phenology or plant height. The majority of loci uncovered here were novel, with favorable alleles widespread in Asian and African landraces providing opportunities for their incorporation into modern varieties through breeding. Using residual heterozygosity in lines from a nested association mapping population, we were able to rapidly develop near-isogenic lines for important target loci. One target locus on chromosome 6A contributed to higher grain weight, harvest index, thousand kernel weight, and grain number under drought and heat stress in field conditions consistent with allelic effects demonstrated in the genome-wide association study.

Keywords: genome-wide association, quantitative trait loci, near-isogenic lines, *Triticum*, abiotic, genetic diversity

OPEN ACCESS

Edited by:
Sonia Negrao,
University College Dublin, Ireland

Reviewed by:
Ahmad M. Alqudah,
Leibniz Institute of Plant Genetics and Crop Plant Research (IPK), Germany
Shun Sakuma,
Tottori University, Japan
Eduard Akhunov,
Kansas State University, United States

****Correspondence:***
Melissa Garcia
melissa.garcia@adelaide.edu.au

Specialty section:
This article was submitted to Plant Abiotic Stress, a section of the journal Frontiers in Plant Science

Received: *09 September 2019*
Accepted: *23 December 2019*
Published: *31 January 2020*

Citation:
Schmidt J, Tricker PJ, Eckermann P, Kalambettu P, Garcia M and Fleury D (2020) Novel Alleles for Combined Drought and Heat Stress Tolerance in Wheat. Front. Plant Sci. 10:1800. doi: 10.3389/fpls.2019.01800

INTRODUCTION

Bread wheat (*Triticum aestivum* L.) is one of the leading crops with an annual production of 730.9 million tons globally. However, the world's wheat consumption is expected to expand beyond production raising concerns about future food security (FAO, 2018; FAO, 2019). Wheat production is constrained by abiotic stresses such as drought and heat causing yield losses of up to 40% and 60% in the field, respectively (Zampieri et al., 2017). In many cropping regions these stresses occur simultaneously leading to almost total yield loss. For instance, wheat production in Mediterranean climate zones such as Australia, southern Europe and the northwest of the United States is largely based on dry land, characterized by drought in combination with high temperatures around anthesis and early grain filling (Izanloo et al., 2008; Schillinger et al., 2008; Gbegbelegbe et al., 2016; Toreti et al., 2019). At reproductive stages wheat yields are especially vulnerable with drought and heat stress reducing spikelet fertility, grain number, single grain weight, and grain filling duration (Prasad et al., 2011; Mahrookashani et al., 2017).

To reduce yield losses, the identification and incorporation of favorable alleles controlling grain yield and its components into cultivated varieties is crucial (Furbank and Tester, 2011). While bi-

parental mapping populations include only a limited number of parental lines, genome-wide association studies (GWAS) are suitable for exploring larger and more diverse panels without the requirement to develop mapping populations (Zhu et al., 2008). To date, several quantitative trait loci (QTL) for yield and its components have been identified under drought, heat, and under combined drought and heat stress in field environments [reviewed in (Tricker et al., 2018)]. The identification of stress tolerance QTL in field conditions is, however, extremely difficult due to multigenic control, low heritability and large genotype × environment interactions, as well as the influence of several stresses at the same time (Fleury et al., 2010; Dolferus et al., 2011). In addition, most of the yield QTL found in these studies were associated with flowering time and plant height controlling genes, in particular photoperiod (*Ppd*), vernalization (*Vrn*), and reduced height (*Rht*) genes. The strong effect of flowering time and plant height on yield often masks the effects of other loci of smaller effects, limiting the detection of yield-regulating QTL. To minimize their cofounding effects, studies either account for flowering time and plant height by including them as covariates in statistical models or by calculating the residual effect of QTL unrelated to flowering time and plant height, but often find very few QTL (Lopes et al., 2015; Ogbonnaya et al., 2017; Mason et al., 2018).

The first genetic studies of wheat under a combination of drought and heat stress under controlled conditions were carried out by Aprile et al. (2013) in durum wheat and by Qaseem et al. (2018) in bread wheat. Experiments in pots under controlled conditions enable a more precise control of the environmental variables and the time of treatment. The disadvantage, however, is that results are not always reproducible in the field although they might be suitable for preliminary discovery and for avoiding high costs of field trials (Passioura, 2006; Izanloo et al., 2008). Qaseem et al. (2018) identified several QTL under well-watered and heat stressed conditions and one QTL under combined drought and heat stress for grain weight not linked to plant phenology.

In this study, we conducted a GWAS over 2 years using a diverse bread wheat collection consisting of 315 accessions. We measured yield components and traits previously hypothesized to be associated with combined drought and heat stress tolerance. Our aim was to identify novel QTL and alleles associated with combined drought and heat tolerance but independent from plant phenology. We used a semi-controlled pot system that allowed us to treat plants individually according to their flowering time. We developed near-isogenic lines (NILs) for one of the QTL and exposed these to combined drought and heat stress in field conditions to validate the effect of the locus.

MATERIALS AND METHODS

Plant Material

For the GWAS, diversity panels composed of a total of 315 spring wheat accessions were evaluated in two independent experiments in 2016 and 2017. The two panels represented a reduced set of the panel described in Garcia et al. (2019) and differed in 110 accessions between both years due to identity issues, missing genotypic data, or late maturing types in 2016 (**Supplementary Table 1**). Accessions with uncertain identity were excluded from the analysis in 2016, resulting in a subset of 273 lines. Plants which flowered much later than the majority of the plants (i.e., seven and six plants in 2016 and 2017, respectively) were also excluded to avoid different treatment conditions due to the rising temperatures at the end of the experiments. Seeds for the 2016 panel were obtained from a pilot experiment in 2015 at Urrbrae (South Australia, Australia) grown in pots under well-watered conditions, whereas seeds for the 2017 panel were obtained from three different sources: a 2013 field trial at Urrbrae (South Australia, Australia; 293 accessions), a 2015 pilot experiment (16 accessions), and the Australian Grains Genebank (6 accessions).

Plant material for the validation of a target QTL identified during the GWAS in 2016, which was located on chromosome 6A, derived from an existing nested association mapping (NAM) population. Parents of the nested association mapping population formed part of the diversity panel and are listed in **Supplementary Table 1**. Twenty-eight BC1F4 families from the existing NAM population were available and used for screening for the target QTL. Four hundred and eighty recombinant inbred lines of the 20 families (BC1F4) were genotyped with the 90,000 single nucleotide polymorphism (SNP) marker "RAC875_s119505_143" (Wang et al., 2014), which was shown to have the strongest association within the QTL, to find lines that were heterozygous at this locus. Genotyping was performed using Kompetitive Allele Specific Polymerase Chain Reaction (KASP™) technology (LGC Limited, London, United Kingdom). KASP™ assays were designed in-house (**Supplementary Table 2**) and SNP and sequence information were obtained through the Diversity Among Wheat geNomes platform (Watson-Haigh et al., 2018). One hundred twenty-seven BC1F5 derived from single seed descendent of heterozygous recombinant inbred lines were genotyped using the selected marker to identify pairs of NILs carrying the allele from either the recurrent or diverse parent. Ten additional KASP SNP markers located on different chromosomes were used to validate the genetic background of the NILs and to select NIL pairs with similar phenology (**Supplementary Table 2**). In total, four NIL pairs (BC1F6) were identified. Three of the four NIL pairs derived from a cross between Gladius and a diverse donor (i.e., one from a cross with Taferstat, NIL pair 1, and two from a cross with Thori, NIL pairs 2 and 3), whereas one of the NIL pairs derived from a cross between Scout and Zilve (NIL pair 4).

Plant Growth Conditions

The phenotyping for the GWAS was carried out in pots under semi-controlled conditions in a polytunnel facility at the University of Adelaide (Urrbrae, South Australia, Australia, 35° S 139° E) from May to November in 2016 and 2017. A split-plot design with three biological replications per treatment surrounded by a line of border pots was adopted in both years (**Supplementary Figure 1**). Plants were randomized over three blocks (i.e., one replicate per block) and randomized differently in each year to avoid that genotypes were located at the same spot

as the year before. The polytunnel facility consisted of a main area with tables at the back to dry the pots down for the drought treatment and an adjacent heat chamber for the heat treatment. Single plants were grown in pots filled with 0.5 kg of a substrate mix of clay-loam, sand, and coco peat in a 1:1:1 ratio and supplemented with a basal, slow-release fertilizer. Plants were additionally fertilized at tillering (All-Purpose Soluble Fertilizer, Hortico, Australia) and heading (Trace Element Soluble Powder, Manutec, Australia) in 2016 and at early booting in 2017 (All-Purpose Soluble Fertilizer, Hortico, Australia). Pesticides were used for an adequate pest and disease control. Temperature and relative humidity were recorded throughout both experiments in the main and in the heat area. Temperature was monitored at 10 minutes intervals with the Hobo Monitoring Station Data Logger RX3000 (Onset Computer Corporation, United States). Sensors were installed at 10 cm above pot level at the beginning of each experiment and adjusted fortnightly to plant canopy height. Relative humidity was recorded every 10 minutes in the heat chamber with a hobo sensor and in the main area with four dataloggers (model KG100, Kongin, China), placed at each of the corners of main area at pot level. Soil moisture was monitored on the last day of treatment. Plants were supplied with sufficient water from sowing to anthesis. The primary tiller of each plant was tagged at anthesis. At 3 days after anthesis, plants were subjected to either drought treatment (D): irrigation withheld for 6 days; or combined drought and heat (DH) treatment: irrigation withheld for 6 days and 35/25°C day/night from the fourth day of D treatment on. After 6 days of treatment, plants were re-irrigated and kept under well-watered conditions until the end of the experiment.

NILs were grown in micro-plots under semi-controlled conditions in a polytunnel facility at the University of Adelaide (Urrbrae, South Australia, Australia) in 2018. A randomized block design with three biological replications was implemented. NILs of the same pair were kept next to each other to minimize spatial heterogeneity. A border around each plot was planted to reduce interplot competition (Rebetzke et al., 2014). For each plot, two rows of eight seeds were sown with a plant density of 190 plants m-2 and a plot size of 20 x 42 cm. Sowing was later (20th of June) than the normal commercial sowing time in South Australia (April/May) to assure temperatures above 35°C during anthesis and grain filling. Plants which did not germinate by the 11th July 2018 were replaced by 6-days old seedlings grown in petri dishes. Two soil probes (Measurement Engineering Australia, Australia), one at 10 and one at 40 cm soil depth, were installed in each block to measure the soil water potential every 10 minutes during the experiment. Soil probes were placed between the same NIL pairs in each block to prevent differences in soil water potential caused by different genotypes. Temperature and relative humidity were recorded at 10 minutes intervals by installing one datalogger in the middle of each block. Plants were fertilized at 5-leaf stage with 50 kg/ha nitrogen (Urea, Richgro, Australia) and 10 kg/ha phosphate (Superphosphate, Richgro, Australia). A second nitrogen (30 kg/ha, Urea, Richgro, Australia) application was performed at the end of stem elongation. Pesticides were applied according to usual field practices. Plants were regularly irrigated using a drip-irrigation system maintaining the soil water potential below −100 kPA. The Zadoks' stage of each plot was recorded three times a week. At Zadoks' stage 39 (i.e., the flag leaf collar was visible in more than 50% of the plots) irrigation was stopped to impose severe drought stress during early grain filling. Plots were lightly re-irrigated three times during the course of the experiment (i.e., drip irrigation for 11 minutes, corresponding to 17 mm of rain fall) the day after all six soil sensors marked −633 kPa to mimic cyclic drought events. To subject plants to a combination of drought and heat stress during early grain filling, the polytunnel was partly closed at Zadoks' stage 65 (i.e., anthesis half complete in more than 50% of the plots) for three weeks.

Phenotypic Data

Morphological, physiological, and grain traits were measured in the pot experiment for all three replicates under both treatments. Days to anthesis was defined as the time from sowing until the first visible anther of the primary tiller. The leaf water potential of the second leaf of the primary tiller was measured on the fifth day of treatment. Leaf samples were collected daily between 8:30 and 11:00 am and placed into a plastic cup, sealed with parafilm, and kept in a moist bag until they were measured with a water potential meter (WP4C, Meter Group, United States) in precise mode for 5 minutes. A self-calibrating chlorophyll meter (SPAD 502 Plus, Spectrum Technologies, United States) was used to measure the chlorophyll content in the center of the flag leaf at 9 days after anthesis as an average of three measurements. At physiological maturity, plant height of the primary tiller was measured from the base of the plant to the tip of the spike excluding awns. Spike length of the primary tiller was determined by measuring the distance between the base of first rachis to the tip of the last spikelet without awns. Number of spikes per plant and total above-ground biomass, including leaves, stem, and spikes of all tillers, were recorded. Spikes of the primary tiller and other tillers were kept separate and threshed by hand. Grain screenings were obtained for the primary tiller and the whole plant with a wheat grain sieve (2.0 mm, Graintec, Australia) and determined as the percentage of the ratio between small grain weight (i.e., non-filled grains) and total grain weight. Number of grains of > 2.0 mm of size (i.e., filled grains) were counted for primary tiller and plant. Grain weight was determined as the weight of grains > 2.0 mm in primary tiller and plant. Single grain weight was calculated for both primary tiller and whole plant as the ratio between grain weight and the number of grains. Harvest index was estimated by dividing grain weight of the whole plant by the above-ground biomass.

In 2018, days to anthesis was defined as the time from sowing until more than half of the plants in a plot reached Zadoks' stage 65 (Zadoks et al., 1974). Plant height and spike length of the primary tiller (i.e., the tallest tiller of each plant) of five randomly chosen plants of each plot were measured at physiological maturity as described above. Spikes of the primary tiller of the five selected plants were harvested separately from the rest of the plants of each plot to potentially increase the statistical power

due to an increased sample size. Single spikes and whole plants per plot were oven-dried in a paper bag at 37°C for 10 days. Subsequently, number of spikes per plot and total above-ground biomass per plot including all spikes were measured. Single spikes were threshed by hand, while the rest of the spikes were threshed with a conventional threshing machine. Both parts were sieved separately by hand (wheat grain sieve 2.0 mm, Graintec, Australia). For the single spikes, grain weight, grain number, and single grain weight of grains > 2.0 mm and screenings were determined as described before. Traits per plot included grain weight, grain number, screenings, and thousand kernel weight. Harvest index was calculated as the ratio between grain weight per plot and above-ground biomass.

Genotyping and Population Structure of Diversity Panels

Genotyping and the population structure analysis of the original diversity panel are described in Garcia et al. (2019). A total of 563 accessions were genotyped using the wheat iSelect 90K SNP genotyping array (Wang et al., 2014). After filtering for SNPs with minor allele frequency of < 5% and missing values > 5%, 30,533 unique, high-quality SNPs remained and were used for association analyses. Additionally, the genotypic data of ten markers associated with genes known to affect plant phenology (*Ppd-A1*, *Ppd-B1*, *Ppd-D1*; *Vrn-A1*, *Vrn-D1*), plant height (*Rht-B1*, *Rht-D1*, *Rht24*), and grain weight (*TaGW2-6A*, *TaGW2-6B*) were included.

Statistical Analysis of Phenotypic Data

Adjusted means (BLUEs) were calculated for each trait under D and DH treatment in both GWAS using the R package ASReml (Butler et al., 2009), fitting accessions and treatments as fixed effects and factors relating to the experimental design as random effects. Days to anthesis was significantly associated with all traits. Predicted means were therefore calculated twice as previously done in durum wheat by Sukumaran et al. (2018): i) without including days to anthesis as a covariate (i.e., not adjusted) and ii) including days to anthesis as a covariate (i.e., adjusted). To assess the heat response under drought of each genotype, a ratio of the predicted, non-adjusted means under DH divided by the predicted, non-adjusted means under D was calculated for all traits, except for days to anthesis. The outputs for D (adjusted and non-adjusted means), DH (adjusted and non-adjusted means), and the ratio were used for genome-wide association analysis. The heritability of each trait under D and DH was calculated according to Cullis et al. (2006) using a secondary model with accessions as random effects. Two-way analysis of variance and Tukey's HSD test were carried out to test for significant differences between non-adjusted means. Pearson correlation coefficients were estimated to investigate the relationship among traits and represented in a principal component analysis biplot.

Means for traits per spike and per plot in 2018 were predicted for each NIL pair separately using ASReml. The two NILs of each pair were implemented as fixed effects and factors relating to the experimental design as random effects. Days to anthesis, defined as the days from sowing until Zadoks' stage 65, was included as fixed effect if significantly associated with the trait, which was the case for NIL pair 1 for biomass, grain weight and grain number per plot, NIL pair 4 for grain number, single grain weight and screenings per spike, and NIL pair 2 and 3 for plant height. Significant differences among NIL pairs were estimated conducting Tukey's HSD test. Correlations between traits were calculated using Pearson coefficients.

Genome Wide Association Analysis

Genome-wide association analysis was performed with the adjusted means for each of the two treatments and the ratio in both years. We used the compressed mixed linear model of Zhang et al. (2010) implemented in the R package "Genomic Association and Prediction Integrated Tool" (GAPIT) (Lipka et al., 2012) and accounted for population structure and genetic relatedness. A model selection procedure was run to determine the optimal number of principal components per trait to be included in the association analysis, with a maximum of four principal components. A two-level false discovery rates (FDR) (Benjamini and Hochberg, 1995) of 0.05 and 0.20 was used as threshold for declaring significant MTA. FDR adjusted p-values were obtained from the GAPIT output files. The difference between the variation explained by the MTA with and without the strongest associated SNP was used to estimate the allelic effect of each MTA (Sun et al., 2010). The order of significant and indicative MTA was determined based on the wheat consensus map of Wang et al. (2014). The position on the physical map was determined by aligning the sequences of the markers to the RefSeq v1.0 (IWGSC, 2018), using BLASTN with an e-value cut-off of 10^{-5}. MTA which could not be assigned to a chromosome were not considered. The intervals for the QTL were defined by comparing the position of the significant markers on the consensus and physical maps. Map graphics were drawn using the R package ggplot 2 (Wickham, 2016).

RESULTS

Effects of Drought or Combined Drought and Heat Stress on Phenotypic Traits

Two treatments, drought (D), and combined drought and heat stress (DH) were imposed 3 days after anthesis of each individual plant. Plants were subjected to D by withholding water for 6 days while plants in the DH treatment were subjected to the same treatment for 3 days and then moved to a heat chamber for another 3 days without watering. This resulted in a severe post-anthesis drought stress of 3.1% average soil water content, coupled, in plants under DH treatment, with high temperature stress of 31.0/23.4°C day/night in 2016 and 32.2/24.4°C day/night in 2017 (**Supplementary Figure 2**). Weather conditions for both years were similar with average temperatures of 17.3/11.6°C day/night in 2016 and 16.8/13.2°C day/night in 2017 in the main area outside the heat chamber. Maximum temperatures were slightly higher in the main area in 2016 with 25 days above 30°C in comparison to 8 days in 2017. On average, relative humidity

reached 69.0% in 2016 and 68.9% in 2017 in the main area and 50.7% in 2016 and 44.1% in 2017 in the heat chamber.

Heritability estimates (H^2) were similar in both years ranging from 40.9% for grain weight of primary tiller to 99.6% for the number of days to anthesis (**Table 1**). Moderate H^2 were found for grain traits and harvest index under DH (40.9–66.3%) while under D, H^2 were high (73.7–91.3%). The lower H^2 under DH is probably due to an increased number of plants with zero grain weight caused by severe stress.

Under DH, grain weight, single grain weight, and the number of grains > 2.0 mm were significantly lower ($p \leq 0.001$) compared to D with similar results in primary tillers and whole plants (**Table 1**, **Supplementary Figure 3**). Screenings significantly increased ($p \leq 0.001$) under DH compared to D. Grain weight was the trait most severely affected by DH with an average reduction of 92.1% in primary tillers and 93.1% in whole plants across years, followed by grain number and single grain weight with average reductions of 87.8–89.6% and 82.9–86.5%, respectively. Screenings was the least affected grain trait, increasing on average by 71.2–75.6%. Similar to grain weight, leaf water potential, biomass, and harvest index were significantly reduced by DH compared to D in both years ($p \leq 0.001$), whereas no significant effect was observed for plant height and spike length in 2016 and 2017 and for spike number and chlorophyll content in 2017.

Grain weight of the primary tiller and whole plant did not differ under DH between the years, while grain components (i.e., grain number, single grain weight, and screenings) were significantly more affected by DH in 2017 compared to 2016 ($p \leq 0.001$) in both primary tillers and whole plants. D had a similar effect in both years on grain weight, grain number, and single grain weight per primary tiller but had a significantly higher impact on grain weight and grain number per plant in 2016 compared to 2017 ($p \leq 0.001$). In contrast, screenings per primary tiller and plant were more affected in 2017 than in 2016 ($p \leq 0.05$ and $p \leq 0.001$, respectively). Number of days to anthesis was reduced by 23 days in 2017 compared to 2016 due to the replacement of late maturing types. A narrowed flowering time window would suggest a decreased exposure to higher temperatures, as they often occur toward the end of the season, and might therefore explain the higher number of grains and grain weight per plant under D in 2017. Differences in grain components between years under DH were, in contrast, most likely caused by the overall 1°C increase in temperature in the heat chamber in 2017.

Phenotypic correlations (R^2) between traits under D and DH treatment are presented in **Supplementary Table 3** and **Figure 1**. Under D and DH, 43.1–43.5% and 19.0–19.9% of the variation is explained by the first and second dimension, respectively, explaining thus more than (62.1–63.4%) half of the variation

TABLE 1 | Predicted means, minimum, and maximum values as well as heritability (H^2) under drought and combined drought and heat stress in 2016-2017.

Trait	Treatment	2016				2017			
		Mean	Min	Max	H^2 (%)	Mean	Min	Max	H^2 (%)
Days to anthesis	Pre-treatment	121.8	91.6	186.2	99.6	119.2	95.7	162.8	98.7
Leaf water potential (MPa)	Drought	-6.5	-65.2	-2.0	85.7	-13.2	-77.3	-1.5	78.4
	Drought & Heat	-21.3	-171.4	-3.4	84.3	-45.6	-132.8	-3.5	84.3
Chlorophyll content	Drought	26.4	4.2	55.8	76.7	39.5	9.8	63.1	75.9
	Drought & Heat	24.3	1.2	60.7	79.8	43.5	12.3	73.6	75.9
Number of spikes	Drought	2.7	1.2	5.1	57.0	3.3	1.0	6.0	68.3
	Drought & Heat	2.8	1.5	5.4	56.7	3.3	1.4	6.5	70.4
Spike length (cm)	Drought	10.4	5.2	13.9	73.8	11.5	4.5	16.7	91.2
	Drought & Heat	10.6	4.7	14.3	75.5	11.6	4.9	18.7	90.7
Plant height (cm)	Drought	104.2	50.9	149.5	92.6	114.1	58.8	173.0	94.8
	Drought & Heat	104.2	51.5	155.1	92.9	114.5	56.3	164.5	95.7
Biomass (g)	Drought	12.7	4.4	31.0	77.5	17.6	4.5	42.5	79.0
	Drought & Heat	10.9	3.3	24.7	87.3	14.0	3.1	40.4	93.3
Screening per primary tiller (% small grain weight)	Drought	10.1	0.0	100.0	78.7	15.1	0.0	100.0	74.0
	Drought & Heat	83.3	7.63	100.00	42.4	90.6	0.0	100.0	63.2
Screening per plant (% small grain weight)	Drought	9.1	0.0	100.0	82.6	14.3	0.0	100.0	74.3
	Drought & Heat	80.3	6.2	100.0	50.1	89.8	0.0	100.0	63.7
Number of grains per primary tiller	Drought	41.8	0.0	72.4	84.4	39.9	0.0	80.2	76.9
	Drought & Heat	6.7	0.0	47.3	43.2	3.4	0.0	33.0	57.7
Number of grains per plant	Drought	88.0	0.0	155.3	77.6	104.6	3.3	176.1	73.7
	Drought & Heat	13.4	0.0	100.6	48.6	5.8	0.0	67.0	57.0
Single grain weight per primary tiller (mg)	Drought	42.3	0.0	64.7	83.1	40.5	0.0	67.7	84.2
	Drought & Heat	7.2	0.0	42.8	41.9	4.1	0.0	51.3	66.3
Single grain weight per plant (mg)	Drought	41.7	0.0	70.0	81.3	39.7	0.0	67.1	82.5
	Drought & Heat	9.4	0.0	38.1	50.2	4.6	0.0	47.2	66.2
Grain weight per primary tiller (g)	Drought	1.90	0.00	3.81	84.0	1.80	0.00	3.86	81.3
	Drought & Heat	0.20	0.00	1.34	40.9	0.10	0.00	1.68	63.8
Grain weight per plant (g)	Drought	3.79	0.00	6.55	82.4	4.50	0.11	9.00	78.3
	Drought & Heat	0.38	0.00	2.38	44.6	0.17	0.00	3.28	63.1
Harvest Index	Drought	0.32	0.00	0.51	91.3	0.26	0.00	0.47	84.7
	Drought & Heat	0.04	0.00	0.24	45.1	0.01	0.00	0.23	64.6

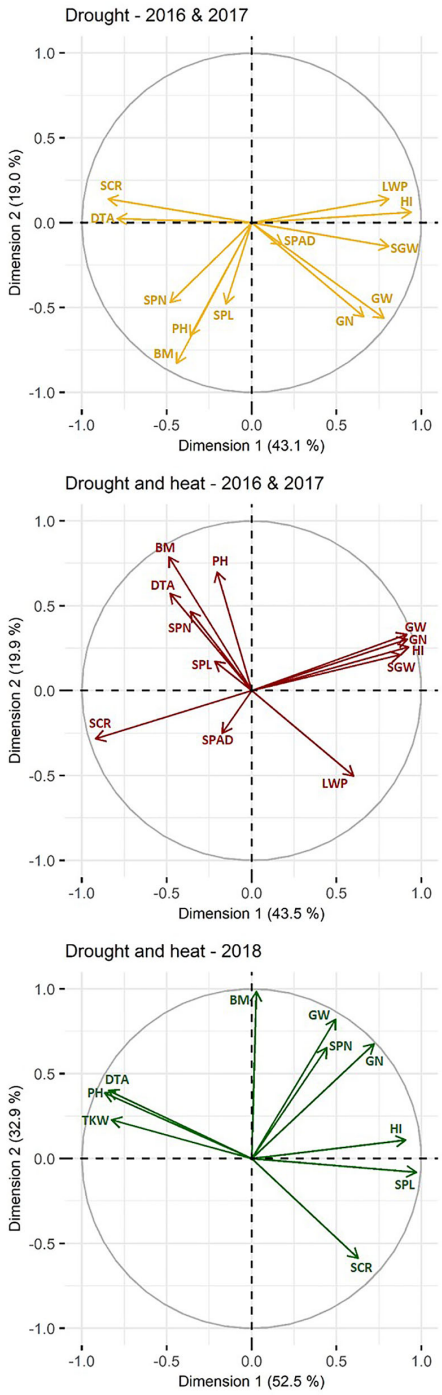

FIGURE 1 | Continued

FIGURE 1 | Principal component analysis biplot of correlations among traits. Traits studied in 2016 and 2017 under drought are marked in yellow, under combined drought and heat in red and traits studied in 2018 under combined drought and heat are marked in green. Positively correlated traits are grouped together, whereas negatively correlated traits are positioned on opposite quadrants. The distance between traits and the plot origin indicates the quality of representation of the trait within the principle component analysis (i.e., the further away, the better represented). For simplicity, grain traits measured in 2016 and 2017 are only given for whole plant and grain traits measured in 2018 are given per plot. DTA, days to anthesis; HI, harvest index; LWP, leaf water potential; SPAD, chlorophyll content; SPN, number of spikes; SPL, spike length; PH, plant height; BM, biomass; SCR, screenings; GN, grain number; SGW, single grain weight; SW, grain weight; single grain weight per spike; TKW, thousand kernel weight.

(**Figure 1**). All traits, except chlorophyll content and spike length were well represented by the principal component analysis. Adjusted means of grain weight, screenings, grain number, and single grain weight of the primary tiller were highly correlated with those of whole plants under D and DH with R^2 between 0.75 and 0.95 ($p \leq 0.001$). Under D and DH, grain weight had a significant ($p \leq 0.001$) and positive correlation with leaf water potential, grain number, single grain weight, and harvest index. In contrast, days to anthesis, spike number, and screenings were negatively associated with grain weight in both treatments.

Genome-Wide Association Studies

Identified markers and their corresponding QTL are shown in **Figure 2**, except for QTL for grain weight which are summarized in **Table 2**. Details of QTL including number of associated markers, position on genetic and physical map, and allelic effect can be found in **Supplementary Table 4**. Examples of Manhattan plots and Q-Q plots are given in **Supplementary Figure 4**. A total of 256 and an additional 216 QTL were identified using a FDR of 0.05 and 0.20, respectively, representing an average of 5 QTL per trait, treatment, and year with an average QTL interval of 1.2 Mbp. QTL were found on all chromosomes with most QTL located on chromosomes 3B, 5A, 5B, and 6B. Of the 472 QTL, 133 QTL were associated with D, 53 with DH, and 276 were found for the heat response under drought. Three hundred twenty-seven QTL co-located with QTL across more than one treatment, of which 81 QTL were pleiotropic for D, DH, and the heat response under drought. No QTL for leaf chlorophyll content were found.

QTL for Flowering Time and Plant Height

The strongest locus for days to anthesis was the known photoperiod sensitive locus *Ppd-D1* (*QDTA.aco-2D*) on chromosome 2D explaining 3.5–6.3% of the phenotypic variation. *Ppd-D1* was also associated with biomass under DH in 2016 and co-located with two QTL for single grain weight per primary tiller for the heat response under drought (*QSGWt.ara-2D*) and leaf water potential under D (*QLWP.adr-2D.2*). Further QTL for days to anthesis were found on chromosomes 2A, 4A, 5A, 5D, and 7B of which seven co-located with QTL for grain weight. QTL on chromosome 5A (*QDTA.aco-5A.1*) and 5D (*QDTA.aco-5D*) co-located also with QTL for plant height (*QPH.adh-5A*, *QPH.adh-5D*). The major loci associated with

FIGURE 2 | Physical position of marker trait associations (MTA). A false discovery rate of 0.20 was set as threshold. Physical positions are based on IWGSC RefSeq v1.0. Traits in yellow represent MTA identified under drought, red represents MTA identified under combined drought and heat, and orange represents MTA identified for the ratio (i.e., heat response under drought). Markers associated with days to anthesis are in grey. MTA identified in 2016 are represented as a circle and MTA identified in 2017 as triangle. The size of the circle and triangle corresponds to the allelic effect of each MTA.

plant height were *Rht-B1* (*QPH.adr-4B*, *QPH.adh-4B*) and *Rht-D1* (*QPH.adr-4D*, *QPH.adh-4D*) on chromosome 4B and 4D, respectively. Both QTL appeared under D and DH and in both years. Another QTL for plant height (*QPH.adh-2B*) was identified under DH in 2016 located on chromosome 2B. None of the five QTL for plant height was associated with grain weight components.

QTL for Combined Drought and Heat

QTL under DH explained, on average, 4.4% of the phenotypic variation with QTL for plant height having the largest allelic effect (8.7%), followed by QTL for screenings per primary tiller and plant (6.2–7.6%) and for leaf water potential (6.4%). QTL for grain weight and grain number explained 3.3–5.2% and 3.9–4.8% of the phenotypic variation, whereas QTL for biomass accounted for the smallest phenotypic variation (2.4%). The maximum allelic effect of QTL for harvest index under DH was 4.9%.

Six QTL for grain weight per primary tiller and per plant independent from flowering time were identified under DH on chromosome 3A, 3B, 5B, and 7B using a FDR of 0.20 (**Table 2**). The strongest QTL was detected on the long arm of chromosome 3A. QTL for grain weight for the heat response co-located with two of the QTL for grain weight under DH on chromosome 3B (*QGWp.adh-3B.2*) and 5B (*QGWp.adh-5B*). QTL for harvest index, leaf water potential, screenings, and grain number co-located with seven, five, three, and two of the eight QTL for grain weight, respectively. The positive allele of the QTL for grain weight on 3B (*QGWp.adh-3B.2*) was mostly found in Asian landraces. Breeding lines from the International Maize and Wheat Improvement Center (CIMMYT) in Mexico and Australia carried mostly the positive allele for QTL located on chromosome 3A (*QGWp.adh-3A*), whereas the positive allele of the second 3B QTL (*QGWp.adh-3B.1*) was predominantly found in the North American germplasm. The positive alleles of

TABLE 2 | QTL controlling grain weight.

Chr	QTL	Trait	Treatment	Year	Position (cM)	Position (bp)	Allelic effect (%)	Traits with same QTL location (Treatment)
QTL for combined drought and heat								
3A	*QGWt.adh-3A*	GWt	DH	2017	347.9-349.3	647,474,241-647,508,573	3.9-4.0	LWP (D), GNp (DH), HI (DH)
	QGWp.adh-3A	GWp						
3B	*QGWp.adh-3B.1*	GWp	DH	2017	56.4	14,985,191-14,985,392	3.7	HI (DH)
3B	*QGWp.adh-3B.2*	GWp	DH	2017	119.8	26,650,089-29,356,945	3.8	SCRp (D), GWt (Ratio), HI (DH)
5B	*QGWp.adh-5B*	GWp	DH	2017	401.5-403.3	622,066,480-623,585,489	3.5	LWP (D), GWt (Ratio), HI (Ratio)
6B	*QGWp.adh-6B*	GWp	DH	2017	na	71,040,399-71,495,726	3.3	LWP (D), SCRt (D), SCRp (D)
QTL for drought								
2D	*QGWt.adr-2D*	GWt	D	2017	109.7-114.4	73,570,876-78,765,908	4.1-4.7	GNt (D), HI (D)
2D	*QGWp.adr-2D*	GWp	D	2016	133.2	146,305,492-146,305,593	7.9	LWP (D)
QTL for the heat response								
1A	*QGWt.ara-1A.6*	GWt	Ratio	2016, 2017	431.5-435.2	579,299,114-581,438,572	5.0-8.7	SGWt (Ratio), SGWp (Ratio), HI (Ratio)
3D	*QGWt.ara-3D.1*	GWt	Ratio	2016, 2017	na	1,698,974-4,394,598	5.2-9.0	LWP (D), GNt (Ratio), SGWp (Ratio), HI (Ratio)
6B	*QGWt.ara-6B.7*	GWt	Ratio	2016, 2017	375.2-388.2	705,384,526-712,346,484	4.8-5.8	SCRp (D), SGWp (Ratio), HI (Ratio)
	QGWp.ara-6B.3	GWp						
6D	*QGWt.ara-6D.2*	GWt	Ratio	2016, 2017	330.3	461,924,775-471,922,386	5.0-14.0	SCRp (D), GNp (Ratio), SGWp (Ratio), HI (D)
	QGWp.ara-6D	GWp						
7A	*QGWt.ara-7A.1*	GWt	Ratio	2016, 2017	262	62,528,244-63,443,715	11.8-14.7	SCRt (Ratio), SGWt (Ratio), SGWp (Ratio), HI (D, Ratio)
7B	*QGWt.ara-7B.1*	GWt	Ratio	2016, 2017	61.4-87.3	1,258,258-6,393,796	4.6-10.8	LWP (D), SCRt (D), SCRp (D), HI (Ratio)
	QGWp.ara-7B	GWp						
Stable QTL under drought and heat stress								
3B	*QGWt.ara-3B.3*	GWt	Ratio	2017	na	44,283,482-44,283,582	9.2	LWP (D, DH), SPN (Ratio), HI (Ratio)
4A	*QGWt.ara-4A.1*	GWt	Ratio	2017	na	21,063,714-21,635,963	4.4-9.1	LWP (D), BM (DH), SCRt (D), HI (Ratio)
	QGWp.ara-4A	GWp						
5B	*QGWt.ara-5B.6*	GWt	Ratio	2017	242.8-247.3	539,296,240-559,072,690	3.6-3.7	LWP (D, DH), SGWt (Ratio), SGWp (Ratio)
6A	*QGWt.ara-6A.1*	GWt	Ratio	2016, 2017	77.7-80.1	12,837,679-16,232,972	4.8-11.8	SCRt (DH), SCRp (D), GNp (Ratio), SGWp (Ratio), HI (Ratio)
	QGWp.ara-6A	GWp						
6A	*QGWt.ara-6A.3*	GWt	Ratio	2017	178.6	85,756,394-99,014,241	3.6	LWP (D), BM (DH)
6B	*QGWt.ara-6B.6*	GWt	Ratio	2017	259.8	646,565,102-652,374,782	12.4-15.4	LWP (D), BM (DH), SCRt (D), SCRp (D), HI (Ratio)
7B	*QGWt.ara-7B.6*	GWt	Ratio	2017	463.6	701,871,740-712,736,264	5.6-5.8	LWP (D), BM (D, DH), SCRt (D), HI (Ratio)

Position in base pairs corresponds to RefSeq v1.0. (IWGSC, 2018). Positions in centimorgan are according to the consensus map from Wang et al. (2014). bp, base pairs; BM, biomass; Chr, chromosome; cM, centimorgan; D, drought; DH, combined drought and heat; HI, harvest index; LWP, leaf water potential; SCRt, screenings per primary tiller; SCRp, screenings per plant; GNt, number of grains per primary tiller; GNp, grain number per plant; SPN, number of spikes; SGWt, single grain weight per primary tiller; SGWp, single grain weight per plant; GWt, grain weight per primary tiller; GWp, grain weight per plant.

QGWp.adh-5B and *QGWp.adh-6B* were common among all accessions and wheat types, but less common in Asian accessions and landraces.

QTL Under Drought

Under D, the identified QTL explained on average 5.9% of the phenotypic variation with the strongest QTL associated with leaf water potential accounting for 16.9% of the variation. Allelic effects at QTL for biomass (3.4–4.6%) explained the least phenotypic variation. The allelic effects of QTL for the yield component traits grain weight, grain number, and screenings ranged from 3.5 to 12.0% with the highest percentage of phenotypic variation explained for screenings per primary tiller.

Two QTL for grain weight per primary tiller and plant under D were identified with a FDR of 0.20 on chromosome 2D (*QGWt.adr-2D*, *QGWp.adr-2D*) accounting for a maximum of 4.7 and 7.9% of the phenotypic variation. Both QTL clustered together with QTL for leaf water potential. *QGWt.adr-2D* also

coincided with QTL for grain number and harvest index. The positive alleles for *QGWt.adr-2D* and *QGWp.adr-2D* were common in breeding lines from CIMMYT and Australia.

QTL for the Heat Response Under Drought

QTL for the heat response under drought elucidated an average of 7.3% of the phenotypic variation. QTL for biomass, spike number, and screenings accounted for the least phenotypic variation (4.7–5.9, 5.4–6.3, and 4.1–6.3%, respectively), while QTL for grain weight explained most of the phenotypic variation (3.6–21.2%). The allelic effects of QTL for single grain weight, grain number, and harvest index ranged from 3.5 to 19.0%. Allelic effects were potentially inflated by the calculation of the ratio. However, the use of a ratio also increased the statistical power allowing us to detect a larger number of QTL and a strong target QTL on chromosome 6A.

Using the ratio between environments, a total of 88 genomic regions were associated with grain weight per primary tiller and per plant with a FDR of 0.05. The most important pleiotropic regions were located on chromosome 1A (*QGWt.ara-1A.6*), 3D (*QGWt.ara-3D.1*), 6B (*QGWt.ara-6B.7*, *QGWp.ara-6B.3*), 6D (*QGWt.ara-6D.2*, *QGWp.ara-6D*), 7A (*QGWt.ara-7A.1*), and 7B (*QGWt.ara-7B.1*, *QGWp.ara-7B*) with chromosome 7A having the strongest allelic effect on grain weight (11.8–14.7%). All six regions were associated with harvest index and five of the six regions included QTL for single grain weight (i.e., all except the one on chromosome 7B). QTL for screenings were located within four (on chromosome 6B, 6D, 7A, and 7B) genomic regions. Grain number and leaf water potential were associated with two of the six genomic regions on chromosomes 3D and 6D and on chromosomes 3D and 7B, respectively. QTL for grain weight appeared in both years in all genomic regions and positive alleles were predominantly found in Asian and African landraces.

Stable QTL Under Drought and Heat Stress

Fourteen genomic regions independent from plant phenology were significantly associated with the two treatments and the heat response under drought of which half were also stable across years. The seven genomic regions were located on chromosomes 3B, 4A, 5B, 6A, 6B, and 7B and were associated with grain weight per primary tiller and plant for the heat response under drought. Six of the nine QTL for grain weight (*QGWt.ara-3B.3*, *QGWt.ara-4A.1*, *QGWp.ara-4A*, *QGWp.ara-6A*, *QGWt.ara-6B.6*, *QGWt.ara-7B.6*) were detected with an FDR of 0.05 and allelic effects ranged from 3.6 to 15.4% with the strongest QTL located on chromosome 6B. The positive alleles of *QGWt.ara-3B.3*, *QGWt.ara-4A.1*, *QGWp.ara-4A*, *QGWt.ara-6A.1*, *QGWp.ara-6A*, *QGWt.ara-6A.3*, *QGWt.ara-6B.6,* and *QGWt.ara-7B.6* were common in Asian and African landraces, whereas the positive allele of *QGWt.ara-5B.6* was mostly present in North American breeding lines. Six of the seven genomic regions were also associated with leaf water potential, four with biomass, harvest index, and screenings, two with single grain weight and one with grain number and spike number per plant.

Validation of Candidate QTL in Near Isogenic Lines

NILs were developed for the validation of a target QTL in semi-controlled field plots. The selected QTL on chromosome 6A (*QGWt.ara-6A.1*, *QGWp.ara-6A*) (**Table 2**) belonged to one of the seven genomic regions which were stable across years, traits, and treatments. It was also the only genomic region which was associated with a grain weight component under DH in 2016 (*QSCRt.adh-6A*) and co-located with QTL for grain number per plant, single grain weight per plant, and plant and harvest index (*QGNp.ara-6A*, *QSGWp.ara-6A*, *QHI.ara-6A.1*). In addition, the positive alleles of *QGWt.ara-6A.1*, *QGWp.ara-6A*, *QGNp.ara-6A*, *QSGWp.ara-6A,* and *QHI.ara-6A.1* were predominantly in African and Asian landraces and not present in most breeding lines, representing a potential candidate for the integration of novel alleles in current breeding programs. Plants of the four NIL pairs at the target region on chromosome 6A were exposed to high temperature stress and cyclic drought (**Supplementary Figure 2**) with relative humidity reaching 56.8%.

Descriptive statistics of phenotypic data are given in **Supplementary Table 5** and represented in **Figure 3**. Correlations between traits are shown in **Supplementary Table 3** and **Figure 1**. Both dimensions of the principal component analysis explained 85.0% of the variation and all traits were well presented. A strong correlation between spike- (i.e., average of five spikes) and plot-based measurements was found for screenings (0.73, $p \leq 0.05$) as well as single grain weight and thousand kernel weight (0.98, $p \leq 0.001$). Correlations between spikes and plots for grain number and grain weight were only moderate (0.50–0.56) and insignificant. Among the plot-based measurements, grain weight showed the highest positive correlation with grain number (0.95, $p \leq 0.001$), followed by biomass with a correlation of 0.85 ($p \leq 0.01$). Flowering time and plant height were similar across all NILs with no differences within NIL pairs, except for NIL pair 2 with an average difference of 6 cm in plant height. Nevertheless, the increase in plant height was not significantly associated with the increase in grain weight in NIL pair 2.

Consistent with the findings from the GWAS in 2016, grain weight per spike and per plot, grain number per plot, and harvest index were increased under DH by the allele from the exotic parents (i.e., Taferstat, Thori, or Zilve) in at least three of the four NIL pairs, whereas screenings per spike and per plot were increased by the non-exotic allele in three NIL pairs. Increases in grain weight per plot ranged between 9.0% (NIL pair 1, $p = 0.038$) to 26.4% in NIL pair 3 ($p = 0.061$), followed by grain number per plot with an increase of 8.7 to 18.2% (NIL pair 1 $p = 0.012$ and NIL pair 3 $p = 0.117$, respectively). Screenings per spike showed the smallest impact of the QTL with 0.1 to 0.6% (NIL pair 4 $p = 0.054$ and NIL pair 2 $p = 0.012$, respectively). Screenings in both GWAS and QTL validation were not normally distributed. Nevertheless, findings from the QTL validation coincided with results from the GWAS in 2016, indicating that the results were sufficiently explained by a linear model. The exotic allele also increased single grain weight, thousand kernel weight, spike number, and biomass

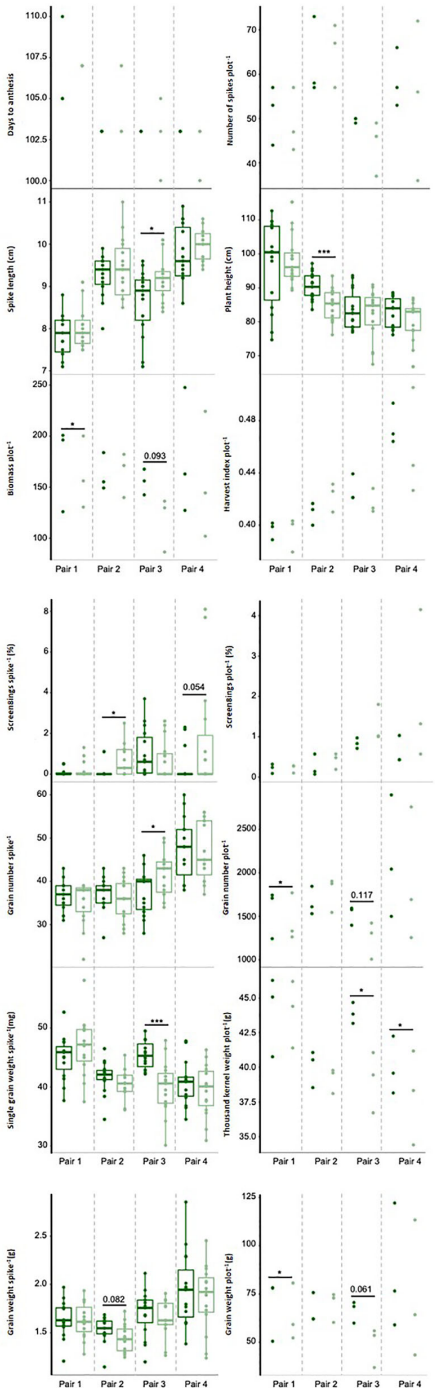

FIGURE 3 | Continued

FIGURE 3 | Phenotypic traits measured in 2018 under combined drought and heat stress. Near isogenic lines (NILs) of the same pair are next to each other carrying either the exotic (dark green) or non-exotic (light green) allele at the target region. Dots represent raw values of NILs. * and *** indicate statistical significance at $p \leq 0.05$, $p \leq 0.01$, and $p \leq 0.001$, respectively, based on Tukey's HSD test. Numbers above black line represent p-values which are marginally significant.

with a significant increase in single grain weight in NIL pair 3 ($p \leq 0.001$, 12.2%), thousand kernel weight in NIL pair 3 and 4 ($p = 0.023$, 2.9–11.0%), and biomass in NIL pair 1 ($p = 0.013$) and marginally significant differences in NIL pair 3 ($p = 0.093$). In contrast, the non-exotic allele increased spike length with significant differences found for NIL pair 3 ($p = 0.041$). The only inconsistency with the previous results in pot-based GWAS experiments was the significant, positive effect of the non-exotic allele on grain number per spike in one of the four NIL pairs. The QTL interval contains 68 high-confidence genes in the Chinese Spring reference genome (**Supplementary Table 6**) but the gene content might differ in the parents of the NILs.

DISCUSSION

Drought and heat constrain wheat yields in many wheat growing regions of the world and their combined effect can cause severe yield losses (Toreti et al., 2019). A comprehensive understanding of the traits and loci conferring drought and heat tolerance will be therefore critical for future crop production in terms of climate change and climate variability.

Important Drought and Heat Tolerance Traits

Grain components between treatments were positively but weakly correlated, indicating that accessions which performed well under D, were often susceptible to the combination of both drought and heat stresses. Accessions which performed well under both stresses were mostly Australian and Mexican varieties, which have been selected for their yield performance in dry and hot climates and represented about 70% of the diversity panels. However, approximately one fifth of the tolerant accessions were varieties from various origins such as the Middle East, Central Africa, the United States, Canada, and India. Landraces from Middle Eastern countries, which represented only about 7% of the panels, accounted for approximately 6% of the tolerant accessions in 2017. Of the number of accessions represented in both diversity panels, all three types (i.e., landraces, varieties from Australia and Mexico, and varieties from other origins) accounted for approximately one third of the tolerant accessions.

Grain number was mostly increased by the same allele as grain weight in both GWAS and NILs, indicating an important factor under post-anthesis drought and heat stress. Grain number is known to be affected by pre-anthesis stress (Fabian et al., 2019) but has also been found to be decreased by post-anthesis stress (Prasad et al., 2011; Qaseem et al., 2018). Grain number, in our experiments, accounted for only well-filled grains

(i.e., grains of size > 2.0 mm). The trait therefore represents grain filling ability. The allele increasing grain number also promoted single grain weight and thousand kernel weight with a significant increase in thousand kernel weight in NIL pairs 3 and 4. In NILs, spike length, spike number, as well as screenings (i.e., percentage of small, empty or partly filled grains) were negatively associated with grain weight under DH and were increased by the opposite allele than grain weight. A reduced tiller and initial grain set (sink strength) might be therefore an advantage when followed by combined drought and heat stress during grain-filling due limited assimilate availability (source strength) (Gupta et al., 2011).

Leaf water potential was the physiological trait with the strongest correlation with grain weight. Plants which maintained a less negative leaf water potential during stress had an increased grain weight, suggesting the role of this trait as both a stress and a stress tolerance indicator. Plants with a less negative leaf water potential had also a higher harvest index and a reduced spike number. Apart for the potential advantage of a limited sink strength, the reduced spike number and thus reduced surface area might have led to a decrease in transpiration rate (i.e., water loss) and water use in comparison to plants with more spikes. This would be especially important under severe drought and heat stress conditions (Tricker et al., 2018).

Phenology and Plant Height Independent QTL

Significant marker-trait associations (MTA) were initially selected using the Bonferroni threshold (i.e., -log10 (p) ≥ 5.68), however, we could not find any marker associated with grain weight or grain weight components under D or DH. Due to the high stringency of the Bonferroni threshold, type II error (i.e., false negative) is inflated drastically reducing the power of detection of loci with smaller allelic effects especially of more complex traits such as yield. In contrast, a low threshold bears the risk of increasing the detection of false-positive MTA (type I error) (Hamblin et al., 2011). We, therefore, chose FDR of 0.05 and 0.20 which have been considered sensible measures to balance between the type I error and type II error in GWAS (Benjamini and Hochberg, 1995; Storey and Tibshirani, 2003). To minimize the risk of potential false positive markers, we only considered QTL which co-located with at least one other QTL. Using the FDR as thresholds, we found and validated a strong QTL on chromosome 6A, confirming the findings from our GWAS.

Some of the QTL identified here were associated with well-known genes that are commonly used in marker assisted selection. For instance, days to anthesis was associated with the photoperiod sensitive gene *Ppd-D1* on chromosome 2D. Even though *Ppd-D1* has been shown to affect grain yield (Arjona et al., 2018; Mason et al., 2018), no significant association between *Ppd-D1* and grain weight or its components was found in this study, regardless whether grain traits were adjusted or not for days to anthesis. Eight additional QTL for days to anthesis were identified on chromosomes 2A, 4A, 5A, 5D, and 7B. The QTL on the short arm of chromosome 2A (*QDTA.aco-2A.1*) and the long arm of chromosome 5A (*QDTA.aco-5A.2*) were located in close proximity to the photoperiod sensitive gene *Ppd-A1* and the vernalization gene *Vrn-A1*, respectively (Yan et al., 2004; Wilhelm et al., 2009). The second QTL on chromosome 5A (*QDTA.aco-5A.1*) co-located with a QTL for plant height (*QPH.adh-5A*, non-adjusted and adjusted for anthesis) and QTL for days to heading and anthesis under combined drought and heat field conditions identified by Maccaferri et al. (2008) and Pinto et al. (2010). QTL for days to maturity under well-watered conditions and plant height were reported (Zanke et al., 2014; Qaseem et al., 2019) close to the ones identified in this study for days to anthesis and plant height on chromosome 5D (*QDTA.aco-5D*, *QPH.adh-5D*—non-adjusted and adjusted for anthesis). The QTL for plant height on chromosome 2B (*QPH.adh-2B*) co-located with the one previously detected by Sun et al. (2017).

Overall, 134 out of 145 identified QTL for grain weight were not related to days to anthesis or plant height. A pot-based system enabling the individual treatment of plants seemed therefore to be advantageous for the identification of QTL associated with drought and heat stress tolerance in comparison to field trials. However, drought and heat tolerance traits influenced by pot size such as root architecture, biomass, and spike number might need to be analyzed in a different setting as low correlations between these traits and grain weight in our GWAS indicated.

Novel QTL for Drought and Heat Tolerance

Allelic effects for grain weight and grain weight components were low to moderate ranging between 3.3% and 21.2% as often the case for complex traits such as yield (Hamblin et al., 2011; Zanke et al., 2015). Nevertheless, several major QTL for grain weight and its components were identified in this study. Identified QTL for grain weight co-located with previously detected QTL in wheat, except for *QGWt.ara-6A.3*. While half of the previously identified QTL have been associated with yield components and a third were controlling yield or grain weight itself, only four have previously been identified under combined drought and heat stress.

Important loci associated with grain weight under drought, heat or the heat response under drought were identified on chromosomes 1A, 2D, 3A, 3B, 3D, 5B, 6B, 6D, 7A, and 7B, of which most grain weight-related QTL were located on 7B. Apart from grain weight, the loci were pleotropic for harvest index, screenings, grain number, single grain weight, and leaf water potential. Ten of the 16 identified QTL for grain weight corresponded to QTL identified by Sun et al. (2017), of which two, located on chromosomes 1A and 7A, regulated grain weight per spike. Six other QTL associated with grain weight were detected under well-watered, rainfed, or heat conditions (Sukumaran et al., 2015; Valluru et al., 2017; Wang et al., 2017; Qaseem et al., 2018) and coincided with the QTL for grain weight under DH and the heat response under drought on chromosome 3B, 5B, and the long arm of chromosome 6B (*QGWp.adh-3B.1*, *QGWp.adh-3B.2*, *QGWp.adh-5B*, *QGWt.ara-6B.7*, *QGWp.ara-6B.3*). The QTL on the long arm of chromosome 6B also co-

located with QTL for harvest index under combined drought and heat stress (Garcia et al., 2019) as well as single grain weight and leaf chlorophyll content under heat (Shirdelmoghanloo et al., 2016). Regions on chromosome 3B co-located with QTL for tiller number under combined drought and heat stress, grain number, biomass, and harvest index under well-watered conditions (Qaseem et al., 2018), while the region on chromosome 7A coincided with QTL for spike length and water-soluble carbohydrates (Gao et al., 2015; Dong et al., 2016; Sun et al., 2017).

Seven of the here identified genomic regions which have not been previously associated with grain weight itself were located on chromosomes 2D, 3A, 3D, 6B (short arm), 6D, and 7B. QTL previously found on chromosomes 2D, 3A, 3D, 6D, and 7B for grain number (Gao et al., 2015; Shi et al., 2017; Sun et al., 2017), on chromosomes 3A, 3D, and 6D for thousand kernel weight (Zanke et al., 2015; Sun et al., 2017), and on chromosomes 1A, 3A, 3D, 6B, and 6D for grain size (Sun et al., 2017) were mapped to similar positions in the wheat reference genome sequence (RefSeq v1.0) to the QTL identified in this study. Under controlled heat conditions, Shirdelmoghanloo et al. (2016) identified QTL for grain filling duration, flag leaf length, shoot length, and harvest index which coincided with QTL for grain weight and harvest index for the heat response under drought on chromosome 7B (*QGWt.ara-7B.1*, *QGWp.ara-7B*, *QHI.ara-7B.1*). QTL associated with leaf chlorophyll content co-located with QTL on chromosome 2D (Gao et al., 2015).

Stable QTL for Yield and Yield Components

Seven genomic regions on chromosomes 3B, 4A, 5B, 6A, 6B, and 7B were particularly of interest as they were stable across treatments, traits, and years. Three of the genomic regions, located on chromosome 4A, 6B, and 7B, were associated with grain weight for the heat response under drought, harvest index, biomass, screenings, and leaf water potential. QTL for grain weight under single and combined drought and heat stress co-located with the QTL on chromosomes 6B and 7B (Valluru et al., 2017; Garcia et al., 2019; Qaseem et al., 2019) and QTL for harvest index and biomass were previously found under heat conditions on chromosome 7B (Qaseem et al., 2019). Using two QTL were reported, mainly wheat accessions from China, for grain number at all three regions (Shi et al., 2017; Sun et al., 2017). Further QTL for water-soluble carbohydrates, normalized difference vegetation index, and canopy temperature depression were found in 3–10 Mbp distance on RefSeq v1.0 on chromosomes 4A and 6B (Sukumaran et al., 2015; Dong et al., 2016; Gao et al., 2016). The genomic region on chromosome 5B regulated a total of four traits including grain weight per primary tiller, leaf water potential, and single grain weight per primary tiller and per plant. Sun et al. (2017) and Wang et al. (2017) reported QTL for thousand kernel weight and spike number at this region. The QTL on 3B co-located with QTL for anther extrusion (Muqaddasi et al., 2017).

On the short arm of chromosome 6A, we detected QTL for the heat response under drought of grain weight per primary tiller and per plant, grain number per plant, single grain weight per plant and harvest index, as well as screenings per primary tiller and per plant under D and DH (*QGWt.ara-6A.1*, *QGWp.ara-6A*, *QGNp.ara-6A*, *QSGWp.ara-6A*, *QHI.ara-6A.1*, *QSCRt.adh-6A*, *QSCRp.adr-6A.1*). QTL for grain weight, grain number, spike length, and tiller number in proximity to our region were associated with well-watered and drought conditions, but not with combined drought and heat stress (Sun et al., 2017; Qaseem et al., 2018; Qaseem et al., 2019). In fact, no QTL for grain weight under combined drought and heat stress has been identified at this locus to date, making it thus a promising target for the discovery of novel genes under drought and heat stress.

Field Validation

We developed NILs which differed at the 6A target QTL to validate our findings from the GWAS. By using an existing nested association mapping population, we were able to rapidly introduce the allele commonly distributed in Asian and African landraces into an Australian elite cultivar background. Findings were in accordance with the results from the GWAS in 2016, except for NIL pair 2. Results of the NIL pair 2 showed an opposite but not significant trend from the other three NIL pairs for most of the grain traits per plot (i.e., spike number, biomass, screenings, grain number, grain weight, and harvest index). Even if the genotyping results assumed uniformity among all four NIL pairs at the target region, the developed markers might not cover the target region sufficiently and differences in recombination events might not be visible. The genetic background might also be different between different pairs, containing potential cis- or trans- regulating elements controlling the target region. A whole genome sequencing of all NILs might therefore be required.

Clear trends were visible for all measured traits and significant differences were observed for six of the eight grain related traits. To potentially increase the statistical power by an increased sample size, traits of five randomly chosen spikes for each plot were measured. High correlation between measurements made per plot and per single spikes were observed for screenings and single grain weight, whereas grain number and grain weight per spike were not representative of the entire plot explaining the inconsistency of grain number per spike in comparison to the rest of the results. Even though grain weight per spike and per plot were not significantly correlated, both were increased in the NILs carrying the allele donated by the exotic parent in comparison to NILs carrying the allele donated by the adapted parent among three of the four NIL pairs. The biggest increase of grain weight was found in NIL pair 3 with 26.4% which would mean an immense yield gain in dry and hot environments. In both GWAS and the QTL validation, we applied severe DH stress, probably causing an inflation of the effect of the allele. We therefore would not expect an impact of 26.4% under actual field conditions but the incorporation of this allele could still be a significant contribution to future wheat breeding.

The GWAS and the validation of the QTL also showed an independency between this locus and QTL from plant phenology. This is important considering most studies in field conditions show

a strong effect of *Ppd-D1* that can potentially mask other loci affecting grain weight (Mason et al., 2018; Garcia et al., 2019). The use of a semi-controlled pot system allowed us to treat plants individually and to identify several QTL for D, DH, and heat response under drought. To confirm the effect of our target QTL in actual field conditions, the testing of NIL pairs in multi-environment trials over several years is required. A semi- or completely controlled pot system might therefore be a useful and cost-effective approach for the preliminary detection of QTL.

DATA AVAILABILITY STATEMENT

The raw data supporting the conclusions of this article will be made available by the authors, without undue reservation, to any qualified researcher.

AUTHOR CONTRIBUTIONS

PT and DF conceived the study. JS, PT, PE, MG, and DF designed the experiments. JS and PK conducted the experiments. JS wrote the manuscript and performed the statistical analysis. PE gave support in the statistical analysis. PT, PE, PK, MG, and DF edited the manuscript.

FUNDING

The project was funded by the Australian Research Council Industrial Transformation Research Hub for Genetic Diversity and Molecular Breeding for Wheat in a Hot and Dry Climate (project number IH130200027).

ACKNOWLEDGMENTS

The authors thank Beata Sznajder for the support in creating the figures and Larissa Chirkova, Martha Van Os, Alex Kovalchuk, Hui Zhou, and Stephan Haefele for their technical support. The authors also would like to thank the Australian Grains Genebank for supplying seeds for the experiments.

SUPPLEMENTARY MATERIAL

The Supplementary Material for this article can be found online at: https://www.frontiersin.org/articles/10.3389/fpls.2019.01800/full#supplementary-material

REFERENCES

Aprile, A., Havlickova, L., Panna, R., Mare, C., Borrelli, G. M., Marone, D., et al. (2013). Different stress responsive strategies to drought and heat in two durum wheat cultivars with contrasting water use efficiency. *BMC Genomics* 14, 821–838. doi: 10.1186/1471-2164-14-821

Arjona, J. M., Royo, C., Dreisigacker, S., Ammar, K., and Villegas, D. (2018). Effect of *Ppd-A1* and *Ppd-B1* allelic variants on grain number and thousand kernel weight of durum wheat and their impact on final grain yield. *Front. Plant Sci.* 9, 888. doi: 10.3389/fpls.2018.00888

Benjamini, Y., and Hochberg, Y. (1995). Controlling the false discovery rate: a practical and powerful approach to multiple testing. *J. R. Stat. Soc.* 57, 289–300. doi: 10.1111/j.2517-6161.1995.tb02031.x

Butler, D. G., Cullis, B. R., Gilmour, A. R., and Gogel, B. J. (2009). *Analysis of mixed models for S language environments: ASReml-R reference manual* (Brisbane: DPI Publications).

Cullis, B. R., Smith, A. B., and Coombes, N. E. (2006). On the design of early generation variety trials with correlated data. *J. Agri. Biol. Environ. Stat.* 11, 381–393. doi: 10.1198/108571106X154443

Dolferus, R., Ji, X., and Richards, R. A. (2011). Abiotic stress and control of grain number in cereals. *Plant Sci.* 181, 331–341. doi: 10.1016/j.plantsci.2011.05.015

Dong, Y., Liu, J., Zhang, Y., Geng, H., Rasheed, A., Xiao, Y., et al. (2016). Genome-wide association of stem water soluble carbohydrates in bread wheat. *PLoS One* 11, 11. doi: 10.1371/journal.pone.0164293

Fabian, A., Safran, E., Szabo-Eitel, G., Barnabas, B., and Jager, K. (2019). Stigma functionality and fertility are reduced by heat and drought co-stress in wheat. *Front. Plant Sci.* 10, 244. doi: 10.3389/fpls.2019.00244

Fleury, D., Jefferies, S., Kuchel, H., and Langridge, P. (2010). Genetic and genomic tools to improve drought tolerance in wheat. *J. Exp. Bot.* 61, 3211–3222. doi: 10.1093/jxb/erq152

Food and Agriculture Organization of the United Nations (FAO). (2018). Food Outlook. Biannual report on the global food markets. Available at: http://www.fao.org/3/CA0239EN/ca0239en.pdf (Accessed May 20, 2019).

Food and Agriculture Organization of the United Nations (FAO). (2019). World food situation. Available at: http://www.fao.org/worldfoodsituation/csdb/en/ (Accessed May 26, 2019).

Furbank, R. T., and Tester, M. (2011). Phenomics – technologies to relieve the phenotyping bottleneck. *Trends Plant Sci.* 16, 635–644. doi: 10.1016/j.tplants.2011.09.005

Gao, F., Wen, W., Liu, J., Rasheed, A., Yin, G., Xia, X., et al. (2015). Genome-wide linkage mapping of QTL for yield components, plant height and yield-related physiological traits in the Chinese wheat cross Zhou 8425B/Chinese Spring. *Front. Plant Sci.* 6, 1099. doi: 10.3389/fpls.2015.01099

Gao, F., Liu, J., Yang, L., Wu, X., Xiao, Y., Xia, X., et al. (2016). Genome-wide linkage mapping of QTL for physiological traits in a Chinese wheat population using the 90k SNP array. *Euphytica* 209, 789–804. doi: 10.1007/s10681-016-1682-6

Garcia, M., Eckermann, P., Haefele, S., Satija, S., Sznajder, B., Timmins, A., et al. (2019). Genome-wide association mapping of grain yield in a diverse collection of spring wheat (*Triticum aestivum* L.) evaluated in southern Australia. *PLoS One* 14, 2. doi: 10.1371/journal.pone.0211730

Gbegbelegbe, S., Cammarano, D., Asseng, S., Robertson, R., Chung, U., Adam, M., et al. (2016). Baseline simulation for global wheat production with CIMMYT mega-environment specific cultivars. *Field Crops Res.* 202, 122–135. doi: 10.1016/j.fcr.2016.06.010

Gupta, A. K., Kaur, K., and Kaur, N. (2011). Stem reserve mobilization and sink activity in wheat under drought conditions. *Am. J. Plant Sci.* 2, 70–77. doi: 10.4236/ajps.2011.21010

Hamblin, M. T., Buckler, E. S., and Jannink, J. L. (2011). Population genetics of genomics-based crop improvement methods. *Trends Genet.* 27, 98–106. doi: 10.1016/j.tig.2010.12.003

International Wheat Genome Sequencing Consortium (IWGSC). (2018). Shifting the limits in wheat research and breeding using a fully annotated reference genome. *Science* 361, 6403. doi: 10.1126/science.aar7191

Izanloo, A., Condon, A. G., Langridge, P., Tester, M., and Schnurbusch, T. (2008). Different mechanisms of adaptation to cyclic water stress in two South Australian bread wheat cultivars. *J. Exp. Bot.* 59, 3327–3346. doi: 10.1093/jxb/ern199

Lipka, A. E., Tian, F., Wang, Q., Peiffer, J., Li, M., Bradbury, P. J., et al. (2012). GAPIT: genome association and prediction integrated tool. *Bioinf. Appl. Note* 28, 2397–2399. doi: 10.1093/bioinformatics/bts444

Lopes, M. S., Dreisigacker, S., Peña, R. J., Sukumaran, S., and Reynolds, M. P. (2015). Genetic characterization of the wheat association mapping initiative (WAMI) panel for dissection of complex traits in spring wheat. *Theor. Appl. Genet.* 128, 453–464. doi: 10.1007/s00122-014-2444-2

Maccaferri, M., Sanguineti, M. C., Corneti, S., Araus, J. L., Ben Salem, M., Bort, J., et al. (2008). Quantitative trait loci for grain yield and adaptation of durum wheat (*Triticum durum* Desf.) across a wide range of water availability. *Genetics* 178, 489–511. doi: 10.1534/genetics.107.077297

Mahrookashani, A., Siebert, S., Hüging, H., and Ewert, F. (2017). Independent and combined effects of high temperature and drought stress around anthesis on wheat. *J. Agron. Crop Sci.* 203, 453–463. doi: 10.1111/jac.12218

Mason, R. E., Addison, C. K., Babar, A., Acuna, A., Lozada, D., Subramanian, N., et al. (2018). Diagnostic markers for vernalization and photoperiod loci improve genomic selection for grain yield and spectral reflectance in wheat. *Crop Sci.* 58, 242–252. doi: 10.2135/cropsci2017.06.0348

Muqaddasi, Q. H., Brassac, J., Börner, A., Pillen, K., and Röder, M. S. (2017). Genetic architecture of anther extrusion in spring and winter wheat. *Front. Plant Sci.* 8, 754. doi: 10.3389/fpls.2017.00754

Ogbonnaya, F. C., Rasheed, A., Okechukwu, E. C., Jighly, A., Makdis, F., Wuletaw, T., et al. (2017). Genome-wide association study for agronomic and physiological traits in spring wheat evaluated in a range of heat prone environments. *Theor. Appl. Genet.* 130, 1819–1835. doi: 10.1007/s00122-017-2927-z

Passioura, J. B. (2006). The perils of pot experiments. *Funct. Plant Biol.* 33, 1075–1079. doi: 10.1071/FP06223

Pinto, R. S., Reynolds, M. P., Mathews, K. L., McIntyre, C. L., Olivares-Villegas, J. J., and Chapman, S. C. (2010). Heat and drought adaptive QTL in a wheat population designed to minimize confounding agronomic effects. *Theor. Appl. Genet.* 121, 1001–1021. doi: 10.1007/s00122-010-1351-4

Prasad, P. V. V., Pisipati, S. R., Momcilovic, I., and Ristic, Z. (2011). Independent and combined effects of high temperature and drought stress during grain filling on plant yield and chloroplast EF-Tu expression in spring wheat. *J. Agron. Crop Sci.* 197, 430–441. doi: 10.1111/j.1439-037X.2011.00477.x

Qaseem, M. F., Qureshi, R., Muqaddasi, Q. H., Shaheen, H., Kousar, R., and Röder, M. S. (2018). Genome-wide association mapping in bread wheat subjected to independent and combined high temperature and drought stress. *PLoS One* 13, 6. doi: 10.1371/journal.pone.0199121

Qaseem, M. F., Qureshi, R., Shaheen, H., and Shafqat, N. (2019). Genome-wide association analyses for yield and yield-related traits in bread wheat (*Triticum aestivum* L.) under pre-anthesis combined heat and drought stress in field conditions. *PLoS One* 14, 3. doi: 10.1371/journal.pone.0213407

Rebetzke, G. J., Fischer, R. A., van Herwaarden, A. F., Bonnett, D. G., Chenu, K., Rattey, A. R., et al. (2014). Plot size matters: interference from intergenotypic competition in plant phenotyping studies. *Funct. Plant Biol.* 41, 107–118. doi: 10.1071/FP13177

Schillinger, W. F., Schofstoll, S. E., and Alldredge, J. R. (2008). Available water and wheat grain yield relations in a Mediterranean climate. *Field Crops Res.* 109, 45–49. doi: 10.1016/j.fcr.2008.06.008

Shi, W., Hao, C., Zhang, Y., Cheng, J., Zhang, Z., Liu, J., et al. (2017). A combined association mapping and linkage analysis of kernel number per spike in common wheat (*Triticum aestivum* L.). *Front. Plant Sci.* 8, 1412. doi: 10.3389/fpls.2017.01412

Shirdelmoghanloo, H., Taylor, J. D., Lohraseb, I., Rabie, H., Brien, C., Timmins, A., et al. (2016). A QTL on the short arm of wheat (*Triticum aestivum* L.) chromosome 3B affects the stability of grain weight in plants exposed to a brief heat shock early in grain filling. *BMC Plant Biol.* 16, 100. doi: 10.1186/s12870-016-0784-6

Storey, J. D., and Tibshirani, R. (2003). Statistical significance for genomewide studies. *PNAS* 100, 9440–9445. doi: 10.1073/pnas.1530509100

Sukumaran, S., Dreisigacker, S., Lopes, M., Chavez, P., and Reynolds, M. P. (2015). Genome-wide association study for grain yield and related traits in an elite spring wheat population grown in temperate irrigated environments. *Theor. Appl. Genet.* 128, 353–363. doi: 10.1007/s00122-014-2435-3

Sukumaran, S., Reynolds, M. P., and Sansaloni, C. (2018). Genome-wide association analyses identify QTL hotspots for yield and component traits in durum wheat grown under yield potential, drought, and heat stress environments. *Front. Plant Sci.* 9, 81. doi: 10.3389/fpls.2018.00081

Sun, G., Zhu, C., Kramer, M. H., Yang, S. S., Song, W., Piepho, H. P., et al. (2010). Variation explained in mixed-model association mapping. *Heredity* 105, 333–340. doi: 10.1038/hdy.2010.11

Sun, C., Zhang, F., Yan, X., Zhang, X., Dong, Z., Cui, D., et al. (2017). Genome-wide association study for 13 agronomic traits reveals distribution of superior alleles in bread wheat from the Yellow and Huai Valley of China. *Plant Biotechnol. J.* 15, 953–969. doi: 10.1111/pbi.12690

Toreti, A., Cronie, O., and Zampieri, M. (2019). Concurrent climate extremes in the key wheat producing regions of the world. *Sci. Rep.* 9, 5493. doi: 10.1038/s41598-019-41932-5

Tricker, P. J., ElHabti, A., Schmidt, J., and Fleury, D. (2018). The physiological and genetic basis of combined drought and heat tolerance in wheat. *J. Exp. Bot.* 69, 3195–3210. doi: 10.1093/jxb/ery081

Valluru, R., Reynolds, M. P., Davies, W. J., and Sukumaran, S. (2017). Phenotypic and genome-wide association analysis of spike ethylene in diverse wheat genotypes under heat stress. *New Phytol.* 214, 271–283. doi: 10.1111/nph.14367

Wang, S., Wong, D., Forrest, K., Allen, A., Chao, S., Huang, B. E., et al. (2014). Characterization of polyploid wheat genomic diversity using a high-density 90,000 single nucleotide polymorphism array. *Plant Biotechnol. J.* 12, 787–796. doi: 10.1111/pbi.12183

Wang, S. X., Zhu, Y. L., Zhang, D. X., Shao, H., Liu, P., Hu, J. B., et al. (2017). Genome-wide association study for grain yield and related traits in elite wheat varieties and advanced lines using SNP markers. *PLoS One* 12, 11. doi: 10.1371/journal.pone.0208217

Watson-Haigh, N. S., Suchecki, R., Kalashyan, E., Garcia, M., and Baumann, U. (2018). DAWN: a resource for yielding insights into the diversity among wheat genomes. *BMC Biol.* 19, 941. doi: 10.1186/s12864-018-5228-2

Wickham, H. (2016). *Ggplot2: Elegant graphics for data analysis* (New York: Springer-Verlag). doi: 10.1007/978-3-319-24277-4_9

Wilhelm, E. P., Turner, A. S., and Laurie, D. A. (2009). Photoperiod insensitive *Ppd-A1a* mutations in tetraploid wheat (*Triticum durum* Desf.). *Theor. Appl. Genet.* 118, 285–294. doi: 10.1007/s00122-008-0898-9

Yan, L., Helguera, M., Kato, K., Fukuyama, S., Sherman, J., and Dubcovsky, J. (2004). Allelic variation at the *VRN-1* promoter region in polyploid wheat. *Theor. Appl. Genet.* 109, 1677–1686. doi: 10.1007/s00122-004-1796-4

Zadoks, J. C., Chang, T. T., and Konzak, C. F. (1974). A decimal code for the growth stages of cereals. *Weed Res.* 14, 415–421. doi: 10.1111/j.1365-3180.1974.tb01084.x

Zampieri, M., Ceglar, A., Dentener, F., and Toreti, A. (2017). Wheat yield loss attributable to heat waves, drought and water excess at the global, national and subnational scales. *Environ. Res. Lett.* 12, 6. doi: 10.1088/1748-9326/aa723b

Zanke, C. D., Ling, J., Plieske, J., Kollers, S., Ebmeyer, E., Korzun, V., et al. (2014). Whole genome association mapping of plant height in winter wheat (*Triticum aestivum* L.). *PLoS One* 9, 11. doi: 10.1371/journal.pone.0113287

Zanke, C. D., Ling, J., Plieske, J., Kollers, S., Ebmeyer, E., Korzun, V., et al. (2015). Analysis of main effect QTL for thousand grain weight in European winter wheat (*Triticum aestivum* L.) by genome-wide association mapping. *Front. Plant Sci.* 6, 644. doi: 10.3389/fpls.2015.00644

Zhang, L. Y., Liu, D. C., Guo, X. L., Yang, W. L., Sun, J. Z., Wang, D. W., et al. (2010). Genomic distribution of quantitative trait loci for yield and yield-related traits in common wheat. *J. Integr. Plant Biol.* 62, 996–1007. doi: 10.1111/j.1744-7909.2010.00967.x

Zhu, C., Gore, M., Buckler, E. S., and Yu, J. (2008). Status and prospects of association mapping in plants. *Plant Genome* 1, 5–20. doi: 10.3835/plantgenome2008.02.0089

Conflict of Interest: The authors declare that the research was conducted in the absence of any commercial or financial relationships that could be construed as a potential conflict of interest.

Chapter 3

Transcripts of wheat at a target locus on chromosome 6B associated with increased yield, water use and photosynthetic capacity under combined drought and heat stress

Link to Chapter 3

The aim of this study was to validate a QTL located on the long arm of chromosome 6B, which was associated with seed weight, single seed weight and harvest index for the heat response under drought as well as with screenings (% small seed weight) under drought in the genome-wide association study (Chapter 2). The QTL had also been identified by two former studies under controlled and field conditions. We developed near-isogenic lines for the target region on chromosome 6B and evaluated them under drought and heat stress in glasshouse conditions. This experiment generated results that could help future studies aiming at identifying important tolerance mechanisms associated with drought and heat stress tolerance at this locus, which could potentially be used as target traits in breeding. A gene expression analysis of developing grains was carried out to reduce the number of candidate genes associated with the QTL.

Transcripts of wheat at a target locus on chromosome 6B associated with increased yield, water use and photosynthetic capacity under combined drought and heat stress

Jessica Schmidt[1], Melissa Garcia[1], Chris Brien[1,2], Priyanka Kalambettu[1], Trevor Garnett[2,3], Delphine Fleury[1,4], Penny J Tricker[1]*

[1]School of Agriculture, Food and Wine, The University of Adelaide, Adelaide, South Australia, Australia

[2]The Plant Accelerator, Australian Plant Phenomics Facility, The University of Adelaide, Adelaide, South Australia, Australia

[3]Grains Research and Development Corporation, Adelaide, South Australia, Australia

[4]Innolea, Mondonville, France

* Corresponding author

Penny.tricker@adelaide.edu.au

Abstract

Drought and heat stress constrain wheat yields globally. To identify putative mechanisms and candidate genes associated with combined drought and heat stress tolerance, bread wheat (*Triticum aestivum* L.) near-isogenic lines (NILs) targeting a quantitative trait locus (QTL) on chromosome 6B were developed. Genotyping-by-sequencing was used to identify additional regions that segregated in allelic pairs between the recurrent and the introduced exotic parent, genome-wide. NILs were phenotyped in a gravimetric platform with precision irrigation and exposed to either drought or to combined drought and heat stress from three days after anthesis. An increase in seed weight was associated with thicker leaves, higher photosynthetic capacity and increased water use efficiency. RNA sequencing of developing grains at early and later stages of treatment revealed 75 genes that were differentially expressed between NILs across both treatments and timepoints. Differentially expressed genes coincided with the targeted QTL and regions of genetic segregation on chromosomes 1B, 6B and 7A. Pathway enrichment analysis showed the involvement of these genes in cell and gene regulation, metabolism of amino acids and transport of carbohydrates. The majority of these genes have not been previously characterized under drought or heat stress and they might serve as candidate genes for improved abiotic stress tolerance.

Introduction

Climate change is a threat to future food security. Prolonged drought periods and heatwaves are predicted to become more common by the end of the century having a major impact on economically important crops such as wheat (Trnka et al. 2014, Toreti et al. 2019). Heatwaves in 2003, 2010, 2018 and 2019 broke temperature records across Europe, with 2019 one of the hottest and driest summer ever recorded (Miralles et al. 2014, Albergel et al. 2019, Mitchell et al. 2019). Yield losses of up to 40% (corresponding to 1 million tonnes) were recorded in France, one of the biggest wheat producers in Europe (Zampieri et al. 2017). In Australia, nine of the ten warmest years on record have occurred since 2005 with rainfall and wheat yields below average, so that the climate was both hot and dry (FAO 2019a, FAO 2019b). To minimize yield losses and to keep up with future food demand, the development of climate resilient wheat varieties is required.

One way to develop more resilient crops is the identification and integration of quantitative trait loci (QTL) and the underlying genes associated with abiotic stress tolerance. QTL have been identified for yield in low-yielding growth environments experiencing drought, heat or combined drought and heat stress (reviewed in Tricker et al. 2018). However, phenotyping for grain yield on its own might not be enough to contribute significantly to cultivar improvement given the complexity of the genetic control of stress tolerance (i.e., multigenic, low heritability with high genotype by environment interactions) (Fleury et al. 2010, Mir et al. 2012). The dissection of these QTL into their component physiological traits, which then can serve as target traits for breeding in dry and hot climates, is of similar importance. Potential key traits that have been suggested for drought and heat stress tolerance are the regulation of the water use in plants and the adaption of photosynthetic assimilation to improve radiation use efficiency (Blum et al. 2005, Cossani and Reynolds 2012, Tricker et al. 2018).

Differentially expressed candidate genes under combined drought and heat stress have been identified in tetraploid durum wheat. Combined drought and heat stress triggered the expression of genes encoding trans-membrane proteins, as well as proteins involved in fatty acid β- oxidation (Aprile et al. 2013, Sukumaran et al. 2018). In bread wheat, significant genetic marker-trait associations were identified under combined drought and heat stress on group 7 chromosomes and were associated with phytoene synthase 1, integral membrane glycoproteins and a protein conferring rust resistance (Qaseem et al. 2018).

We developed lines (NILs) that targeted a QTL on the long arm of chromosome 6B of hexaploid bread wheat (*Triticum aestivum* L.). The QTL (*QYld.aww-6B.1*) had previously been

identified in three independent studies. In semi-controlled conditions (Schmidt et al. 2020), the allele predominantly occurring in Asian accessions contributed to higher total seed weight per plant, single seed weight and harvest index for the heat response under drought, while decreasing screenings (% small seed weight) under drought. However, a different effect was observed in hot conditions in the field with the Asian allele reducing harvest index (Garcia et al. 2019). In controlled conditions (Shirdelmoghanloo et al. 2016), the QTL was associated with single seed weight and leaf chlorophyll content following heat stress and for the heat susceptibility index. To find candidate genes associated with the QTL, we performed a gene expression analysis of developing grains collected during early and late drought as well as with drought and heat stress during the grain-filling period. Further, by studying physiological traits such as water use and photosynthesis, we aimed to identify important tolerance mechanisms associated with drought and heat stress tolerance at this locus, which could potentially be used as target traits in crop breeding.

Materials and Methods

Plant material

NILs targeting the *QYld.aww-6B.1* were developed from an existing nested association mapping population. The nested-association mapping population consisted of 73 diverse ('exotic') donors which were crossed with two recurrent ('non-exotic') Australian varieties (cvs. Gladius and Scout), back-crossed with the corresponding recurrent parent and selfed over three generations. 772 recombinant inbred lines of 34 families at BC1F4 were genotyped with the SNP marker "BobWhite_c27364_296" (S1 Table: https://adelaide.figshare.com/s/9f2685cd67f71860520e). The development of molecular markers and genotyping was performed using Kompetitive Allele Specific Polymerase Chain Reaction (KASP^{TM}) technology. Subsequently, the selected SNP marker was used to genotype 663 single seed descendants from heterozygous recombinant inbred lines (BC1F5), identifying pairs of NILs carrying the allele from either the non-exotic or exotic parent at the target region. Additional molecular markers developed in-house (S1 Table: https://adelaide.figshare.com/s/9f2685cd67f71860520e) revealed a NIL pair, resulting from a cross between the Australian variety 'Gladius' and the Algerian variety 'Taferstat'. Seeds (BC1F6) for each line, derived from a single plant, were used for phenotyping and genotyping. DNA of two seedlings of each line was isolated using the DNeasy 96 Plant Kit (Qiagen,

Germany) according to the manufacturer's instructions, of which one sample carrying the non-exotic allele failed (S2 Table: https://adelaide.figshare.com/s/9f2685cd67f71860520e, Fig 1). DNA of two additional samples from plants carrying the non-exotic allele was isolated (as before) of which one was similar (sample ID: 22) and one different in its phenotype (sample ID: B23, reduced biomass and plant height) in comparison to the other replicates. A targeted genotyping by sequencing (tGBS) analysis based on data from the 90k SNP Illumina array was carried out, resulting in 9,424 markers which contained no missing values and could be mapped to a unique position within the bread wheat 'Chinese Spring' reference genome sequence, RefSeq v1.0 (IWGSC et al., 2018).

Fig 1. Illustration of segregating regions within near-isogenic lines at BC1F6 carrying either the allele donated by the non-exotic (Gladius) or exotic (Taferstat) parent at the target region on chromosome 6B (marked in green). Additional regions of segregation were observed on chromosomes 1B and 7A (marked in blue). Regions on chromosomes 1B, 3B, 4A and 7A, which appear to segregate between replicates, are marked in blue-grey. NILs were homozygous for the remaining 16 chromosomes.

Plant growth conditions

Growth chamber and glasshouse conditions

Both NIL allele pairs carried winter alleles at the vernalization gene *Vrn-A1* and were therefore vernalized according to Boyd et al. (2003). For vernalization, 32 seeds were initially germinated for 24 hours in jiffy pots at room temperature (20 ^{o}C) in a reach-in chamber, followed by 4 weeks at 4-8 ^{o}C with a 2-hour photoperiod (2h/22h day/night) and well-watered conditions. At the end of vernalization, sixteen seedlings of each line were transferred to plastic pots together with their jiffy pot and placed on balances in a gravimetric platform (Droughtspotter, Phenospex, Netherlands) which recorded pot weight at 30 min intervals, with precision irrigation. Plastic pots (240 mm high x 165 mm diameter) were filled with 3.5 kg dry weight of a soil mix (1: 1: 1, coco peat-based potting mix: clay loam paddock soil: sand), supplemented with a slow-release fertilizer and covered with a double layer of foam mesh to minimize evaporation. A metal frame was placed around each plant for support. The combinations of sampling dates, treatments and lines were randomized to pots in the glasshouse according to a triple-split-unit design with four biological replicates. Each replicate block was divided into two areas, each of which was, in turn, divided into two subareas. The two sampling dates (i.e. during treatment and at maturity) were randomized to the areas within replicates and

the two treatments (i.e. drought or combined drought and heat) were randomized to the two subareas within each area. The lines were randomized to the pots within an area so that NIL allele pairs occurred together. Pots were manually irrigated and adjusted to their target weight corresponding to 20 % soil water content and -0.44 MPa (S1 Fig) during the first two weeks and then automatically irrigated whenever the pot weight dropped 0.5 % below target weight. Temperatures in the glasshouse were set to 22/15 ºC day/night with a 16 hours day length period and supplemental LED lighting providing approximately 400 μmoles.m^2.s^{-1} at the canopy.

Drought and heat treatment

Plants were grown under well-watered conditions (20 % soil moisture) except for a 9-day drought period commencing three days after anthesis. Drought was imposed by lowering the target weight to 12 % soil water content, corresponding to -0.72 MPa (S1 Fig). Half of the plants were additionally subjected to heat stress (combined drought and heat) by transferring them to a neighbouring glasshouse with 35/25 ºC day/night and similar light settings during the last three days of the drought period. During the heat treatment, plants were irrigated manually to the target weight four times a day. After nine days, plants were moved back to their spot on the gravimetric platform and kept under well-watered conditions until reaching physiological maturity. Transfer of pots and changes in treatments were carried out daily at 8:00 am to maintain a consistent treatment period. Water use, temperature and relative humidity were recorded at 30 min intervals in both gravimetric and neighbouring glasshouses throughout (S2 Fig).

Plant phenotyping

Flowering time, defined as the first anther extrusion of the primary tiller, was scored daily for all plants. Four of the replicates of each line were used for physiological measurements during growth and harvested at maturity, while the other four were used for ribonucleic acid (RNA) sequence analysis (i.e. harvest during treatment). Hyperspectral reflectance measurements (350-2500 nm) were taken daily between 10:30 am and 12:00 pm in the centre of the flag leaf of the primary tiller from anthesis till three days after treatment (0-14 days after anthesis, DAA) using the ASD FieldSpec 3 portable spectroradiometer (Malvern Panalytical, United Kingdom). To transform the obtained wavelength into values of physiological traits, the data were uploaded to the wheat physiology predictor website (Silva-Perez et al. 2017, Coast et al. 2019, Silva-Perez and Ivakov 2019). Physiological traits obtained from hyperspectral

measurements included leaf dry mass per area, chlorophyll index, photosynthetic capacity (normalized to 25 °C), electron transport capacity and mitochondrial respiration rate (normalized to leaf dry mass).

At physiological maturity, plant height of the primary tiller of the four replicates of each NIL was measured as the distance between the base of the stem and the top of the spike excluding awns. Spike length was measured from the base of the first spikelet to the tip of the last spikelet of the primary tiller. The number of spikes per plant was counted. Samples were dried at 37 °C for 10 days and total above-ground biomass per plant was determined including stems, leaves and spikes of all tillers. Seed traits per primary tiller and for the remainder of the spikes were analysed separately. To differentiate between small (< 2.0 mm) and large seeds (> 2.0 mm) a wheat grain sieve (2.0 mm, Graintec, Australia) was used. Seed weight and seed number were determined for seeds > 2.0 mm. Single seed weight was measured as the average of seed weight divided by the number of seeds. Screenings was defined as the difference in percentage of small seed (< 2.0 mm) compared to total seed weight.

Statistical data analysis of phenotypic traits

Means were estimated using the R packages ASReml (Butler et al. 2009) and asremlPlus (Brien 2019). Data for the screenings trait were transformed for normalisation and the statistical significance of differences between NIL pairs and with treatments for all traits were analysed by ANOVA. Random effects for subareas and pairs were included in the model for each harvest time and the variance was allowed to differ between the two treatments. P-values to estimate potential differences between NILs for each trait and treatment were calculated using the Wald test for fixed effects. Days from planting to anthesis and plant height were not significantly associated with yield-related traits and therefore not included as covariates. The average daily water consumption was estimated over three consecutive multiple-days periods: during the first six days of drought (3-8 DAA), during the last three days of drought or combined drought and heat stress (9-11 DAA) and during recovery (12-42 DAA). The daily water use efficiency was calculated by dividing the above-ground biomass measured at maturity by the average daily water consumption during these periods. Physiological traits were assessed across four time-periods: during pre-treatment (0-2 DAA), during the first six days of drought (3-8 DAA), during the last three days of drought or combined drought and heat stress (9-11 DAA) and during the first two days of recovery (12-14 DAA). As there were no significant differences between drought or drought and heat treatment groups prior to the heat treatment (0-8 DAA),

values for water consumption, water use efficiency and other physiological traits were estimated together, independent from the following treatment.

RNA sequencing

Sampling and RNA isolation

The first two spikelets of the primary tiller with extruding anthers were marked at anthesis. For RNA sequencing, two developing grains from the two spikelets were collected on the fifth day of drought treatment (i.e. eight days after anthesis (8 DAA), spikelet number one) and on the last day of either drought or combined drought and heat treatment (i.e. 11 days after anthesis (11 DAA), spikelet number two), snap frozen using liquid nitrogen and stored at -80 °C. All samples were collected between 10:00 and 11:00 am. A total of four replicates per line, treatment and time point were collected. RNA was isolated using the Spectrum Plant Total RNA kit (Sigma-Aldrich, United States) including alpha-amylase (E-BLAAM 54.0 U/mg, Megazyme, United States) and DNAse (On-Column DNase I Digestion Set, Sigma-Aldrich, United States) treatments. Samples were further purified using the RNA Clean & Concentrator-5 kit (Zymo Research, United States) according to the manufacturer's instructions. Samples were subsequently sent for quality check (Agilent Bioanalyzer 2100, Agilent Technologies, United States) and concentration measurement (Qubit 2.0 fluorometer, Thermo Fisher Scientific, United States) to the ACRF Cancer Genomics Facility (Adelaide, Australia). 15 samples with RNA integrity number (RIN) of at least 8.9 collected at 11 DAA (four replicates per treatment and line, except for one sample where RNA extraction failed) and eight samples collected 8 DAA were sent for sequencing and data analysis to NovoGene (Beijing, China). One additional sample collected 8 DAA (ID: B23, sample name: D8_AA4) was included because it differed in its phenotype from the other replicates (i.e. reduced plant height and biomass).

RNA sequencing

Following quality check of the RNAs, mRNA was enriched using oligo beads, followed by a random fragmentation and a single and then double stranded complementary deoxyribonucleic acid (cDNA) synthesis. Further steps including purification, terminal repair, poly-A-tailing, ligation of sequencing adapters, fragments selection and polymerase chain reaction (PCR) enrichment were performed to obtain the final cDNA libraries. Library concentration was first quantified using a Qubit 2.0 fluorometer and then diluted to 1 ng/µl before checking insert size

on an Agilent Bioanalyzer 2100 and quantifying to greater accuracy by quantitative PCR. RNA sequences were obtained through the Illumina sequencing platform (Illumina, United States).

Data analysis

Raw data output from Illumina were transformed to sequence reads by base calling and recorded in a FASTQ file. Initial quality checks included an estimation of error rates for each base along reads and guanine-cytosine content distribution, followed by the removal of reads containing adapters or which were of low quality. After the quality checks, sequences were mapped against the IWGSC reference genome version 2 (https://wheat-urgi.versailles.inra.fr/Seq-Repository/Assemblies) using the hierarchical indexing for spliced alignment of transcripts (HISAT) (Kim et al. 2015) software. Total gene expression was estimated by counting the reads that mapped to genes or exons. Thereby, read count was not only proportional to the actual gene expression level, but also to the gene length and sequencing depth. In order to compare gene expression levels of different genes, the fragments per kilobase of transcript sequence per millions base pairs sequenced (FPKM) were calculated, taking into account the effects of both sequencing depth and gene length (Trapnell et al. 2010). Gene expression levels were analysed using the HTSeq software (Anders et al. 2015). Pearson correlations were calculated to reveal differences in gene expression between samples. Differences in gene expression between treatments, timepoints and alleles including all biological replicates were estimated using the software DESeq (Anders and Huber 2010, Anders and Huber 2012). The resulting P-values were adjusted using the Benjamini and Hochberg's approach for controlling the false discovery rate. Genes with an adjusted P-value <0.05 were assigned as differentially expressed.

Genes with similar expression patterns were clustered together and represented in a heat plot. Gene ontology (http://www.geneontology.org/) enrichment analysis of differentially expressed genes was carried out using the GOseq software (Young et al. 2010) based on the Wallenius non-central hyper-geometric distribution. To assign the differentially expressed genes to their putative biological function and pathway, a Kyoto Encyclopedia of Genes and Genomes (KEGG, https://www.genome.jp/kegg/kegg2.html) pathway enrichment analysis was conducted using *Oryza sativa japonica* as a reference genome. We used KOBAS software to test the statistical enrichment of differential expression genes in KEGG pathways. Genes which were differentially expressed between NILs across treatments and timepoints were aligned to the International Wheat Genome Sequencing Consortium (IWGSC) Chinese Spring (CS)

RefSeq v1.0 [38] using BLASTN with an e-value cutoff of 10^{-40} in order to find their putative locations on the wheat genome.

Results

Genotyping by sequencing of near-isogenic lines

Near-isogenic lines (NILs) were developed targeting a QTL interval of ~7 Mbp on the long arm of chromosome 6B. tGBS data of the five NIL pairs at BC1F6 (Fig. 1, S2 Table: https://adelaide.figshare.com/s/9f2685cd67f71860520e) indicated 93.7 % similarity between NILs segregating for ~17 Mbp, including the target region, on chromosome 6B (RefSeq v1.0). Further segregating regions were detected on chromosomes 1B and 7A. NILs carrying the non-exotic allele (Gladius) were 95.7 % similar to each other and segregated on chromosomes 1B and 4A. NILs carrying the exotic allele from Taferstat were heterozygous for regions on chromosomes 1B, 3B and 7A with a genotypic similarity of 96.1 %. As expected, NILs segregating for the target region were genotypically more different than replicates of the same NIL. Genetic differences between replicates (3.7-4.5 %) could be due residual heterozygosity of the plants which were selected and separately propagated from BC1F5.

Plant growth conditions

Environmental conditions were fairly consistent during the vegetative stage and the crucial experimental period of July and August (-50 to 45 DAA) with maximum and minimum temperatures of 22.0-24.9 and 13.4-15.8 ºC during day and night, respectively, in the unheated treatment (S2 Fig). Maximum temperatures increased towards the end of the experiment up to 30 ºC, when plants were maturing (from 48 DAA onwards). Temperatures during the heat treatment reached 33.5-35.3 ºC maximum during the day and 23.5-24.5 ºC minimum at night. On average, pots reached the targeted drought level of 12 % soil water content after 3.5 days of withholding irrigation.

Phenotypic data

Water use

Average daily water use ranged from 71.0 to 139.7 ml per day during the treatment and recovery period. Daily water use efficiency ranged between 0.55 and 0.66 g biomass ml^{-1} day^{-1} during the drought treatment, but was reduced during the combined drought and heat treatment and during recovery after both treatments (0.32-0.39 and 0.37-0.46 g biomass ml^{-1}

day^{-1}, respectively). On average, plants exposed to drought decreased their water use 52 DAA (i.e., 41 days after treatment), whereas plants exposed to the combined drought and heat treatment reduced their water use 36 days after treatment.

The average water use per day was higher in NILs carrying the exotic allele in comparison to NILs carrying the non-exotic allele throughout the drought treatment and the following recovery period ($p < 0.012$) (Fig 2). Under combined drought and heat stress, daily water use was similar among NILs during treatment, but differed during recovery with NILs carrying the exotic allele consuming on average 5.6 ml less water per day. Daily water use efficiency was increased in NILs carrying the exotic allele during the combined drought and heat treatment ($p = 0.004$) as well as during recovery following both treatments ($p \leq 0.001$) compared with NIL carrying the non-exotic allele.

Fig 2. Predicted means of daily water use and daily water use efficiency (WUE) of near-isogenic lines under drought and combined drought and heat stress. Grey = the non-exotic allele, green = exotic allele. *, ** and *** indicate statistical significance between near-isogenic lines at $p \leq 0.05$, $p \leq 0.01$ and $p \leq 0.001$, respectively, based on Wald test. Error bars are standard error of the mean. n = 8 for traits measured during the first six days of drought treatment (3-8 days after anthesis); n=4 for traits measured from 9 days after anthesis on (i.e. 9-11 and 12-42 days after anthesis). D, drought; DH, drought and heat stress; g_{BM}, g above-ground biomass at maturity.

Photosynthesis-related traits

Chlorophyll index and leaf mass per unit of area were relatively stable throughout the whole measurement period, except for a peak in dry mass during the combined drought and heat treatment (Fig 3). Photosynthetic and electron transport capacity declined slightly over time (0-14 DAA) under drought in both NILs, while the highest capacity was recorded during the combined drought and heat treatment. NILs carrying the exotic allele had increased leaf dry mass in comparison to NILs carrying the non-exotic allele under both drought ($p = <0.013$) and combined drought and heat stress ($p \leq 0.05$) Photosynthetic capacity (Vcmax) was higher in the line carrying the exotic allele during the combined drought and heat treatment ($p \leq 0.05$) but not with drought stress or during recovery, and electron transport capacity (J) did not differ with allele in either treatment. Mitochondrial respiration rate was similar over the measurement period and between NILs carrying the alternate alleles, in both treatments.

Fig 3. Photosynthesis-related traits of near-isogenic lines carrying the non-exotic (grey) or exotic (green) allele at the target region on chromosome 6B under drought and combined drought and heat. *, ** and *** indicate statistical significance between near-isogenic lines at $p \leq 0.05$, $p \leq 0.01$ and $p \leq 0.001$, respectively, based on Wald test. Error bars represent standard error of the mean. n = 8 for traits measured during pre-treatment (Pre) (i.e. 0-2 days of anthesis) and first phase of drought treatment (3-8 days after anthesis); n=4 for traits measured from 9 days after anthesis on (i.e. 9-11 and 12-14 days after anthesis). D, drought; DH, drought and heat stress; g_{DM}, g dry mass; J, electron transport capacity; Vcmax, photosynthetic capacity.

Yield-related traits

NILs carrying the exotic allele at the target region on chromosome 6B (NIL pair 6B-1) flowered, on average, two days earlier ($p = 0.046$) in comparison to NILs carrying the non-exotic allele (Fig 4). Similarly, plant height and biomass were promoted by the exotic allele under drought ($p \leq 0.021$) and plant height under combined drought and heat ($p = 0.014$) with increases of 5.1-9.8 cm in length. However, neither flowering time nor plant height were significantly associated with biomass or any of the yield components. Number of spikes, biomass, seed number, single seed weight and seed weight were reduced under combined drought and heat stress in comparison to drought in both NILs, whereas screenings increased. Spike length and plant height were similar in both treatments.

Fig 4. Yield-related traits of near-isogenic lines carrying the non-exotic (grey) or exotic (green) allele at the 6B QTL under drought and combined drought and heat. *, ** and *** indicate statistical significance between near-isogenic lines at $p \leq 0.05$, $p \leq 0.01$ and $p \leq 0.001$, respectively, based on Wald test. Error bars are standard error of the mean. n = 4, except for day to anthesis (n =8). Tiller refers to the primary tiller of the plant. D, drought; DH, drought and heat stress.

Significant differences for the 6B QTL were found in five of the twelve yield component traits. Seed weight, single seed weight and seed number per primary tiller as well as spike length were increased by the allele derived from Taferstat with seed weight, seed number and spike length being increased under both treatments. Seed weight showed the largest increase with 23.4-32.0 % ($p < 0.001$), followed by seed number 24.3-24.4 % ($p = 0.001$-0.002). Single seed weight and spike length were increased by 10.3 % ($p < 0.001$) and 7.4-8.1 % ($p = 0.003$-0.020),

respectively. In addition, screenings per plant was reduced in NILs carrying the exotic allele ($p = 0.003$) in both treatments. Seed weight, single seed weight and seed number per plant showed the same trend as the primary tiller but were not significantly different. Differences in whole plant measurements between NILs might have been buffered by the tendentially smaller number of spikes in NILs carrying the exotic allele.

Gene expression analysis of developing grains

RNA sequencing data were of good quality with 94.73-99.03 % of clean data in each sample. The percentage of mappable reads for all samples was above 70 % (S5 Table: https://adelaide.figshare.com/s/9f2685cd67f71860520e). Most reads could be mapped to exons (57.6-76.2 %), followed by intergenic regions (22.5-41.5 %). The smallest proportion was mapped to intron regions (0.8-2.0 %). Some of the reads were mapped to more than one exon (17.55-26.35 %) potentially due to repetitive DNA within a chromosome or a gene copy on one of the other two homeologous chromosomes. Read densities were similar for the positive and negative strands of each chromosome.

Overall, all samples showed similar gene expression levels with the majority of genes poorly expressed (FPKM interval of 0-1: ≥55.87 % of the total number of genes) (S6 Table: https://adelaide.figshare.com/s/9f2685cd67f71860520e). Genes with a medium to high expression, i.e., FPKM between 1-3, 3-15, 15-60, accounted for 11.31-13.23 %, 19.31-21.68 % and 6.06-7.96 % of the genes, respectively. Genes with a very high expression (FPKM > 60) accounted for 1.80-2.29 % of the genes. Biological replicates were 90-99 % similar in their gene expression (S7 Table: https://adelaide.figshare.com/s/9f2685cd67f71860520e), except for sample "D8_AA4". The sample "D8_AA4" was included as additional sample because of its phenotypic difference (i.e., reduced plant height and biomass) in comparison to the other replicates. Pearson correlations (R^2) between "D8_AA4" and the other replicates collected at 8 DAA carrying the non-exotic alleles ranged between 0.79 and 0.81, at the limit of the suggested threshold of 0.80 for reliable replicates. tGBS data did not reveal any difference in the genome of plants with reduced biomass and plant height in comparison to plants showing the common phenotype. The markers used for tGBS might not have covered the region associated with this phenotype, or an epigenetic modification might be causing this difference. A total of 42,393 genes were similarly expressed in both NILs and treatments. Genes differentially expressed between the two treatments at 11 DAA (Fig 5 - cluster II, IV, VI and VII, S8 Table: https://adelaide.figshare.com/s/9f2685cd67f71860520e) or timepoints (i.e., 8

DAA and 11 DAA) (Fig 5 - cluster I and VIII, S8 Table: https://adelaide.figshare.com/s/9f2685cd67f71860520e) accounted for 5,507 and 28,371 of the genes, respectively. Of these, 2,278 and 10,579 were differentially expressed between treatment or timepoint in both NILs. Genes differing between timepoints were principally involved in plant and grain development such as cell number regulation, DNA repair mechanisms and transport and hydrolysis of sugars (S9-10 Table: https://adelaide.figshare.com/s/9f2685cd67f71860520e).

Fig 5. Hierarchical cluster analysis of differentially expressed genes in developing grains of near-isogenic lines under drought and combined heat (sourced from NovoGene). Samples were collected on the fifth day of treatment (i.e. 8 days after anthesis) when all plants were subjected to drought and on the last day of treatment (i.e. 11 days after anthesis) when plants were subjected to either drought or drought and heat stress. Red, upregulated genes (> 0); blue, downregulated genes (< 0). The colour range from red to blue represents the $\log_{10}$ (FPKM+1) value from large to small.

NILs carrying the exotic allele differed by 3-11% in their number of expressed genes to NILs carrying the non-exotic allele (S7 Table: https://adelaide.figshare.com/s/9f2685cd67f71860520e) with a total of 2,082, 358 and 164 differentially expressed genes under drought at 8 DAA, under drought at 11 DAA and under drought and heat at 11 DAA, respectively. Differentially expressed genes at 8 DAA were mainly located on the long arms of chromosomes 1B (64 genes), 4B (1,037), 6B (37) and 7A (18) and on the short arm of chromosome 4B (763 genes) (S8 Table: https://adelaide.figshare.com/s/9f2685cd67f71860520e). Most of these genes encode proteins which are cellular components of the cytoplasm and the endomembrane system (S9 Table: https://adelaide.figshare.com/s/9f2685cd67f71860520e). Upregulated genes on chromosome 4B in NILs carrying the exotic allele are mostly involved in alanine, aspartate and glutamate metabolism (Fig 6A, S10 Table: https://adelaide.figshare.com/s/9f2685cd67f71860520e). Genes differently expressed between NILs at 11 DAA under drought were similar to those detected at 8 DAA and mostly, but not significantly, associated with cell components (Fig 6B). Differentially expressed genes under combined drought and heat at 11 DAA were dominantly located on the long arms of chromosomes 1B (51 genes), 6B (48 genes) and 7A (16 genes), but only one of the genes was located on chromosome 4B (S8 Table: https://adelaide.figshare.com/s/9f2685cd67f71860520e). Most of these genes encode binding

proteins which are involved in pathways such as glutathione metabolism, plant-pathogen interactions and RNA transport (not significant) (Fig 6C).

Fig 6. Gene ontology (GO) and Kyoto Encyclopedia of Genes and Genomes (KEGG) enrichment analysis of differentially expressed genes in developing grains of near-isogenic line allele pairs under drought at 8 days after anthesis (A), under drought at 11 days after anthesis (B) and under combined drought and heat stress at 11 days after anthesis (C) (sourced from NovoGene). *, significantly enriched (adjusted p-value < 0.05).

A total of 67 high confidence and 8 low confidence genes were differentially expressed between NILs carrying the opposite allele across treatments and timepoints. with 27 of the genes located on the long arms of chromosome 1B (physical positions 330,193,821-583,693,092 bp), 36 genes located on the long arm of chromosome 6B (703,288,889-720,510,790 bp), one gene located on the long arm of chromosome 6D (462,012,557-462,015,085 bp) as well as 3 and 8 genes located on the short (11,422,765-20,486,172 bp) and long arm (635,069,694-681,015,619 bp) of chromosome 7A, respectively (Fig 5 - cluster V, Table 1). 35 genes were upregulated and 40 downregulated in NILs carrying the exotic allele. Both, upregulated and downregulated genes, are involved in cell and gene regulation, protein binding, disease resistance, carbohydrate transport and metabolic pathways. In addition, two of the upregulated genes are associated with the arginine and proline metabolism (TraesCS6B02G456400) as well as with the development of anatomical structures (TraesCS1B02G269500), whereas one of the downregulated genes (TraesCS1B02G288900) is associated with the Golgi vesicle transport and three encode proteins located in the chloroplast.

Table 1. List of genes which were differently expressed between near-isogenic lines of the opposite allele across treatments and timepoints. Positions in base pairs (bp) are based on the RefSeq v2.0 (IWGSC et al., 2018; http://plants.ensembl.org/Triticum_aestivum/Info/Index). Chr, chromosome; down, downregulated genes in NILs carrying the exotic allele; inf, gene which was exclusively expressed in either NIL carrying the non-exotic or exotic allele; log_2, fold change in gene expression; up, upregulated genes in NILs carrying the exotic allele. P-value corresponds to adjusted p-value.

Old gene name	Updated gene name	Chr	Position (bp)	Corresponding protein	Gene regulation	log2	adjusted p-value
Traes_1BL_58A450CB0	TraesCS1B02G356100LC.1	1B	330,055,731-330,057,688	-	down	inf	8.76E-62
Traes_1BL_927C3ED7B	TraesCS1B02G183200	1B	330,193,821-330,218,044	Myosin-8	down	7.62	4.91E-46
Traes_1BL_A54461172	TraesCS1B02G183700	1B	330,501,851-330,504,531	UPF0415 protein C7orf25 homolog	down	1.80	9.24E-08
Traes_1BL_63F0F0FAA	TraesCS1B02G186500	1B	333,595,520-333,597,852	LanC-like protein GCR2	down	4.17	1.15E-09
Traes_1BL_C80BB3B0D	TraesCS1B02G375500LC.1	1B	348,478,933-348,479,535	-	up	7.91	2.57E-25
Traes_1BL_6956EAF2D1	TraesCS1B02G207100	1B	374,328,133-374,330,340	60S ribosomal export protein NMD3	down	3.20	6.27E-30
Traes_1BL_337760BBE	TraesCS1B02G209600	1B	380,461,431-380,467,221	Nuclease related NERD	up	4.08	3.53E-17
Traes_1BL_42FAD5DBE	TraesCS1B02G216300	1B	392,107,116-392,111,653	MLO-like protein 9	up	1.41	1.29E-10
Traes_1BL_1AA872E89	TraesCS1B02G250600	1B	442,622,871-442,626,924	Probable nitronate monooxygenase	down	2.11	4.08E-05
Traes_1BL_9A1A32022	TraesCS1B02G253700	1B	447,323,125-447,327,142	Protein N-terminal asparagine/ glutamine amidohydrolase	up	5.46	7.98E-16
Traes_1BL_D261AE149	TraesCS1B02G466000LC	1B	456,154,491-456,159,954	26S protease regulatory subunit 10B homolog A	up	8.06	3.17E-122
Traes_1BL_2DF3E745A	TraesCS1B02G258800	1B	456,252,451-456,255,472	-	up	1.14	1.02E-03
Traes_1BL_942C3A057	TraesCS1B02G262200	1B	460,578,389-460,581,993	Bax inhibitorI1-like protein	up	2.35	2.04E-27
Traes_1BL_664BABA7A	TraesCS1B02G262600	1B	461,298,262-461,312,532	Probable manganese-transporting ATPase PDR2	up	0.94	1.00E-04
Traes_1BL_5C0E7A70E	TraesCS1B02G269500	1B	473,864,248-473,868,617	Isopentenyl-diphosphate Delta-isomerase	up	1.22	1.03E-03
Traes_1BL_A762B63A2	TraesCS1B02G272900	1B	478,721,054-478,725,344	Protein root UVB sensitive 6	up	7.57	6.59E-152
Traes_1BL_9AE83440A	TraesCS1B02G279200	1B	487,489,192-487,496,862	CRAL-TRIO lipid binding	up	1.92	9.13E-08
Traes_1BL_BE03D01EF	TraesCS1B02G492100LC	1B	488,037,013-488,038,655	Uncharacterized protein	up	2.81	9.09E-33

Table 1. Continued.

Old gene name	Updated gene name	Chr	Position (bp)	Corresponding protein	Gene regulation	log2	adjusted p-value
Traes_1BL_72FF5A24C	TraesCS1B02G288900	1B	503,622,726-503,624,114	Yos-1 like	up	4.88	1.89E-69
Traes_1BL_4C3C75D3A	TraesCS1B02G289100	1B	503,871,963-503,881,842	Ankyrin-1	down	5.08	1.67E-36
Traes_1BL_7BB61786E	TraesCS1B02G291200	1B	508,553,015-508,555,855	Aldo-keto reductase family 4 member C9	up	1.65	1.91E-09
Traes_1BL_3CB12266D	TraesCS1B02G291500	1B	508,707,538-508,709,360	Aldo-keto reductase family 4 member C10	down	3.21	2.93E-24
Traes_1BL_28B2386DF	TraesCS1B02G292400	1B	509,891,166-509,892,675	Peptidyl-prolyl cis-trans isomerase	down	3.13	7.10E-35
Traes_1BL_2B7961A65	TraesCS1B02G292800	1B	510,598,733-510,602,454	Copper transport protein CCH	up	2.25	2.07E-17
Traes_1BL_9C2B2A24A	TraesCS1B02G298500	1B	520,083,939-520,091,297	Serine/threonine-protein kinase ATR	down	3.08	1.72E-22
Traes_1BL_8FABA743F	TraesCS1B02G559300LC	1B	549,463,918-549,465,895	-	down	4.06	3.31E-19
Traes_1BL_C5C66A768	TraesCS1B02G353500	1B	583,689,036-583,693,092	Probable peptidyl-tRNA hydrolase 2	up	4.42	4.71E-28
Traes_6BL_81481E353	TraesCS6B02G435000	6B	703,288,889-703,290,737	Mitochondrial import protein TIM15	down	7.10	5.28E-14
Traes_6BL_882745936	TraesCS6B02G779400LC	6B	703,941,450-703,945,001		down	1.23	1.94E-06
Traes_6BL_93357D848	TraesCS6B02G436400	6B	704,038,332-704,042,869	Serine/threonine-protein phosphatase PP1	down	0.85	7.06E-03
Traes_6BL_5AF540208	TraesCS6B02G436600	6B	704,153,686-704,156,343	F-box LRR protein	down	2.55	6.18E-05
Traes_6BL_F914C4C3A	TraesCS6B02G437000	6B	704,187,356-704,189,481	Putative ribonuclease H protein At1g65750	down	5.14	9.00E-34
Traes_6BL_A0879077D	TraesCS6B02G783000LC.1	6B	704,949,053-704,949,315	T-complex protein 1 subunit zeta 1	down	1.01	1.96E-05
Traes_6BL_0CB2299E9	TraesCS6B02G437200	6B	712,227,427-712,229,904	-	down	7.80	6.42E-47
Traes_6BL_4704FF2B4	TraesCS6B02G440200	6B	705,377,867-705,385,342	Putative aconitate hydratase, cytoplasmic	down	2.77	5.41E-29
Traes_6BL_FBA80D37C	TraesCS6B02G440500	6B	705,497,114-705,500,519	Probable mediator of RNA polymerase II transcription subunit 36b	down	1.65	2.84E-12
Traes_6BL_B55E3EF6A	TraesCS6B02G441200	6B	705,613,631-705,620,958	Putative disease resistance protein RGA3	down	inf	3.98E-23

Table 1. Continued.

Old gene name	Updated gene name	Chr	Position (bp)	Corresponding protein	Gene regulation	log2	adjusted p-value
Traes_6BL_CD8C2012C1	TraesCS6B02G441400	6B	705,634,389-705,636,966	Probably inactive leucine-rich repeat receptor-like protein kinase IMK2	down	inf	5.66E-09
Traes_6BL_616BBA730	TraesCS6B02G442200	6B	705,885,467-705,886-688	Disease resistance protein RGA2	down	inf	3.43E-26
Traes_6BL_9E98E2626	TraesCS6B02G443700	6B	706,625,650-706,628,754	ATG8-interacting protein 1	down	4.25	9.48E-13
Traes_6BL_55445DC2D	TraesCS6B02G451500	6B	710,149,424-710,152,200	F-box protein	up	4.65	5.09E-38
Traes_6BL_B84BC12EC	TraesCS6B02G452100	6B	710,795,550-710,799,389	-	up	8.84	4.72E-190
Traes_6BL_4C6B99385	TraesCS6B02G452500	6B	711,345,338-711,348,401	Telomere length and silencing protein	up	3.72	2.31E-19
Traes_6BL_55A1538E1	TraesCS6B02G452700	6B	711,372,963-711,375,917	Telomere length and silencing protein 1	up	1.89	3.52E-08
Traes_6BL_E8F3B2953	TraesCS6B02G453300	6B	711,709,311-711,712,023	F-box like protein	up	3.95	4.68E-11
Traes_6BL_7DB204621	TraesCS6B02G454800	6B	712,227,427-712,229,904	L-type lectin-domain containing receptor kinase IV.4	up	3.72	1.67E-02
Traes_6BL_CED3DB508	TraesCS6B02G456000	6B	712,345,436-712,351,600	ABC transporter F family member 3	up	1.85	6.41E-17
Traes_6BL_C48F853F8	TraesCS6B02G456400	6B	712,658,222-712,662,336	Probable prolyl 4-hydroxylase 3	up	2.67	9.19E-19
Traes_6BL_FAD2FD89C	TraesCS6B02G456500	6B	712,665,811-712,674,449	Sucrose transport protein SUT4	up	1.16	1.35E-04
Traes_6BL_E204B7C91	TraesCS6B02G457400	6B	713,114,509-713,117-699	NB-ARC-LRR	up	1.52	5.97E-03
Traes_6BL_FF26CBFBF	TraesCS6B02G460100	6B	713,971,067-713,976,790	Synaptotagmin-like 1 homologous	up	5.84	1.70E-41
Traes_6BL_EE1166E22	TraesCS6B02G465800	6B	716,361,322-716,368,720	Disease resistance protein RPP13	down	inf	2.12E-19
Traes_6BL_7C8EDCF5A	TraesCS6B02G466700	6B	716,622,427-716,628,907	Protein argonaute 1C	down	6.52	6.27E-30
Traes_6BL_2D48C932A	TraesCS6B02G468200	6B	717,861,512-717,874,664	Callose synthase 3	down	1.85	7.33E-18
Traes_6BL_20CA191B4	TraesCS6B02G468300	6B	717,891,358-717,892,813	Outer envelope pore protein 21, chloroplastic	down	1.75	7.57E-08
Traes_6BL_C8ED6D1AF	TraesCS6B02G468600	6B	717,9151,50-717,919,160	Callose synthase 3	down	5.70	8.93E-17
Traes_6BL_1787AAD1C	TraesCS6B02G468900	6B	717,961,216-717,964,216	Metal tolerance protein C2	down	3.69	3.27E-12
Traes_6BL_DF9519C97	TraesCS6B02G470000	6B	718,382,723-718,387,419	Alpha-1,3-mannosyl-glycoprotein 2-beta-N-acetylglucosaminyltransferase	down	0.96	5.48E-04
Traes_6BL_077C91EAE	TraesCS6B02G470700	6B	718,765,354-718,775,528	Protein DETOXIFICATION 45, chloroplastic	down	1.77	1.28E-09
Traes_6BL_5E211AB35	TraesCS6B02G470800	6B	718,919,952-718,923,804	Unknown function	down	0.77	9.79E-03

Table 1. Continued.

Old gene name	Updated gene name	Chr	Position (bp)	Corresponding protein	Gene regulation	log2	adjusted p-value
Traes_6BL_CBDCDEFC5	TraesCS6B02G471700	6B	719,709,634-719,725,528	Protein Furry/ Tao3/ Mor2	down	2.71	5.02E-17
Traes_6BL_71ABF50AC	TraesCS6B02G472700	6B	720,418,530-720,423,497	DEAD-box ATP-dependent RNA helicase 2	down	2.15	1.25E-14
Traes_6BL_ECEBFE4C1	TraesCS6B02G473000	6B	720,505,144-720,510,790	Organellar oligopeptidase A, chloroplastic/mitochondrial	down	2.38	4.71E-28
Traes_6DL_F06F9895B	TraesCS6D02G381700	6D	462,012,557-462,015,085	F-box protein	up	8.14	1.26E-112
Traes_7AS_1DF12C790	TraesCS7A02G031300LC	7A	11,423,423-11,424,188	OTU domain-containing protein At3g57810	down	8.36	2.72E-29
Traes_7AS_D4796D360	TraesCS7A02G040000	7A	18,054,572-18,055,221	Disease resistance RPP8-like protein 3	up	9.64	6.78E-05
Traes_7AS_73D26354E	TraesCS7A02G044300	7A	20,482,829-20,486,172	Disease resistance protein RPM1	up	10.36	2.12E-06
Traes_7AL_2A57956BC	TreasCS7A02G440700	7A	635,069,180-635,069,850	Clathrin heavy chain 1-like	up	7.02	4.57E-06
Traes_7AL_E58674B35	TraesCS7A02G442500	7A	636,889,761-636,906,158	Glutathione synthetase, chloroplastic	up	7.74	3.56E-31
Traes_7AL_060F5996C	TraesCS7A02G448300	7A	642,731,873-642,735,937	26S protease regulatory subunit S10B homolog	up	8.22	2.15E-105
Traes_7AL_6E220ADA0	TraesCS7A02G457200	7A	652,703,802-652,712,442	Mechanosensitive ion channel protein 2, chloroplastic	down	4.31	3.57E-07
Traes_7AL_879EF12ED	TraesCS7A02G479800	7A	672,024,985-672,029,520	Eukaryotic translation initiation factor 5B	up	4.02	2.60E-40
Traes_7AL_1A15283C9	TraesCS7A02G484800	7A	675,587,045-675,590,716	G-type lectin S-receptor-like serine/threonine-protein kinase B120	down	9.11	3.65E-12
Traes_7AL_47158BA7C	TraesCS7A02G491300	7A	680,341,311-680,345,280	Ubiquitin-conjugating enzyme E2	up	1.81	1.26E-07
Traes_7AL_B8CD6C57F	TraesCS7A02G492400	7A	681,011,336-681,015,619	Probable auxin efflux carrier component 2	down	3.27	1.69E-08

Discussion

The identification of QTL and the underlying genes associated with grain yield and yield stability following abiotic stress can be valuable for the development of new, high yielding varieties. Identified QTL and their associated molecular markers can be used for marker-assisted selection, a method which enables the selection of genotypes in large populations without the need of costly and time-consuming phenotyping in the field (Gupta et al. 2010). Knowing the genes and their function, on the other hand, can provide information on key mechanisms associated with stress tolerance and can be used for direct modification of current cultivars by methods such as CRISPR/Cas9 (Kim et al. 2018). Of similar importance is the physiological dissection of these QTL into their component physiological traits, which can then serve as target traits for breeding in dry and hot climates. Using NILs, we studied a target QTL on the long arm of chromosome 6B and its effect on yield components, water use and photosynthesis-related traits. The QTL was previously identified in three independent studies (Shirdelmoghanloo et al. 2016, Garcia et al. 2019, Schmidt et al. 2020), contributing to seed weight, single seed weight, harvest index and leaf chlorophyll content, but with opposite allelic effects under semi-controlled and field conditions.

Water use and photosynthesis-related traits have previously been suggested to be important traits to increase wheat yield potential under drought and heat stress (Cossani and Reynolds 2012, Tricker et al. 2018). Particularly, an increased water use efficiency has often been hypothesized in literature to be associated with a higher stress tolerance (French and Schulz 1984, Richards et al. 2002, Codon et al. 2004, Deng et al. 2006), while others argue that the effective use of water (i.e. maximal soil moisture capture for transpiration) and not water use efficiency are important for crop improvement (Blum et al. 2005, Blum et al. 2009).
In our case, NILs carrying the allele from the exotic parent showed an increase in seed weight, seed number and single seed weight, consistent with results observed under semi-controlled conditions (Schmidt et al. 2020). The water use during the drought treatment and recovery phase following the drought treatment was also increased in these lines, whereas the water consumption under the combined drought and heat treatment was similar in both exotic and non-exotic NILs. During the drought treatment and recovery phase, pots were constantly re-irrigated to a certain target weight instead of withholding irrigation completely, enabling a constant delivery of water. Plants with an increased water use can transpire more to cool down and prevent a negative effect of an increased internal temperature on the metabolic pathways.

Under the combined drought and heat treatment, re-irrigation was less frequent, meaning plants were more restricted in their water use and transpiration. NILs carrying the exotic allele seemed to adapt more easily to different water availabilities and used the water more effectively than NILs carrying the non-exotic allele. In fact, NILs carrying the exotic allele had an increased water use efficiency at all times in comparison to NILs carrying the non-exotic allele even though their water consumption was higher (except under combined drought and heat treatment). Here it seemed that an effective use of water and an increased water use efficiency might, therefore, not rule out but favour each other.

Water use was increased in both NILs during the recovery phase following both treatments, likely due to the higher water availability and resulting in an overall lower water use efficiency. The water use during recovery was, nonetheless, higher in plants exposed to drought than in plants exposed to the combined drought and heat treatment. A potential explanation could be an acceleration in the crop cycle following the drought and heat treatment, reflected by the earlier decline in water use in plants exposed to combined drought and heat in comparison to plants exposed to drought alone.

The chlorophyll index was fairly stable throughout the whole measurement period in both NILs and treatments (0-14 DAA), while the photosynthetic and electron transport capacity declined slowly with a similar magnitude in both NILs during drought and recovery following the drought treatment (3-14 DAA). In contrast, photosynthetic and electron transport capacity were increased in both NILs during the combined drought and heat stress before reaching similar values during recovery as measured before the occurrence of the heat stress (3-8 DAA). To avoid photoinhibition and allow acclimation, plants can optimise the light absorption, through leaf and chlorophyll movement and anthocyanin accumulation, as well as the energy balance of their photosystem, through modifications of CO_2 fixation, photo- and mitochondrial respiration, cyclic electron flow, etc. (Sage and Kubien 2007, Rungrat et al. 2016). In our case, photosynthetic and electron transport capacity were reversibly modified in response to the occurrence and absence of the heat stress but were not modified following the drought treatment. This suggests that NILs were able to acclimate to higher temperatures but not to the drought treatment in both NILs.

NILs carrying the exotic allele maintained their chlorophyll index as well as photosynthetic and electron transport capacity above NILs carrying the non-exotic allele at all times. NILs carrying the exotic allele had also had an increased leaf dry mass (i.e. thicker leaves) compared to NILs carrying the non-exotic allele, which could explain the increase of chlorophyll content

and, in turn, a higher photosynthetic and electron transport capacity in NILs carrying the exotic allele. A higher photosynthetic capacity would suggest a higher contribution to grain yield (Sanchez-Bragado et al. 2014, Dodig et al. 2016), which was the case in our study.

Respiration is an important process to produce energy for biosynthesis and cellular maintenance and can also reduce the formation of reactive oxygen through oxidation of excess cellular redox equivalents (Atkin et al. 2005, Atkin and Macherel 2009). However, respiration also involves the oxidation of carbohydrates to CO_2 (Graham 1980). In our study, respiration rate was similar between both NIL alleles and throughout the measurements period, with the only exception under combined drought and heat stress. NILs carrying the exotic allele showed a decrease in respiration rate compared to NILs carrying the non-exotic allele under combined drought and heat stress, suggesting that a higher respiration rate was negatively associated with yield.

Segregation regions between NILs were observed on chromosome 1B, 6B and 7A, of which one coincided with our target region. The region on chromosome 1B co-located on the Ref Seq v1.0 (IWGSC et al. 2018) with a previously identified QTL for anther extrusion in wheat (Okada et al. 2019). The segregation region on chromosome 7A co-located with QTL identified for thousand kernel weight and spikelet number per spike (Keeble-Gagnère et al. 2018, Kuzay et al. 2019, Voss-Fels et al. 2019). One of our differentially expressed genes (TraesCS7A02G479800, Table 1), encoding a putative Eukaryotic translation initiation factor 5B, was located within the exact same region on the Ref Seq v1.0 as the previously identified QTL and was upregulated in NILs carrying the exotic allele in all treatments and timepoints. A second gene (TraesCS7A02G484800), encoding a G-type lectin S-receptor-like serine/threonine-protein kinase B120 was 1.3 Mb distant from the QTL and downregulated in NILs carrying the exotic allele.

Most genes were differentially expressed at an early drought stage (i.e., 8 DAA), whereas the number of differentially expressed genes decreased with an increase of stress duration (i.e., 11 DAA) and, in case of the combined drought and heat treatment, with intensity. Genes differentially expressed between NILs carrying the opposite allele were located on chromosomes 1B, 4B, 6B, 6D and 7A, i.e. mostly in regions of genotypic differences observed between NILs (Fig 1). Genotyping by sequencing data, however, did not suggest regions of segregation on chromosomes 4B and 6D. Genes underpinning the 6B QTL might therefore

have a trans-regulatory effect. Several of the differentially expressed genes between NILs, in particular those under drought and heat, were associated with regulation of gene expression and RNA processing. MicroRNA, for instance, are an important gene regulation mechanism in plants (Dugas and Bartel 2004), supporting the hypothesis of a trans-acting control.

The majority of differentially expressed genes under drought were located on chromosome 4B with upregulated genes in NILs carrying the exotic allele being involved in alanine, aspartate and glutamate metabolism. All three amino acids have been observed to increase in developing grains of drought-resistant wheat plants when subjected to drought (Casartelli et al. 2019) and form part of the photorespiratory cycle (Betsche 1983, Wingler et al. 2000). Differentially expressed genes under combined drought and heat stress were dominantly located on chromosomes 1B, 6B and 7A and were associated with the metabolism of glutathione, a component of the antioxidative system in plants, which is synthetised from glycine, a by-product of photorespiration (Wingler et al. 2000). Photorespiration, the fixation of O_2 by ribulose-1,5- bisphosphate, is mostly perceived as a negative trait in crop yield, degrading sugars which have been produced in energy-consuming reactions during photosynthesis, releasing CO_2 and producing reactive oxygen species which can harm the cell. The ascorbate/ glutathione cycle is an important component in the regeneration of antioxidant scavengers and glutathione reductase and peroxidase have been previously observed to be specifically induced by drought and heat stress in tobacco (Rizhsky et al., 2002).

A total of 36 differentially expressed genes across treatments and timepoints could be mapped to our target region on the long arm of chromosome 6B (Table 1). Several of these genes were associated with a wide range of functions such as carbohydrate transport, gene regulation, protein binding, disease resistance and various enzymatic activities, whereas others were of unknown function. To our knowledge, none of these genes has been previously characterized under drought or heat stress in wheat, except for one of the genes (TraesCS6B02G456400) whose predicted protein functions in hydroxylation of the well-studied amino acid Proline. Proline has been shown to accumulate in plants in response to drought, heat and combined drought and heat stress (Dobra et al. 2010, Qaseem et al. 2019). Its accumulation has been associated with tolerance mechanisms such as reactive-oxygen species scavenging, osmotic adjustment, signalling and the stabilisation of proteins (Szabados and Savoure 2009, Verbruggen and Hermans 2008) as well as with an increase in grain yields (Mafakheri et al. 2010, Qaseem et al. 2019).

We could not draw a conclusion about the opposite allele effects observed in the field by Garcia et al. (2019). However, performances in field trials are influenced by season to season environmental variation, additional and interacting biotic and abiotic stresses and, therefore, a number of field trials are required to confirm results. The higher harvest index promoted by the Australian allele in the field might have resulted from one of these factors rather than from actual drought or heat stress. On the other hand, a positive effect of the non-Australian allele was always found in pot experiments. Pot systems, however, often differ in their water relations, the structure and temperature of the soil as well as the available root space compared to field conditions, all of which strongly influence root architecture and physiology as well as the interactions in the rhizosphere (Passioura 2006). These factors could play a role in whether the exotic allele had a positive or negative effect.

Conclusions

Allelic effects on seed weight, single seed weight and seed number under drought and combined drought and heat stress were consistent with results from the genome-wide association study (Schmidt et al. 2020). An increase in yield was also associated with thicker leaves, a higher photosynthetic capacity as well as a better acclimation to different water availabilities and a higher water use efficiency. Using gene expression analysis, we could narrow down our target region on chromosome 6B to 36 potential candidate genes with a further 39 genes of interest differentially expressed across treatments and timepoints in the NIL. Candidate differentially expressed genes were usually associated with genetic segregation illustrating the value of the NAM population for the rapid incorporation and validation of the beneficial exotic alleles. The majority of these genes have not previously been associated with drought or heat stress tolerance in wheat and might serve as candidate genes for crop improvement in dry and hot climates. Further analysis regarding their involvement in the observed changes in physiology and yield components is required.

Acknowledgments

This work was supported by the Australian Research Council Industrial Transformation Research Hub for Wheat in a Hot and Dry Climate (IH130200027) and an Australian Plant Phenomics Facility (APPF) Postgraduate Internship Award to JS. We acknowledge and thank

NovoGene for the RNA sequencing and data analysis including quality checks, mapping of sequences, differential expression analysis and GO and KEGG enrichment analyses. We also acknowledge the use of the facilities, and scientific and technical assistance of the APPF, which is supported by the Australian Government's National Collaborative Research Infrastructure Strategy (NCRIS).

References

Albergel C, Dutra E, Bonan B, Zheng Y, Munier S, Balsamo G, et al. Monitoring and forecasting the impact of the 2018 summer heatwave on vegetation. Remote Sens. 2019;11: 520.

Anders S, Huber W. Differential expression analysis for sequence count data. Genome Biol. 2010;11: R106.

Anders S, Huber W. Differential expression of RNA-Seq data at the gene level - the DESeq package. 2012 [cited 17 September 2019]. In: Bioconductor [Internet]. Available from: https://pdfs.semanticscholar.org/6262/6783bba 72d2bec4ec3424baf7dca7f8416bf.pdf.

Anders S, Pyl PT, Huber W. HTSeq - A Python framework to work with high-throughput sequencing data. Bioinformatics. 2015;31: 166-10.

Aprile A, Havlickova L, Panna R, Mare C, Borrelli GM, Marone D, et al. Different stress responsive strategies to drought and heat in two durum wheat cultivars with contrasting water use efficiency. BMC Genomics. 2013;14: 821-838.

Atkin OK, Bruhn D, Hurry VM, Tjoelker MG. The hot and the cold: unravelling the variable response of plant respiration to temperature. Funct Plant Biol. 2005;32: 87-105.

Atkin OK, Macherel D. The crucial role of plant mitochondria in orchestrating drought tolerance. Ann Bot. 2009;103: 581-597.

Betsche T. Aminotransfer from alanine and glutamate to glycine and serine during photorespiration in oat leaves. Plant Physiol. 1983;71: 961-965.

Blum A. Drought resistance, water-use efficiency, and yield potential are they compatible, dissonant, or mutually exclusive? Aust J Agric Res. 2005;56: 1159-1168.

Blum A. Effective use of water (EUW) and not water-use efficiency (WUE) is the target of crop yield improvement under drought stress. Field Crops Res. 2009;112: 119-123.

Boyd WJR, Li CD, Grime CR, Cakir M, Potipibool S, Kaveeta L, et al. Conventional and molecular genetic analysis of factors contributing to variation in the timing of heading among spring barley (*Hordeum vulgare* L.) genotypes grown over a mild winter growing season. Aust J Agric Res. 2003;54: 1277-1301.

Brenchley R, Spannagl M, Pfeifer M, Barker GLA, D'Amore R, Allen AM, et al. Analysis of the bread wheat genome using whole-genome shotgun sequencing. Nature. 2012;491: 705-710.

Brien CJ. asremlPlus: Augments ASReml-R in fitting mixed models and packages generally in exploring prediction differences. Version 4.1-10. 2019 [cited 17 July 2019] In: The Comprehensive R Archive Network [Internet]. Available from: http://cran.r-project.org/package=asremlPlus/.

Butler DG, Cullis BR, Gilmour AR and Gogel BJ. ASREML-R Reference Manual. Release 3.0. 2009. Technical Report, Queensland Department of Primary Industries, Australia.

Casartelli A, Melino VJ, Baumann U, Riboni M, Suchecki R, Jayasinghe NS, et al. Opposite fates of the purine metabolite allantoin under water and nitrogen limitations in bread wheat. Plant Mol Biol. 2019;99: 477-497.

Coast O, Shah S, Ivakov A, Gaju O, Wilson PB, Posch BC, et al. Predicting dark respiration rates of wheat leaves from hyperspectral reflectance. Plant Cell Environ. 2019;42: 2133-2150.

Condon AG, Richards RA, Rebetzke GJ, Farquhar GD. Breeding for high water-use efficiency. J Exp Bot. 2004;55: 2447-2460.

Cossani CM, Reynolds MP. Physiological traits for improving heat tolerance in wheat. Plant Physiol. 2012;160: 1710-1718.

Deng X, Shan L, Zhang H, Turner NC. Improving agricultural water use efficiency in arid and semiarid areas of China. Agric Water Manag. 2006;80: 23-40.

Dobra J, Motyka V, Dobrev P, Malbeck J, Prasil IT, Haisel D, et al. Comparison of hormonal responses to heat, drought and combined stress in tobacco plants with elevated proline content. J Plant Physiol. 2010;167: 1360-1370.

Dodig D, Savic J, Kandic V, Zoric M, Radovic BV, Popovic, et al. Responses of wheat plants under post-anthesis stress induced by defoliation: I. Contribution of agro-physiological traits to grain yield. Expl Agric. 2016;52: 203-223.

Dugas DV, Bartel B. MicroRNA regulation of gene expression in plants. Curr Opin Plant Biol. 2004;7: 512-520.

Fleury D, Jefferies S, Kuchel H, Langridge P. Genetic and genomic tools to improve drought tolerance in wheat. J Exp Bot. 2010;61: 3211-3222.

Food and Agriculture Organization of the United Nations (FAO). World Food Situation. 2019a [cited 15 July 2019]. In: Food and Agriculture Organization of the United Nations [Internet]. Available from: http://www.fao.org/worldfoodsituation/csdb/en/.

Food and Agriculture Organization of the United Nations (FAO). FAOSTAT - Temperature change. 2019b [cited 15 July 2019]. In: Food and Agriculture Organization of the United Nations [Internet]. Available from: http://www.fao.org/faostat/en/#data/ET.

French RJ, Schulz JE. Water use efficiency of wheat in a Mediterranean-type environment. I. The relation between yield, water use and climate. Aust J Agric Res. 1984;35: 743-764.

Garcia M, Eckermann P, Haefele S, Satija S, Sznajder B, Timmins A, et al. Genome-wide association mapping of grain yield in a diverse collection of spring wheat (*Triticum aestivum* L.) evaluated in southern Australia. PLoS one. 2019;14: 2.

Graham D. Effects of light and "dark" respiration. In: Davies DD, editor. The biochemistry of plants. A comprehensive treatise; volume 2, metabolism and respiration. New York: Academic Press; 1980. pp. 525-579.

Gupta PK, Langridge P, Mir RR. Marker-assisted wheat breeding: present status and future possibilities. Mol Breed. 2010;26: 145-161.

International Wheat Genome Sequencing Consortium (IWGSC), et al. Shifting the limits in wheat research and breeding using a fully annotated reference genome. Science. 2018;361: 7191.

Izanloo A, Condon AG, Langridge P, Tester M, Schnurbusch T. Different mechanisms of adaptation to cyclic water stress in two South Australian bread wheat cultivars. J Exp Bot. 2008;59: 3327-3346.

Keeble-Gagnère G, Rigault P, Tibbits J, Pasam R, Hayden M, Forrest K, et al. Optical and physical mapping with local finishing enables megabase-scale resolution of agronomically important regions in the wheat genome. Genome Biol. 2018;19: 112.

Kim D, Langmead B, Salzberg SL. HISAT: a fast spliced aligner with low memory requirements. Nat Methods. 2015;12: 357-360.

Kim D, Alptekin B, Budak H. CRISPR/Cas9 genome editing in wheat. Funct Integr Genomics. 2018;18: 31-41.

Kuzay S, Xu Y, Zhang J, Katz A, Pearce S, Su Z, et al. Identification of a candidate gene for a QTL for spikelet number per spike on wheat chromosome arm 7AL by high-resolution genetic mapping. Theor Appl Genet. 2019;132: 2689-2705.

Mafakheri A, Siosemardeh A, Bahramnejad B, Struik PC, Sohrabi Y. Effect of drought stress on yield, proline and chlorophyll contents in three chickpea cultivars. Aust J Crop Sci. 2010;4: 580-585.

Mir RR, Zaman-Allah M, Sreenivasulu N, Trethowan R, Varshney RK. Integrated genomics, physiology and breeding approaches for improving drought tolerance in crops. Theor Appl Genet. 2012;125: 625-645.

Miralles DG, Teuling AJ, van Heerwaarden CC, Vila-Guerau de Arellano J. Mega-heatwave temperatures due to combined soil desiccation and atmospheric heat accumulation. Nat Geosci. 2014;7: 345-349.

Mitchell D, Kornhuber K, Huntingford C, Uhe P. The day the 2003 European heatwave record was broken. Lancet Planet Health. 2019; doi: 10.1016/ S2542-5196(19)30106-8.

Okada T, Jayasinghe JEARM, Eckermann P, Watson-Haigh NS, Warner P, Hendrikse Y, et al. Effects of *Rht-B1* and *Ppd-D1* loci on pollinator traits in wheat. Theor Appl Genet. 2019;132: 1965-1979.

Passioura JB. The perils of pot experiments. Funct Plant Biol. 2006;33: 1075-1079.

Peterhansel C, Maurino VG. Photorespiration redesigned. Plant Physiol. 2011;15: 49-55.

Qaseem MF, Qureshi R, Muqaddasi QH, Shaheen H, Kousar R, Roder MS. Genome-wide association mapping in bread wheat subjected to independent and combined high temperature and drought stress. PLoS one. 2018;13: 6.

Qaseem, MF, Qureshi R, Shaheen H. Effects of pre-anthesis drought, heat and their combination on the growth, yield and physiology of diverse wheat (*Triticum aestivum* L.) genotypes varying in sensitivity to heat and drought stress. Sci Rep. 2019;9: 6955.

Reddy VR, Baker DN, Hodges HF. Temperature effects on cotton canopy growth, photosynthesis, and respiration. Agron J. 1991;83: 699-704.

Richards RA, Rebetzke GJ, Condon AG, van Herwaarden AF. Breeding opportunities for increasing efficiency of water use and crop yield in temperate cereals. Crop Sci. 2002;42: 111-121.

Rungrat T, Awlia M, Brown T, Cheng R, Sirault X, Fajkus J, et al. Using phenomic analysis of photosynthetic function for abiotic stress response gene discovery. Arabidopsis Book. 2016;14: e0185.

Sage, RF, Kubien DS. The temperature response of C_3 and C_4 photosynthesis. Plant Cell Environ. 2007;30: 1086-1106.

Sanchez-Bragado R, Molero G, Reynolds MP, Araus JL. Relative contribution of shoot and ear photosynthesis to grain filling in wheat under good agronomical conditions assessed by differential organ δ13C. J Exp Bot. 2014;65: 5401-5413.

Schmidt J, Tricker P, Eckermann P, Kalambettu P, Garcia M, Fleury D. Novel alleles for combined drought and heat stress tolerance in wheat. Front Plant Sci. 2019; doi: 10.3389/fpls.2019.01800.

Shirdelmoghanloo H, Taylor JD, Lohraseb I, Rabie H, Brien C, Timmins A, et al. A QTL on the short arm of wheat (*Triticum aestivum* L.) chromosome 3B affects the stability of grain weight in plants exposed to a brief heat shock early in grain filling. BMC Plant Biol. 2016;16: 100.

Silva-Perez V, Molero G, Serbin SP, Condon AG, Reynolds MP, Furbank RT, et al. Hyperspectral reflectance as a tool to measure biochemical and physiological traits in wheat. J Exp Bot. 2017;69: 483-496.

Silva-Perez V, Ivakov A. Wheat physiology predictor. 2019 [cited 6 September 2019]. In: Metabolome Express [Internet]. Available from: https://www.metabolome-express.org/pheno/.

Sukumaran S, Reynolds MP, Sansaloni C. Genome-wide association analyses identify QTL hotspots for yield and component traits in durum wheat grown under yield potential, drought, and heat stress environments. Front Plant Sci. 2018;9: 81.

Szabados L, Savoure A. Proline: a multifunctional amino acid. Trends Plant Sci. 2009;15: 2.

Toreti A, Cronie O, Zampieri M. Concurrent climate extremes in the key wheat producing regions of the world. Sci Rep. 2019;9: 5493.

Trapnell C, Roberts A, Goff L, Pertea G, Kim D, Kelley DR., et al. Differential gene and transcript expression analysis of RNA-seq experiments with TopHat and Cufflinks. Nat Protoc. 2012;7: 562-578.

Tricker PJ, ElHabti A, Schmidt J, Fleury D. The physiological and genetic basis of combined drought and heat tolerance in wheat. J Exp Bot. 2018;69: 3195-3210.

Trnka M, Rötter RP, Ruiz-Ramos M, Kersebaum KC, Olesen JE, Žalud Z, et al. Adverse weather conditions for European wheat production will become more frequent with climate change. Nat Clim Chang. 2014;4: 637-643.

Verbruggen N, Hermans C. Proline accumulation in plants: a review. Amino Acids. 2008;35: 753-759.

Voss-Fels KP, Keeble-Gagnère G, Hickey LT, Tibbits J, Nagornyy S, Hayden MJ, et al. High-resolution mapping of rachis nodes per rachis, a critical determinant of grain yield components in wheat. Theor Appl Genet. 2019;132: 2707-2719.

Watson-Haigh NS, Suchecki R, Kalashyan E, Garcia M, Baumann U. DAWN: A resource for yielding insights into the diversity among wheat genomes. BMC Genomics. 2018;19: 941.

Wingler A, Lea PJ, Quick WP, Leegood RC. Photorespiration: metabolic pathways and their role in stress protection. Philos Trans R Soc Lond B Biol Sci. 2000;355: 1517-1529.

Young MD, Wakefield MJ, Smyth G K, Oshlack A. Gene ontology analysis for RNA-seq: accounting for selection bias. Genome Biol. 2010;11: R14.

Zampieri M, Ceglar A, Dentener F, Toreti A. Wheat yield loss attributable to heat waves, drought and water excess at the global, national and subnational scales. Environ Res Lett. 2017;12: 6.

Supporting information captions

S1 Fig. Soil water potential – soil water content curve of the drought soil mix. Eight pots of the same size and filled with the same substrate mix as used in the experiment were first watered and then drained out until reaching ~5 % soil water content. The water content and water potential of the soil were measured daily by coring a of sample of 15 mm diameter and 200 mm length. The water content in soil was determined by calculating the weight difference between fresh soil sample and the oven-dried soil sample (at 65 ºC for 72 hours), divided by the oven-dried sample. The water potential of the fresh soil sample was measured using a water potential meter (WP4C, Meter Group, United States) in continuous mode until the value maintained stable. Dots, raw values of the eight pots. Blue line, logarithmic trendline.

S2 Fig. Daily temperature and relative humidity records in the DroughtSpotter glasshouse and the glasshouse used for the combined drought and heat treatment over the course of the experiment. The target temperatures were 22/15 ºC day/night and 35/25 ºC day/night in the DroughtSpotter and heated glasshouse, respectively. Anthesis date (i.e., 0 days after anthesis) represents the mean anthesis date. Relative humidity was not recorded from 18 to 22 days after anthesis and 33 to 41 days after anthesis due to a system failure.

S1 Table. KASP marker assisted selection for the development of near-isogenic lines. Grey indicates the allele derived from the non-exotic parent (Gladius) in the target regions of chromosome 6B. Green indicates the allele derived from the exotic parent (Taferstat).

S2 Table. Targeted genotypic by sequencing data of near-isogenic lines for the target QTL on chromosome 6B. The target region (T) and segregating regions (S) between NILs of the same pair as well as between replicates are marked in yellow. Exotic, allele from the diverse parent (Taferstat); non-exotic, allele from the Australian parent (Gladius).

S3 Table. Quality and concentration of extracted RNA samples of near-isogenic lines. DAA, days after anthesis; QTL, quantitative trait locus. The phenotype of plants with ID E1 and B23 was slightly different (i.e., reduced plant height and biomass) from the rest of the replicates.

S4 Table. Quality assessment of the sequencing data. Raw reads refer to the total number of reads, clean reads to the number of filtered reads. GC content, guanine-cytosine content; Q20, percentage of bases whose correct base recognition rates are greater than 99 % in total bases. Q30, percentage of bases whose correct base recognition rates are greater than 99.9 % in total bases.

S5 Table. Overview of mapping status. Total reads, total number of filtered reads (clean data); total mapped, total number of reads that could be mapped to the reference genome; uniquely mapped, number of reads that were uniquely mapped to the reference genome; multiple mapped, number of reads that were mapped to multiple sites in the reference genome; reads map to '+', number of reads that map to the positive strand; reads map to '-', number of reads that map to the negative strand; exons, percentage of reads mapped to exons; introns, percentage of reads mapped to introns; intergenic, percentage of reads mapped to intergenic regions; non-splice reads, reads that were mapped entirely to a single exon; splice reads, reads that were mapped to two exons.

S6 Table. Total number of expressed genes. FPKM, fragments per kilobase of transcript sequence per million mapped reads. The higher the FPKM, the higher the gene expression level.

S7 Table. Pearson correlation (R^2) of number of expressed genes between samples. D8_AA, samples under drought collected 8 days after anthesis of NILs carrying the non-exotic allele (n=5); D8_BB, samples under drought collected 8 days after anthesis of NILs carrying the exotic allele (n=4); D11_AA, samples under drought collected 11 days after anthesis of NILs carrying the non-exotic allele (n=3); D11_BB, samples under drought collected 11 days after anthesis of NILs carrying the exotic allele (n=4); DH11_AA, samples under combined drought and heat collected 11 days after anthesis of NILs carrying the non-exotic allele (n=4); D11_BB, samples under combined drought and heat treatment collected 11 days after anthesis of NILs carrying the exotic allele (n=4).

S8 Table. Differently expressed genes comparing alleles, timepoints and treatments. -, no data available; D8_AA, samples under drought collected 8 days after anthesis of NILs carrying the non-exotic allele; D8_BB, samples under drought collected 8 days after anthesis of NILs carrying the exotic allele; D11_AA, samples under drought collected 11 days after anthesis of NILs carrying the non-exotic allele; D11_BB, samples under drought collected 11 days after anthesis of NILs carrying the exotic allele; DH11_AA, samples under combined drought and heat collected 11 days after anthesis of NILs carrying the non-exotic allele; D11_BB, samples under combined drought and heat treatment collected 11 days after anthesis of NILs carrying the exotic allele; log2, magnitude (fold-change) of gene expression.

S9 Table. Gene ontology enrichment analysis of differentially expressed genes. Statistical test method: hypergeometric test / Fisher's exact test. -, no significant enrichment; FDR, false discovery rate; D8_AA, samples under drought collected 8 days after anthesis of NILs carrying the non-exotic allele; D8_BB, samples under drought collected 8 days after anthesis of NILs carrying the exotic allele; D11_AA, samples under drought collected 11 days after anthesis of NILs carrying the non-exotic allele; D11_BB, samples under drought collected 11 days after anthesis of NILs carrying the exotic allele; DH11_AA, samples under combined drought and heat collected 11 days after anthesis of NILs carrying the non-exotic allele; D11_BB, samples under combined drought and heat treatment collected 11 days after anthesis of NILs carrying the exotic allele.

S10 Table. Kyoto Encyclopedia of Genes and Genomes (KEGG) enrichment analysis of differentially expressed genes. Reference genome: Oryza sativa. -, no significant enrichment; FDR, false discovery rate; D8_AA, samples under drought collected 8 days after anthesis of NILs carrying the non-exotic allele; D8_BB, samples under drought collected 8 days after anthesis of NILs carrying the exotic allele; D11_AA, samples under drought collected 11 days after anthesis of NILs carrying the non-exotic allele; D11_BB, samples under drought collected 11 days after anthesis of NILs carrying the exotic allele; DH11_AA, samples under combined drought and heat collected 11 days after anthesis of NILs carrying the non-exotic allele; D11_BB, samples under combined drought and heat treatment collected 11 days after anthesis of NILs carrying the exotic allele.

Figures

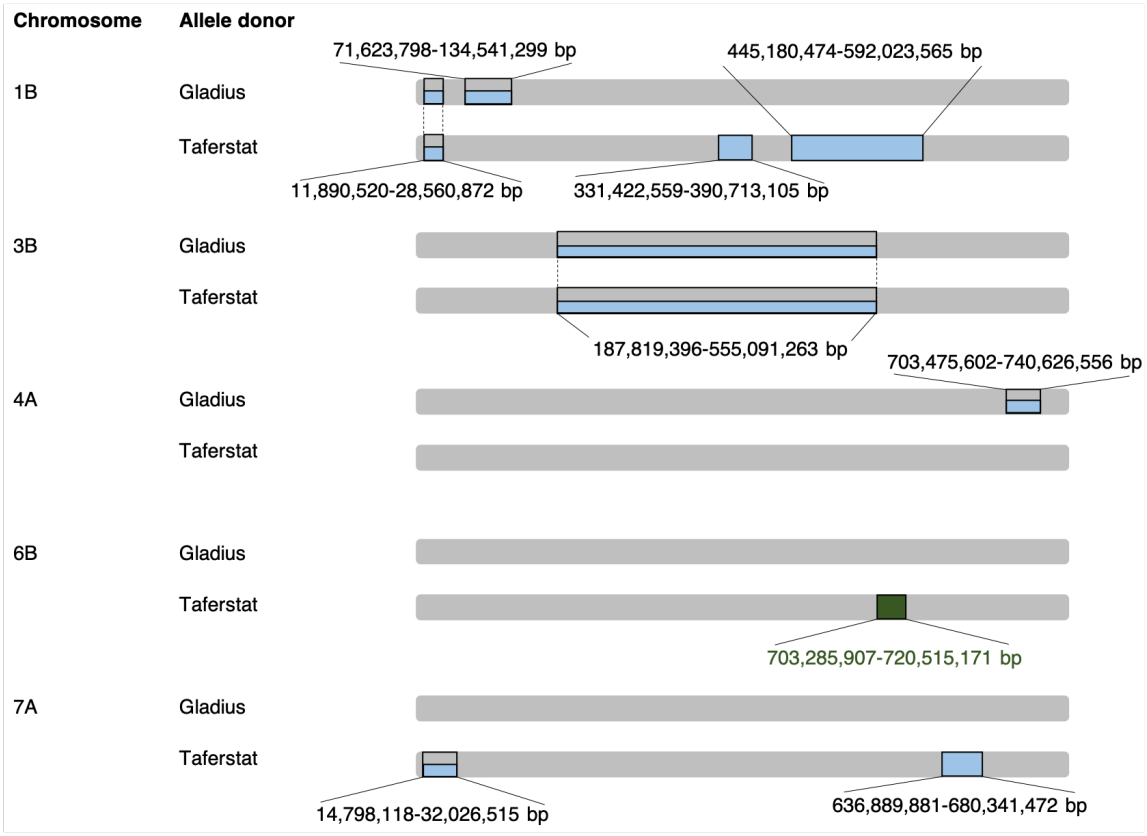

Fig 1.

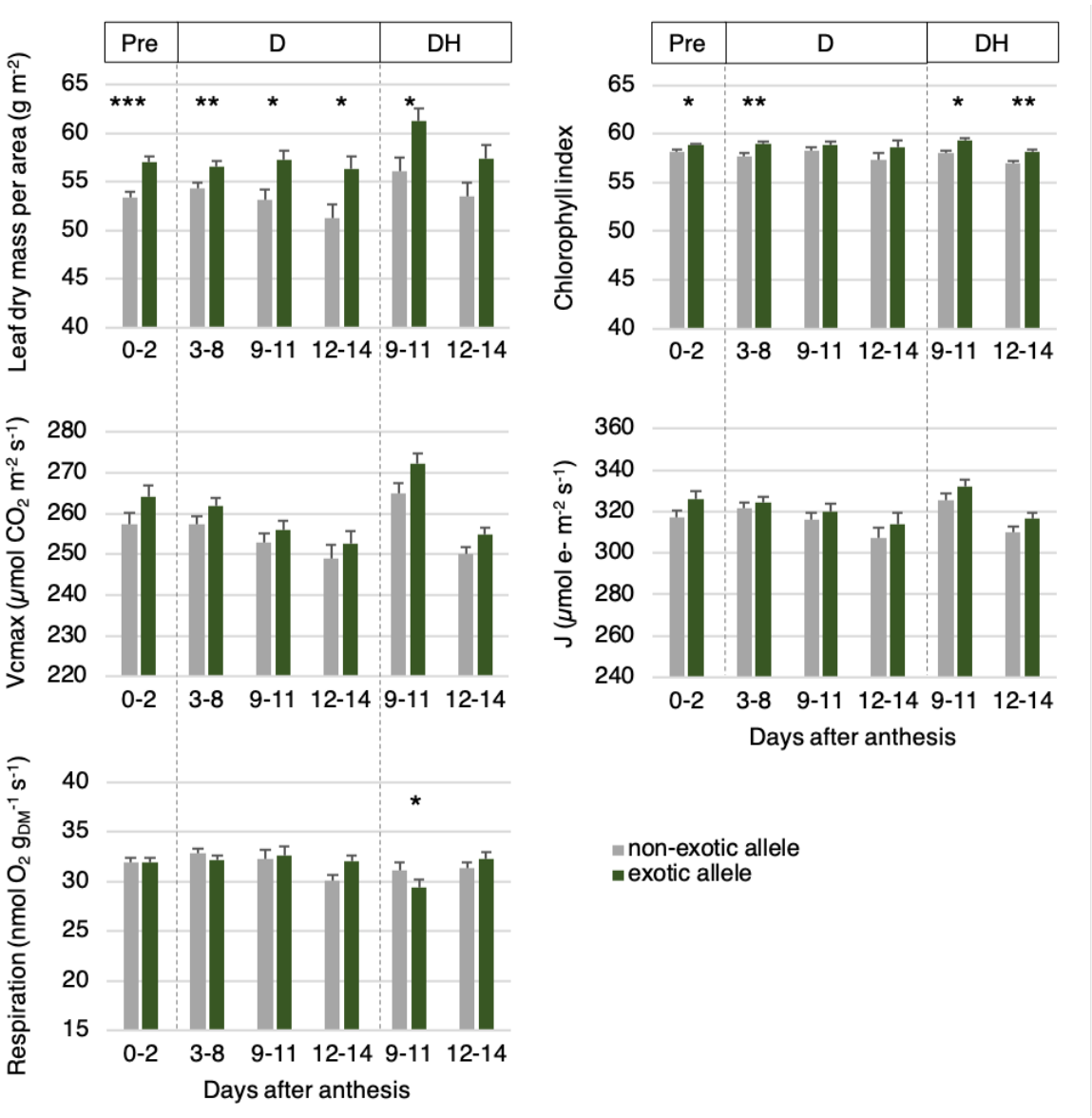
Pre
D
DH
Leaf dry mass per area (g m-2)
Chlorophyll index
Vcmax (µmol CO2 m-2 s-1)
J (µmol e- m-2 s-1)
Respiration (nmol O2 gDM-1 s-1)
0-2
3-8
9-11
12-14
Days after anthesis
non-exotic allele
exotic allele

Fig 2.

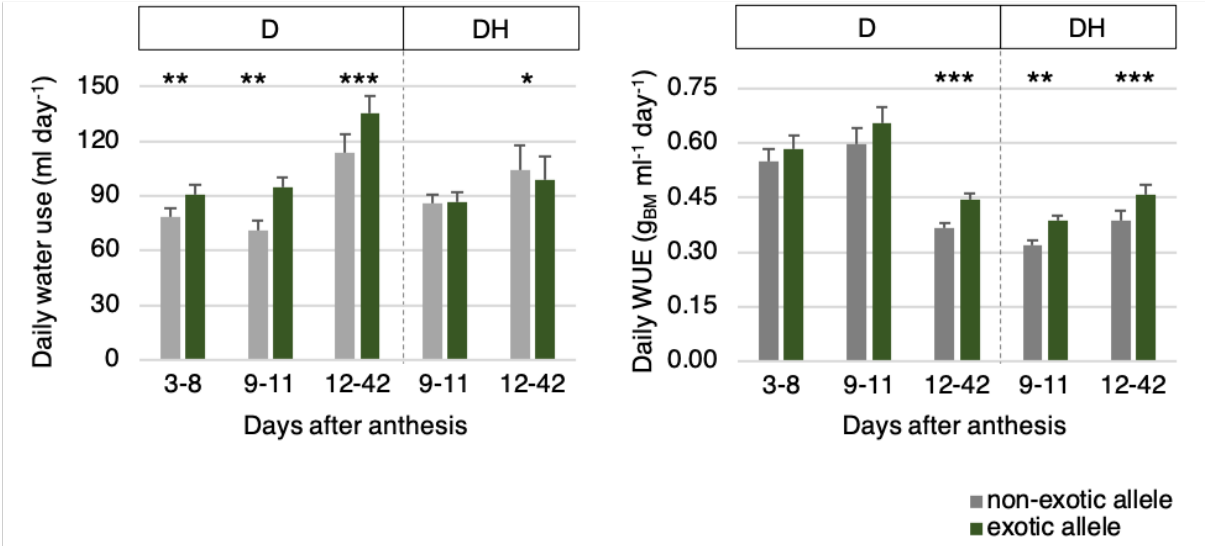
D
DH
Daily water use (ml day-1)
150
120
90
60
30
0
**
**
***
*
3-8
9-11
12-42
9-11
12-42
Days after anthesis
Daily WUE (gBM ml-1 day-1)
0.75
0.60
0.45
0.30
0.15
0.00
***
**
***
non-exotic allele
exotic allele

Fig 3.

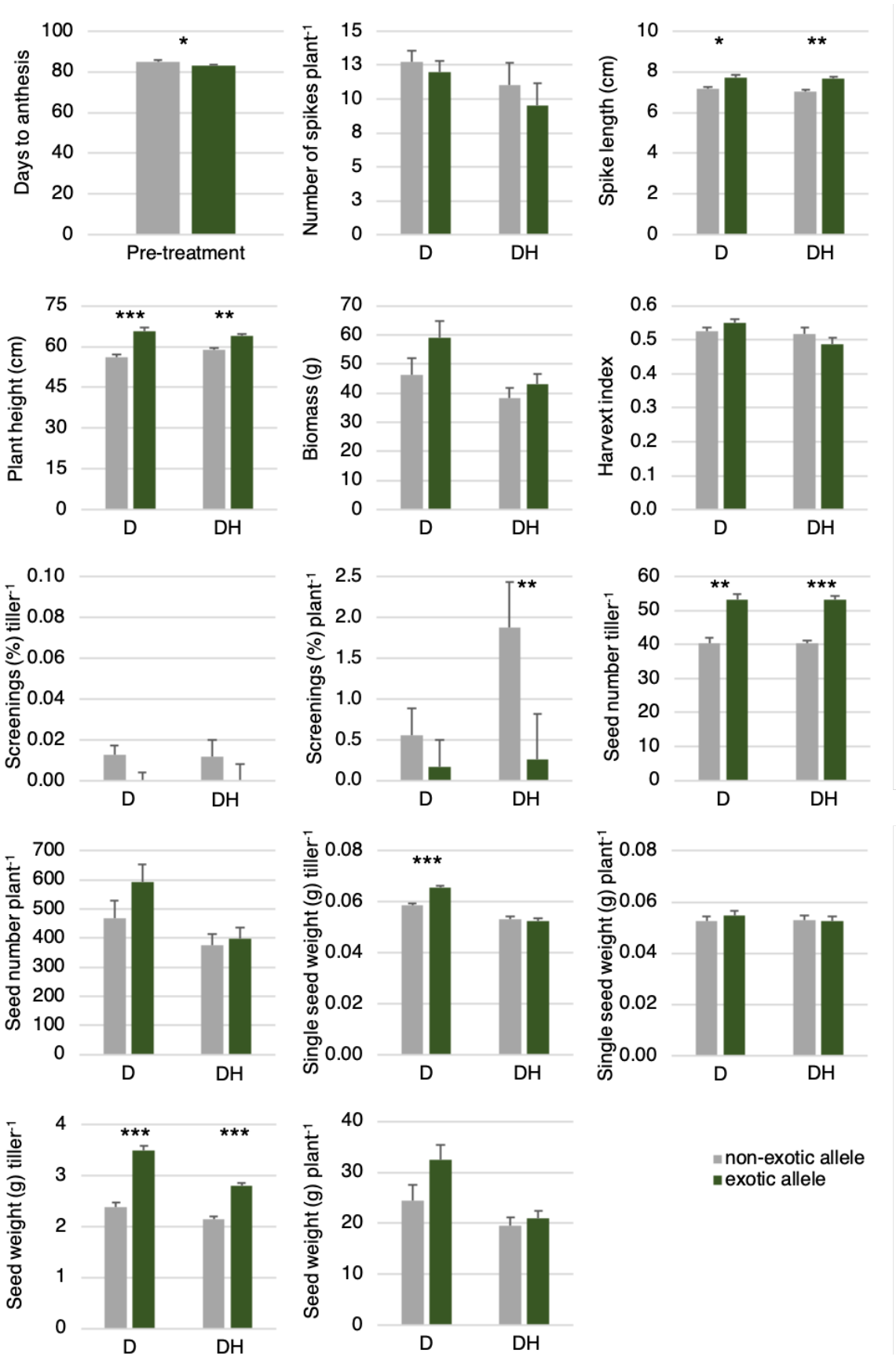
Days to anthesis
Pre-treatment
Number of spikes plant-1
Spike length (cm)
Plant height (cm)
Biomass (g)
Harvext index
Screenings (%) tiller-1
Screenings (%) plant-1
Seed number tiller-1
Seed number plant-1
Single seed weight (g) tiller-1
Single seed weight (g) plant-1
Seed weight (g) tiller-1
Seed weight (g) plant-1
D
DH
non-exotic allele
exotic allele

Fig 4.

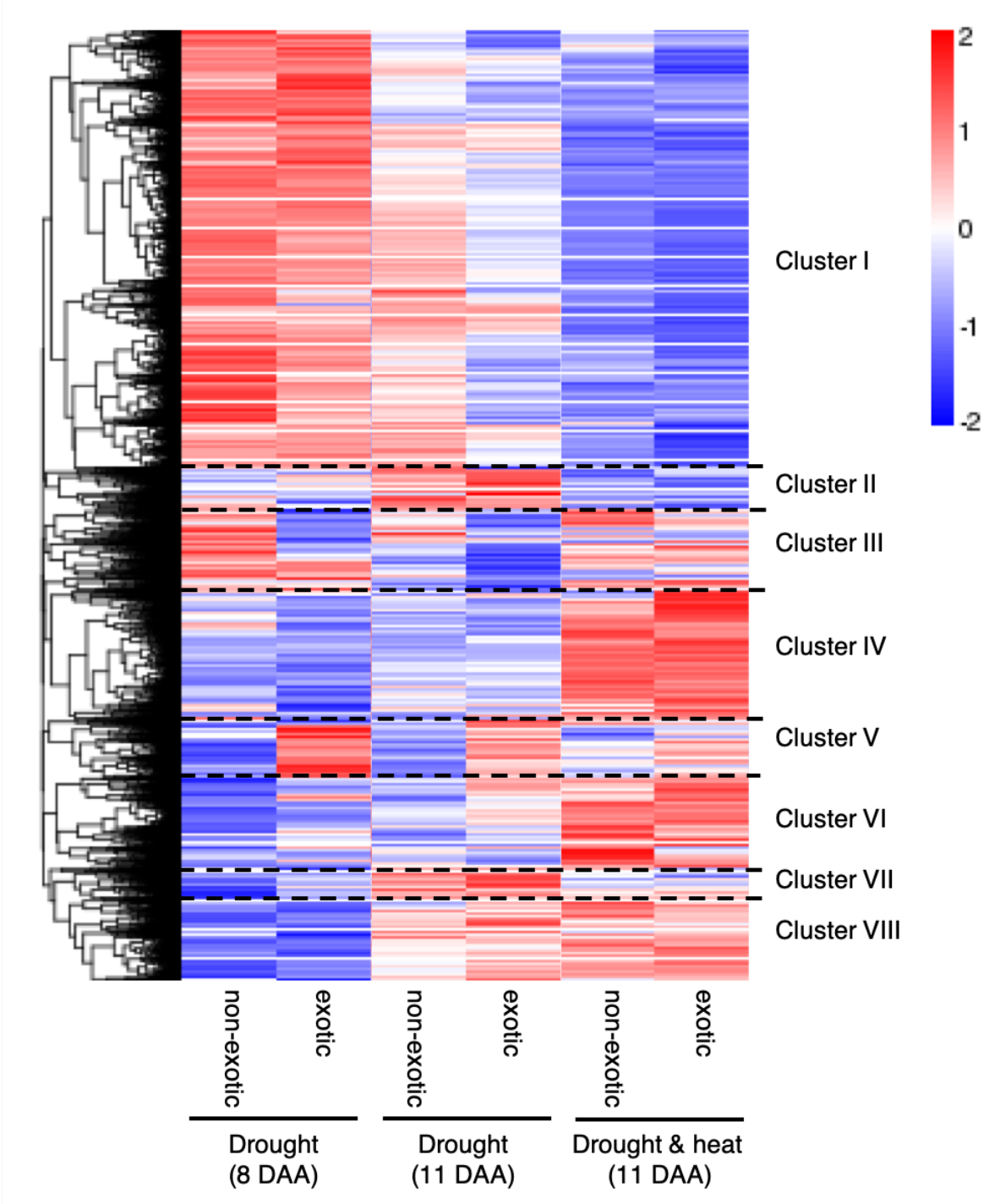
2
1
0
-1
-2
Cluster I
Cluster II
Cluster III
Cluster IV
Cluster V
Cluster VI
Cluster VII
Cluster VIII
non-exotic
exotic
non-exotic
exotic
non-exotic
exotic
Drought
(8 DAA)
Drought
(11 DAA)
Drought & heat
(11 DAA)

Fig 5.


A
Organonitrogen compound biosynthesis
Organonitrogen compound metabolic process
Cellular aldehyde metabolic process
Cellular amino acid biosynthesis
Organonitrogen metabolic process
Aromatic amino acid family biosynthesis
Pyridoxal phosphate metabolic process
Cytoplasm
Endomembrane system
Cell
Cell part
Cytoplasmatic part
Intracellular part
Intracellular
Intracellular organelle
Organelle
Cytoplasmic vesicle
Bounding membrane of organelle
Cytoplasmic vesicle part
Cytoplasmic membrane-bound vesicle
Vesicle
Cytoplasmic vesicle membrane
Intracellular membrane-bounded organelle
Membrane-bounded organelle
Membrane-bounded vesicle
Cellular component
Vesicle membrane
Structural molecule activity
Ribonuclease P activity
tRNA-specific ribonuclease activity
GO term
0
200
400
600
Gene number
Type
Biological process
Cellular component
Molecular function
Sulfur relay system
Spliceosome
Sesquiterpenoid and triterpenoid biosynthesis
Selenocompound metabolism
RNA transport
Riboflavin metabolism
Purine metabolism
Proteasome
Phosphatidylinositol signaling system
Pentose phosphate pathway
mRNA surveillance pathway
Lysine degradation
Linoleic acid metabolism
Inositol phosphate metabolism
Homologous recombination
Glutathione metabolism
Fatty acid elongation
Biosynthesis of amino acids
Ascorbate and aldarate metabolism
Alanine, aspartate and glutamate metabolism
KEGG pathway
0.20
0.25
0.30
0.35
0.40
Rich factor (degree of enrichment)
Adjusted p-value
1.00
0.75
0.50
0.25
0.00
Gene number
10
20
30
40

Fig 6A.


B
Glutathione biosynthetic process
Ribosomal peptide biosynthesis
Glutathione metabolic process
DNA-templated transcription
Glycerol metabolic process
Androgen receptor signalling
Circulatory system process
Vascular process
Blood circulation
Regulation of tube size
Regulation of blood vessel size
Regulation of blood circulation
Alditol metabolic process
Sulphur compound biosynthetic process
Cellular nitrogen compound biosynthesis
System process
Golgi stack
Organelle sub-compartment
Golgi sub-compartment
Elongator holoenzyme complex
Cellular component
Cell
Cell part
Glutathione synthase activity
Alpha-1,6-maanosylglycoprotein activity
Glycerol kinase activity
RNA polymerase II transcription activity
Androgen receptor activity
Transcription factor activity
Acid-amino acid ligase activity
GO term
0
20
40
60
80
100
120
Gene number
Type
Biological process
Cellular component
Molecular function
Sulfur relay system
Spliceosome
RNA transport
RNA polymerase
Plant-pathogen interaction
Phosphatidylinositol signaling system
Other glycan degradation
N-Glycan biosynthesis
mRNA surveillance pathway
Linoleic acid metabolism
Inositol phosphate metabolism
Glycosphingolipid biosynthesis - globo series
Glycosphingolipid biosynthesis - ganglio series
Glycosaminoglycan degradation
Glycerolipid metabolism
Glutathione metabolism
Galactose metabolism
Fatty acid elongation
Basal transcription factors
alpha-Linolenic acid metabolism
KEGG pathway
0.04
0.08
0.12
0.16
Rich factor (degree of enrichment)
Adjusted p-value
1.00
0.75
0.50
0.25
0.00
Gene number
1
2
3
4
5
6

Fig 6B.

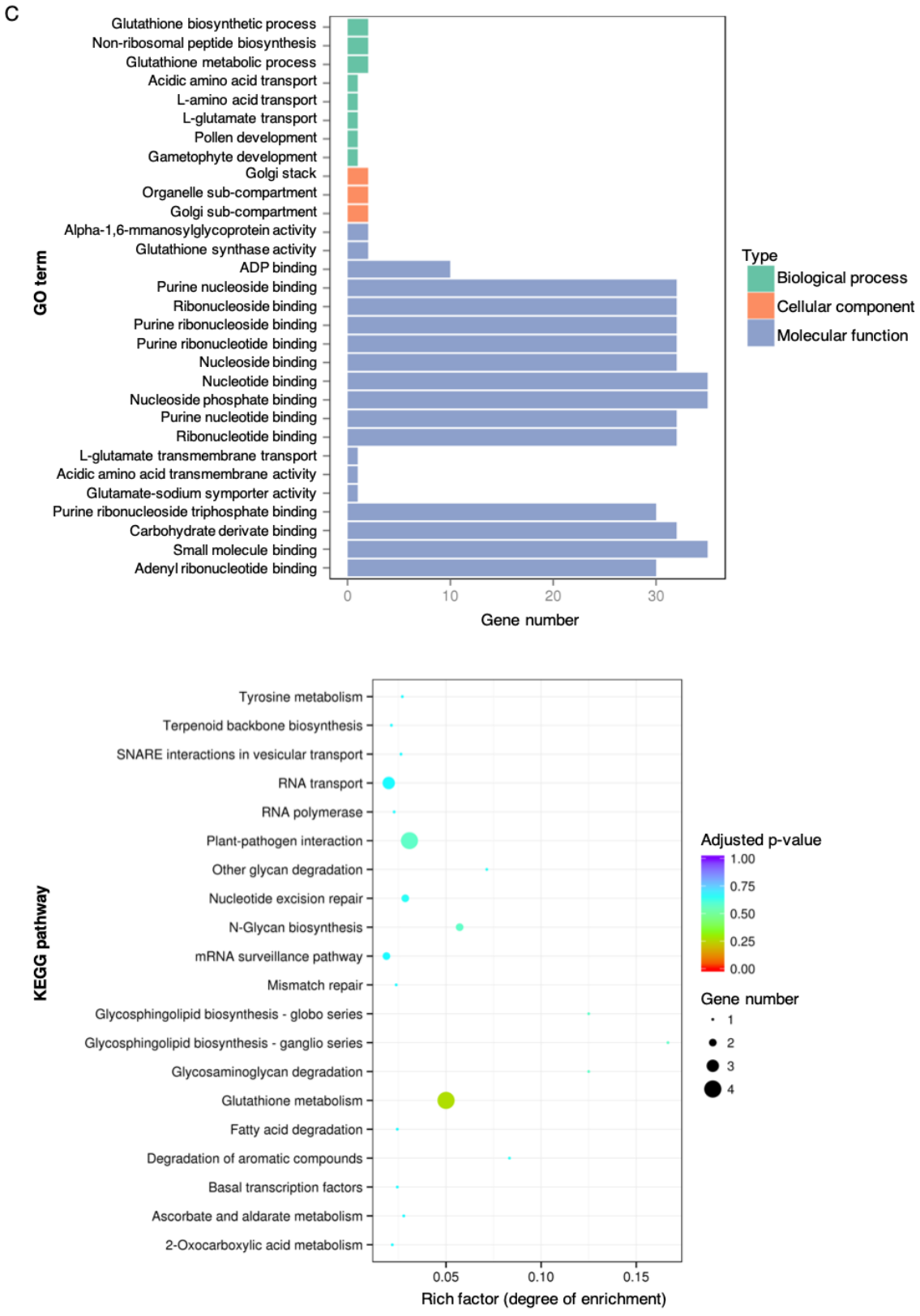
C
Glutathione biosynthetic process
Non-ribosomal peptide biosynthesis
Glutathione metabolic process
Acidic amino acid transport
L-amino acid transport
L-glutamate transport
Pollen development
Gametophyte development
Golgi stack
Organelle sub-compartment
Golgi sub-compartment
Alpha-1,6-mmanosylglycoprotein activity
Glutathione synthase activity
ADP binding
Purine nucleoside binding
Ribonucleoside binding
Purine ribonucleoside binding
Purine ribonucleotide binding
Nucleoside binding
Nucleotide binding
Nucleoside phosphate binding
Purine nucleotide binding
Ribonucleotide binding
L-glutamate transmembrane transport
Acidic amino acid transmembrane activity
Glutamate-sodium symporter activity
Purine ribonucleoside triphosphate binding
Carbohydrate derivate binding
Small molecule binding
Adenyl ribonucleotide binding
GO term
0
10
20
30
Gene number
Type
Biological process
Cellular component
Molecular function
Tyrosine metabolism
Terpenoid backbone biosynthesis
SNARE interactions in vesicular transport
RNA transport
RNA polymerase
Plant-pathogen interaction
Other glycan degradation
Nucleotide excision repair
N-Glycan biosynthesis
mRNA surveillance pathway
Mismatch repair
Glycosphingolipid biosynthesis - globo series
Glycosphingolipid biosynthesis - ganglio series
Glycosaminoglycan degradation
Glutathione metabolism
Fatty acid degradation
Degradation of aromatic compounds
Basal transcription factors
Ascorbate and aldarate metabolism
2-Oxocarboxylic acid metabolism
KEGG pathway
0.05
0.10
0.15
Rich factor (degree of enrichment)
Adjusted p-value
1.00
0.75
0.50
0.25
0.00
Gene number
1
2
3
4

Fig 6C.

Supporting figures

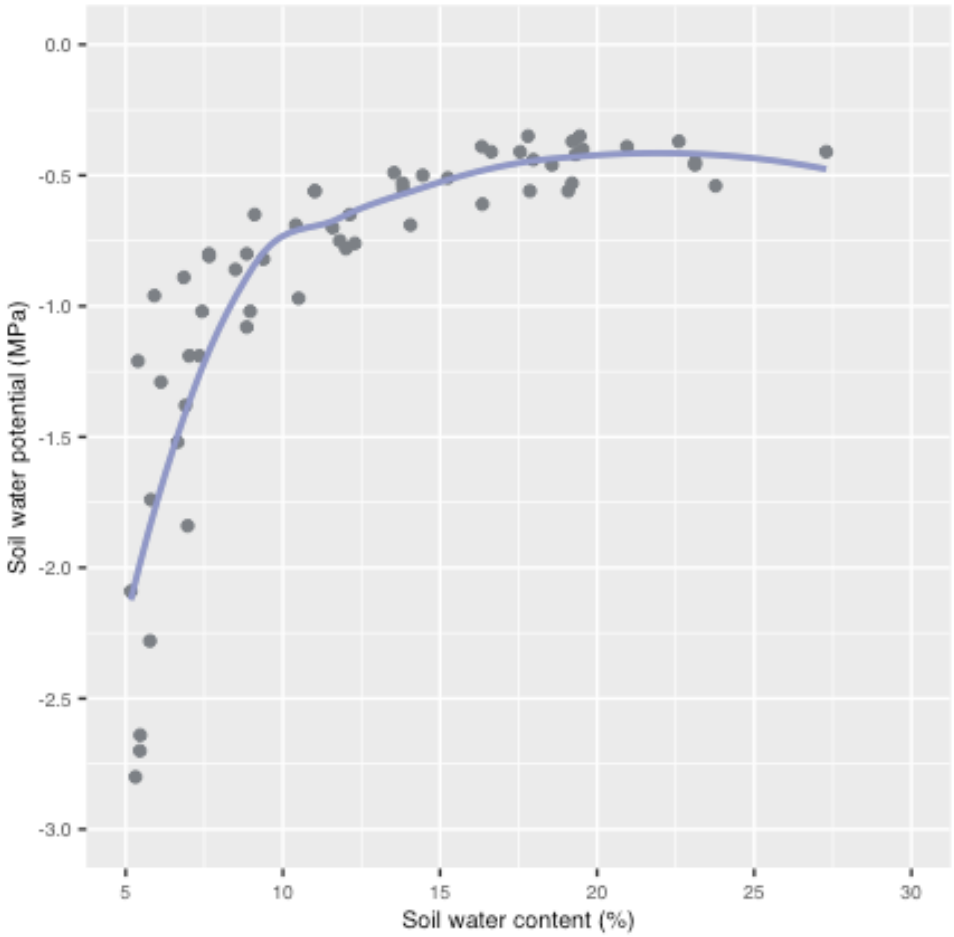

S1 Fig.

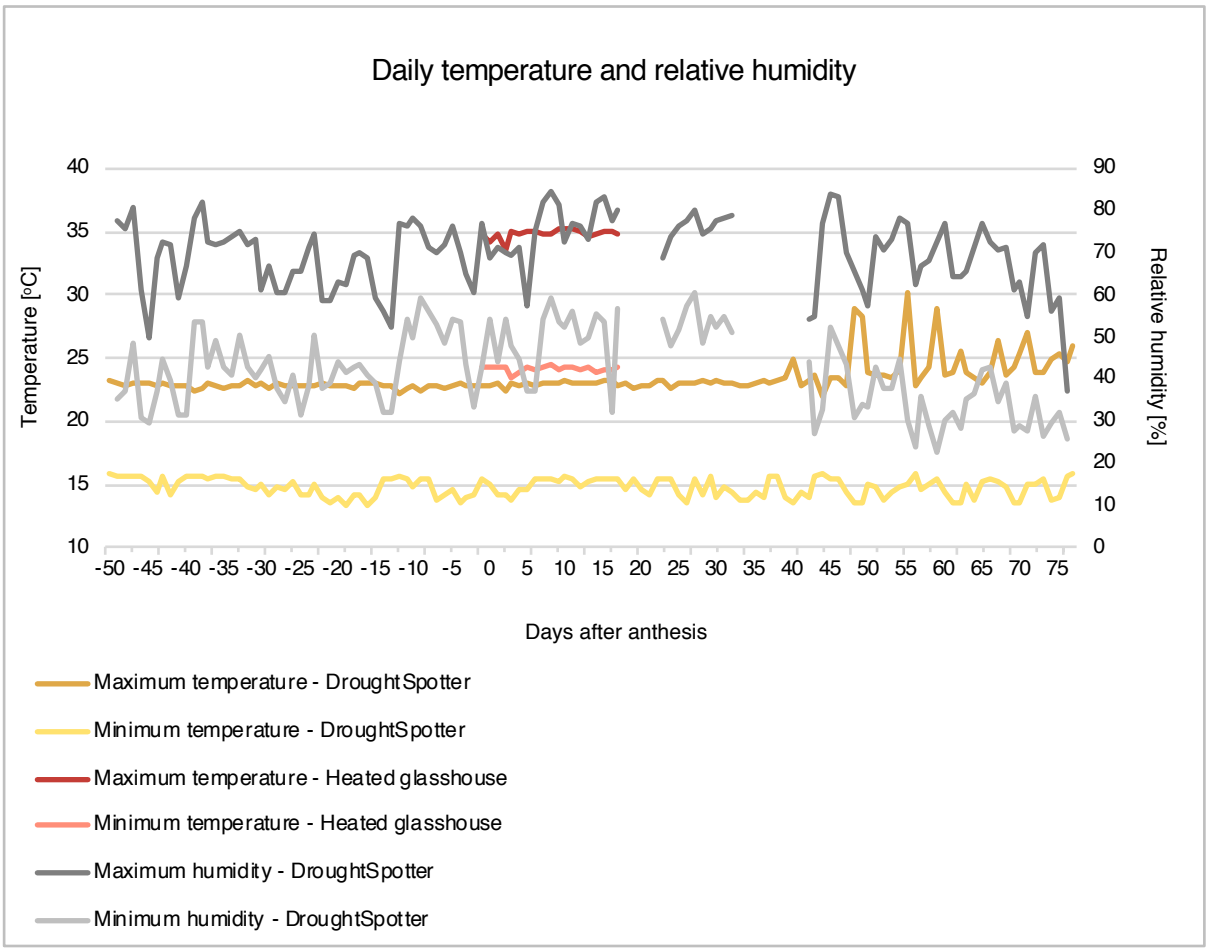
Daily temperature and relative humidity
Temperature [°C]
Relative humidity [%]
Days after anthesis
Maximum temperature - DroughtSpotter
Minimum temperature - DroughtSpotter
Maximum temperature - Heated glasshouse
Minimum temperature - Heated glasshouse
Maximum humidity - DroughtSpotter
Minimum humidity - DroughtSpotter

S2 Fig.

Chapter 4

Drought and heat stress tolerance screening in wheat using computed tomography

Statement of Authorship

Title of Paper	Drought and heat stress tolerance screening in wheat using computed tomography
Publication Status	☐ Published ☐ Accepted for Publication ☑ Submitted for Publication ☐ Unpublished and Unsubmitted w ork w ritten in manuscript style
Publication Details	Schmidt J., Claussen, J., Wörlein, N., Eggert, A., Fleury, D., Garnett, T., & Gerth, S. Drought and heat stress tolerance screening in wheat using computed tomography.

Principal Author

Name of Principal Author (Candidate)	Jessica Schmidt
Contribution to the Paper	Designed and performed the experiment to acquire plant material. Measured wheat spikes manually and using computed tomography. Wrote the manuscript.
Overall percentage (%)	55%
Certification:	This paper reports on original research I conducted during the period of my Higher Degree by Research candidature and is not subject to any obligations or contractual agreements with a third party that would constrain its inclusion in this thesis. I am the primary author of this paper.
Signature	Date 23/09/19

Co-Author Contributions

By signing the Statement of Authorship, each author certifies that:

i. the candidate's stated contribution to the publication is accurate (as detailed above);
ii. permission is granted for the candidate in include the publication in the thesis; and
iii. the sum of all co-author contributions is equal to 100% less the candidate's stated contribution.

Name of Co-Author	Joelle Claussen
Contribution to the Paper	Helped with the X-ray scanning of the wheat spikes. Created the figures and carried out the statistical analysis. Edited the manuscript.
Signature	Date 11.09.19

Name of Co-Author	Norbert Wörlein
Contribution to the Paper	Developed the algorithm. Analysed the data output.
Signature	Date 11.09.19

Name of Co-Author	Anja Eggert		
Contribution to the Paper	Helped with the X-ray scanning and manual measurements of the wheat spikes.		
Signature		Date	11.9.19

Name of Co-Author	Delphine Fleury		
Contribution to the Paper	Designed and supervised the experiment at the University of Adelaide. Edited the manuscript.		
Signature		Date	23/09/2019

Name of Co-Author	Trevor Garnett		
Contribution to the Paper	Conceived and designed the X-ray experiment. Edited the manuscript.		
Signature		Date	16/5/19

Please cut and paste additional co-author panels here as required.

Name of Co-Author	Stefan Gerth		
Contribution to the Paper	Supervised the X-ray scanning and algorithm development. Conceived and designed the X-ray experiment. Helped with the X-ray scanning of the wheat spikes. Edited the manuscript.		
Signature		Date	11.9.19

Link to Chapter 4

In our pot experiments (Chapter 2 and Chapter 3), we struggled with the manual threshing and phenotyping of the wheat spikes due to the amount of time and work it required. We, therefore, developed a method that replaced the threshing for glasshouse experiments and accelerated the evaluation of agronomic grain set traits. An X-ray computed tomographic analysis was carried out on 291 spikes of wheat plants which had been exposed to either drought or combined drought and heat stress during the second year of genome-wide association study. An algorithm was developed and evaluated comparing actual measurements of seed weight and seed number per spike to the virtual measurements. Results demonstrated that our computed tomography pipeline was capable of evaluating those traits with an accuracy of 95-99 %. Subsequently, the algorithm was used to acquire further grain set characteristics such as seed weight along the spike, single seed weight, seed size, seed shape and seed surface area, enabling a detailed analysis of the performance of genotypically very diverse wheat accessions under both stress regimes. The chapter has been published as follows: Schmidt, J., Claussen, J., Wörlein, N., Eggert, A., Fleury, D., Garnett, T., & Gerth, S. (2020). Drought and heat stress tolerance screening in wheat using computed tomography. *Plant Methods,* 16.

Schmidt *et al. Plant Methods* (2020) 16:15
https://doi.org/10.1186/s13007-020-00565-w

Plant Methods

RESEARCH Open Access

Drought and heat stress tolerance screening in wheat using computed tomography

Jessica Schmidt[1], Joelle Claussen[2*], Norbert Wörlein[2], Anja Eggert[2], Delphine Fleury[1,3], Trevor Garnett[1] and Stefan Gerth[2]

Abstract

Background: Improving abiotic stress tolerance in wheat requires large scale screening of yield components such as seed weight, seed number and single seed weight, all of which is very laborious, and a detailed analysis of seed morphology is time-consuming and visually often impossible. Computed tomography offers the opportunity for much faster and more accurate assessment of yield components.

Results: An X-ray computed tomographic analysis was carried out on 203 very diverse wheat accessions which have been exposed to either drought or combined drought and heat stress. Results demonstrated that our computed tomography pipeline was capable of evaluating grain set with an accuracy of 95–99%. Most accessions exposed to combined drought and heat stress developed smaller, shrivelled seeds with an increased seed surface. As expected, seed weight and seed number per ear as well as single seed size were significantly reduced under combined drought and heat compared to drought alone. Seed weight along the ear was significantly reduced at the top and bottom of the wheat spike.

Conclusions: We were able to establish a pipeline with a higher throughput with scanning times of 7 min per ear and accuracy than previous pipelines predicting a set of agronomical important seed traits and to visualize even more complex traits such as seed deformations. The pipeline presented here could be scaled up to use for high throughput, high resolution phenotyping of tens of thousands of heads, greatly accelerating breeding efforts to improve abiotic stress tolerance.

Keywords: X-ray, High-throughput, Phenotyping, Yield, Seed morphology, Genetic diversity

Background

Wheat (*Triticum aestivum* L.) is one of the most important crops worldwide, accounting for 20% of the total calories and proteins in the human diet [1]. Its global production reaches 757.6 million tonnes per year with an annual consumption of 734 million tonnes [2]. Wheat yields are increasingly affected by global climate changes raising concerns regarding future food security. To increase wheat yields the understanding and genetic dissection of quantitative traits, especially those related to yield and stress tolerance, are required [3, 4].

Abiotic stresses such as heat, drought and frost negatively affect grain yield by reducing grain number, grain size and single grain weight. However, how and which yield component a certain stress affects varies with its duration, intensity and timing [5–7]. For instance, the occurrence of a stress before and during anthesis reduces the number of grains per ear due to an increased seed abortion, whereas grain weight is hardly affected. In contrast, an abiotic stress occurring after anthesis does not influence grain number but reduces grain size and single grain weight by impeding grain filling [5, 7, 8]. Further differences in the stress symptoms arise from temporal

*Correspondence: joelle.claussen@iis.fraunhofer.de
[2] Fraunhofer Development Center X-Ray Technology, Fürth, Germany
Full list of author information is available at the end of the article

variation in flowering between and within ears of a single plant [9, 10]. In order to identify genomic regions responsible for grain yield and stress tolerance, the precise analysis of the grain yield components per ear and along the ear is crucial.

Currently, yield data is obtained by machine threshing in the field [11] or hand threshing for pot experiments. In wheat, about 10% of the seeds are lost during machine threshing, of which 4 to 6% is due to broken seeds compared with 1% seed breakage in samples threshed by hand [12, 13]. Hand threshing, on the other hand, is laborious, costly, time-consuming, and particularly difficult for wild accessions and hulled landraces [14]. The evaluation of yield-related traits such as seed weight, seed size and seed number require additional labour and restricts the number of samples which can be processed [15–17]. This is problematic for genetic experiments consisting in studying hundreds or thousands different genotypes of large populations, gene banks or mutant collections.

In order to improve the efficiency and accuracy of grain yield components measurements in large experiments, a number of automated approaches have been developed in the last few years. For instance, hyperspectral and RGB imaging have been used for the high-throughput measurement of yield-correlated traits such as plant height, ground cover, above-ground biomass and growth dynamics [18–22]. However, these methods do not allow researchers to directly assess grain yield components. More recently, computed tomography, a well-established technique in medicine, has been successfully adapted to plant phenotyping, showing a greater potential compared to hyperspectral and RGB imaging. In fact, along with measuring visible traits such as tiller number [23], computed tomography was employed to gain new insights into root growth plasticity within soil [24–26] and the internal and outer characteristics of seeds, such as size, porosity, infections and cracks [27–30]. Computed tomography has also been applied to predict yield components in rice and wheat [15, 31, 32] but with technical limitations so far.

Given the potential of computed tomography in plant phenotyping, this study aimed to develop an automatic, non-destructive and accurate method to measure a wide range of wheat grain set characteristics under different abiotic stresses. Previously used X-ray scanners were limited by the size of the computed tomography instrument that enable to fit ears of a maximum length of 10 cm [31, 32]. Larger ears had therefore to be cut in half leading to potential losses of seeds, useful data regarding ear architecture and seed position and causing longer preparation time. Further, scanning times were prolonged with up to 40–80 min per wheat ear. To keep scanning times moderate, lower resolutions had to be used hindering the analysis of morphological variations such as germ deformations and estimation of the weight of smaller seeds (< 2.0 mm) which are important to calculate stress tolerance traits. In contrast, the system we used in our study features a high-resolution flat-panel detector with a pixel pitch of only 49.5 µm and about 2304 pixel in the horizontal direction. Thus, scanning the ears close to the detector enables a large field of view while maintaining a voxel sampling of 31.25 µm.

We used a computed tomography scanner with integrated helix function that allowed us to analyse four intact ears with lengths up to 20 cm (including awns) at the same time with a two- to three-times higher resolution. As a result, we increased our throughput and were able to accurately assess total seed weight per ear, seed number per ear, seed weight along the ear and single seed characteristics such as single seed weight, seed size, seed shape, seed surface area and physical density of seeds. Additionally, we were able to reconstruct morphological deformations which are symptomatic of wheat grown under drought and frost stress. We tested the method on material with a broad genetic diversity and under two abiotic stress regimes.

Results

Computed tomography measurements

Our aim was to develop a non-invasive method to automate grain set measurements of wheat ears exposed to different abiotic stresses. The measured parameters included total seed weight per ear, seed number per ear (> 2.0 mm), seed weight along the ear and single seed characteristics such as single seed weight, seed size (volume), seed shape (spherical ratio) and seed surface area. Total seed weight refers to the sum of the weight of all seeds per ear. The single seed weight is the weight of one individual seed. Seed weight along the ear was calculated as the sum of the measured weight of seeds at the particular position for all ears. Single seed characteristics were measured for each seed individually and then averaged per ear.

Ears of plants subjected to either drought or combined drought and heat stress were initially measured with a total of 8441 projections and a scanning time of ~ 70 min for four ears. To increase the throughput, a lower number of projections (3082 projections) was tested which produced images of similar quality and were still accurate enough for data acquisition and analysis. Scanning time decreased to ~ 25 min, resulting in a scanning time of 7 min per ear. These settings were used for routine scans.

3D reconstruction and seed trait extraction

After the image acquisition of the raw 2D projections each stack of helical computed tomography scans is reconstructed using a Filtered-Back-Projection-Algorithm developed within the Development of X-ray Center (Fraunhofer Institute of Integrated Circuits, Germany). This reconstruction algorithm is implemented following the principle described in Buzug et al. [33]. This algorithm normalize the output 3D volume via the automatic detection of the unattenuated intensity on each projection. Thus, variations in the primary beam intensity does not change the calculated absorption within a voxel. Additionally, the algorithm convert the same range of absorption values within the raw 3D volume to an unsigned 16-bit grey value volume. Doing so, the grey values within the resulting 3D dataset represent the physical absorption within the ears for the specific x-ray beam spectrum used during the measurement. Without this normalization approach in the Filtered-Back-Projection, it is not possible to use the apparent grey values as a measure of the absorption. Within this publication all grey values mentioned are reconstructed as described above. If the physical absorption is mentioned, the derived float value of the reconstruction algorithm is meant.

After the segmentation, the four ears within the volumes were manually divided into individual sub volumes. The EarS segmentation algorithm was used to segment the individual 3D volumes of an ear. An example of the visualization and segmentation is shown in Fig. 1. Additionally to the 3D visualization for two different ears (Fig. 1a), a 2D cross-section and the segmentation overview is shown (Fig. 1b). The algorithm is segmenting all seeds along the ear in 3D. Subsequently, each seed is stored in a small 3D volume for feature extraction. Additionally, a 2D cross section is created alongside the largest diameter within the seed (Fig. 1b).

Using a subset of about 10% ears, the correction factor between the virtual seed weight and the measured seed weight was determined. This correction factor was later on used for the calibration of the virtual total seed weight. For all the individual seed volumes a set of volumetric features is calculated and stored in a comma separated file.

Evaluation of the image analysis algorithm

The performance of the algorithm was evaluated by comparing estimated (virtual) versus manually measured (actual) traits including total seed weight and number of seeds of > 2.0 mm size from the 291 wheat ears. The 2 mm diameter was selected to virtually represent the sieve during the threshing process. Thus, all seeds

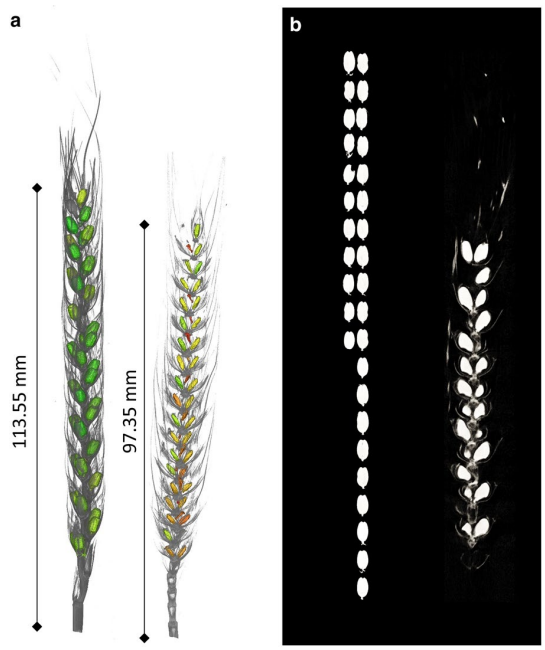

Fig. 1 Reconstruction of wheat ears. **a** Virtual cross-section of the three-dimensional reconstruction of two wheat ears subjected to drought (left) and combined drought and heat (right) stress. **b** 2D representation of each seed at its maximum diameter of one ear

featuring a diameter smaller than 2 mm in every direction are omitted virtually. Scatter plots of virtual versus actual measurements are shown in Fig. 2a for the weight and 2b for the number of seeds > 2.0 mm. Total seed weight per ear was reduced ($p \leq 0.001$) under combined drought and heat (DH) stress in comparison to the single drought stress (D). Seed weight under DH ranged from 0.03 to a maximum of 1.97 g per ear with an average of 0.40 g, whereas values ranged from 0.06 to 3.22 g with an average of 1.57 g per ear under D. Both plants with very small seed weight and with big seed weight were represented well by the algorithm, capturing a wide range of seed weights. Coefficients of determination (r^2) were high between virtual and actual seed weight per ear with an r^2 of 0.83 and 0.96 under D and DH, respectively.

Number of seeds > 2.0 mm of size were severely reduced ($p \leq 0.001$) under DH in comparison to D. Under DH, only 25.7% of the plants contained seeds above 2.0 mm, whereas under D 87.4% of the plants produced larger seeds. In addition, plants under DH produced a maximum of 49 seeds per ear, while plants under D produced up to 73 seeds per ear. By contrast, the amount of small seeds (< 2.0 mm) per ear was increased under DH in comparison to D. The coefficient of determination between virtual and actual seed numbers were highest

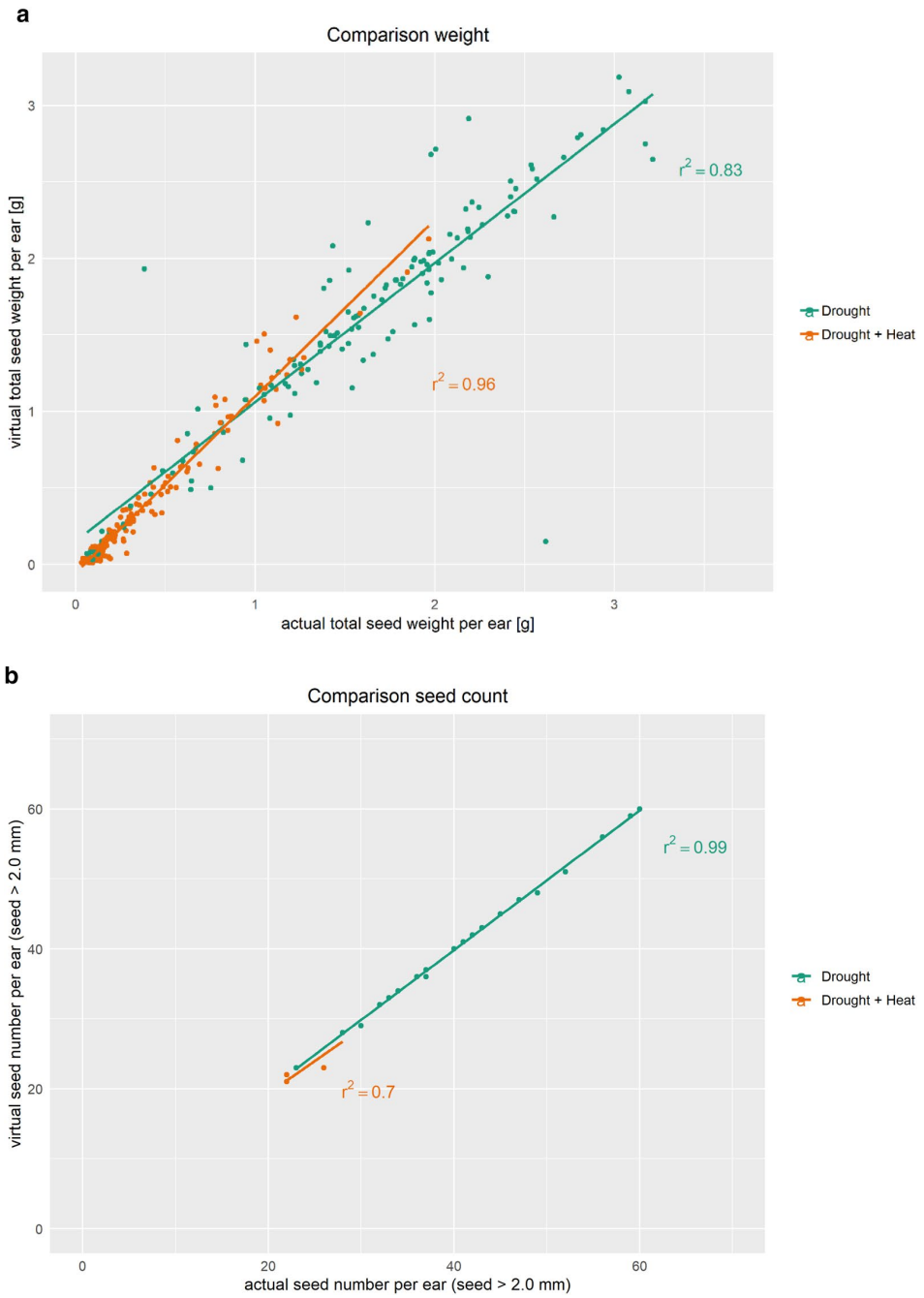

Fig. 2 Predictions of seed weight and seed number per ear. Comparison of **a** virtual total seed weight per ear with actual total seed weight per ear and **b** comparison of virtual seed number per ear (seeds > 2.0 mm) with actual seed number of per ear. Under drought, 125 out of the 143 plants produced seeds above 2.0 mm, under combined drought and heat only 38 out of the 148 plants produced seeds of > 2.0 mm of size. r^2, correlation coefficient

under D (r^2 of 0.99). The coefficient of determination under DH were high (r^2 of 0.70) but lower in comparison to D probably due to reduced number of plants containing big seeds.

Ears of the same accession but under different treatments showed mostly an average to good performance (i.e., seed weight $\geq$ 1.50 g, seed number $\geq$ 36) under D, but a bad performance under DH (i.e., seed number of zero). Ten out of the 46 accessions with ears exposed to D and DH were susceptible to both treatments with most of them being Australian varieties. Eight accessions performed relatively well under D and DH (i.e. seed weight ranging between 0.68 and 1.58 g with 17 to 45 seeds per ear) of which most were older varieties from Australia, Mexico, Asia and Canada. Even if some accessions performed well under both treatments, their performance under DH was never higher than the one under D which is not surprising since two stresses have a more severe impact on seed weight and seed number than a single stress alone.

Virtual measurements of wheat grain set in response to drought and heat stress

The EarS algorithm was used to acquire seed set characteristics and to estimate the performance of diverse wheat accessions under two stress regimes. Significant differences between D and DH treatments were observed for four of the six virtually measured seed set characteristics (Fig. 3). Under DH, single seed weight as well as seed size (i.e. seed volume) were reduced in comparison to D. Seeds under D weight on average 0.03 g, whereas seed under DH were on average 0.02 g lighter, probably due to a reduced seed size. Seeds from plant under DH were also less round (i.e. reduced spherical ratio) but had an increased surface compared to seeds from plants subjected to D. Mean attenuation value is representing the physical density and were similar under both treatments with an average value of 0.80.

Decrease in spherical ratio of seeds under DH in comparison to D correlated with a decreased seed size, meaning that ears exposed to DH developed mostly seeds which were smaller and less round (Fig. 4). Ears of plants exposed to D contained mostly larger and rounder seeds with an average seed volume of 23.04 mm^3 and a spherical ratio of 0.53 compared to an average seed volume of 7.98 mm^3 and a spherical ratio of 0.46 under DH. Larger seeds had a fully developed crease and germ. The majority of the plants under DH showed severe seed deformations with large hollow cavities in the middle of the seeds (crease) and a not fully developed germ indicating an inhibition of grain filling or a late abortion. Those cavities lead to a larger surface area of seeds under DH compared to most seeds under D. The relative number of surface voxel is calculated as the ration of number of surface voxel divided by the volume of the seed. Which means that this value is close to zero for objects close to a sphere and close to one for a plane.

To represent variations in the impact of both stress regimes on seed weight along the ear, the average virtual seed weight was plotted against the normalised ear position (Fig. 5). The central region of the ear contained more large seeds (seed size > 2.0 mm) than the top and bottom of the ear for both D and DH treatments. However, clear differences in seed weight between D and DH were observed. Under DH, seed weight was in general low along the whole ear with a slight decrease at the top and bottom of the ear (average 0.01 g) and the highest seed weight at position 0.55 (centre of ear, average 0.02 g). Average seed weight under DH was always below the seed weight under D along the whole ear (Fig. 5). Under D, average seed weight was severely decreased at the top and base of the ear (average 0.03 g) in comparison to rest of the ear. Interestingly, the highest seed weight was not located directly in the centre (position 0.50) but rather shifted towards the top of the ear (around 0.65–0.70, average 0.036 g).

Discussion

Although the application of computed tomography to plants has been published before [23–32], our method enabled us to considerably increase speed and accuracy of grain measurement as well as to measure small genetic differences between wheats under stress conditions. Previously implemented computed tomography pipelines in wheat struggled with fusion problems between seeds due to the use of a low resolution. Further, due to long preparation and scanning times, only a small number of accessions and ears could be measured [30–32]. Our aim was therefore to develop a non-destructive, faster and more accurate computed tomography pipeline to predict yield related traits for a wide range of wheat accessions under different abiotic stress regimes.

Scanning time for each ear was around seven minutes in comparison to 40- and 80-min scanning time per ear in Hughes et al. [31] and Strange et al. [30], respectively, while using a two- to three-times higher resolution. The higher resolution allowed us to get a more detailed view of seeds and to reduce fusion issues achieving a higher accuracy of 0.83–0.96 for seed weight and 0.70–0.99 for seed number. In order to establish a computed tomography pipeline capable of predicting most accurately seed weight per ear and the derived seed traits, we calculated a virtual seed weight instead of seed volume only [31, 32]. Current pipelines tested in wheat work for fully developed, well filled seeds but would struggle to identify underdeveloped, poorly filled seeds. This is of

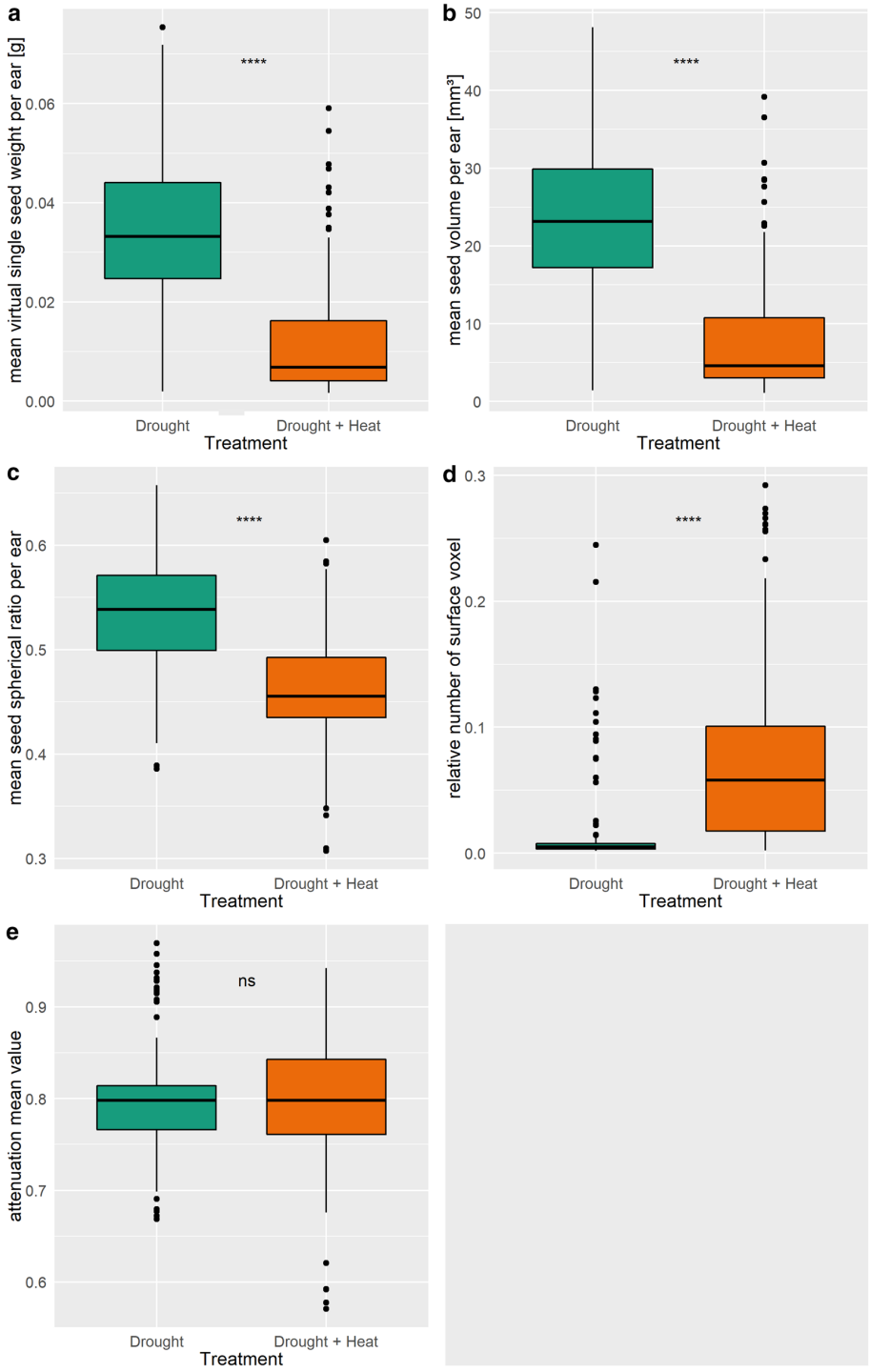

Fig. 3 Virtually measured seed set characteristics under drought and combined drought and heat treatment. Mean attenuation mean value are representing the physical density of the seeds. Seed set characteristics were measured for each seed individually and subsequently averaged per ear. Drought: n = 143; drought and heat: n = 148. *, **, ***, ****Indicate $p \leq 0.05$, 0.01, 0.001 and 0.0001, respectively. *Ns* not significant

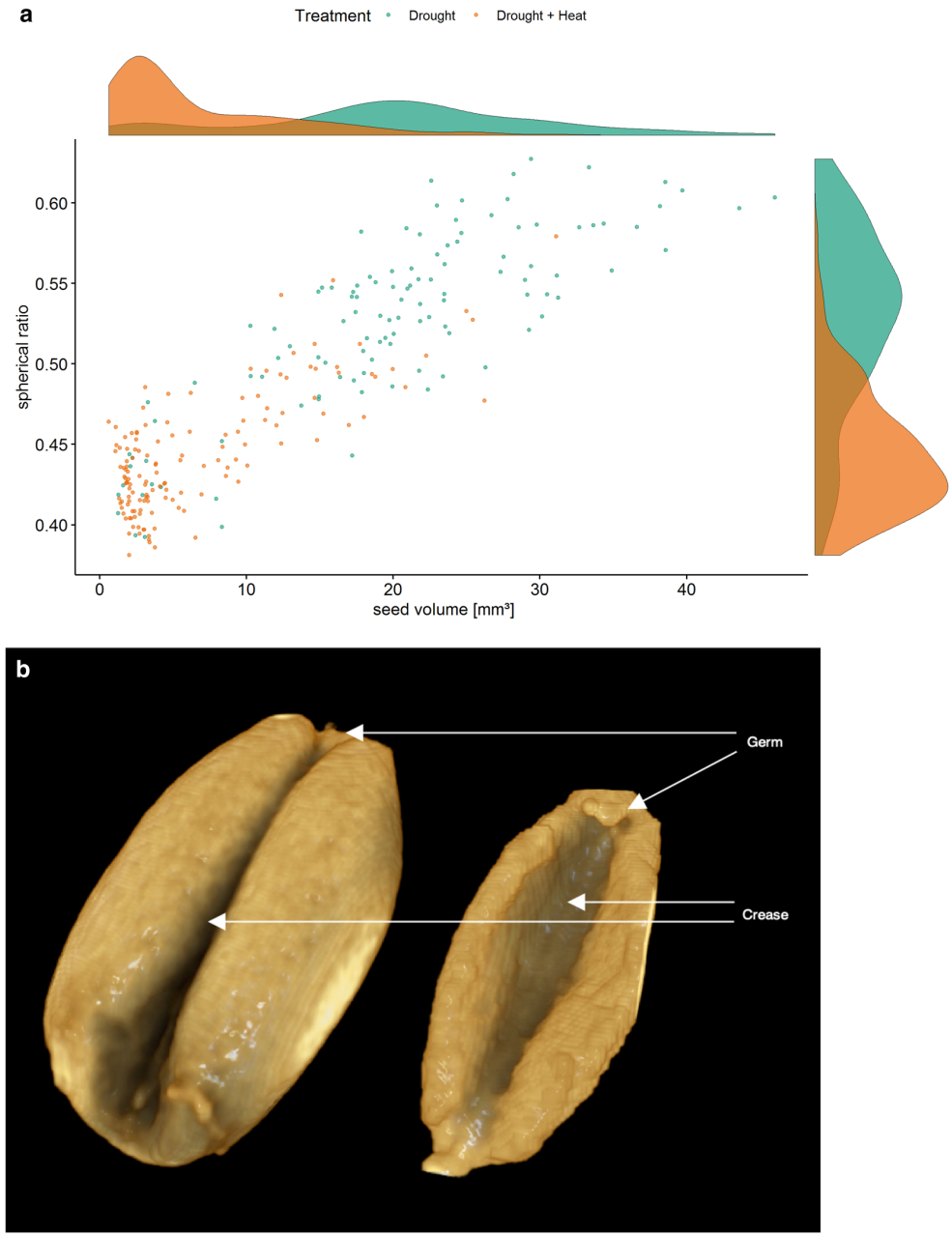

Fig. 4 Seed morphology analysis. **a** Virtual spherical ratio versus virtual seed volume of single seeds under drought and drought and heat stress. **b** 3D reconstruction of a seed under drought stress with a length of 4.9 mm (left) and drought and heat stress with a length of 3.7 mm (right)

importance due to the increased occurrence of underdeveloped seeds under abiotic stresses which feature a relative volume but are mainly hollow inside caused by the impediment in the development and grain filling of the seeds [34–36]. Poorly filled seeds affect negatively seed test weight and are diminished in their milling and baking qualities in comparison to well filled seeds. The differentiation between poorly and well filled seeds is therefore crucial in order to estimate the actual grain production and quality outcome [37].

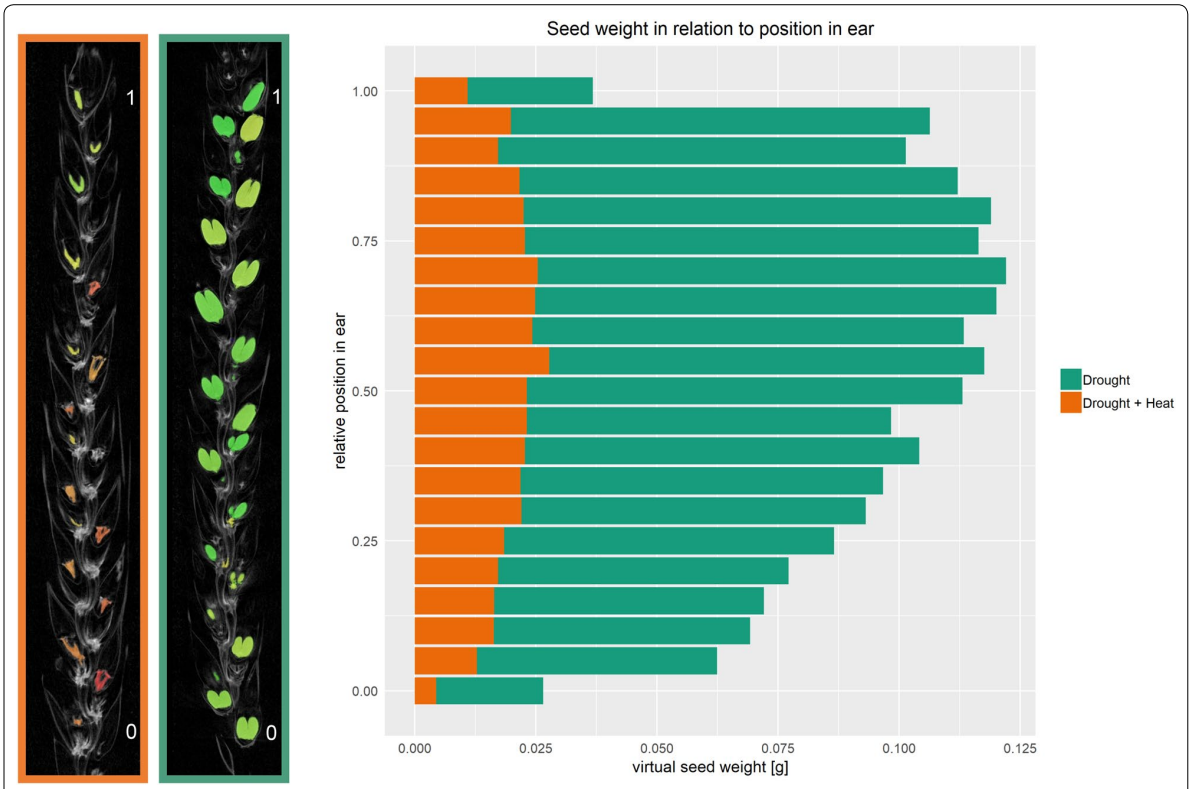

Fig. 5 Virtual seed weight in relation to position in ear. 0 marks the first seed detected at the bottom of the ear including big (seed size > 2.0 mm) and small seeds (seed size < 2.0 mm) and 1 the last seed detected at the top of the ear. For illustration, a wheat ear subjected to drought (green background) and to drought and heat (orange background) are attached. Drought: n = 143; drought and heat: n = 148

Under D and DH, we detected small, underdeveloped seeds with a "shrivelled" appearance. This phenomenon has been previously observed visually in wheat by Cromey et al. [35] and Gaines et al. [37] under rainfed and frost conditions but has not been shown with any of the so far implemented computed tomography pipelines. Most shrivelled seeds occurred in plants exposed to DH indicating a synergistic effect of both abiotic stresses. Apart from the "shrivelled" appearance, we could also observe a stress induced deformation of the germ and an increased crease cavity explaining the increase in seed surface of smaller seeds (Fig. 4b). Future investigation of why and when these deformations occur might be possible using computed tomography scans gaining new insight into seed and ear morphology under different abiotic stresses. In contrast, the mean attenuation value was similar under both treatments, indicating that the starch density was only slightly affected by the heat component of the DH treatment. Smaller seeds seem therefore to accumulate starch in the same density but in less amount than bigger seeds causing potentially the described cavities.

As in previous studies, we could demonstrate the synergistic effect of D and H on seed weight, single seed weight and number of seeds > 2.0 mm [38, 39]. All traits were similarly affected with a decrease between 64 and 83%, the highest decrease being in seed number. Seed number explains up to 84% of the variation in yield and is therefore a crucial component for improving yield under abiotic stress [40–42]. Most studies report a decrease in seed number if the stress occurs during meiosis,however, recent papers showed also an effect on seed number under post-anthesis stress [38, 39, 43]. Average seed weight was decreased at the top and bottom of the ear under both treatments with a more severe effect of DH. The decrease of seed weight at the extremes of the ears is likely due to the spatial differences in the development of the ear with the middle flowering usually earlier than top and bottom parts [9, 10].

Using a genetically diverse material enabled us to capture a broad variation in seed weight and components for implementing our pipeline to identify germplasm with an increased drought and heat tolerance. In our study, eight accessions, predominantly from countries characterized

by dry and hot summers (i.e., Australia, Iraq, Tunisia, India and Mexico) showed relatively good performances under both treatments in regard to seed weight. Those accessions produced on average more seeds and seeds of increased weight, size and rounder shape. Screening genetic diversity for tolerant germplasms is essential for mining novel candidate genes underlying traits of agricultural importance such as abiotic stress tolerance. Novel genes and alleles can then be implemented in breeding programmes to breed high-yielding crops adapted to future climates [44].

Future perspectives

The combination of both molecular and high-throughput phenotyping technologies is important for the improvement of crops under abiotic stresses [45]. The computed tomography pipeline we developed enables the analysis of thousands of ears in a relative short time, numbers that would allow to study precisely the genetic of grain set development in large genetic populations and mutant collections. The approach could also be used to screen large and diverse collections preserved in gene banks allowing to explore distant gene pools and possibly preselect material with high yield potential for breeding. The method could also be adapted to other crops such as barley. Single time point measurements could also be replaced by dynamic data such as kinetics of grain growth and potentially embryo development as well as developmental alterations over time induced by abiotic stresses.

Conclusions

We developed a robust, fast and accurate computed tomography pipeline for wheat which can measure seed traits under various stress conditions and for a broader range of wheat accessions. We demonstrated that our method can detect small genetic differences between wheats, ears and even single seeds, which is essential to improve grain yield and produce resilient varieties. More importantly our method is amenable to automation enabling us to phenotype, with high resolution, one hundred thousand wheat heads in 6 weeks only. This throughput is compatible with large scale genetic studies and breeding programmes where hundred thousand yield plots have to be assessed every year in the field. Additional morphological traits such as seed shrivelling and germ deformation have been measured for the first time under combined drought and heat stress. Our computed tomography pipeline is therefore a quick method enabling the measurements of common seed traits in combination with a detailed analysis of seed and ear morphology.

Methods

Plant material

A panel of 315 diverse bread wheat accessions was sown in 2017 (from May to November) on the Waite Campus of the University of Adelaide (Urrbrae, South Australia). Plants were grown in a polyurethane tunnel in pots filled with a substrate mix (clay-loam, sand and coco peat, 1:1:1) supplemented with a basal, slow-release fertilizer. Pots were watered from underneath and kept under well-watered conditions until anthesis. Three days after anthesis of the primary tiller, plants were exposed individually to either drought or combined drought and heat, mimicking growing conditions common in the southern Australian climate. Drought was imposed by stopping irrigation for 6 days. The heat treatment was applied on the 4th day of the drought treatment by moving the plants in a heat chamber to expose plants to 35/25 °C day/night for three days. Treatments were arranged in a randomized split-plot design with three replications. A subset of 291 ears of the primary tiller which varied regarding yield and yield-related traits (143 drought-treated and 148 combined drought and heat-treated) were selected from 203 of the 315 accessions with 46 accessions represented in both treatments. A list of accessions is given in Additional file 1.

Computed tomography measurements

X-ray computed tomography measurements were performed at the Development Center X-Ray Technology (EZRT) of the Fraunhofer Institute of Integrated Circuits (Fürth, Germany) using the "CTportable160.90". The scanner consisted of a cone beam X-ray source with voltage ranging from 20 to 90 kV, current up to 89 µA and a detector size of 2304 × 1278 pixels (49.5 µm pixel size). The system consists of a Thermo Scientific PXS5-928 microfocus monoblock X-ray source, featuring a transmission target with only 6 mm spot to window spacing. Additionally, the focal spot size of the source is dependent on the actual power (4 µm @ 2 watts). The sample stage can be positioned between X-ray source and detector with a minimum focus object distance (FOD) of 10 mm and a maximum FOD of 285 mm. The focus detector distance (FDD) is fixed to 290 mm. Thus, the maximum nominal magnification is 29 for objects with diameters below 8 mm. However, limiting the maximum magnification to about 18 will result in an acceptable edge blurring of 1.4 pixel due to the focal spot size of 4 µm. The resulting maximum resolution is 2.8 µm. The detector is a 14 bit CMOS sensor (Teledyne DALSA Shad-o-Box 3K HS) with a direct-contact Gd_2O_2S scintillator (Kodak Min-R 2190) scintillation foil.

Within this experiment, the system was operated at 90 kV and 80 µA and a nominal spatial voxel sampling of 31.25 µm to cover the biggest field of view during the scan. To extend the vertical field of view a helical scanning geometry was used to scan four ears simultaneously (i.e. vertical movement during several 360° rotations). Thus, ears were scanned in their full length and at the same time Feldkamp artefacts are avoided. A total of 3082 projections within 4.24 times 360° rotations in a helical scan were taken with an exposure time of 500 ms in a FlyBy acquisition allowing the system to rotate the ear constantly during the image exposure. Each scan lasted about 27 min producing images with a spatial voxel sampling of 31.25 µm pixel^{-1}. The software Volex 6 (Fraunhofer Institute of Integrated Circuits, Germany) was used for controlling the system.

3D reconstruction and seed trait extraction

Images were 3D reconstructed with a filtered back projection (Fraunhofer Institute for Integrated Circuits, Germany, REL-2.1.1) and cropped using the software VolumePlayerPlus (Fraunhofer Institute for Integrated Circuits, Germany, 8.1.9). The algorithm EarS (Fraunhofer Institute for Integrated Circuits, Germany, Revision number 227116) determines a wide range of wheat ear and grain components. To evaluate the performance of the image analysis algorithm, ears were carefully threshed by hand and total seed weight and seed number (seeds > 2.0 mm of size) were measured. The obtained parameters were correlated with the data from the X-ray scans. The EarS algorithm first separates each individual grain from the ear itself. Each grain is automatically oriented using a principal axis transformation in 3D. Thus, 2D cross sections alongside the largest slice can be used for fast visual inspection of the performance of the algorithm. Additionally, for each individual grain different features are analysed in 3D and stored in a csv file. With the current revision number 227116 of EarS, for each grain, following digital traits are calculated within the ear:

- Amount of voxel in the grain.
- Corresponding volume of the grain in mm^3.
- Virtual weight in g.
- Centre of mass of the grain in the 3D volume in x, y, z coordinates.
- Mean attenuation value of the grain.
- Aspect ratio of the grain.
- Surface of the grain.
- Ratio between volume and surface of the grain.

The amount of voxel is gathered by automatically separating the grain from the surrounding biological material. Having the voxel sampling size calibrated within the system, the volume of the whole grain is derived multiplying the physical voxel size with the amount of voxel within a seed. Using the volume and the mean physical absorption, a virtual weight can be calculated and therefore the position of the centre of the mass of each grain [46]. The value of the mean physical absorption is directly generated from the normalization of the FireFly Filtered-Back-Projection. The centre of mass is used to calculate the distances between individual grains alongside the ear. The surface is approximated by counting the number of voxels connected to the binary background of the volume. Out of this, it is possible to calculate the surface to volume ratio for each grain. Another morphological trait is the aspect ratio calculated by comparing the radius of the minimum covering sphere with the radius of a sphere featuring the same volume as the grain. Values between 0 and 1 are derived, where 0 would be an infinite long and thin rod, and 1, a perfect sphere. Whereas most of the calculations for the aspect ratio are in 2D [47], the EarS algorithm expands the aspect ratio calculation to 3D.

Supplementary information

Supplementary information accompanies this paper at https://doi.org/10.1186/s13007-020-00565-w.

Additional file 1. List of *Triticum aestivum* accessions.

Abbreviations

2D: Two-dimensional; 3D: Three-dimensional; D: Drought; DH: Combined drought and heat stress; r^2: Correlation coefficient; RGB: Red–green–blue.

Acknowledgements

The authors would like to thank the Australian Grains Genebank for supplying seeds for the experiment at the University of Adelaide.

Authors' contributions

JS conducted the experiment at the University of Adelaide and wrote the manuscript. JC, DF, TG, and SG edited the manuscript. JC created the figures and carried out the statistical analysis. JS, JC, SG and AE performed the X-ray scanning. NW developed the algorithm. DF designed and supervised the experiment at the University of Adelaide. SG supervised the X-ray scans and algorithm development. TG and SG conceived and designed the X-ray experiment. All authors read and approved the final manuscript.

Funding

The project was funded by the Australian Research Council Industrial Transformation Research Hub for Genetic Diversity and Molecular Breeding for Wheat in a Hot and Dry Climate (Project number IH130200027).

Availability of data and materials

Not applicable.

Ethics approval and consent to participate

Not applicable.

Consent for publication

Not applicable.

Competing interests
The authors declare that they have no competing interests.

Author details
[1] School of Agriculture, Food and Wine, The University of Adelaide, Glen Osmond, SA, Australia. [2] Fraunhofer Development Center X-Ray Technology, Fürth, Germany. [3] Innolea, 6 chemin de Panedautes, 31700 Mondonville, France.

Received: 16 October 2019 Accepted: 6 February 2020
Published online: 13 February 2020

References

1. Shiferaw B, Smale M, Braun HJ, Duveiller E, Reynolds M, Muricho G. Crops that feed the world 10. Past successes and future challenges to the role played by wheat in global food security. Food Secur. 2013;5:291–317.
2. Food and Agriculture Organization of the United Nations. World food situation. 2018. https://www.fao.org/worldfoodsituation/csdb/en/. Accessed 5 Oct 2018.
3. Tester M, Langridge P. Breeding technologies to increase crop production in a changing world. Science. 2010;327:818–22.
4. He Z, Joshi AK, Zhang W. Climate vulnerabilities and wheat production. In: Pielke RA, editor. Climate vulnerability: understanding and addressing threats to essential resources. Waltham: Academic Press; 2013. p. 57–67.
5. Demotes-Mainard S, Doussinault S, Meynard JM. Effects of low radiation and low temperature at meiosis on pollen viability and grain set in wheat. Agronomie. 1995;15:357–65.
6. Foulkes MJ, Sylvester-Bradley R. The ability of wheat cultivars to withstand drought in UK conditions: formation of grain yield. J Agric Sci. 2002;138:153–69.
7. Weldearegay DF, Yan F, Jiang D, Liu F. Independent and combined effects of soil warming and drought stress during anthesis on seed set and grain yield in two spring wheat varieties. J Agron Crop Sci. 2012;198:245–53.
8. Blum A. Improving wheat grain filling under stress by stem reserve mobilisation. Euphytica. 1998;100:77–83.
9. Whaley JM, Kirby EJM, Spink JH, Foulkes MJ, Sparkes DL. Frost damage to winter wheat in the UK: the effect of plant population density. Eur J Agron. 2004;21:105–15.
10. Lukac M, Gooding MJ, Griffiths S, Jones HE. Asynchronous flowering and within-plant flowering diversity in wheat and the implications for crop resilience to heat. Ann Bot. 2012;109:843–50.
11. Macdonald S. The progress of the early threshing machine. Agric Hist Rev. 1975;23:63–77.
12. Tuff DW, Telford HS. Wheat fracturing as affecting infestation by *Cryptolestes ferrugineus*. J Econ Entomol. 1964;57:513–6.
13. Basavaraja H, Mahajanashetti SB, Udagatti NC. Economic analysis of postharvest losses in food grains in India: a case study of Karnataka. Agric Econ Res Rev. 2007;20:117–26.
14. Tzarfati R, Saranga Y, Barak V, Gopher A, Korol AB, Abbo S. Threshing efficiency as an incentive for rapid domestication of emmer wheat. Ann Bot. 2013;112:829–37.
15. Duan L, Yang W, Huang C, Liu Q. A novel machine-vision-based facility for the automatic evaluation of yield-related traits in rice. Plant Methods. 2011;7:44–57.
16. Dencic S, Kastori R, Kobiljski B, Duggan B. Evaluation of grain yield and its components in wheat cultivars and landraces under near optimal and drought conditions. Euphytica. 2000;113:43–52.
17. Nicol JM, Ortiz-Monasterio I. Effects of the root-lesion nematode *Pratylenchus thornei* on wheat yields in Mexico. Nematology. 2004;6:485–93.
18. Shanahan JF, Schepers JS, Francis DD, Varvel GE, Wilhelm WW, Tringe JM, et al. Use of remote-sensing imagery to estimate corn grain yield. Agron J Abstr. 2001;93:583–9.
19. Golzarian MR, Frick RA, Rajendran K, Berger B, Roy S, Tester M, et al. Accurate inference of shoot biomass from high-throughput images of cereal plants. Plant Methods. 2011;7:2.
20. Tisne S, Serrand Y, Bach L, Gilbault E, Ben Ameur R, Balasse H, et al. Phenoscope: an automated large-scale phenotyping platform offering high spatial homogeneity. Plant J. 2013;74:534–44.
21. Muraya MM, Chu J, Zhao Y, Junker A, Klukas C, Reif JC, Altmann T. Genetic variation of growth dynamics in maize (*Zea mays* L.) revealed through automated non-invasive phenotyping. Plant J. 2017;89:366–80.
22. Jimenez-Berni JA, Deery DM, Rozas-Larraondo P, Condon AG, Rebetzke GJ, James RA, et al. High throughput determination of plant height, ground cover, and above-ground biomass in wheat with LiDAR. Front Plant Sci. 2018;9:237.
23. Yang W, Xu X, Duan L, Luo Q, Chen S, Zeng S, Liu Q. High-throughput measurement of rice tillers using a conveyor equipped with X-ray computed tomography. Rev Sci Instrum. 2011;82:025102–9.
24. Gregory PJ, Hutchison DJ, Read DB, Jenneson PM, Gilboy WB, Morton E. Non-invasive imaging of roots with high resolution X-ray micro-tomography. Plant Soil. 2003;255:351–9.
25. Pfeifer J, Kirchgessner N, Colombi T, Walter A. Rapid phenotyping of crop root systems in undisturbed field soils using X-ray computed tomography. Plant Methods. 2015;11:1–8.
26. Metzner R, Eggert A, van Dusschoten D, Pflugfelder D, Gerth S, Schurr U, Uhlmann N, Jahnke S. Direct comparison of MRI and X-ray CT technologies for 3D imaging of root systems in soil: potential and challenges for root trait quantification. Plant Methods. 2015;11:1–11.
27. Moreira de Carvalho ML, van Aelst AC, van Eck JW, Hoekstra FA. Preharvest stress cracks in maize (*Zea mays* L.) kernels as characterized by visual, X-ray and low temperature scanning electron microscopical analysis: effect on kernel quality. Seed Sci Res. 1999;9:227–236.
28. Narvankar DS, Singh CB, Jayas DS, White NDG. Assessment of soft X-ray imaging for detection of fungal infection in wheat. Biosyst Eng. 2009;103:49–56.
29. Frisullo P, Laverse J, Barnaba M, Navarini L, Del Nobile MA. Coffee beans microstructural changes induced by cultivation processing: an X-ray microtomographic investigation. J Food Eng. 2012;109:175–81.
30. Strange H, Zwiggelaar R, Sturrock C, Mooney SJ, Doonan JH. Non-destructive, high-content analysis of wheat grain traits using X-ray micro computed tomography. Funct Plant Biol. 2015;42:452–9.
31. Hughes N, Askew K, Scotson CP, Williams K, Sauze C, Corke F, et al. Non-destructive, high-content analysis of wheat grain traits using X-ray micro computed tomography. Plant Methods. 2017;13:76.
32. Hughes N, Oliveira HR, Fradgley N, Corke FMK, Cockram J, Doonan JH, et al. CT trait analysis reveals morphometric differences between domesticated temperate small grain cereals and their wild relatives. Plant J. 2019;99:98–111.
33. Buzug TM. Computed tomography: from photon statistics to modern cone-beam CT. Berlin: Springer; 2008.
34. Pena RJ, Nagarajan P, Bates LS. Grain shriveling in secondary hexaploid triticale. II. Morphology of mature and developing grains related to grain shriveling. Cereal Chem. 1982;59:459–68.
35. Cromey M, Wright D, Boddington H. Effects of frost during grain filling on wheat yield and grain structure. N Z J Crop Hortic Sci. 1998;26:279–90.
36. Zakaria S, Matsuda T, Tajima S, Nitta Y. Effect of high temperature at ripening stage on the reserve accumulation in seed in some rice cultivars. Plant Prod Sci. 2002;5:160–8.
37. Gaines CS, Finney PF, Fleege LM, Andrews LC. Use of aspiration and the single-kernel characterization system to evaluate the puffed and shriveled condition of soft wheat grain. Cereal Chem. 1998;75:207–11.
38. Prasad PVV, Pisipati SR, Momcilovic I, Ristic Z. Independent and combined effects of high temperature and drought stress during grain filling on plant yield and chloroplast EF-Tu expression in spring wheat. J Agron Crop Sci. 2011;197:430–41.
39. Pradhan GP, Prasad PV, Fritz AK, Kirkham MB, Gill BS. Effects of drought and high temperature stress on synthetic hexaploid wheat. Funct Plant Biol. 2012;39:190–8.
40. Frederick JR, Bauer PJ. Physiological and numerical components of wheat yield. In: Satorre EH, Slafer GA, editors. Wheat: ecology and physiology of yield determination. New York: Haworth Press; 1999. p. 45–65.
41. Pinto RS, Reynolds MP, Mathews KL, McIntyre CL, Olivares-Villegas JJ, Chapman SC. Heat and drought adaptive QTL in a wheat population designed to minimize confounding agronomic effects. Theor Appl Genet. 2010;121:1001–21.
42. Dolferus R, Ji X, Richards RA. Abiotic stress and control of grain number in cereals. Plant Sci. 2011;181:331–41.
43. Qaseem MF, Qureshi R, Muqaddasi QH, Shaheen H, Kousar R, Roder MS. Genome-wide association mapping in bread wheat subjected to

independent and combined high temperature and drought stress. PLoS ONE. 2018;13:6.
44. Feuillet C, Langridge P, Waugh R. Cereal breeding takes a walk on the wild side. Trends Genet. 2008;24:24–322.
45. Furbank RT, Tester M. Phenomics—technologies to relive the phenotyping bottleneck. Trends Plant Sci. 2011;16:1360–85.
46. Ruina A, Pratap R. Center of mass and gravity. In: Introduction to statics and dynamics. Oxford University Press; 2015. p. 138–47 **(Pre-print)**.
47. Ahn SJ, Rauh W, Recknagel M. Circular coded landmark for optical 3D-measurement and robot vision. In: Proceedings of the IEEE/RSJ international conference on intelligent robots and systems. Korea: Kyunghee Printing; 1999. p. 1128–33.

Publisher's Note

Chapter 5

General discussion

The purpose of this study was to improve our genetic and physiological understanding of the complex quantitative trait of drought and heat stress tolerance at early grain filling in bread wheat by i) identifying and validating novel loci and alleles associated with combined drought and heat stress tolerance, ii) identifying and characterizing drought and heat-responsive wheat genes and iii) developing a high-throughput method that allowed us to automate the evaluation of yield components and morphological changes in seeds in response to abiotic stresses in glasshouse experiments.

Significance of the work

Wheat is one of the most important cereals worldwide with bread wheat (*Triticum aestivum* L.) accounting for 90 % of the world wheat production (Feuillet et al. 2008). However, wheat production is facing new challenges to ensure global food security due to climate change and a constantly growing world population (Rosenzweig and Parry 1994). One of the consequences of climate change is the increase in magnitude and frequency of abiotic stresses such as drought and heat causing vast yield losses in bread wheat (Trnka et al. 2014, Zampieri et al. 2016, Zampieri et al. 2017). Breeders will need to select for the best traits and quantitative trait loci (QTL) to improve and develop crop varieties tolerant to future drought and heat stress scenarios (Reynolds et al. 2010).

Until recently, most studies focussed on either drought or heat stress. However, in many wheat growing regions of the world, drought and heat stresses occur simultaneously during the crop cycle (Gbegbelegbe et al. 2016, Toreti et al., 2019). The effect of drought and heat stress on plant physiology and performance can either be synergistic (e.g., relative water content in plants) (Machado and Paulsen 2001), hypo-additive (e.g., yield) (Pradhan et al. 2012) or even antagonistic (e.g., stomatal conductance) (Perdomo et al. 2015). The combination of both stresses has therefore to be considered as a unique stress, rather than simply the sum of both stresses (Mittler 2006). In our genome-wide association study (GWAS) (Chapter 2), we were able to analyse drought, the heat response under drought and combined drought and heat treatment effects separately and identified QTL associated with either one, two or all three conditions. We also found 55 QTL which were common across treatments and years. These are important, since QTL with consitent effects are more likely to be used in the development and selection of new varieties.

QTL often interact with the environment (GxE) and with each other (QTLxQTL), meaning their allelic effects depend on environmental fluctuations and the presence and absence of other

QTL (Brennan and Byth 1979, Gupta et al. 2017). Our target QTL on chromosome 6B shows interaction with the environment. In the genome-wide association study (semi-controlled pot system, Chapter 2) and the glasshouse experiment (controlled pot system, Chapters 3) results were consistent with the non-Australian allele increasing seed weight, seed number and single seed weight. However, results in South Australian field trials (Garcia et al. 2019) using a similar diversity panel as used in Chapter 2 showed the opposite allelic effect. Even if pot systems might be a useful way to identify preliminary QTL, these QTL need to be validated in field-like conditions and in different genetic backgrounds, years and environments (Knoll and Ejeta 2008). One of our target QTL on chromosome 6A was validated under semi-controlled drought and heat stress field conditions using near-isogenic lines (NILs), showing consistent results with previous years (Chapter 2) and making it a reliable candidate. NILs for the 6A QTL are also tested in larger field trials this year. Markers have been developed for both target loci offering potential for marker-assisted selection in wheat breeding programs. Nevertheless, traits like yield are under multigenic control and the selection for single QTL will not be enough to achieve significant yield increases. Pyramiding of several of the identified QTL will be required.

Using gene expression analysis, we also identified 41 genes at our target region on chromosome 6B (Chapter 3). Some of these genes were associated with previously known proteins such as proline, whereas most of the identified genes have not yet-been characterized. Unknown genes and gene functions offer the potential for the discovery of novel candidate genes that might be used for direct manipulation in current cultivars, or cloned and used as finer markers in breeding. Transgenic wheat plants, for instance, have been developed for a range of well-known drought and heat stress genes, including ABA-responsive genes, proline biosynthesis genes, glycinebetaine encoding genes as well as stress-responsive promoter and transcription factors; with yield increases of up to 21.4 % under drought or heat stress (Sivamani et al. 2000, Vendruscolo et al. 2007, Wang et al. 2010, Freeman et al. 2011, Saint Pierre et al. 2012, Rong et al. 2014). Several of the genes we found, particularly under combined drought and heat stress, were involved in regulating gene expression and RNA processing, indicating trans-regulatory elements. The lack of specificity of trans-regulatory elements and their potential variation in effect within different genetic backgrounds might make them a difficult target for crop improvement. Nonetheless, work has shown that the effect in trans is often determined by genetic polymorphisms at target genes or motifs (e.g., Ferdous et al. 2017). In these cases, trans regulation can be explored by the genetic identification of interacting QTL, epistasis and genome-transcriptome studies.

A range of physiological traits have been hypothesized to play key roles in the combined drought and heat stress tolerance of wheat (Tricker et al. 2018). In this study, we found water relations were important stress tolerance mechanisms. More than a third of the QTL for seed weight identified during GWAS (Chapter 2) co-located with QTL for leaf water potential, indicating an important link between seed weight and leaf water potential under stress conditions. We also found a strong correlation between seed weight and leaf water potential under drought and combined drought and heat stress, with higher-yielding plants maintaining an overall lower leaf water potential. Differences in the ability to efficiently use and acclimate to different water availabilities have been observed in NILs for the target region on chromosome 6B (Chapter 3). Appropriate and effective water use seem like an obvious choice for combined drought and heat stress tolerance since drought causes a loss of water and turgor in plants, while high temperatures exacerbate the drought stress by increasing water evaporation and transpiration (Levitt 1980a, Levitt 1980b). However, water use is a broad term and might be regulated by several molecular (eg., osmoprotectants, hormones) and anatomical (e.g., root architecture, leaf morphology) parameters (Izanloo et al. 2008, Batool et al. 2019). A more detailed analysis of water use and its regulation will help our understanding of combined drought and heat stress tolerance and potentially become a valuable target for plant breeders. Here the timing of increased water use and water use efficiency driven by the stress responses were differed between the exotic allele conferring yield benefit and the non-exotic allele and likely played a role in tolerance. The ability to increase the temporal precision of phenotyping for water use was important to enable us to dissect this trait.

The manual measurement of physiological traits such as photosynthesis, water use and leaf water potential is often time-consuming and, in case of leaf water potential, also destructive. In recent years, technologies to accelerate the phenotyping of large and diverse populations, especially in field, such as drones and phenomobiles have been implemented (Araus et al. 2018). Automated phenotyping platforms in glasshouse like the here used ‘DroughtSpotter’ and so called ‘Smarthouses’ enable the measurement of plant growth, plant health and precise water consumption over whole crop cycles (Ge et al. 2016, Chen et al. 2019). Most developed phenotyping tools, however, can assess physiological traits but not yield itself. The computed tomography platform developed in this study (Chapter 4) will facilitate not only yield measurements per se but also allow us a much more detailed analysis of yield components such as single seed weight, seed number as well as seed morphology, traits which we were previously not able to assess due to their time- and work-intensity. The method will support future projects in their evaluation and selection of tolerant germplasms for crop improvement.

In conclusion, the results from this study contributed to the genetic and physiological dissection of combined drought and heat stress with the discovery of two novel target QTL, candidate genes and water relations as potential stress tolerance trait. We also implemented a more accurate and faster phenotyping platform for the evaluation of yield components, which enables the mining of candidate germplasm and genes.

Future research directions

The results obtained are encouraging; however, further research is required and the limitations in this study will be discussed.

1. Using GWAS allowed us to identify several drought and heat stress tolerance QTL of which the majority were novel and with favourable alleles rare in Australian cultivars and breeding lines (Chapter 2). This offers opportunities for the yield improvement in Australian wheat breeding programs. Nevertheless, as many studies before us (e.g., Sukumaran et al. 2015, Muqaddasi et al. 2017, Valluru et al. 2017, Wang et al. 2017), we struggled to find significant association between molecular markers and traits. For instance, we did not find any QTL for yield or yield components under drought or combined drought and heat stress when applying the Bonferroni threshold. Apart from the phenotypic variation within the population explained by the molecular markers, the power of GWAS to identify true marker-trait associations is influenced by a number of factors such as i) population structure, ii) population size, iii) marker density and iv) allele frequency within the population (Korte and Farlow 2013). Other mapping populations might be a better option to overcome these issues. Nested-association mapping (NAM) populations, for example, have been shown to be more powerful when it comes to the identification of QTL (Zhu et al. 2008). NAM populations are not as restricted in their genetic diversity as bi-parental populations, as a much larger number of diverse donors are crossed, and struggle less with the detection of rare alleles and with population structure than GWAS (Yu et al. 2008, Rafalski 2010, Korte and Farlow 2013). The drawback of NAM populations is the time it takes to develop these populations (Yu et al. 2008). New approaches like speed breeding (Watson et al. 2018) might help to reduce the time taken to create these populations.

2. QTL are often based on single marker-trait associations, however, haplotyping can be more informative. Several studies showed that the combination of several molecular markers (or single nucleotide polymorphisms) and not only the most significant marker is critical for the phenotype of a plant (Guo et al. 2010, Garcia et al. 2019, He et al. 2019, Nyine et al. 2019). The identification of haplotypes at our target QTL could provide valuable and accurate information for the selection of drought and heat stress tolerant crops.

3. NILs for the target region on chromosome 6B (Chapter 3) segregated additionally for regions on chromosomes 1B and 7A, which co-located with previously identified QTL (Keeble-Gagnère et al. 2018, Okada et al. 2019). Observed differences between NILs might have resulted from, or at least been influenced, by these additional regions. Regions of segregation between replicates have also been observed on chromosomes 1B, 3B, 4A and 7A. The crossing between the two NILs and the selection of suitable progenies might facilitate narrowing down the target region of currently 17.2 Mbp and eliminate the additional regions of segregation between and within NILs. Identified candidate genes underlying the target region on chromosome 6B will also need to be examined further both in terms of gene expression, including differences in gene expression at different development stages and tissues, as well as their association with the observed physiological variations (i.e., water use, photosynthesis, respiration) between NILs. Interestingly, differences in gene expression between NILs were also detected on the short and long arm of chromosome 4B, even though targeted genotyping by sequencing data did not suggest any segregation region on this chromosome. New wheat assemblies for the comparison of multiple wheat genomes such as the 10+ genome project (http://www.10wheatgenomes.com/) are in progress and might help to clarify if those regions are either trans-regulated or present in only one of the NIL parents.

4. The computed tomography platform was developed for the estimation of yield and yield components of single wheat spikes under drought and combined drought and heat stress. The evaluation of other stresses or crops morphologically similar to wheat such as barley might be possible with predictions being adjusted and validated accordingly. The adjustment of the algorithm for morphologically more different crops such as oats might, however, be difficult and new algorithms would probably need to be developed. Computed tomography has also been shown to be useful in the estimation of root growth (de Dorlodot et al. 2017). A scan of a whole plant including spike, stem and roots would provide a comprehensive analysis of the development and growth dynamics of plants in response to different stresses.

References

Araus, J. L., Kefauver, S. C., Zaman-Allah, M., Olsen, M. S., & Cairns, J. E. (2018). Translating high-throughput phenotyping into genetic gain. *Trends in Plant Science*, 23, 5.

Batool, A., Aisha, N., Cheng, Z., Lv, G., Ashraf, M., Afzal, M., Xiong, J., Wang, J., & Xiong, Y. (2019). Physiological and biochemical responses of two spring wheat genotypes to non-hydraulic root-to-shoot signalling of partial and full root-zone drought stress. *Plant Physiology and Biochemistry*, 139, 11-20.

Brennan, P. S., & Byth, D. E. (1979). Genotype x environmental interactions for wheat yields and selection for widely adapted wheat genotypes. *Australian Journal of Agricultural Research*, 30, 221-232.

Chen, S., Guo, Y., Sirault, X., Stefanova, K., Saradadevi, R., Turner, N. C., Nelson, M. N., Furbank, R. T., Siddique, K. H. M., & Cowling, W. A. (2019). Nondestructive phenomic tools for the prediction of heat and drought tolerance at anthesis in Brassica species. *Plant Phenomics*, doi: 10.34133/2019/3264872.

de Dorlodot, S., Forster, B., Pages, L., Price, A., Tuberosa, R., & Draye, X. (2017). Root system architecture: opportunities and constraints for genetic improvement of crops. *Trends in Plant Science*, 12, 10.

Ferdous, J., Sanchez-Ferrero, J. C., Langridge, P., Milne, L., Chowdhury, J., Brien, C., & Tricker, P. J. (2017). Differential expression of microRNAs and potential targets under drought stress in barley. *Plant Cell and Environment*, 40, 11–24.

Feuillet, C., Langridge, P., & Waugh, R. (2008). Cereal breeding takes a walk on the wild side. *Trends in genetics,* 24, 24-32.

Freeman, J., Sparks, C. A., West, J., Shewry, P. R., & Jones, H. D. (2011). Temporal and spatial control of transgene expression using a heat-inducible promoter in transgenic wheat. *Plant Biotechnology Journal*, 9, 788-796.

Garcia, M., Eckermann, P., Haefele, S., Satija, S., Sznajder, B., Timmins, A., Baumann, U. Petra Wolters, P., Mather, D. E., & Fleury, D. (2019). Genome-wide association mapping of grain yield in a diverse collection of spring wheat (*Triticum aestivum* L.) evaluated in southern Australia. *PLoS ONE*, 14, 2.

Gbegbelegbe, S., Cammarano, D., Asseng, S., Robertson, R., Chung, U., Adam, M., Abdalla, O., Payne, T., Reynolds, M., Sonder, K., Shiferaw, B., & Nelson, G. (2016). Baseline simulation for global wheat production with CIMMYT mega-environment specific cultivars. *Field Crops Research*, 202, 122-135.

Ge, Y., Bai, G., Stoerger, V., & Schnable, J. C. (2016). Temporal dynamics of maize plant growth, water use, and leaf water content using automated high throughput RGB and hyperspectral imaging. *Computers and Electronics in Agriculture*, 127, 625-632.

Guo, Z., Song, Y., Zhou, R., Ren, Z., & Jia, J. (2010). Discovery, evaluation and distribution of haplotypes of the wheat *Ppd-D1* gene. *New Phytologist*, 185, 841-851.

Gupta, P. K., Balyan, H. S., & Gahlau, V. (2017). QTL analysis for drought tolerance in wheat: present status and future possibilities. *Agronomy*, 7, 5.

He, S., Thistlethwaite, R., Forrest, K., Shi, F., Hayden, M. J., Trethowan, R., & Daetwyler, H. D. (2019). Extension of a haplotype-based genomic prediction model to manage multi-environment wheat data using environmental covariates. *Theoretical and Applied Genetics*, doi: 10.1007/s00122-019-03413-1.

Izanloo, A., Condon, A. G., Langridge, P., Tester, M., & Schnurbusch, T. (2008). Different mechanisms of adaptation to cyclic water stress in two South Australian bread wheat cultivars. *Journal of Experimental Botany,* 59, 3327-3346.

Keeble-Gagnère, G., Rigault, P., Tibbits, J., Pasam, R., Hayden, M., Forrest, K., Frenkel, Z., Korol, A., Huang, B. E., Cavanagh, C., Taylor, J., Abrouk, M., Sharpe, A., Konkin, D., Sourdille, P., Darrier, B., Choulet, F., Bernard, A., Rochfort, S., Dimech, A., Watson-Haigh, N., Baumann, U., Eckermann, P., Fleury, D., Juhasz, A., Boisvert, S., Nolin, M.-A., Doležel, J., Šimková, H., Toegelová, H., Šafář, J., Luo, M.-C., Câmara, F., Pfeifer, M., Isdale, D., Nyström-Persson, J., Iwgsc Koo, D.-H., Tinning, M., Cui, D., Ru, Z., & Appels, R. (2018). Optical and physical mapping with local finishing enables megabase-scale resolution of agronomically important regions in the wheat genome. *Genome Biology*, 19, 112.

Knoll, J., & Ejeta, G. (2008). Marker-assisted selection for early-season cold tolerance in sorghum: QTL validation across populations and environments. *Theoretical and Applied Genetics,* 116, 541-553.

Korte, A., & Farlow, A. (2013) The advantages and limitations of trait analysis with GWAS: a review. *Plant Methods*, 9, 29.

Levitt, J. (1980a). *Responses of plants to environmental stresses. Volume I. Chilling, freezing, and high temperature stresses.* Second edition. Sydney: Academic Press.

Levitt, J (1980b). *Responses of plants to environmental stresses. Volume II. Water, radiation, salt, and other stresses.* Second edition. Sydney: Academic Press.

Mittler, R. (2006). Abiotic stress, the field environment and stress combination. *Trends in Plant Science*, 11, 1.

Muqaddasi, Q. H., Reif, J. C., Li, Z., Basnet, B. R., Dreisigacker, S., & Röder, M. S. (2017). Genome-wide association mapping and genome-wide prediction of anther extrusion in CIMMYT spring wheat. *Euphytica*, 213, 73.

Nyine, M., Wang, S., Kiani, K., Jordan, K., Liu, S., Byrne, P., Haley, S., Baenziger, S., Chao, S., Bowden, R., & Akhunov, E. (2019). Genotype imputation in winter wheat using first-generation haplotype map SNPs improves genome-wide association mapping and genomic prediction of traits. *Genes Genomes Genetics*, 9, 125-133.

Okada, T., Jayasinghe, J. E. A. R. M., Eckermann, P., Watson-Haigh, N. S., Warner, P., Hendrikse, Y., Baes, M., Tucker, E. J., Laga, H., Kato, K., Albertsen, M., Wolters, P., Fleury, D., Baumann, U., & Whitford, R. (2019). Effects of *Rht-B1* and *Ppd-D1* loci on pollinator traits in wheat. *Theoretical and Applied Genetics*, 132, 1965-1979.

Perdomo, J. A., Conesa, M. A., Medrano, H., Ribas-Carbó, M., & Galmes, J. (2015). Effects of long-term individual and combined water and temperature stress on the growth of rice, wheat and maize: relationship with morphological and physiological acclimation. *Physiologia Plantarum,* 155, 149-165.

Pradhan, G. P., Prasad, P. V., Fritz, A. K., Kirkham, M. B., & Gill, B. S. (2012). Effects of drought and high temperature stress on synthetic hexaploid wheat. *Functional Plant Biology,* 39, 190-198.

Rafalski, J. A. (2010) Association genetics in crop improvement. *Current Opinion in Plant Biology*, 13, 174-180.

Reynolds, M. P., Hays, D., & Chapman, S. (2010). Breeding for adaptation to heat and drought stress. In: *Climate change and crop production, volume 13* (Reynolds, M. P., ed.), pp. 71-91. Chippenham: CABI.

Rong, W., Qi, L., Wang, A., Ye, X., Du, L., Liang, H., Xin, Z., & Zhang, Z. (2014). The *ERF* transcription factor *TaERF3* promotes tolerance to salt and drought stresses in wheat. Plant Biotechnology Journal, 12, 468-479.

Rosenzweig, C., & Parry, M. L. (1994). Potential impact of climate change on world food supply. *Nature,* 367, 133-138.

Saint Pierre, C., Crossa, J. L., Bonnett, D., Yamaguchi-Shinozaki, K., & Reynolds, M. P. (2012). Phenotyping transgenic wheat for drought resistance. *Journal of Experimental Botany*, 63, 1799-1808.

Sivamani, E., Bahieldin, A., Wraith, J. M., Al-Niemi, T., Dyer, W. E., Ho, T. D., & Qu, R. (2000). Improved biomass productivity and water use efficiency under water deficit conditions in transgenic wheat constitutively expressing the barley *HVA1* gene. *Plant Science*, 155, 1-9.

Sukumaran, S., Dreisigacker, S., Lopes, M., Chavez, P., & Reynolds, M. P. (2015). Genome-wide association study for grain yield and related traits in an elite spring wheat population grown in temperate irrigated environments. *Theoretical and Applied Genetics,* 128, 353-363.

Toreti, A., Cronie, O., & Zampieri, M. (2019). Concurrent climate extremes in the key wheat producing regions of the world. *Scientific reports*, 9, 5493.

Tricker, P. J., ElHabti, A., Schmidt, J., & Fleury, D. (2018). The physiological and genetic basis of combined drought and heat tolerance in wheat. *Journal of Experimental Botany*, 69, 3195-3210.

Trnka, M., Rötter, R. P., Ruiz-Ramos, M., Kersebaum, K. C., Olesen, J. E., Žalud, Z., & Semenov, M. A. (2014). Adverse weather conditions for European wheat production will become more frequent with climate change. *Nature Climate Change*, 4, 637-643.

Valluru, R., Reynolds, M.P., Davies, W.J., & Sukumaran, S. (2017). Phenotypic and genome-wide association analysis of spike ethylene in diverse wheat genotypes under heat stress. *New Phytologist,* 214, 271-283.

Vendruscolo, E. C., Schuster, I., Pileggi, M., Scapim, C. A., Molinari, H. B., Marur, C. J., & Vieira, L. G. (2007). Stress-induced synthesis of proline confers tolerance to water deficit in transgenic wheat. *Journal of Plant Physiology*, 164, 1367-1376.

Wang, G. P., Zhang, X. Y., Li, F., Luo, Y., & Wang, W. (2010). Overaccumulation of glycine betaine enhances tolerance to drought and heat stress in wheat leaves in the protection of photosynthesis. *Photosynthetica*, 48, 117-126.

Wang, S. X., Zhu, Y. L., Zhang, D. X., Shao, H., Liu, P., Hu, J. B., Zhang, H., Zhang, H. P., Chang, C., Lu, J., Xia, X. C., Sun, G. L. & Ma, C. X. (2017). Genome-wide association study for grain yield and related traits in elite wheat varieties and advanced lines using SNP markers. *PLoS ONE,* 12, 11.

Watson, A., Ghosh, S., Williams, M. J., Cuddy, W. S., Simmonds, J., Rey, M. D., Asyraf Md Hatta, M., Hinchliffe, A., Steed, A., Reynolds, D., Adamski, N. M., Breakspear, A., Korolev, A., Rayner, T., Dixon, L. E., Riaz, A., Martin, W., Ryan, M., Edwards, D., Batley, J., Raman, H., Carter, J., Rogers, C., Domoney, C., Moore, G., Harwood, W., Nicholson, P., Dieters, M. J., DeLacy, I. H., Zhou, J., Uauy, C., Boden, S. A., Park, R. F., Wulff, B. B. H., & Hickey, L. T. (2018). Speed breeding is a powerful tool to accelerate crop research and breeding. *Nature Plants*, 4, 23-29.

Yu, J., Holland, J. B., McMullen, M. D., & Buckler, E. S. (2008). Genetic design and statistical power of nested association mapping in maize. *Genetics*, 178, 539-551.

Zampieri, M., Russo, S., di Sabatino, S., Michetti, M., Scoccimarro, E., & Gualdi, S. (2016). Global assessment of heat wave magnitudes from 1901 to 2010 and implications for the river discharge of the Alps. *Science of the Total Environment*, 571, 1330-1339.

Zampieri, M., Ceglar, A., Dentener, F., & Toreti, A. (2017). Wheat yield loss attributable to heat waves, drought and water excess at the global, national and subnational scales. *Environmental Research Letters*, 12, 6.

Zhu, C., Gore, M., Buckler, E. S., & Yu, J. (2008). Status and Prospects of Association Mapping in Plants. *The plant genome,* 1, 5-20.

Appendices

Appendix A

Supplementary to Chapter 2 - Genotypic data analysis and validation of near-isogenic lines for the target QTL on chromosome 6A under controlled conditions.

Introduction

We performed a Genome-wide Association Study (GWAS) and identified a QTL for single seed weight, seed number and screenings at 12,837,679-16,232,972 bp on chromosome 6A in the RefSeq v1.0 assembly (IWGSC 2018) under combined drought and heat stress in 2016 and 2017 (Chapter 2). The aim of the experiment described here was to evaluate the 6A QTL effect on yield components and water relations by phenotyping near-isogenic lines (NILs) under controlled conditions.

Material and Methods

Plant material

Three of the four NIL pairs validated in the polytunnel in 2018, were phenotyped under controlled condition in a glasshouse with precision irrigation located at the Plant Accelerator ('DroughtSpotter' glasshouse, University of Adelaide, Australia). One of the NIL pairs (NIL pair 1, Chapter 2 – Supplementary Table 2) carried wild type alleles at the dwarfing loci *Rht-B1* and *Rht-D1* and exceeded the height limit of the facility. We replaced NIL pair 1 with a semi-dwarf NIL pair (NIL pair 5, Table 1), deriving from a cross between the Australian variety 'Gladius' and the Portuguese variety 'Mocho de Espiga Branca'. A targeted genotyping by sequencing (tGBS) analysis based on data from the 90k SNP Illumina array was carried out for all five NIL pairs in the polytunnel and DroughtSpotter glasshouse. A detailed genotyping data file ("Supplementary Table_Appendix.xlxs", Supplementary Table 1) is available on Figshare (https://adelaide.figshare.com/s/fb22de5ba3ab7cb4d059).

Plant growth conditions

A total of 32 seeds of each of the near-isogenic lines were germinated in jiffy pots at room temperature (i.e., 20 ºC) for 24 hours in darkness in a reach-in chamber at the Plant Accelerator (University of Adelaide, Australia). A Latin square design with eight trays, each consisting of 10 rows of four plants, was implemented. One of the NIL pairs (NIL pair 4, Chapter 2 – Supplementary Table 2) for the DroughtSpotter glasshouse experiment carried winter alleles at the vernalisation gene *Vrn-A1* on chromosome 5A and required vernalisation. In order to avoid having lines grown under different conditions, all lines were vernalized for a total of four weeks at 4-8 ºC with a 2-hour photoperiod under well-watered conditions, as adapted from Boyd et al. (2003). At the end of vernalization, sixteen seedlings of each line were transferred to plastic pots together with their jiffy pot and placed on balances in the DroughtSpotter glasshouse. The size of the plastic pots (240 mm high x 165 mm diameter) represented approximately the available space for plants in the field and was filled with 3.5 kg dry weight of a drought mix (1 : 1 : 1, coco peat : clay loam : sand) supplemented with a slow-release, basal fertilizer. A frame was put around each pot for support and a double foam matt was placed on the top of the soil in each pot to minimize evaporation. Pots were randomized according to a quadruple-split-unit design with four biological replicates per treatment (drought or drought and heat stress) and harvest date (harvest during early grain filling or at maturity). Each replicate was divided into two areas, which were, in turn, divided into two subareas. The four NIL pairs were randomly allocated to each of the subareas and NILs of the same pair were kept together to maximize the precision of comparison within NIL pairs.

Similar to the treatment applied in the GWAS (Chapter 2), plants were grown under well-watered conditions (20% soil moisture) until three days after anthesis when plants were exposed to either drought or combined drought and heat stress. Drought was imposed by lowering the target weight of the pot to 12 % soil water content, corresponding to -0.72 MPa (Chapter 3), for a total of nine days instead of six days as carried out in the GWAS to compensate for the slower drying out of the pots (Figure 1). A combination of drought and heat stress was applied by exposing plants to nine days of drought treatment coupled with heat stress at 35/25 ºC day/night during the last three days of treatment. During the heat treatment, plants were irrigated manually to the target weight four times a day. After the treatment, plants were moved back to their spot in the DroughtSpotter glasshouse and kept under well-watered conditions until reaching physiological maturity.

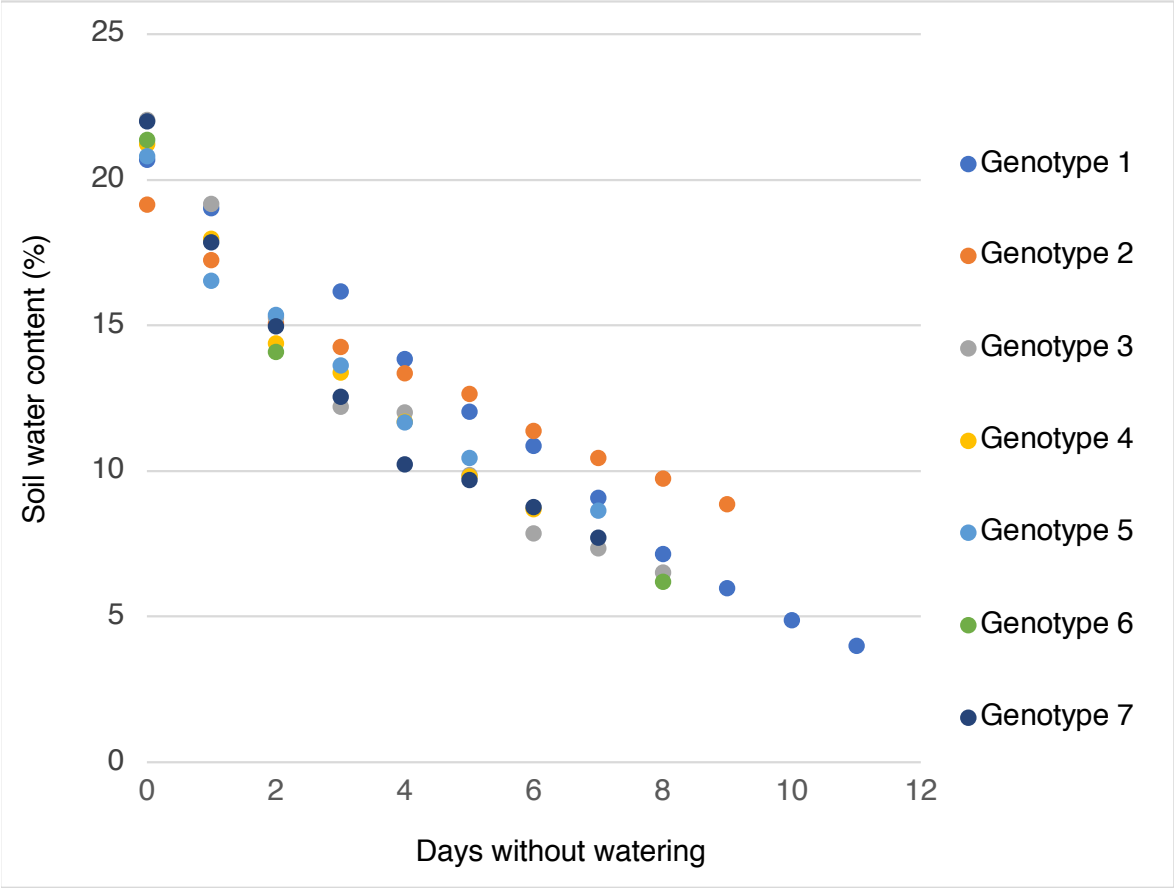

Figure 1. Water loss over time at early grain-filling. To estimate the time it would take to decrease the soil water content from 20 to 12 %, seven different genotypes were grown in pots of the same size and filled with the same substrate mix as used in the DroughtSpotter glasshouse experiment. All genotypes were semi-dwarf, having thus a similar biomass than plants used in the actual experiment. Plants were kept under well-watered conditions (i.e., ~20 % soil water content) in a glasshouse at the Plant Research Centre (Adelaide, Australia) until anthesis. At anthesis, irrigation was stopped, and the water content was measured by extracting daily soil samples of 15 mm diameter and 200 mm length and by calculating the weight difference between fresh soil sample and the dry soil sample (oven-dried at 65 ºC for 72 hours), divided by the dry weight. On average, soil water content reached 12 % after 5 days of withholding irrigation. The drought treatment in the experiment was therefore extended to a total of nine days instead of six days.

Plant phenotyping

Four of the replicates of each line were used for harvesting at maturity, while the other four were sampled (but finally not used) for RNA sequence analysis (i.e., harvest during early grain filling). At physiological maturity, plant height and spike length of the primary tiller as well as the number of spikes per plant were recorded. Samples were subsequently oven-dried at 37 ºC for 10 days and total aboveground biomass per plant was determined including stems, leaves and spikes of all tillers. Seed traits per primary tiller and the rest of the spikes were analysed separately. To differentiate between small (< 2.0 mm) and big seeds (> 2.0 mm) a wheat grain sieve (2.0 mm, Graintec, Australia) was used. Seed weight and seed number were determined for seeds > 2.0 mm. Single seed weight was measured as the average of seed weight divided by the number of seeds. Screenings was defined as the difference in percentage of small seeds (< 2.0 mm) compared to total seed weight.

Statistical analysis

The best linear unbiased estimators (BLUEs) of each trait under drought and combined drought and heat treatment were calculated separately for each NIL pair using the R package ASReml (Butler et al. 2009). NILs were treated as fixed effect and the experimental design as random effect. Plant height was included as covariant if significantly associated with seed weight, which was the case for seed weight per plant under combined drought and heat of NIL pair 4. Screenings per main spike was not normally distributed among two NIL pairs: NIL pair 4 under drought and NIL pair 3 under combined drought and heat stress. Single seed weight of main spike under combined drought and heat stress was not normally distributed within NIL pair 3.

Results

Genotyping by sequencing

A total of 29,663 polymorphic SNP markers were obtained by the tGBS approach, of which 4,297 markers were mapped to a single locus within the Chinese Spring RefSeq v1.0, (IWGSC 2018) and contained less than 5 % of missing data. The 4,297 markers were used for comparison between replicates and NILs. Replicates of NILs carrying the same allele at the target region were to 96.6-97.1, 96.5-97.4, 92.3-95.9, 96.4-97.4 and 96.4-96.5 % similar within NIL pairs 1-5, respectively. NILs carrying the opposite allele at the target region were to 95.4-

96.3, 95.9-96.8, 91.5-94.2, 96.1-97.0 and 96.3-96.6 % similar within NIL pairs 1-5, respectively.

NILs within each NIL pair segregated for the 6A QTL at 1,495,513-17,912,935 bp in NIL pair 1; 11,168,878-11,964,467 bp in NIL pair 2; 17,898,981-61,387,479 bp in NIL pair 3; 14,354,220-33,953,480 bp in NIL pair 4; and 17,898,981-22,524,655 bp on RefSeq v1.0 in NIL pair 5 (Figure 2). Even if tGBS data did not suggest a separation within NIL pairs 2, 3 and 5 at the exact target region (12,837,679-16,232,972 bp on RefSeq v1.0), in-house developed KASP markers (Table 1, Chapter 2 – Supplementary Table 2) suggested a segregation at the target region from 15,728,423 to 15,748,761 bp. This region might not have been sampled in the tGBS approach. A second region of segregation between NILs of the pair 1 was observed on chromosomes 6B (50,990,872-146,145,061), which most likely had an effect on yield components observed in Chapter 2 since the region coincided with a QTL for seed weight and seed number per spike as well as shoot weight under heat stress (QTL26) identified by Shirdelmoghanloo et al. (2016). Regions segregating within replicates were identified on 16 of the 21 chromosomes of which 20 out of the 31 segregating regions were found within NIL pair 3. Plants were selected and separately propagated from BC1F5 on. We therefore would expect a residual heterozygosity of 3.13 %. However, the extremely high number and size of segregation regions found in NIL pair 3 would rather suggest a genotyping error.

Table 1. Kompetitive Allele Specific Polymerase Chain Reaction (KASP) marker assisted selection for the development of near-isogenic lines of the NIL pair 5 for the target region on chromosome 6A**.** Chr: chromosome. Grey indicates the allele derived from the non-exotic parent (Gladius), whereas green indicates the allele derived from the exotic parent (Mocho de Espiga Branca). Positions are based on Ref Seq v1.0 (IWGSC 2018).

				Genotyping results BC1F5		**Genotyping results BC1F6**			
Marker name	**Chr**	**Positon (bp)**	**Corresponding gene**	non-exotic	exotic	non-exotic		exotic	
						Replicate 1	Replicate 1	Replicate 1	Replicate 2
6A_118917_01	6A	15,728,423-15,728,470	TraesCS6A01G030700	C	A	C	A	A	C
6A_118917_03	6A	15,737,660-15,737,717	TraesCS6A01G038900LC			G	A	A	G
6A_118917_04	6A	15,744,580-15,744,628	TraesCS6A01G038900LC			C	T	T	C
6A_118917_05	6A	15,748,713-15,748,761	TraesCS6A01G030900			C	T	T	C
6B_119265_02	6B	713,513,485-713,513,529	-	G	G	G	G	G	G
6B_119265_06	6B	713,149,515-713,149,563	TraesCS6B01G458800			G	G	G	G
6B_119265_08	6B	713,462,432-713,462,498	TraesCS6B01G458200			C	C	C	C
6B_119265_10	6B	712,997,417-712,997,467	TraesCS6B01G456800			A	A	A	A
6B_39100_04	6B	708,047,370-708,047,414	TraesCS6B01G447700			C	C	C	C
BS00017267	4A	21,063,786-21,063,839	TraesCS4A01G028900	G	G	G	?	?	G
KASParMAS021	1D	410,464,670-410,464,717	*GluD1*	5+10	5+10				
wMAS000001	4B	30,861,518-30,861,590	*Rht-B1*	WT	WT	WT	WT	WT	WT
wMAS000002	4D	18,781,193-18,781,262	*Rht-D1*	DWARF	DWARF				
wMAS000018	5D	3,609,867-3,609,911	*Pinb-D1*	WT	WT	WT	WT	WT	WT
wMAS000024	2D	33,957,749-33,957,796	*Ppd-D1*	INSENS	INSENS	INSENS	INSENS	INSENS	INSENS
wMAS000033	5A	588,550,239-588,550,309	*Vrn-A1*	SPRING	SPRING	SPRING	SPRING	SPRING	SPRING
wMAS000035	5A	587,423,348-587,423,416	*Vrn-A1*	WINTER	WINTER	WINTER	WINTER	WINTER	WINTER

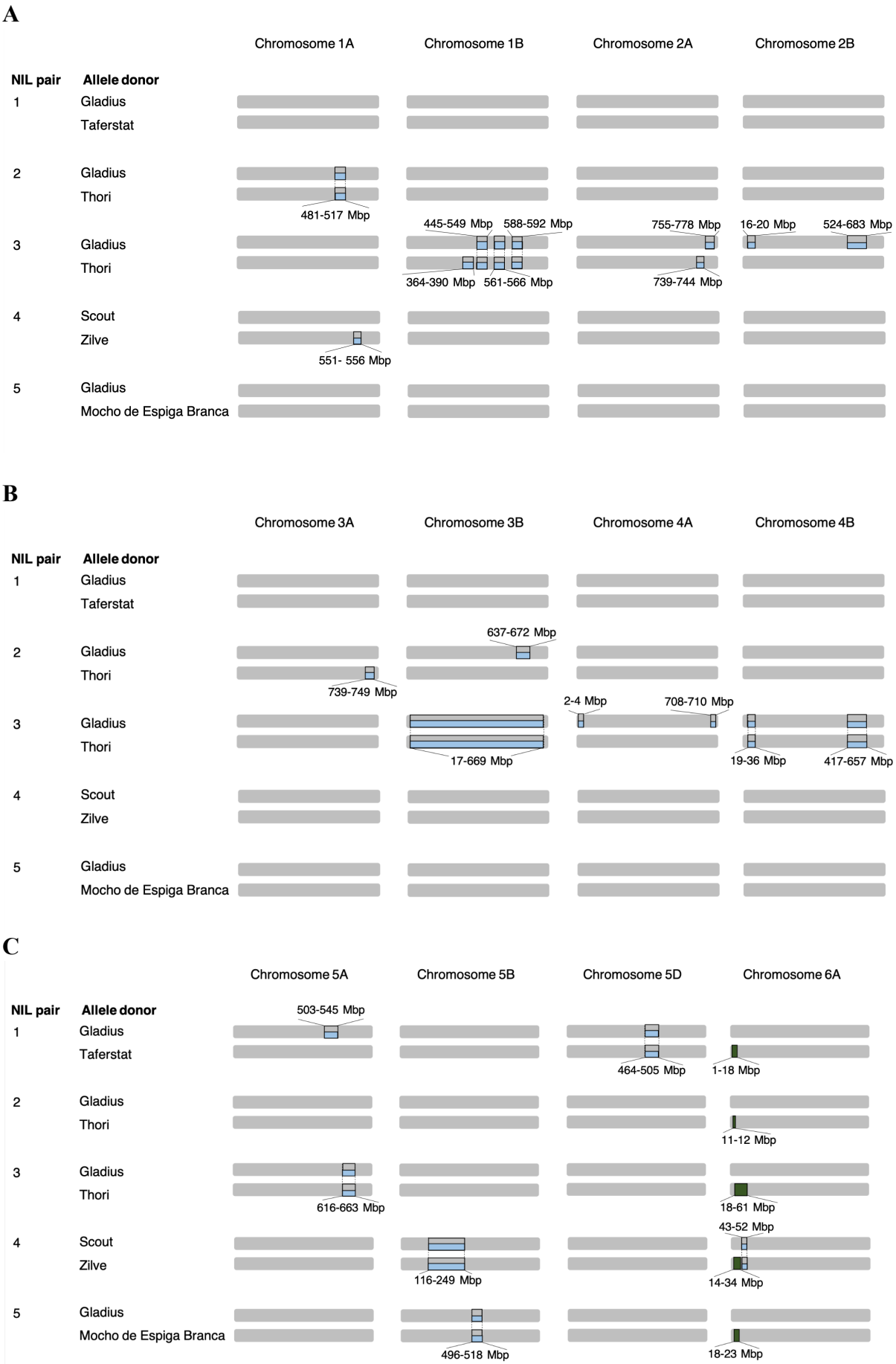
A
Chromosome 1A
Chromosome 1B
Chromosome 2A
Chromosome 2B
NIL pair
Allele donor
1
Gladius
Taferstat
2
Gladius
Thori
481-517 Mbp
3
Gladius
Thori
445-549 Mbp
588-592 Mbp
364-390 Mbp
561-566 Mbp
755-778 Mbp
739-744 Mbp
16-20 Mbp
524-683 Mbp
4
Scout
Zilve
551- 556 Mbp
5
Gladius
Mocho de Espiga Branca
B
Chromosome 3A
Chromosome 3B
Chromosome 4A
Chromosome 4B
NIL pair
Allele donor
1
Gladius
Taferstat
2
Gladius
Thori
637-672 Mbp
739-749 Mbp
3
Gladius
Thori
2-4 Mbp
708-710 Mbp
17-669 Mbp
19-36 Mbp
417-657 Mbp
4
Scout
Zilve
5
Gladius
Mocho de Espiga Branca
C
Chromosome 5A
Chromosome 5B
Chromosome 5D
Chromosome 6A
NIL pair
Allele donor
1
Gladius
Taferstat
503-545 Mbp
464-505 Mbp
1-18 Mbp
2
Gladius
Thori
11-12 Mbp
3
Gladius
Thori
616-663 Mbp
18-61 Mbp
4
Scout
Zilve
43-52 Mbp
116-249 Mbp
14-34 Mbp
5
Gladius
Mocho de Espiga Branca
496-518 Mbp
18-23 Mbp

D

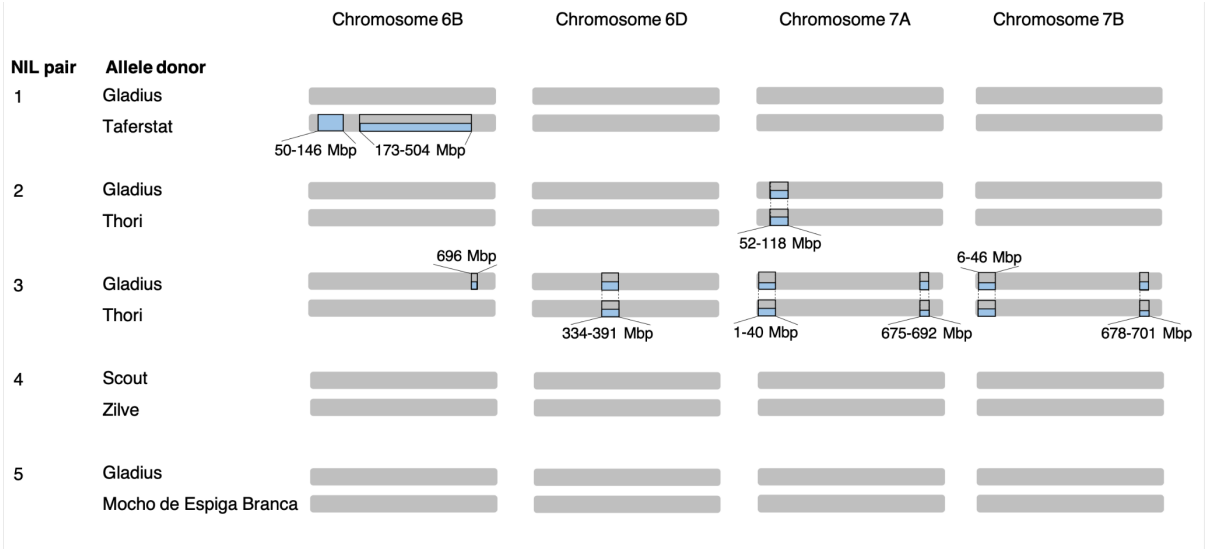

Figure 2. Schematic of genotyping by sequencing results of the five near-isogenic line (NIL) pairs (A-D). All NIL pairs segregate at the target region with NILs either carrying the allele donated by a recurrent parent (Gladius or Scout) or the allele donated by the exotic parent (marked in green). An additional region of segregation between NILs of the pair 1 was observed on chromosomes 6B and is marked in blue. Regions which appear to segregate within replicates, are marked in blue-grey. NILs were homozygous for the remaining 5 chromosomes. Positions are based on RefSeq v1.0 (IWGSC 2018). Mbp, Mega base pairs.

Plant growth conditions

Growth conditions in the DroughtSpotter glasshouse were stable during vegetative stage and grain filling with maximum and minimum temperatures of 22.0-24.9 and 13.4-15.8 ºC during day and night, respectively (Chapter 3). Maximum temperatures increased towards the end of the experiment up to 30 ºC, when plants were maturing (from 133 days after planting onwards). Temperatures during the heat treatment reached the aimed target temperatures of 33.5-35.3 ºC during the day and 23.5-24.5 ºC during night.

Phenotypic data

No significant differences for any of the measured traits could be found within the four NIL pairs, except for NIL pair 5. The NILs in pair 5 that carried the exotic allele (donated by Mocho de Espiga Branca) had a significantly reduced seed weight per primary tiller under combined

drought and heat stress (p = 0.047) in comparison to those carrying the non-exotic allele (donated by Gladius) (Table 2).

Table 2. Predicted mean, standard error and p-value of phenotypic traits of near-isogenic lines grown under drought and combined drought and heat stress.

Trait	NIL pair	Condition	Predicted mean		Standard error	p-value
			non-exotic allele	exotic allele		
Days to anthesis	6A-2	Pre-treatment	77.8	78.6	0.6	0.337
	6A-3	Pre-treatment	80.4	80.9	0.5	0.511
	6A-4	Pre-treatment	81.3	80.6	0.5	0.369
	6A-5	Pre-treatment	83.8	84.3	0.6	0.568
Spike number per plant	6A-2	Drought	7.8	9.8	1.1	0.235
		Drought&Heat	6.5	7.3	1.0	0.613
	6A-3	Drought	10.3	12.5	1.6	0.345
		Drought&Heat	7.8	11.0	1.3	0.136
	6A-4	Drought	16.0	14.3	1.4	0.400
		Drought&Heat	11.5	11.8	1.3	0.895
	6A-5	Drought	8.5	9.8	0.8	0.317
		Drought&Heat	7.0	8.8	1.1	0.286
Spike length (cm)	6A-2	Drought	7.3	7.1	0.4	0.684
		Drought&Heat	7.8	7.1	0.3	0.147
	6A-3	Drought	7.3	7.8	0.3	0.301
		Drought&Heat	7.8	7.5	0.2	0.240
	6A-4	Drought	9.3	9.2	0.3	0.866
		Drought&Heat	9.4	9.5	0.2	0.705
	6A-5	Drought	9.1	9.0	0.2	0.781
		Drought&Heat	9.2	9.0	0.3	0.633
Plant height (cm)	6A-2	Drought	65.6	65.9	2.0	0.918
		Drought&Heat	66.6	65.7	1.1	0.586
	6A-3	Drought	57.3	66.6	2.3	0.031
		Drought&Heat	61.1	64.4	1.5	0.180
	6A-4	Drought	70.8	69.7	1.2	0.549
		Drought&Heat	69.5	69.5	1.3	0.978
	6A-5	Drought	70.5	69.1	2.0	0.648
		Drought&Heat	73.3	69.1	2.1	0.215
Biomass (g)	6A-2	Drought	30.0	35.6	5.4	0.077
		Drought&Heat	24.8	26.2	3.6	0.794
	6A-3	Drought	46.4	54.9	6.2	0.368
		Drought&Heat	34.5	42.6	4.7	0.272
	6A-4	Drought	55.2	52.7	4.0	0.674
		Drought&Heat	39.8	43.2	4.0	0.577
	6A-5	Drought	50.6	51.1	3.8	0.932
		Drought&Heat	41.0	44.4	4.9	0.639

Table 2. Continued.

Trait	NIL pair	Condition	Predicted mean		Standard error	p-value
			non-exotic allele	exotic allele		
Screenings per primary tiller (% small seed weight)	6A-2	Drought	0.000	0.000	0.000	1.000
		Drought&Heat	0.232	0.009	0.102	0.174
	6A-3	Drought	0.066	0.018	0.043	0.647
		Drought&Heat	0.000	0.106	0.075	0.356
	6A-4	Drought	0.003	0.000	0.002	0.356
		Drought&Heat	0.225	0.238	0.187	0.780
	6A-5	Drought	0.013	0.007	0.004	0.350
		Drought&Heat	0.113	0.003	0.634	0.261
Screenings per plant (% small seed weight)	6A-2	Drought	0.026	0.428	0.259	0.237
		Drought&Heat	0.142	0.525	0.339	0.603
	6A-3	Drought	2.068	1.362	0.815	0.563
		Drought&Heat	0.177	0.727	0.353	0.332
	6A-4	Drought	1.084	1.762	1.036	0.660
		Drought&Heat	0.985	0.078	0.634	0.304
	6A-5	Drought	0.089	0.261	0.096	0.253
		Drought&Heat	0.123	0.105	0.025	0.634
Seed number per primary tiller	6A-2	Drought	29.8	30.3	2.0	0.864
		Drought&Heat	34.3	31.5	2.0	0.368
	6A-3	Drought	45.3	47.5	2.9	0.599
		Drought&Heat	47.5	43.5	2.1	0.219
	6A-4	Drought	51.8	54.0	2.4	0.533
		Drought&Heat	53.8	56.3	2.6	0.518
	6A-5	Drought	48.0	47.8	1.8	0.923
		Drought&Heat	50.5	42.5	2.4	0.054
Seed number per plant	6A-2	Drought	269.8	338.3	44.3	0.317
		Drought&Heat	227.3	249.3	34.4	0.667
	6A-3	Drought	495.0	546.3	63.9	0.591
		Drought&Heat	322.8	430.5	47.7	0.161
	6A-4	Drought	600.3	494.8	44.9	0.148
		Drought&Heat	376.5	416.5	39.1	0.497
	6A-5	Drought	398.8	378.3	27.9	0.623
		Drought&Heat	275.8	323.5	26.2	0.244
Single seed weight per primary tiller (g)	6A-2	Drought	0.053	0.051	0.001	0.077
		Drought&Heat	0.047	0.047	0.001	0.693
	6A-3	Drought	0.048	0.055	0.002	0.054
		Drought&Heat	0.043	0.046	0.001	0.198
	6A-4	Drought	0.057	0.056	0.001	0.417
		Drought&Heat	0.047	0.047	0.002	0.887
	6A-5	Drought	0.066	0.068	0.001	0.212
		Drought&Heat	0.059	0.056	0.001	0.258
Single seed weight per plant (g)	6A-2	Drought	0.050	0.047	0.001	0.239
		Drought&Heat	0.049	0.048	0.001	0.511
	6A-3	Drought	0.044	0.048	0.002	0.145
		Drought&Heat	0.048	0.046	0.002	0.455
	6A-4	Drought	0.048	0.052	0.001	0.079
		Drought&Heat	0.048	0.051	0.001	0.109
	6A-5	Drought	0.060	0.061	0.002	0.769
		Drought&Heat	0.061	0.059	0.001	0.288

Table 2. Continued.

Trait	NIL pair	Condition	Predicted mean		Standard error	p-value
			non-exotic allele	exotic allele		
Seed weight per primary tiller (g)	6A-2	Drought	1.6	1.5	0.1	0.872
		Drought&Heat	1.6	1.5	0.1	0.443
	6A-3	Drought	2.1	2.6	0.2	0.096
		Drought&Heat	2.1	2.0	0.1	0.665
	6A-4	Drought	3.0	3.0	0.2	0.813
		Drought&Heat	2.5	2.6	0.1	0.624
	6A-5	Drought	3.1	3.2	0.1	0.554
		Drought&Heat	3.0	2.4	0.2	0.047
Seed weight per plant (g)	6A-2	Drought	13.5	16.2	2.4	0.448
		Drought&Heat	11.2	11.9	1.6	0.743
	6A-3	Drought	21.9	26.4	2.8	0.301
		Drought&Heat	15.3	19.6	2.1	0.211
	6A-4	Drought	28.7	25.7	2.1	0.349
		Drought&Heat	18.2	21.3	2.2	0.369
	6A-5	Drought	24.0	22.9	1.3	0.550
		Drought&Heat	16.9	18.9	1.6	0.418
Harvest index	6A-2	Drought	0.448	0.458	0.014	0.609
		Drought&Heat	0.451	0.456	0.013	0.758
	6A-3	Drought	0.473	0.482	0.012	0.620
		Drought&Heat	0.445	0.460	0.005	0.092
	6A-4	Drought	0.521	0.486	0.011	0.070
		Drought&Heat	0.457	0.489	0.013	0.135
	6A-5	Drought	0.477	0.452	0.015	0.271
		Drought&Heat	0.419	0.431	0.018	0.306

Discussion

The QTL on chromosome 6A at 12,837,679-16,232,972 bp on RefSeq v1.0 was previously identified to be associated with total seed weight, single seed weight, seed number and screenings in GWAS experiments in 2016 and 2017 and under semi-controlled field conditions in 2018 (Chapter 2). However, no significant differences were observed under controlled glasshouse conditions even though both KASP markers and tGBS indicated a separation of NILs at the target region. In case of the pairs 1 and 3, NILs also segregated for regions on chromosomes 2B and 6B. Three of the four NIL pairs have also been evaluated under field conditions where we did observe significant differences.

A possible explanation for these contrasting results might be genotype by environment interactions. QTL effects often vary and might even be reversed when tested under different environmental conditions (Bonneau et al. 2013). It is therefore important to define a specific target environment including stress type, severity and timepoint of stress. Similar to the

GWAS, the treatment started three days after anthesis of the primary tiller, however, the drought stress applied was less severe in this experiment (12% soil water content) in comparison to the previous experiments (average of 3% soil water content). Screenings per primary tiller, for instance, was low in the DroughtSpotter glasshouse experiment with an average of 0.006 and 0.089 % under drought and combined drought and heat stress, respectively, whereas screenings in the GWAS ranged between 10.1 and 90.6 %. Plants were also re-irrigated constantly to maintain the target soil water content, whereas plants in the GWAS were not re-irrigated until the end of the treatment or were exposed to cyclic drought as in the case of the validation under field conditions in 2018. Cyclic drought has been suggested to affect plant growth in wheat more severely than a constant drought level (Cousins et al. 2019). Further, the heat treatment was delayed by three days due to the additional time required to dry pots down to 12 % soil water content. Pradhan et al. (2012) demonstrated that seed weight and seed weight components were much more affected the closer the stress occurred towards anthesis. We hypothesise that the applied stress was not severe enough and that the QTL effect is not significant under mild stress conditions.

References

Bonneau, J., Taylor, J., Parent, B., Bennett, D., Reynolds, M., Feuillet, C., Langridge, P., & Mather, D. (2013). Multi-environment analysis and improved mapping of a yield-related QTL on chromosome 3B of wheat. *Theoretical and Applied Genetics*, 126, 747-761.

Boyd, W. J. R., Li, C. D., Grime, C. R., Cakir, M., Potipibool, S., Kaveeta, L., Men, S., Jalal Kamali, M. R., Barr, A. R., Moody, D. B., Lance, R. C. M., Logue, S. J., Raman, H., & Read, B. J. (2003). Conventional and molecular genetic analysis of factors contributing to variation in the timing of heading among spring barley (*Hordeum vulgare* L.) genotypes grown over a mild winter growing season. *Australian Journal of Agricultural Research*, 54, 1277-1301.

Butler, D. G., Cullis, B. R., Gilmour, A. R., & Gogel, B. J. (2009). Analysis of mixed models for S language environments: ASReml-R reference manual. Brisbane: DPI Publications.

Cousins, O. H., Garnett, T. P., Rasmussen, A., Moone, S. J., Smernik, R. J., Brien, C. J., & Cavagnaro, T. R. (2019). Variable water cycles have a greater impact on wheat growth and soil nitrogen response than constant watering. *Plant Science*, doi: 10.1016/j.plantsci.2019.05.009.

International Wheat Genome Sequencing Consortium (IWGSC) (2018). Shifting the limits in wheat research and breeding using a fully annotated reference genome. *Scienc*e, 361, 7191.

Pradhan, G. P., Prasad, P. V., Fritz, A. K., Kirkham, M. B., & Gill, B. S. (2012). Effects of drought and high temperature stress on synthetic hexaploid wheat. *Functional Plant Biology,* 39, 190-198.

Shirdelmoghanloo, H., Taylor, J. D., Lohraseb, I., Rabie, H., Brien, C., Timmins, A., Martin, P., Mather, D. E., Emebiri, L., & Collins, N. C. (2016). A QTL on the short arm of wheat (*Triticum aestivum* L.) chromosome 3B affects the stability of grain weight in plants exposed to a brief heat shock early in grain filling. *BMC Plant Biology*, 16, 100.

Appendix B

The physiological and genetic basis of combined drought and heat tolerance in wheat.

Statement of Authorship

Title of Paper	The physiological and genetic basis of combined drought and heat tolerance in wheat
Publication Status	☑ Published ☐ Accepted for Publication ☐ Submitted for Publication ☐ Unpublished and Unsubmitted work written in manuscript style
Publication Details	Tricker, P. J., ElHabti, A., Schmidt, J., & Fleury, D. (2018) The physiological and genetic basis of combined drought and heat tolerance in wheat. Journal of Experimental Botany, 69, 3195-3210.

Principal Author

Name of Principal Author (Candidate)	Penny Tricker
Contribution to the Paper	Wrote the manuscript. Edited the figure and table.
Overall percentage (%)	40%
Certification:	This paper is not subject to any obligations or contractual agreements with a third party that would constrain its inclusion in this thesis. I am the primary author of this paper.
Signature	Date 11/9/19

Co-Author Contributions

By signing the Statement of Authorship, each author certifies that:

i. the candidate's stated contribution to the publication is accurate;
ii. permission is granted for the candidate in include the publication in the thesis; and
iii. the sum of all co-author contributions is equal to 100% less the candidate's stated contribution.

Name of Co-Author	Abdeljalil ElHabti
Contribution to the Paper	Wrote part of the manuscript, created the figure and reference list.
Signature	Date 11/9/19

Name of Co-Author	Jessica Schmidt
Contribution to the Paper	Wrote part of the manuscript, created the table and edited the figure.
Signature	Date 11/9/19

Name of Co-Author	Delphine Fleury		
Contribution to the Paper	Wrote part of the manuscript. Edited the manuscript and acted as corresponding author.		
Signature		Date	23/09/2019

Journal of Experimental Botany, Vol. 69, No. 13 pp. 3195–3210, 2018
doi:10.1093/jxb/ery081 Advance Access publication 17 March 2018

REVIEW PAPER

The physiological and genetic basis of combined drought and heat tolerance in wheat

Penny J. Tricker, Abdeljalil ElHabti, Jessica Schmidt and Delphine Fleury*

School of Agriculture, Food and Wine, University of Adelaide, PMB1, Glen Osmond, SA 5064, Australia

* Correspondence: delphine.fleury@adelaide.edu.au

Received 6 October 2017; Editorial decision 20 February 2018; Accepted 14 March 2018

Editor: Rajeev K Varshney, International Crops Research Institute for the Semi-Arid Tropics (ICRISAT), India

Abstract

Drought and heat stress cause losses in wheat productivity in major growing regions worldwide, and both the occurrence and the severity of these events are likely to increase with global climate change. Water deficits and high temperatures frequently occur simultaneously at sensitive growth stages, reducing wheat yields by reducing grain number or weight. Although genetic variation and underlying quantitative trait loci for either individual stress are known, the combination of the two stresses has rarely been studied. Complex and often antagonistic physiology means that genetic loci underlying tolerance to the combined stress are likely to differ from those for drought or heat stress tolerance alone. Here, we review what is known of the physiological traits and genetic control of drought and heat tolerance in wheat and discuss potential physiological traits to study for combined tolerance. We further place this knowledge in the context of breeding for new, more tolerant varieties and discuss opportunities and constraints. We conclude that a fine control of water relations across the growing cycle will be beneficial for combined tolerance and might be achieved through fine management of spatial and temporal gas exchange.

Keywords: Cereal, climate, stress, temperature, water, yield.

Introduction

Wheat is the major food for numerous regions around the world, providing approximately 20% of daily calories and protein for 4.5 billion people (Shiferaw *et al.*, 2013). Wheat ranks first in terms of harvested area (223.67 million hectares in 2016) and is the second most produced crop with a global production of 735.3 million tons in 2016 (USDA, 2017). A recent study predicted that wheat yields will decline by 4.1% to 6.4% for each global increase of 1 °C due to climate change (Liu *et al.*, 2016) while wheat consumption is expected to increase by over 30% in the next 40 years (Weigand, 2011). Wheat production would need to reach 858 million tons by 2050 in order to match the predicted global food demand (Alexandratos and Bruinsma, 2012).

Drought and heat are two major abiotic stresses constraining wheat productivity worldwide, causing yield losses of up to 86% and 69%, respectively (Fischer and Maurer, 1978; Prasad *et al.*, 2011). Both stresses are more likely to occur simultaneously rather than separately in semi-arid and hot growing regions in North Africa, Argentina, Mexico, Australia, South Africa, and the Mediterranean countries, and in high latitude, semi-arid growing regions of central and eastern Asia, Canada, the USA, and Kazakhstan (Mooney and Di Castri, 1973; Araus *et al.*, 2002; Pradhan *et al.*, 2012; Tricker *et al.*, 2016). Yield penalty is associated with long periods of drought coinciding with heat waves above 32 °C during heading and grain filling stages (Wardlaw and Wrigley, 1994). In

Abbreviations: G×E, genotype by environment; GS, genomic selection; HI, harvest index; HSF, heat shock factor; HSP, heat shock protein; QTL, quantitative trait locus; ROS, reactive oxygen species; VPD, vapour pressure deficit; WU, water use; WUE, water use efficiency.

the Australian wheat belt, average daily maximum temperatures and numbers of days over 30 °C during the period of grain filling have been steadily increasing over the past three decades, and further rises are projected with climate change (ABS, 2012). The major decrease in wheat production across central Europe in the exceptionally hot summer of 2003 was likely to be due to short, but severe, heat waves during reproductive development (Wheeler, 2012). Stress tolerance is particularly critical in growing regions where the gap between attained yields and maximum yields is highest, and may have more consequence globally than where differences are lower (Tester and Langridge, 2010). Hence, producing wheat varieties with high and stable yield under these environmental stresses is one of the most important aims of breeding (Gavuzzi *et al.*, 1997; Tilman *et al.*, 2011).

Whereas responses to either drought or heat stress have been studied extensively in wheat, the combination of both environmental stresses has only recently become a matter for research. When irrigated, and with saturated atmospheric humidity (low vapour pressure deficit; VPD) at high temperatures, Australian modern wheat varieties did not show symptoms of heat stress: plants were lush and produced up to 6.8 t ha^{-1} (Parent *et al.*, 2017). This example and others demonstrate that wheat is heat tolerant when water is available. To improve wheat for dual tolerance, plants must be studied under the combination of stresses.

Overall, the combination of both high temperature and drought has a negative, additive impact on plant phenology and physiology, i.e. growth, chlorophyll content, leaf photosynthesis, grain number, spikelet fertility, grain filling duration, and grain yield (Altenbach *et al.*, 2003; Shah and Paulsen, 2003; Prasad *et al.*, 2011; Pradhan *et al.*, 2012; Perdomo *et al.*, 2015, 2017). Although responses to the two stresses share some common mechanisms, other physiological processes are antagonistic (Machado and Paulsen, 2001). For instance, combined drought and heat stress decreases leaf chlorophyll content by 49% while drought or heat alone reduce it by 9% or 27%, respectively (Pradhan *et al.*, 2012; Awasthi *et al.*, 2014). This early senescence of green tissues affects the total amount of carbohydrates transported to the grains and final grain weight. Delayed senescence, a stay-green phenotype, has been associated with drought tolerance (e.g. Pinto *et al.*, 2010) and with heat tolerance in experiments using irrigation (e.g. Shirdelmoghanloo *et al.*, 2016) where water reserves are available and accessible in deep soils for continued water use and transport of assimilates to grains post-anthesis (Reynolds *et al.*, 2005; Christopher *et al.*, 2008). In contrast, a stay-green phenotype is unlikely to contribute to combined drought and heat tolerance where no water reserves are available for continuous water use and might exacerbate the combined stress.

Although plants' responses to the combination of drought and heat have been described (reviewed in Zandalinas *et al.* 2018), few models or explanations are proposed for the physiological traits underlying combined tolerance (Pinto and Reynolds, 2015), and very little is known about genes and loci underlying these physiological mechanisms in wheat. Quantitative trait loci (QTLs) for drought and heat tolerance have, to date, mostly been reported for low-yield field environments where stress is present (such as the mega-environments 1 and 4 defined by CIMMYT, http://wheatatlas.org/), but not controlled and often not measured (Table 1). Complex interactions between QTLs and environments exist that may limit the usefulness of a particular allele. For example, using multi-environment analysis, Bonneau *et al.* (2013) showed that alternative parental alleles of a major QTL for yield in dry and hot environments (*qDHY.3B*) were positive, depending on the severity of the water deficit, soil depth, and co-occurrence with high temperatures.

A greater understanding of the physiology underlying combined drought and heat tolerance should enable researchers and breeders to discriminate between traits and loci useful for improvement. With improving genomic resources and high-throughput phenotyping methods, it becomes possible to identify loci and genes for tolerance and incorporate favourable alleles into breeding programmes. In this review, we outline what is known in wheat of the physiology and genetic variation underlying drought and heat tolerance – defined here as the ability to maintain yield under stress. We propose traits to measure in genetic mapping populations that are likely to prove beneficial for combined tolerance (Fig. 1) and discuss opportunities and constraints for incorporating alleles into breeding for tolerant wheat.

Wheat growth, architecture and biomass partitioning under drought and heat

Water deficit and high temperature affect every aspect of wheat growth from germination to maturity. The impact on yield components depends on the duration and the severity of the stress as well as the stage of plant development when stress occurs (Salter and Goode, 1967; Barnabás *et al.*, 2008; Parent *et al.*, 2017). As water stress reduces plant growth through reduced tillering and leaf expansion (Acevedo *et al.*, 1971), and high temperature accelerates plant growth and shortens developmental stages (Parent and Tardieu, 2012), under combined stress plants flower earlier and produce less biomass than under single stress. Reproductive organs are especially sensitive to drought and heat stress (Stone and Nicolas, 1995; Saini and Lalonde, 1997). Episodes of drought and heat stress around anthesis severely reduce the final number of grains per spike by more than either individual stress due to an increased abortion of ovules (Asana and Williams, 1965; Hochman, 1982; Saini and Aspinall, 1982; Pradhan *et al.*, 2012; Weldearegay *et al.*, 2012). During grain filling, combined drought and high temperature, as frequently occur in major growing regions, reduce the size and weight of individual grains by reducing the division rate of endosperm cells and shortening the duration of grain filling (Jenner, 1994; Barnabás *et al.*, 2008; Prasad *et al.*, 2011; Pradhan *et al.*, 2012).

Complex source–sink interactions underlie tolerance to drought and heat stress, and remobilization of stored assimilates to grain filling following stress at sensitive periods is dependent on sink strength. In maize, grain size, determining

Table 1. *QTL identified in wheat under combined dry and hot conditions, drought or heat stress*

Trait	Chromosome	References
Combined dry and hot conditions		
Grain yield	1AL, 1B, 1D, 2A, 2BL, 3A, 3B, 4AL, 4B, 5A, 6A, 6B, 7A, 7B, 7D	Kirigwi *et al.* (2007)[a], Maccaferri *et al.* (2008)[a,b], Pinto *et al.* (2010)[a], Golabadi *et al.* (2011)[a], Bennett *et al.* (2012)[a], Merchuk-Ovnat *et al.* (2016)[a], Tahmasebi *et al.* (2017)[a]
Thousand grain weight	1D, 2B, 3A, 3B, 4A, 6A, 7A, 7B, 7D	Pinto *et al.* (2010)[a], Golabadi *et al.* (2011)[a], Bennett *et al.* (2012)[a], Tahmasebi *et al.* (2017)[a]
Kernel weight index (large grains–all grains)	1A, 2B, 6A	Pinto *et al.* (2010)[a]
Grain weight spike^{-1}	5B, 6A, 7B	Golabadi *et al.* (2011)[a]
Grain number m^{-2}	1B, 2A, 3B, 3D, 4AL, 6B, 7A	Kirigwi *et al.* (2007)[a], Pinto *et al.* (2010)[a], Bennett *et al.* (2012)[a]
Grain number spike^{-1}	2B, 7B	Golabadi *et al.* (2011)[a], Tahmasebi *et al.* (2017)[a]
Harvest index	1B, 2A, 2B, 3B, 4A, 5A, 5B, 6A, 6B, 7B	Peleg *et al.* (2009)[d], Golabadi *et al.* (2011)[a]
Spike weight	1B, 2A, 4A, 6A, 7A, 7B	Peleg *et al.* (2009)[d], Golabadi *et al.* (2011)[a]
Spike number m^{-2}	2B, 4AL, 5B	Kirigwi *et al.* (2007)[a], Golabadi *et al.* (2011)[a]
Spike harvest index	2B, 3B	Golabadi *et al.* (2011)[a]
Spikelet number spike^{-1}	5A	Tahmasebi *et al.* (2017)[a]
Biomass	2BS, 4AL, 4B, 5A, 7AS	Kirigwi *et al.* (2007)[a], Peleg *et al.* (2009)[d], Merchuk-Ovnat *et al.* (2016)[a]
Plant height	1A, 1B, 2BL, 3AL, 3BS, 4A, 4B, 5A, 7AS	Maccaferri *et al.* (2008)[ab], Pinto *et al.* (2010)[a], Tahmasebi *et al.* (2017)[a]
Shoot length	2B, 3B, 4A, 4B, 6B, 7A, 7B	Peleg *et al.* (2009)[d]
Peduncle length	3A, 3B	Bennett *et al.* (2012)[a]
Flag leaf width	2B, 3B	Bennett *et al.* (2012)[a]
Days to heading	1A, 1B, 1D, 2AS, 2BS, 2BL, 3A, 3B, 4AL, 4B, 4D, 5A, 6A, 7AS, 7BS, 7D	Kirigwi *et al.* (2007)[a], Maccaferri *et al.* (2008)[a,b], Peleg *et al.* (2009)[d], Pinto *et al.* (2010)[a], Merchuk-Ovnat *et al.* (2016)[a], Ogbonnaya *et al.* (2017)[a], Tahmasebi *et al.* (2017)[a]
Days to maturity	1A, 1D,5A, 7B, 7D	Pinto *et al.* (2010)[a], Tahmasebi *et al.* (2017)[a]
Days from heading to maturity	1B, 2B, 4A, 4B, 5A, 5B, 7A, 7B	Peleg *et al.* (2009)[d]
NDVI at the vegetative stage	1B, 3B, 4A, 7A	Pinto *et al.* (2010)[a], Bennett *et al.* (2012)[a]
NDVI at the grain filling stage	1B, 1D, 2A, 2B, 4A, 4B, 5A, 6A, 6B, 7A, 7B	Pinto *et al.* (2010)[a]
Stem WSC	1A, 1B, 3A, 3B, 4A, 6D	Pinto *et al.* (2010)[a], Bennett *et al.* (2012)[a]
Grain fill rate	4AL	Kirigwi *et al.* (2007)[a]
Grain fill duration	4AL	Kirigwi *et al.* (2007)[a]
Canopy temperature at the vegetative stage	1B, 2B, 3B, 4A, 4B, 6B, 7A	Pinto *et al.* (2010)[a], Tahmasebi *et al.* (2017)[a]
Canopy temperature at the grain filling stage	1A, 1B, 2B, 3B, 4A, 5A, 6B, 7A	Pinto *et al.* (2010)[a]
Canopy temperature depression	1A, 2A, 2B, 3A, 3B, 4A, 4B, 5A, 5B, 6A, 6B, 7A, 7B	Diab *et al.* (2008)[a]
Flag leaf rolling	1A, 2A, 2B, 4B, 5A, 5B, 6B, 7A, 7D	Peleg *et al.* (2009)[d], Tahmasebi *et al.* (2017)[a]
Early vigour	2B, 2D, 3B, 4A	Bennett *et al.* (2012)[a]
Early ground cover	6AS	Mondal *et al.* (2017)[a]
Chlorophyll content	1A, 1B, 3A, 4A, 4B, 4D, 5A, 5B, 6A, 6B, 7A	Diab *et al.* (2008)[a], Peleg *et al.* (2009)[d], Bennett *et al.* (2012)[a]
Chlorophyll fluorescence	1A, 1B, 2A, 2B, 3A, 3B, 4A, 4B, 5A, 5B, 6A, 6B, 7A, 7B	Diab *et al.* (2008)[a]
Carbon isotope discrimination	1B, 2A, 2B, 3A, 3B, 4A, 4B, 5A, 5B, 6B, 7A, 7B	Diab *et al.* (2008)[a], Peleg *et al.* (2009)[d]
Photosynthetically active radiation	1A, 1B, 2B, 3A, 3B, 4A, 4B, 5A, 5B, 6A, 6B, 7A, 7B	Diab *et al.* (2008)[a]
Stomatal density	4AS, 5AS, 7AL	Shahinnia *et al.* (2016)[a]
Stomatal index	2BL, 7BL	Shahinnia *et al.* (2016)[a]
Stomatal aperture area	7AL	Shahinnia *et al.* (2016)[a]
Stomatal aperture length	2BS, 2BL, 7AL	Shahinnia *et al.* (2016)[a]
Guard cell length	1AS, 3BL, 7AL	Shahinnia *et al.* (2016)[a]
Guard cell area	1BL, 4BL, 5AL, 5DL	Shahinnia *et al.* (2016)[a]

Table 1. *Continued*

Trait	Chromosome	References
Transpiration efficiency	1A, 1B, 2B, 3A, 3B, 4A, 4B, 5A, 5B, 6A, 6B, 7A, 7B	Diab *et al.* (2008)[a]
Leaf relative water content	1B, 2B, 3A, 3B, 4A, 4B, 5A, 5B, 6A, 6B	Diab *et al.* (2008)[a]
Water index	1A, 1B, 2A, 2B, 3A, 3B, 4A, 4B, 5A, 5B, 6A, 6B, 7A, 7B	Diab *et al.* (2008)[a]
Leaf osmotic potential	2A, 2B, 3A, 3B, 4B, 5A, 5B, 6B	Peleg *et al.* (2009)[d]
Osmotic adjustment	1A, 3A, 3B, 4A, 7A	Diab *et al.* (2008)[a]
Metabolites (mQTL)	2B, 4A, 5A, 7A, 7D	Hill *et al.* (2015)[a]
Expression of stress-related genes (eQTL)	6BL	Aprile *et al.* (2013)[c]
Drought stress		
Grain yield	2D, 3D, 3DL, 4AL, 4BS, 4DL, 5A, 5B, 5DL, 6B, 6D, 7AL, 7BL, 7D	Quarrie *et al.* (2005)[a], Czyczyło-Mysza *et al.* (2011)[d], Kadam *et al.* (2012)[c], Tahmasebi *et al.* (2017)[a]
Grain weight spike^{-1}	1B, 1D	Xu *et al.* (2017)[a]
Thousand grain weight	1B, 1D, 2A, 2B, 3A, 3D, 4A, 4D, 5A, 6A, 6D, 7A, 7B	Quarrie *et al.* (2005)[a], Dashti *et al.* (2007)[c], Yang *et al.* (2007)[a], Tahmasebi *et al.* (2017)[a], Xu *et al.* (2017)[a]
Grain number m^{-2}	1B, 5B, 7D	Tahmasebi *et al.* (2017)[a]
Grain number spike^{-1}	1A, 2A, 2B, 2D, 3A, 3B, 4A, 4B, 5A, 5B, 5D, 6A, 6B, 6D, 7A, 7B	Quarrie *et al.* (2005)[a], Czyczyło-Mysza *et al.* (2011)[d], Xu *et al.* (2017)[a]
Harvest index	1B, 2D, 4BS, 5A	Kadam *et al.* (2012)[c], Xu *et al.* (2017)[a]
Spike number plant^{-1}	1A, 2A, 2B, 2D, 4B, 5A, 7B	Quarrie *et al.* (2005)[a], Xu *et al.* (2017)[a]
Spikelet compactness	6A, 7A	Xu *et al.* (2017)[a]
Spikelet number spike^{-1}	1A, 7D	Tahmasebi *et al.* (2017)[a], Xu *et al.* (2017)[a]
Sterile spikelet number spike^{-1}	7A	Xu *et al.* (2017)[a]
Fertile spikelet spike^{-1}	2A	Xu *et al.* (2017)[a]
Biomass	1B	Xu *et al.* (2017)[a]
Shoot biomass	4B	Kadam *et al.* (2012)[c]
Root biomass	2D, 4BS	Kadam *et al.* (2012)[c]
Plant height	1B, 4B, 7D	Tahmasebi *et al.* (2017)[a], Xu *et al.* (2017)[a]
Peduncle length	3B	Dashti *et al.* (2007)[c]
Coleoptile length	6AS	Spielmeyer *et al.* (2007)[c]
Spike length	2B, 7A, 7B	Xu *et al.* (2017)[a]
Root length	2D, 4B, 5D, 6B	Kadam *et al.* (2012)[c]
Growth rate	5BL	Parent *et al.* (2015)[c]
Relative growth rate	4AL	Parent *et al.* (2015)[c]
Inflexion point in growth curves	7DS	Parent *et al.* (2015)[c]
Leaf expansion rate	5BL	Parent *et al.* (2015)[c]
Inflexion point in leaf expansion curves	5BL	Parent *et al.* (2015)[c]
Days to heading	1D, 4B, 7D	Tahmasebi *et al.* (2017)[a]
Days to flowering	2D	Kadam *et al.* (2012)[c]
Stem WSC at the flowering stage	1A, 1D, 2D, 4A, 4B, 7B	Yang *et al.* (2007)[a]
Stem WSC at the grain filling stage	4A	Yang *et al.* (2007)[a]
Stem WSC at the maturity stage	6B	Yang *et al.* (2007)[a]
Accumulation efficiency of stem WSC	1A, 2A, 5A, 7B	Yang *et al.* (2007)[a]
Remobilization efficiency of stem WSC	7A	Yang *et al.* (2007)[a]
Grain filling efficiency	2A, 4B, 5A,	Yang *et al.* (2007)[a]
Flag leaf rolling	4B, 5A	Tahmasebi *et al.* (2017)[a]
Chlorophyll content	1B, 2B, 5B, 7A, 7B	Ilyas *et al.* (2014)[c], Tahmasebi *et al.* (2017)[a], Xu *et al.* (2017)[a]
Flag leaf persistence	2D, 3B, 4B, 5A, 6A	Verma *et al.* (2004)[a]
Net photosynthetic rate	6B	Xu *et al.* (2017)[a]
Chlorophyll fluorescence	1B, 2A, 2D, 3A, 3B, 3D, 4A, 4B, 4D, 5A, 5B, 6A, 6B, 7A, 7B, 7D	Czyczyło-Mysza *et al.* (2011)[d]
Stomatal conductance	5A	Xu *et al.* (2017)[a]

Table 1. *Continued*

Trait	Chromosome	References
Stomatal density	5BS	Shahinnia *et al.* (2016)[c]
Stomatal index	5BS, 6DL	Shahinnia *et al.* (2016)[c]
Stomatal aperture length	2BL, 4BS, 7AS, 7DL	Shahinnia *et al.* (2016)[c]
Guard cell area	1BL, 5BS	Shahinnia *et al.* (2016)[c]
Guard cell length	1BL, 4BS, 7AS	Shahinnia *et al.* (2016)[c]
Transpiration rate	3Al, 4BL, 6D	Parent *et al.* (2015)[c], Xu *et al.* (2017)[a]
Water use efficiency	2AL, 4D	Parent *et al.* (2015)[c], Xu *et al.* (2017)[a]
Heat stress		
Grain yield	1A, 1BL, 1D, 2BS, 3A, 3BS, 3BL, 3D, 4A, 4B, 4DL, 5A, 5B, 6A, 6B, 6D, 7AS, 7AL, 7BS, 7BL	Quarrie *et al.* (2005)[a], Maccaferri *et al.* (2008)[a,b], Pinto *et al.* (2010)[a], Golabadi *et al.* (2011)[a], Bennett *et al.* (2012)[a], Paliwal *et al.* (2012)[a], Merchuk-Ovnat *et al.* (2016)[a], Ogbonnaya *et al.* (2017)[a]
Grain weight spike^{-1}	3A, 3BS, 6A, 7A, 7B	Golabadi *et al.* (2011)[a], Shirdelmoghanloo *et al.* (2016)[c], Ogbonnaya *et al.* (2017)[a]
Thousand grain weight	1A, 2A, 2B, 2D, 3A, 3BS, 3D, 4A, 4B, 4D, 5A, 5B, 5D, 6A, 6B, 6D, 7A, 7D	Quarrie *et al.* (2005)[a], Pinto *et al.* (2010)[a], Golabadi *et al.* (2011)[a], Bennett *et al.* (2012)[a], Ogbonnaya *et al.* (2017)[a], Tahmasebi *et al.* (2017)[a]
Single grain weight	2D, 3BS, 5B, 6A	Shirdelmoghanloo *et al.* (2016)[c]
Kernel weight index (large grains–all grains)	1A, 1D, 2B, 3B, 4B, 5A, 5B, 6A, 6B, 6D	Pinto *et al.* (2010)[a]
Grain number m^{-2}	1A, 1B, 1D, 3BS, 3BL, 3D, 4A, 4B, 4D, 5B, 6A, 6B, 6D, 7A	Pinto *et al.* (2010)[a], Bennett *et al.* (2012)[a]
Grain number spike^{-1}	1A, 1B, 2A, 3B, 4B, 4D, 5D, 6A, 7B, 7D	Quarrie *et al.* (2005)[a], Golabadi *et al.* (2011)[a], Ogbonnaya *et al.* (2017)[a], Tahmasebi *et al* (2017)[a]
Threshing index	1A, 1B, 5B	Ogbonnaya *et al.* (2017)[a]
Harvest index	1B, 2B, 3B, 4A, 5A, 5B, 6A, 6B, 7B	Peleg *et al.* (2009)[d]
Spike number m^{-2}	1A, 1B, 3A, 3B, 4B, 5A, 5B, 7B, 7D	Golabadi *et al.* (2011)[a], Ogbonnaya *et al.* (2017)[a]
Spike number plant^{-1}	3A	Quarrie *et al.* (2005)[a]
Spike weight	1B, 2B, 2D, 3D, 4A, 5D, 6A, 7B	Peleg *et al.* (2009)[d], Golabadi *et al.* (2011)[a], Ogbonnaya *et al.* (2017)[a]
Spike harvest index	2B, 5B, 7A, 7B	Golabadi *et al.* (2011)[a]
Spikelet compactness	1A	Tahmasebi *et al.* (2017)[a]
Spikelet number spike^{-1}	1B, 1D, 2B, 4A, 5B, 6A, 6B	Ogbonnaya *et al.* (2017)[a], Tahmasebi *et al.* (2017)[a]
Number of productive tiller	1B	Sharma *et al.* (2016)[a]
Biomass	1BL, 2BS, 7AS, 7BS	Merchuk-Ovnat *et al.* (2016)[a]
Shoot biomass	3BS, 4A, 6B	Shirdelmoghanloo *et al.* (2016)[c]
Plant height	1A, 1B, 2A, 2B, 2D, 3A, 3B, 3D, 4A, 4B, 5A, 5B, 6A, 6D, 7A, 7B, 7D	Maccaferri *et al.* (2008)[a,b], Pinto *et al.* (2010)[a], Ogbonnaya *et al.* (2017)[a], Tahmasebi *et al.* (2017)[a]
Shoot length	1B, 2B, 3A, 3B, 4A, 4B, 5D, 7A, 7B	Peleg *et al.* (2009)[d], Ogbonnaya *et al.* (2017)[a]
Peduncle length	1A, 1B, 2B, 3A, 3B, 5B, 7A	Ogbonnaya *et al.* (2017)[a]
Flag leaf length	3B, 5B	Mason *et al.* (2010)[c]
Flag leaf width	1D, 2B, 3BL, 7A, 3BL	Mason *et al.* (2010)[c], Bennett *et al.* (2012)[a]
Wax score	1B, 2A, 2B, 2D, 3A, 3B, 5A, 6A, 6B, 7B	Mason *et al.* (2010)[c], Ogbonnaya *et al.* (2017)[a]
Days to heading	1BL, 1D, 2A, 2BS, 3B, 3A, 4A, 4B, 4D, 5A, 6A, 7AS, 7BS, 7D	Maccaferri *et al.* (2008)[a,b], Peleg *et al.* (2009)[d], Pinto *et al.* (2010)[a], Merchuk-Ovnat *et al.* (2016)[a], Ogbonnaya *et al.* (2017)[a]
Days to flowering	1B, 1D, 4A, 4B, 4D, 5B	Mason *et al.* (2010)[c], Pinto *et al.* (2010)[a]
Days to maturity	1B, 1D, 2A, 2B, 3B, 4D, 5A, 5B, 5D, 6A, 6B, 6D, 7A, 7B, 7DS	Pinto *et al.* (2010)[a], Bennett *et al.* (2012)[a], Paliwal *et al.* (2012)[a], Ogbonnaya *et al.* (2017)[a]
NDVI at the vegetative stage	1B, 1D, 2B, 2D, 3A, 3B, 4A, 4D, 5A, 6A, 6B, 6D, 7A	Pinto *et al.* (2010)[a], Bennett *et al.* (2012)[a]
NDVI at the grain filling stage	1A, 1B, 3A, 4A, 4B, 5A, 5B, 6A, 7B	Pinto *et al.* (2010)[a]
Stem WSC	1A, 1B, 2D, 3A, 3BL, 5A, 5B, 6A	Pinto *et al.* (2010)[a], Bennett *et al.* (2012)[a]
Grain filling duration	1B, 1D, 2A, 2B, 2D, 3BS, 5A, 6A, 6B, 6D	Mason *et al.* (2010)[c], Shirdelmoghanloo *et al.* (2016)[c], Ogbonnaya *et al.* (2017)[a]
Canopy temperature at the vegetative stage	1A, 1B, 1D, 2B, 3A, 3BL, 4A, 4B, 5B, 6B, 7A	Pinto *et al.* (2010)[a], Bennett *et al.* (2012)[a]
Canopy temperature at the grain filling stage	1A, 1B, 1D, 2B, 3BS, 3BL, 4A, 4D, 5A, 5D, 7A, 7B	Pinto *et al.* (2010)[a], Bennett *et al.* (2012)[a]
Canopy temperature depression	7BL	Paliwal *et al.* (2012)[a]
Flag leaf rolling	1A, 2A, 2B, 2D, 3D, 4B, 5A, 5B, 6A, 6B, 7A, 7B	Peleg *et al.* (2009)[d], Ogbonnaya *et al.* (2017)[a], Tahmasebi *et al.* (2017)[a]
Early vigour	2B, 2D, 3BL	Bennett *et al.* (2012)[a]

Table 1. *Continued*

Trait	Chromosome	References
Chlorophyll content	1A, 1B, 1D, 2B, 3A, 3BS, 4A, 4D, 5A, 5B, 6A, 6D, 7A, 7B, 7D	Peleg *et al.* (2009)[d], Pinto *et al.* (2010)[a], Bennett *et al.* (2012)[a], Tahmasebi *et al.* (2017)[a]
Flag leaf persistence	1B, 1D, 2A, 3A, 3BS, 6A, 6B, 7A,	Vijayalakshmi *et al.* (2010)[c], Talukder *et al.* (2014)[c], Shirdelmoghanloo *et al.* (2016)[c]
Chlorophyll loss rate	3BS, 6BL	Shirdelmoghanloo *et al.* (2016)[c]
Chlorophyll fluorescence	7A	Vijayalakshmi *et al.* (2010)[c]
Carbon isotope discrimination	1A, 2A, 4A, 5B, 6A, 6B, 7B	Peleg *et al.* (2009)[d]
Leaf osmotic potential	2A, 3A, 3B, 5A, 5B, 6A, 6B	Peleg *et al.* (2009)
Plasma membrane damage	1D, 2B, 7A	Talukder *et al.* (2014)[c]
Thylakoid membrane damage	1D, 6A, 7A	Talukder *et al.* (2014)[c]

Dry and hot field conditions are defined using the CIMMYT mega-environments 1 and 4 (Rajaram *et al.*, 1994). NDVI, near differential vegetative index; WSC, water-soluble carbohydrates
[a] Field conditions.
[b] Trials in Italy, Tunisia and Morocco with maximum temperature at grain filling ≤26.1 °C.
[c] Controlled conditions.
[d] Semi-controlled conditions.

sink strength for grain filling, is determined by expansive plant growth, which is the increase in volume due to water entry into growing cells (Tardieu *et al.*, 2014). There is limited evidence for differences in carbon metabolism or status in ovules under stress, but many studies demonstrate reductions in organ elongation rates at sensitive periods with either drought or heat stress. In maize, silk growth and leaf elongation rate are highly correlated (Parent and Tardieu, 2012; Tardieu *et al.*, 2014). When the *PLASTOCHRON1* (Zm*PLA1*) gene was expressed in maize, increasing the length of the cell division zone, the duration of cell division, the duration of leaf elongation, kernel number, and size were increased in field experiments under mild drought (Sun *et al.*, 2017). QTLs for organ size and growth and expansion rates have been identified in wheat under drought (Table 1) but have not been studied under combined drought and heat stress, and no studies of genetic variation for the expansive growth trait have yet been carried out. Theoretically, increased expansive growth will be beneficial for combined drought and heat tolerance where loss of grain number is due to reduction in spike growth and development. Expansive growth will increase sink strength and be beneficial for remobilization of assimilates to the grain during filling.

Traits that increase overall assimilation should increase drought and heat tolerance when partitioned beneficially to the grain. Several QTLs for harvest index (HI) have been reported (Table 1). Meta-analysis of reported QTLs for drought or heat stress revealed meta-QTLs for spike weight/density and plant height were significantly (at $P<0.1$) associated with meta-QTL regions for yield under drought or heat in wheat (Acuña-Galindo *et al.* 2015). Major clusters were located at the *Rht-B1* and *Rht-D1* dwarfing loci. Plant height restriction due to the *Rht-B1* allele increases HI and is due to gibberellin insensitivity (Peng *et al.*, 1999). In barley, exogenous gibberellin application increases sensitivity to high temperature stress (Vettakkorumakankav *et al.*, 1999), so it is possible that widely used dwarfing alleles in modern, semi-dwarf wheat varieties already contribute to heat tolerance through the gibberellin pathway. Modern, semi-dwarf phenotypes are already widely used to prevent undesirable lodging, but there are alleles that appear more or less beneficial in particular environments. For example, Wang *et al.* (2014*b*) suggested that the *Rht13* or combination of *Rht13* + *Rht8* alleles could be favourable in water-limited environments. Thus, there is scope to study and improve wheat drought and heat tolerance through the deployment of new combinations of dwarfing alleles, identification of genes controlling the gibberellin pathway, and optimization of expansive growth (Fig. 1).

Breeding for canopy temperature and evapotranspiration under drought and heat

The main mechanism wheat plants use to decrease their internal temperatures under heat stress is evaporative cooling, driven by transpiration. Under drought, plants close their stomata to avoid excessive water loss; this reduces transpiration and evaporative cooling and, as a result, drought-stressed plants display higher leaf and canopy temperatures than well-watered plants (Reynolds *et al.*, 2009). Cool canopies were always associated with better yield performance (Pinto and Reynolds, 2015). Several QTLs have been reported for canopy temperature depression under drought and heat in wheat grown in deep soils of northern Mexico (Pinto *et al.*, 2010; Pinto and Reynolds, 2015). The major QTLs on chromosome 2B were shown to be associated with root distribution, with cool canopy genotypes able to extract more water at depth under water stress due to a greater proportion of deeper roots (Pinto and Reynolds, 2015). The deep root trait was not recapitulated under heat stress alone (with irrigation) (Pinto and Reynolds, 2015). This suggested that the beneficial physiological trait conferred by the 2B QTL was not a different root system architecture or distribution *per se*, but the ability to optimize root distribution to capture water for continued cooling dependent on water distribution in the soil.

Transpiration efficiency is a ratio between biomass and transpiration, while water use efficiency (WUE) is the biomass

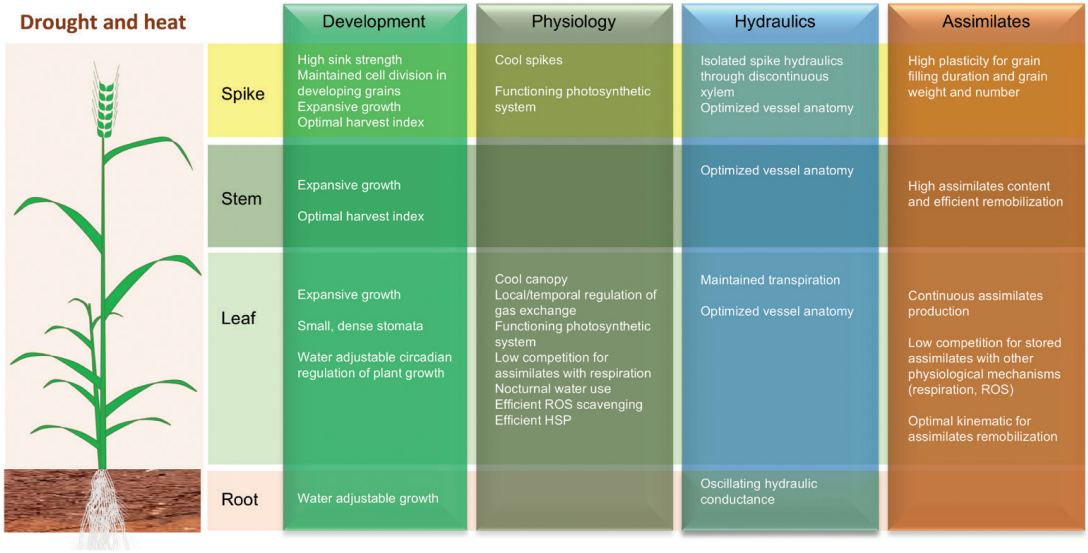

Fig. 1. Beneficial traits for combined drought and heat tolerance in wheat.

produced per unit of water used, at the whole plant level or whole plot in the field. Carbon isotope discrimination ($^{12}C/^{13}C$ ratio) in dry matter is negatively correlated to transpiration efficiency in wheat and a surrogate for this trait (Condon *et al.*, 1990). It has been successfully used for breeding water use efficient wheat for dry regions in Australia (Condon *et al.*, 1990, 2002). Increased transpiration efficiency alone might not improve tolerance. The equation for grain yield in water-limited environments includes harvest index (HI) and water use (WU) as well as WUE (Passioura, 1977; Passioura, 1996): GY=HI×WU×WUE. The theoretical physiology underlying this relationship has been extensively explained and reviewed (Ehrler *et al.*, 1978; Araus *et al.*, 2002; Blum, 2005; Reynolds *et al.*, 2007; Fischer, 2011; Vadez *et al.*, 2014). It has been argued that, if transpiration efficiency is increased by a reduction in the transpiration term of the equation, a low intrinsic stomatal conductance and transpiration reduces growth, biomass accumulation and light interception. Therefore, selecting plants with high transpiration efficiency might select for smaller plants (Blum, 2009). When small plants are selected, sink strength is lost and fewer assimilates are mobilized to the grain. Under the combination of drought and heat, low intrinsic transpiration could, additionally, penalize evaporative cooling. Reynolds *et al.* (2007) found that carbon isotope discrimination, together with canopy temperature linked to water uptake, was associated with improved performance in drought-stressed environments. Diab *et al.* (2008) found QTLs associated with tolerance in wheat for canopy temperature depression, transpiration efficiency, water index, and grain carbon isotope discrimination in dry and hot field conditions (Table 1).

Evaporative demand, or VPD, which depends on the amount of moisture in the air and the air temperature, also plays a critical role in transpiration and transpiration efficiency. Different sensitivities of transpiration to high VPD have been found amongst wheats and its genetic control described in the Australian wheat population RAC875/Kukri (Schoppach *et al.*, 2016). Six QTLs were identified for transpiration response to VPD, with one QTL on chromosome 5A individually explaining 25.4% of the genetic variance (Schoppach *et al.*, 2016). A study of 23 Australian wheat varieties released from 1890 to 2008 showed that whole-plant transpiration rate in response to VPD was limited at VPD above a breakpoint of about 2 kPa (Schoppach *et al.*, 2016). The breakpoint and transpiration response at VPD>2 kPa were correlated with the year of release indicating that breeders, by selecting for yield in the hot and dry climate of southern Australia, selected lines with limited whole-plant transpiration rate.

Transpiration rate might also be moderated by patchy stomatal closure and the threshold for closure might differ in sensitivity between VPD and soil moisture deficit (Vadez *et al.*, 2014). In maize, the relationship between expansive growth (leaf expansion rate; LER) and stomatal conductance was rapid and linear in contrast to the relationship between LER and transpiration rate (Caldeira *et al.*, 2014*b*). Tardieu *et al.* (2014) suggest that this is because increases in biomass and in expansive growth in volume are under different genetic controls and that, under water deficit, they are uncoupled over time. Because of the dependence of transpiration efficiency on both the biomass term and VPD, transpiration response traits should be evaluated in QTL studies. To keep an optimal balance between evaporative cooling and water saving, plants with fine adjustment of transpiration should have an advantage under combined drought and heat (Fig. 1).

Temporal regulation of gas exchange

Vadez *et al.* (2014) have argued that the total plant water use over the growing season and WUE for yield depend on available water and use at critical stages. Plants can increase

effective use of water by timely modifications of water uptake at critical stages. Timely modifications in stomatal conductance, transpiration, and water use might include different patterns of stomatal opening with developmental stage, time of the day, time of season, and microclimate VPD driven by differences in plant architecture.

High stomatal densities and conductance are associated with increased yield potential in both well-watered and water-limited environments (reviewed in Roche, 2015). High stomatal density could give more flexibility to the plant to adjust stomatal opening depending on the local environmental conditions and ensure continued water uptake and use under favourable conditions. For example, the Australian line RAC875, which is drought and heat tolerant, has many small stomata by contrast with the susceptible Australian variety Kukri with fewer large stomata (Shahinnia *et al.*, 2016). QTLs for stomatal size and density have been identified in dry and hot field conditions in wheat (Table 1). While no correlation was found between yield and stomatal traits in the RAC875/Kukri population, we found a locus for stomatal density and size on chromosome 7A that overlaps with QTLs for grain number per spike, normalized difference vegetation index, harvest index, and yield in the same population (Shahinnia *et al.*, 2016).

When heat stress is severe, leaf stomata will open to allow evaporative cooling despite water limitation. At very high temperatures, the photosynthetic machinery is damaged (Berry and Bjorkman, 1980) and leaf or other vegetative tissues may be sacrificed (Lohraseb *et al.*, 2017). Under combined drought and heat stress, this balance between open stomata and damaged photosynthetic machinery can become critical to allow continued assimilation and can depend on the fine spatiotemporal regulation of gas exchange. That is, continued assimilation in periods of lower stress, as temperatures rise and cool diurnally, may make a plant more tolerant (Richards *et al.*, 1986). Diurnal regulation of gas exchange will make a difference during stress exposure and circadian use of water and regulation of transpiration may both alleviate combined drought and heat stress and be a source of tolerance. A shift in transpiration to cooler times of the day could confer tolerance.

Nocturnal water use, particularly night-time transpiration, is of increasing interest for its role in sustaining sugars export at night (Marks and Lechowicz, 2007) and its potential role in drought tolerance in wheat (Schoppach *et al.*, 2014; Resco de Dios *et al.*, 2016; Sadok, 2016). Genotypic variation for night-time transpiration and its sensitivity to VPD has been documented in wheat and influences the next day's gas exchange under normal conditions and drought (Schoppach and Sadok, 2013; Schoppach *et al.*, 2014; Claverie *et al.*, 2017). Night-time transpiration rate in response to VPD varied consistently with the sensitivity of the genotypes to drought and increased under soil water deficit (Claverie *et al.*, 2017). The effect of night-time temperature was also significant, with an increase in transpiration with increasing temperature observed, as well as genotypic variation. Despite the importance of nocturnal water use for potential drought and heat stress tolerance, no genetic studies have yet been carried out in wheat and no QTLs are known. The interplay between night-time export of assimilates and day-time gas exchange is also yet to be explored. Supply and demand ratios are likely to play a role in determining assimilation and export and, as yet, no studies of circadian regulation in wheat have been carried out in plants during grain filling when grains determine sink strength. With the development of non-destructive phenotyping methods, it will become possible to collect plant data over time and examine the kinematics of plant physiology.

Optimal hydraulic conductance for drought and heat tolerance

Hydraulic conductance is a measure of the flow induced by a pressure or water potential gradient normalized to the plant/organ geometry. Caldeira *et al.* (2014*b*) proposed that circadian oscillations of hydraulic conductance accounted for fluctuating growth (leaf elongation rates) in Arabidopsis. The degree of oscillation was highly dependent on evaporative demand and water stress. High root hydraulic conductance oscillation under water deficit likely led to the ability to control water uptake in response to available soil water when needed. Soil water status regulates the root hydraulic conductance of maize (Caldeira *et al.*, 2014*a*) adjusting growth to water availability. Maintenance of high hydraulic conductance in spikes of long-awned cultivars of wheat significantly reduces spike temperature during grain filling (Maydup *et al.*, 2014). The end of grain filling correlates with a loss of hydraulic conductance at the rachis-xylem conduit (Neghliz *et al.*, 2016). Thus, we hypothesize that by maintaining optimal hydraulic conductance in the different tissues under drought and heat stress (Fig. 1), wheat plants could extend grain filling duration, cool down grain and spike, and optimize water uptake for expansive growth.

In grapevine, soil–leaf differences in water potential among genotypes were shown to be less related to sensitivity of transpiration to soil water deficit than to change in soil–leaf hydraulic conductance, likely due to rapid changes in water transport within the plant (Scharwies and Tyerman, 2017). The ability to partition and channel water between stem, leaf, tillers, and spikes determines both expansive growth in these tissues and remobilization of assimilates following stress. Differences in hydraulic resistances in different tissues influence water transport capacity and drought and heat tolerance (Coupel-Ledru *et al.*, 2014; Bramley *et al.*, 2015). Hydraulic resistance may be determined by differences in structure and architecture of stems, peduncles, and rachis, and differences in xylem vessel diameter and leaf venation (Scharwies and Tyerman, 2017). Vessel structure has an important role in the control of water conductivity in plants in water-limited environments (Tixier *et al.*, 2013; Caringella *et al.*, 2015; Kadam *et al.*, 2015). In wheat, Barlow *et al.* (1980) demonstrated that a xylem discontinuity at the base of the peduncle permitted the isolation of spike hydraulics from the rest of the plant, and that this anatomical feature was crucial during water scarcity, resulting in the independence of water relations in the spike from the rest of the plant. The xylem in wheat is

also discontinuous between rachis and grains, isolating grains and, potentially, preventing water loss during stress (Zee and O'brien, 1970). Photoperiod response (*Ppd* loci) genes have pleiotropic effects on plant growth and development (Cockram *et al.*, 2007) that can modify plant hydraulics. The photoperiod sensitive allele *Ppd-D1* increases daytime and night-time transpiration while decreasing whole-plant leaf area in response to VPD increase in wheat (Schoppach *et al.*, 2016). This suggests that whole-plant hydraulics are developmentally controlled. Deciphering the relationship between vessel structure and plant hydraulics and the genetic control of plant development in wheat will provide a better understanding of the involvement of these physiological mechanisms in tolerance to combined drought and heat stress and their potential for breeding tolerant varieties.

Competition for assimilates under drought and heat stress

Redox balance is crucial for the normal function of many cellular processes. Its fine control is essential for a proper integration of environmental and developmental stimuli and signal transduction (Choudhury *et al.*, 2017). Recent studies demonstrated the important role of photorespiration in maintaining redox homeostasis (Scheibe and Dietz, 2012), mitigating oxidative stress and protecting the photosynthetic apparatus from photoinhibition (Rivero *et al.*, 2009; Peterhansel and Maurino, 2011; Voss *et al.*, 2013). With either drought or heat stress, net photosynthesis is reduced and photorespiration increased (Long and Ort, 2010), but the relative contributions of photorespiration and mitochondrial respiration to combined drought and heat stress tolerance in wheat are unknown and genetic variation for this ratio has not been explored.

Heat stress affects membrane stability and the quantum efficiency of photosystem II, which can be measured, respectively, as cell viability and chlorophyll fluorescence (Blum, 1988; Mohammed and Tarpley, 2009). Drought stress also affects chlorophyll fluorescence with a dramatic decrease of F_v/F_m ratio in susceptible wheat compared with tolerant lines (Izanloo *et al.*, 2008). QTLs have been reported for chlorophyll fluorescence in drought- or heat-stressed wheat (Table 1), but studies in other species suggest that responses to combined drought and heat stress are unique in comparison with either individual stress (Mittler, 2006). At the ecosystem level, drought may actually reduce heat-driven increases in plant respiration due to reduction in carbon substrates available (Schauberger *et al.*, 2017). However, if stored carbohydrates are used for respiration and less available for remobilization following heat stress, drought may exacerbate the effect of heat stress-induced increases in respiration. The rate of grain filling from stem reserves is increased with increasing temperature, reducing grain filling duration (Blum *et al.*, 1994). Tolerance to drought and heat stress will then depend on both the initial concentration of remobilizable carbohydrates and the use of these reserves for respiration. Genetic variation for stem water-soluble carbohydrate content has been explored with known QTLs in drought or heat stress and in combined drought and heat stress (Table 1). Yang *et al.* (2007) also investigated genotype × environment (G×E) interactions for QTLs for stem water-soluble carbohydrate content and remobilization efficiency under water stress in wheat and found significant interactions for all traits. They showed that not all reserves were translocated to grain following water stress and suggested that losses due to respiration could be significant. Zhang *et al.* (2014) explicitly investigated water-soluble carbohydrate QTLs under drought, heat, and combined drought and heat stress and were able to identify additive effects and combinations of favourable alleles for both content and remobilization, suggesting that the genetic mechanisms underlying tolerance will not depend purely on accumulation of stored carbohydrates. QTLs for respiration are now being studied in wheat for the first time under the International Wheat Yield Partnership umbrella (http://iwyp.org/wp-content/; accessed 5 February 2018).

Under prolonged stress exposure, photosynthetic activity is further inhibited by excessive accumulation of reactive oxygen species (ROS), causing damage to the membranes, proteins, and chlorophyll molecules of the photosynthetic apparatus (Price and Hendry, 1991; Jiang and Huang, 2001; Allakhverdiev *et al.*, 2008; Silva *et al.*, 2010; Redondo-Gómez, 2013; Awasthi *et al.*, 2014; Das *et al.*, 2016). Plants use a complex antioxidant system to regulate ROS levels and avoid toxicity, but changes in redox status are also perceived by plants as a signature of a specific stress that will result in a corresponding acclimation response (Foyer and Noctor, 2005; Choudhury *et al.*, 2017). The balance between accumulation of ROS in response to stress and their signalling role under stress is yet to be defined. ROS scavenging is generally induced under drought and heat stress, and higher antioxidant capacity is generally correlated with tolerance to stress (Koussevitzky *et al.*, 2008; Suzuki *et al.*, 2014; Wang *et al.*, 2014*a*). In some wheat genotypes, tolerance to drought or heat stress was associated with increased antioxidant capacity and reduced oxidative damage (Sairam and Saxena, 2000; Sairam *et al.*, 2000; Lascano *et al.*, 2001; Almeselmani *et al.*, 2006; Sečenji *et al.*, 2010; Lu *et al.*, 2017; Zang *et al.*, 2017; Zhang *et al.*, 2017). The effects of combined drought and heat on the ROS system in wheat are unknown, but recent studies highlight the importance of modulation of ROS scavenging, some pathways being specifically induced by combined stress (Rizhsky *et al.*, 2002; Koussevitzky *et al.*, 2008; Demirevska *et al.*, 2010; Zandalinas *et al.*, 2017). The alleles that regulate photorespiration, membrane stability and antioxidant capacity under drought and heat are yet to be discovered in wheat.

As genomics and phenomics advance, the ability to analyse differences in physiological traits in empirical experiments has improved. Important advances in phenotyping with imaging or other equipment mean that it is possible to, for example, measure senescence or canopy temperature in real time in fields (Araus and Cairns, 2014). Further advances that allow, for example, field-scale simultaneous measurements of gas exchange, or non-destructive measurements of water-soluble carbohydrate movement can be anticipated. For researchers,

these will provide a wealth of previously unquantifiable data for physiological traits.

Breeding for stability, plasticity, and G×E interaction under drought and heat

In past breeding of tolerant varieties, efforts have been concentrated on the search for stable QTLs that show the same allelic effect across environments to produce generalist, high-yielding varieties (Eberhart and Russell, 1966). Acuña-Galindo *et al.* (2015) conducted a meta-QTL analysis of 24 genetic studies where QTLs had been mapped for drought, heat, or combined stress in wheat. Co-localization with meta-QTLs for yield was only significant (at $P<0.1$) for the maturity/date of anthesis, spike weight/density, plant height, and canopy temperature depression QTLs. This analysis underscored the pleiotropic effects of phenology and dwarfing alleles on wheat stress response. These generalist QTLs are already bred for with *Ppd* and *Vrn* alleles routinely used in marker-assisted selection. Other stress tolerance QTLs are not generalist and have strong G×E interaction.

In wheat, directional selection (Chapman *et al.*, 2012) has been used to breed varieties that respond consistently to the target environment and management practice. Whilst this approach has been successful in achieving yield gains in some tested environments, strong G×E interactions mean that it is difficult to identify genotypes responding consistently positively in a range of stressful environments, even for a single physiological trait (Reynolds *et al.*, 2009; Lopes *et al.*, 2012). When testing lines bred in high- and low-moisture and reciprocal environments at different sites, Kirigwi *et al.* (2004) found significant environment × selection regime interactions. In this study, development in alternating high-to-low or low-to-high-moisture regimes facilitated the selection of lines that performed well for yield in both, whereas lines selected in either continuous high- or continuous low-moisture regimes had lower yields in these respective environments. The authors suggested that selection under these alternating environmental conditions favoured retention of both high yield under stress and high responsiveness to water input.

In a changing environment, trait plasticity is theoretically beneficial (Bradshaw, 1965; Aspinwall *et al.*, 2015). Plasticity can be defined as the variance in genotypic response across an environmental gradient – that is the slope of its reaction to change, with a steeper slope indicating higher plasticity (Nicotra *et al.*, 2010). Plasticity can be measured as phenotype versus an environmental range for any trait and considered as a trait in itself (Sadras and Slafer, 2012), i.e. it has its own genetic variation and underlying QTLs. Phenotypic plasticity should be advantageous for fitness in variable environments and neutral in stable environments (Bradshaw, 1965; Nicotra *et al.*, 2010). It can be argued that selection for plasticity QTLs, against the background of the increased pace of climate change, will prove beneficial for maintaining or improving agricultural yields (Aspinwall *et al.*, 2015). However, plasticity is particular to the trait. For example, Sadras *et al.* (2009) found that high yield plasticity in wheat was disadvantageous in low-yield environments when it was associated with low plasticity of post-anthesis development. Breeding for plasticity in grain yield components coupled with plasticity for the length of the grain-filling phase will be useful but is limited due to a trade-off between low plasticity in grain size and high plasticity in grain number during this stage.

Many QTLs have been found for grain production in dry and hot climates (Table 1), but very few (possibly none) are used in breeding programs. The main limiting factor to the deployment of these QTLs in breeding is the inconsistency in performances of the introgressed lines due to the strong QTL×E interaction. Although only field experiments are relevant for evaluating crop tolerance to stress as performance in an agricultural system, most studies fail to explain why a QTL is significant in one environment and not in another. Field trials are usually considered as a qualitative factor, which enables detection of G×E interactions but not its measurement (Acuña-Galindo *et al.*, 2015). Recent development in phenomics and sensors means that we can now continuously measure soil water potential and air temperature across the crop cycle in field conditions. But how can we use these data to understand G×E?

Uncoupling responsive and adaptive physiological traits is often complex and disentangling the effect of a specific environmental condition is not simple in experiments and often requires complex analysis and modelling (reviewed by Parent and Tardieu, 2014). Parent *et al.* (2017) described new models that exploit such data and measure a plant's response to quantitative variations in drought and heat stress. Applied to lines that segregated for specific yield QTLs, such models revealed, in Australian wheats, that a QTL on chromosome 1B was constitutively expressed under various combinations of soil water potential and high temperature, while a QTL on chromosome 3B was heat responsive with a positive effect of the drought-tolerant parental line RAC875 when temperature was above 23 °C around flowering stage (Parent *et al.*, 2017). This information is highly valuable as it enables us to understand a QTL's function and use it in appropriate environments. By equipping national variety trials with sensors to measure soil moisture and air temperature, such models could also predict the level of tolerance of new varieties to quantified drought and heat. Combined with whole genome genotyping, this would provide information on the effects of haplotypes on yield in response to specific environmental conditions.

Find the drought and heat tolerance genes and design the genome

Another obstacle in using yield QTLs in breeding programmes is the small effect of a single QTL and the need to introgress several QTLs to gain a significant increment in yield improvement. As breeders can only recombine as many loci as the size of their breeding programmes allows, they prioritize those with strong and stable effects, such as phenology, plant height, and disease resistance, and select for yield

under dry and hot environment empirically or, more recently, by genomic selection (GS). So, were the efforts in finding QTLs for drought and heat tolerance wasted? The answer is probably yes, unless we carry on the positional cloning of these QTLs and find the genes controlling combined drought and heat tolerance. Gene-level knowledge of the control of drought and heat tolerance will enable the identification and creation of new sequence variants.

Although many QTLs have been found for drought or heat tolerance (Table 1), little is known about the genes underlying these effects in wheat. The molecular network of drought and heat stress response in model species includes heat shock proteins (HSPs, chaperone proteins that protect the cell machinery), a number of drought stress response or heat stress transcription factors (DSF, HSF), and signal transduction proteins (Mittler *et al.*, 2012). A study in adult durum plants identified genes that respond specifically to combined drought and heat including a chaperone homologous to a putative t-complex protein 1 theta chain (Rizhsky *et al.*, 2002, 2004; Rampino *et al.*, 2012). Two classes of heat shock factors, A6 and C2, have been shown recently to enhance heat tolerance in transgenic wheat (Xue *et al.*, 2014; Hu *et al.*, 2018). Overexpression of TaHsfC2a-B in transgenics up-regulated a cascade of HSP genes in grains during grain filling under heat and also in leaves under drought stress. Combining positive alleles of HSF and DSF such as dehydration-responsive element-binding (DREB) proteins (Morran *et al.*, 2011) might be a way to enhance wheat tolerance to simultaneous stress, but the positive effects will need to be tested in the field in dry and hot climates and redundancy and interactions measured. The forward genetics approach starting with a locus with a demonstrated yield effect is attractive but, to date, none of the QTLs for drought and heat tolerance (Table 1) has been cloned in wheat.

While GS is an efficient tool to quickly identify the best haplotypes, it still requires the incorporation of new alleles into the breeding programme New alleles can also be found in wild relatives of wheat and landraces well adapted to local environments (Lopes *et al.*, 2015), including hot and arid environments. Natural diversity encompasses adaptive mechanisms that wheat plants developed to cope with harsh conditions (Huang and Han, 2014). Emmer wheat and cultivated wheat's wild relatives are sources of tolerance to high temperature or water limitation that could be used to overcome the bottleneck in genetic diversity within the cultivated wheat genepool (Feuillet *et al.*, 2008). The usefulness of a wider germplasm is illustrated by the QTLs deriving from wild emmer wheat for drought (Peleg *et al*, 2005; 2009) and QTLs for salinity tolerance from *Triticum monococcum* (Munns *et al.*, 2012). This is a rare example of successful introgression of a locus (*Nax2*) for abiotic stress tolerance in wheat, following both physiological characterization (James *et al.*, 2006) and positional cloning of the causative gene (*TmHKT1;5-A*) and demonstrates the power of this approach.

New alleles of known genes can also be created by deliberate mutagenesis or genome design (E. Buckler, Plant and Animal Genome conference XXVI, 2018). The ability to efficiently screen for mutations by sequencing (TILLING (Targeting Induced Local Lesions IN Genomes) by sequencing) is quite recent in wheat (Tsai *et al.*, 2011) and is based on both an increased understanding of genomics and advances in next generation sequencing and analysis. Using this approach, Simmonds *et al.* (2016) were able to rapidly identify the causative mutation for the locus *TaGW2-A1* and cross the mutant allele into durum and bread wheat to develop isogenic lines with increased grain weight. The advantage of a mutant collection over wild germplasm is that the new alleles are in agronomically relevant backgrounds where their effect can be readily measured. As the current sequenced collections are in English and US genetic backgrounds, namely Kronos and Cadenza (Tsai *et al.*, 2011), the sequencing of new TILLING collections in varieties that are locally relevant to hot and dry climates is urgently needed.

An alternative method is to specifically edit genes for drought and heat tolerance in a modern, relevant variety. The ability to specifically edit the wheat genome using CRISPR-cas9 ribonucleoproteins has been demonstrated in bread wheat (Liang *et al.*, 2017). This technique promises transgene-free modification of the genome to enhance traits of agronomic interest including abiotic stress tolerance. The use of this technique, however, depends on a detailed knowledge of the sequences underlying tolerance and is likely to require cassettes of sequence edits in the case of editing for combined drought and heat tolerance for wheat. With three highly similar sub-genomes, the majority of wheat gene sequences have homeologues and the contributions of these homeologues to copy number variation and dosage-dependent expression as well as functional redundancy are often unknown in wheat but will influence the success of gene editing approaches. In some cases, a gene/QTL effect could be increased if we were to combine the positive alleles of the three homeologous copies. On a whole genome level, pan-genome data are now being used to understand and mark structural variation of this kind, for instance in maize (Lu *et al.*, 2015). The coming together of advances in genome editing and pan-genomics in wheat should facilitate editing for the future.

Conclusions

Because wheat is heat tolerant when water is available (Parent *et al.*, 2017), to improve wheat for dual tolerance, plants must be studied under the combination of stresses. Results from experiments with heat treatments and well-watered conditions are unlikely to be relevant when water is limiting in the field. There is a large body of evidence showing that water use is essential for either drought or heat tolerance and that, for tolerance of the combined stress, fine control of water relations across the growing cycle will be beneficial. This might be achieved through fine management of spatial and temporal gas exchange. For a wheat plant to be drought and heat tolerant, beneficial traits likely include the following: finely regulated transpiration through small, dense stomata, able to respond to the micro-environment (shade, water, VPD, radiation); maintenance of optimal hydraulic conductance in different tissues; a root system able to grow fast in response

to water availability; water-adjustable circadian regulation of plant growth; ability to retain water in essential organs to avoid tissue dehydration; efficient HSPs to protect enzymes and membranes against high temperature; efficient carbohydrate synthesis, export, and remobilization; and an efficient ROS scavenging system (Fig. 1).

The rationale for identifying and deploying alleles for combined drought and heat tolerance in wheat breeding is compelling. Improvements in phenotyping of physiological traits and genomic information are particularly encouraging as we seek to discover and incorporate, possibly, rare, novel tolerance alleles in breeding programmes. Improvement of methods capturing plant and environmental data over time will enable us to phenotype genetic populations for kinematic traits, and this will help us unravel the genetic basis of complex biological processes. Although wheat physiology under drought and heat stress is complex, this complexity and plasticity in itself provides sources of tolerance and hope.

Modifying a single trait might not have a significant effect on yield under stress as some of these traits are co-dependent and would be effective only in combination. Rather than improving a single trait at a time, we might need to combine them in order to increase yield. With underscoring genetic resources and a clear picture of valuable physiological traits, combined drought and heat tolerance in wheat can now be realized in research for use in breeding programmes.

Acknowledgements

The authors' research is supported by the Australian Research Council Industrial Transformation Research Hub for Genetic Diversity and Molecular Breeding for Wheat in a Hot and Dry Climate (project number IH130200027).

References

ABS (Australian Bureau of Statistics). 2012. Year Book Australia. Canberra: Australian Bureau of Statistics.

Acevedo E, Hsiao TC, Henderson DW. 1971. Immediate and subsequent growth responses of maize leaves to changes in water status. Plant Physiology **48,** 631–636.

Acuña-Galindo MA, Mason RE, Subramanian NK, Hays DB. 2015. Meta-analysis of wheat QTL regions associated with adaptation to drought and heat stress. Crop Science **55,** 477–492.

Alexandratos N, Bruinsma J. 2012. World agriculture towards 2030/2050: the 2012 revision. ESA Working paper No. 12-03. Rome: Food and Agriculture Organization of the United Nations.

Allakhverdiev SI, Kreslavski VD, Klimov VV, Los DA, Carpentier R, Mohanty P. 2008. Heat stress: an overview of molecular responses in photosynthesis. Photosynthesis Research **98,** 541–550.

Almeselmani M, Deshmukh PS, Sairam RK, Kushwaha SR, Singh TP. 2006. Protective role of antioxidant enzymes under high temperature stress. Plant Science **171,** 382–388.

Altenbach SB, DuPont FM, Kothari KM, Chan R, Johnson EL, Lieu D. 2003. Temperature, water and fertilizer influence the timing of key events during grain development in a US spring wheat. Journal of Cereal Science **37,** 9–20.

Aprile A, Havlickova L, Panna R, *et al.* 2013. Different stress responsive strategies to drought and heat in two durum wheat cultivars with contrasting water use efficiency. BMC Genomics **14,** 821.

Araus JL, Cairns JE. 2014. Field high-throughput phenotyping: the new crop breeding frontier. Trends in Plant Science **19,** 52–61.

Araus JL, Slafer GA, Reynolds MP, Royo C. 2002. Plant breeding and drought in C3 cereals: what should we breed for? Annals of Botany **89 Spec No,** 925–940.

Asana R, Williams R. 1965. The effect of temperature stress on grain development in wheat. Australian Journal of Agricultural Research **16,** 1–13.

Aspinwall MJ, Loik ME, Resco de Dios V, Tjoelker MG, Payton PR, Tissue DT. 2015. Utilizing intraspecific variation in phenotypic plasticity to bolster agricultural and forest productivity under climate change. Plant, Cell & Environment **38,** 1752–1764.

Awasthi R, Kaushal N, Vadez V, Turner NC, Berger J, Siddique KHM, Nayyar H. 2014. Individual and combined effects of transient drought and heat stress on carbon assimilation and seed filling in chickpea. Functional Plant Biology **41,** 1148–1167.

Barlow E, Lee J, Munns R, Smart M. 1980. Water relations of the developing wheat grain. Functional Plant Biology **7,** 519–525.

Barnabás B, Jäger K, Fehér A. 2008. The effect of drought and heat stress on reproductive processes in cereals. Plant, Cell & Environment **31,** 11–38.

Bennett D, Reynolds M, Mullan D, Izanloo A, Kuchel H, Langridge P, Schnurbusch T. 2012. Detection of two major grain yield QTL in bread wheat (*Triticum aestivum* L.) under heat, drought and high yield potential environments. Theoretical and Applied Genetics **125,** 1473–1485.

Berry J, Bjorkman O. 1980. Photosynthetic response and adaptation to temperature in higher plants. Annual Review of Plant Physiology **31,** 491–543.

Blum A. 1988. Plant breeding for stress environments. Boca Raton, FL, USA: CRC Press.

Blum A. 2005. Drought resistance, water-use efficiency, and yield potential are they compatible, dissonant, or mutually exclusive? Australian Journal of Agricultural Research **56,** 1159–1168.

Blum A. 2009. Effective use of water (EUW) and not water-use efficiency (WUE) is the target of crop yield improvement under drought stress. Field Crops Research **112,** 119–123.

Blum A, Sinmena B, Mayer J, Golan G, Shpiler L. 1994. Stem reserve mobilisation supports wheat-grain filling under heat stress. Functional Plant Biology **21,** 771–781.

Bonneau J, Taylor J, Parent B, Bennett D, Reynolds M, Feuillet C, Langridge P, Mather D. 2013. Multi-environment analysis and improved mapping of a yield-related QTL on chromosome 3B of wheat. Theoretical and Applied Genetics **126,** 747–761.

Bradshaw AD. 1965. Evolutionary significance of phenotypic plasticity in plants. Advances in Genetics **13,** 115–155.

Bramley H, Bitter R, Zimmermann G, Zimmermann U. 2015. Simultaneous recording of diurnal changes in leaf turgor pressure and stem water status of bread wheat reveal variation in hydraulic mechanisms in response to drought. Functional Plant Biology **42,** 1001–1009.

Caldeira CF, Bosio M, Parent B, Jeanguenin L, Chaumont F, Tardieu F. 2014*a*. A hydraulic model is compatible with rapid changes in leaf elongation under fluctuating evaporative demand and soil water status. Plant Physiology **164,** 1718–1730.

Caldeira CF, Jeanguenin L, Chaumont F, Tardieu F. 2014*b*. Circadian rhythms of hydraulic conductance and growth are enhanced by drought and improve plant performance. Nature Communications **5,** 5365.

Caringella MA, Bongers FJ, Sack L. 2015. Leaf hydraulic conductance varies with vein anatomy across *Arabidopsis thaliana* wild-type and leaf vein mutants. Plant, Cell & Environment **38,** 2735–2746.

Chapman SC, Chakraborty S, Dreccer MF, Howden SM. 2012. Plant adaptation to climate change—opportunities and priorities in breeding. Crop and Pasture Science **63,** 251–268.

Choudhury FK, Rivero RM, Blumwald E, Mittler R. 2017. Reactive oxygen species, abiotic stress and stress combination. The Plant Journal **90,** 856–867.

Christopher JT, Manschadi AM, Hammer GL, Borrell AK. 2008. Developmental and physiological traits associated with high yield and stay-green phenotype in wheat. Australian Journal of Agricultural Research **59,** 354–364.

Claverie E, Meunier F, Javaux M, Sadok W. 2017. Increased contribution of wheat nocturnal transpiration to daily water use under drought. Physiologia Plantarum **162,** 290–300.

Cockram J, Jones H, Leigh FJ, O'Sullivan D, Powell W, Laurie DA, Greenland AJ. 2007. Control of flowering time in temperate cereals: genes, domestication, and sustainable productivity. Journal of Experimental Botany **58,** 1231–1244.

Condon A, Farquhar G, Richards R. 1990. Genotypic variation in carbon isotope discrimination and transpiration efficiency in wheat. Leaf gas exchange and whole plant studies. Functional Plant Biology **17,** 9–22.

Condon AG, Richards RA, Rebetzke GJ, Farquhar GD. 2002. Improving intrinsic water-use efficiency and crop yield. Crop Science **42,** 122–131.

Coupel-Ledru A, Lebon É, Christophe A, Doligez A, Cabrera-Bosquet L, Péchier P, Hamard P, This P, Simonneau T. 2014. Genetic variation in a grapevine progeny (*Vitis vinifera* L. cvs Grenache×Syrah) reveals inconsistencies between maintenance of daytime leaf water potential and response of transpiration rate under drought. Journal of Experimental Botany **65,** 6205–6218.

Czyczyło-Mysza I, Marcińska I, Skrzypek E, *et al*. 2011. Mapping QTLs for yield components and chlorophyll a fluorescence parameters in wheat under three levels of water availability. Plant Genetic Resources **9,** 291–295.

Das A, Eldakak M, Paudel B, Kim DW, Hemmati H, Basu C, Rohila JS. 2016. Leaf proteome analysis reveals prospective drought and heat stress response mechanisms in soybean. BioMed Research International **2016,** 6021047.

Dashti H, Yazdisamadi B, Bihamta Naghavi MR, Quarrie S. 2007. QTL analysis for drought resistance in wheat using doubled haploid lines. International Journal of Agriculture and Biology **9,** 98–101.

Demirevska K, Simova-Stoilova L, Fedina I, Georgieva K, Kunert K. 2010. Response of oryzacystatin I transformed tobacco plants to drought, heat and light stress. Journal of Agronomy and Crop Science **196,** 90–99.

Diab AA, Kantety RV, Ozturk NZ, Benscher D, Nachit MM, Sorrells ME. 2008. Drought-inducible genes and differentially expressed sequence tags associated with components of drought tolerance in durum wheat. Scientific Research and Essays **3,** 009–026.

Eberhart SA, Russell WA. 1966. Stability parameters for comparing varieties. Crop Science **6,** 36–40.

Ehrler WL, Idso SB, Jackson RD, Reginato RJ. 1978. Wheat canopy temperature: relation to plant water potential. Agronomy Journal **70,** 251–256.

Feuillet C, Langridge P, Waugh R. 2008. Cereal breeding takes a walk on the wild side. Trends in Genetics **24,** 24–32.

Fischer RA. 2011. Wheat physiology: a review of recent developments. Crop and Pasture Science **62,** 95–114.

Fischer RA, Maurer R. 1978. Drought resistance in spring wheat cultivars. I. Grain yield responses. Australian Journal of Agricultural Research **29,** 897–912.

Foyer CH, Noctor G. 2005. Oxidant and antioxidant signalling in plants: a re-evaluation of the concept of oxidative stress in a physiological context. Plant, Cell & Environment **28,** 1056–1071.

Gavuzzi P, Rizza F, Palumbo M, Campanile RG, Ricciardi GL, Borghi B. 1997. Evaluation of field and laboratory predictors of drought and heat tolerance in winter cereals. Canadian Journal of Plant Science **77,** 523–531.

Golabadi M, Arzani A, Mirmohammadi Maibody SAM, Sayed Tabatabaei BE, Mohammadi SA. 2011. Identification of microsatellite markers linked with yield components under drought stress at terminal growth stages in durum wheat. Euphytica **177,** 207–221.

Hill CB, Taylor JD, Edwards J, Mather D, Langridge P, Bacic A, Roessner U. 2015. Detection of QTL for metabolic and agronomic traits in wheat with adjustments for variation at genetic loci that affect plant phenology. Plant Science **233,** 143–154.

Hochman Z. 1982. Effect of water stress with phasic development on yield of wheat grown in a semi-arid environment. Field Crops Research **5,** 55–67.

Hu X-J, Chen D, Lynne McIntyre C, Fernanda Dreccer M, Zhang Z-B, Drenth J, Kalaipandian S, Chang H, Xue G-P. 2018. Heat shock factor C2a serves as a proactive mechanism for heat protection in developing grains in wheat via an ABA-mediated regulatory pathway. Plant, Cell & Environment **41,** 79–98.

Huang X, Han B. 2014. Natural variations and genome-wide association studies in crop plants. Annual Review of Plant Biology **65,** 531–551.

Ilyas M, Ilyas N, Arshad M, Kazi AG. 2014. QTL mapping of wheat doubled haploids for chlorophyll content and chlorophyll fluorescence kinetics under drought stress imposed at anthesis stage. Pakistan Journal of Botany **46,** 1889–1897.

Izanloo A, Condon AG, Langridge P, Tester M, Schnurbusch T. 2008. Different mechanisms of adaptation to cyclic water stress in two South Australian bread wheat cultivars. Journal of Experimental Botany **59,** 3327–3346.

James RA, Davenport RJ, Munns R. 2006. Physiological characterization of two genes for Na^+ exclusion in durum wheat, *Nax1* and *Nax2*. Plant Physiology **142,** 1537–1547.

Jenner C. 1994. Starch synthesis in the kernel of wheat under high temperature conditions. Functional Plant Biology **21,** 791–806.

Jiang Y, Huang B. 2001. Drought and heat stress injury to two cool-season turfgrasses in relation to antioxidant metabolism and lipid peroxidation. Crop Science **41,** 436–442.

Kadam NN, Yin X, Bindraban PS, Struik PC, Jagadish KS. 2015. Does morphological and anatomical plasticity during the vegetative stage make wheat more tolerant of water deficit stress than rice? Plant Physiology **167,** 1389–1401.

Kadam S, Singh K, Shukla S, Goel S, Vikram P, Pawar V, Gaikwad K, Khanna-Chopra R, Singh N. 2012. Genomic associations for drought tolerance on the short arm of wheat chromosome 4B. Functional & Integrative Genomics **12,** 447–464.

Kirigwi FM, van Ginkel M, Trethowan R, Sears RG, Rajaram S, Paulsen GM. 2004. Evaluation of selection strategies for wheat adaptation across water regimes. Euphytica **135,** 361–371.

Kirigwi FM, Van Ginkel M, Brown-Guedira G, Gill BS, Paulsen GM, Fritz AK. 2007. Markers associated with a QTL for grain yield in wheat under drought. Molecular Breeding **20,** 401–413.

Koussevitzky S, Suzuki N, Huntington S, Armijo L, Sha W, Cortes D, Shulaev V, Mittler R. 2008. Ascorbate peroxidase 1 plays a key role in the response of *Arabidopsis thaliana* to stress combination. The Journal of Biological Chemistry **283,** 34197–34203.

Lascano HR, Antonicelli GE, Luna CM, Melchiorre MN, Gómez LD, Racca RW, Trippi VS, Casano LM. 2001. Antioxidant system response of different wheat cultivars under drought: field and in vitro studies. Functional Plant Biology **28,** 1095–1102.

Liang Z, Chen K, Li T, *et al*. 2017. Efficient DNA-free genome editing of bread wheat using CRISPR/Cas9 ribonucleoprotein complexes. Nature Communications **8,** 14261.

Liu B, Asseng S, Muller C, *et al*. 2016. Similar estimates of temperature impacts on global wheat yield by three independent methods. Nature Climate Change **6,** 1130–1136.

Lohraseb I, Collins NC, Parent B. 2017. Diverging temperature responses of CO_2 assimilation and plant development explain the overall effect of temperature on biomass accumulation in wheat leaves and grains. AoB Plants **9,** plw092.

Long SP, Ort DR. 2010. More than taking the heat: crops and global change. Current Opinion in Plant Biology **13,** 241–248.

Lopes MS, El-Basyoni I, Baenziger PS, *et al*. 2015. Exploiting genetic diversity from landraces in wheat breeding for adaptation to climate change. Journal of Experimental Botany **66,** 3477–3486.

Lopes MS, Reynolds MP, Jalal-Kamali MR, *et al*. 2012. The yield correlations of selectable physiological traits in a population of advanced spring wheat lines grown in warm and drought environments. Field Crops Research **128,** 129–136.

Lu F, Romay MC, Glaubitz JC, *et al*. 2015. High-resolution genetic mapping of maize pan-genome sequence anchors. Nature Communications **6,** 6914.

Lu Y, Li R, Wang R, Wang X, Zheng W, Sun Q, Tong S, Dai S, Xu S. 2017. Comparative proteomic analysis of flag leaves reveals new insight into wheat heat adaptation. Frontiers in Plant Science **8,** 1086.

Maccaferri M, Sanguineti MC, Corneti S, *et al*. 2008. Quantitative trait loci for grain yield and adaptation of durum wheat (*Triticum durum* Desf.) across a wide range of water availability. Genetics **178,** 489–511.

Machado S, Paulsen GM. 2001. Combined effects of drought and high temperature on water relations of wheat and sorghum. Plant and Soil **233,** 179–187.

Marks CO, Lechowicz MJ. 2007. The ecological and functional correlates of nocturnal transpiration. Tree Physiology **27,** 577–584.

Mason RE, Mondal S, Beecher FW, Pacheco A, Jampala B, Ibrahim AMH, Hays DB. 2010. QTL associated with heat susceptibility index in wheat (*Triticum aestivum* L.) under short-term reproductive stage heat stress. Euphytica **174,** 423–436.

Maydup ML, Antonietta M, Graciano C, Guiamet JJ, Tambussi EA. 2014. The contribution of the awns of bread wheat (*Triticum aestivum* L.) to grain filling: Responses to water deficit and the effects of awns on ear temperature and hydraulic conductance. Field Crops Research **167,** 102–111.

Merchuk-Ovnat L, Fahima T, Krugman T, Saranga Y. 2016. Ancestral QTL alleles from wild emmer wheat improve grain yield, biomass and photosynthesis across environments in modern wheat. Plant Science **251,** 23–34.

Mittler R. 2006. Abiotic stress, the field environment and stress combination. Trends in Plant Science **11,** 15–19.

Mittler R, Finka A, Goloubinoff P. 2012. How do plants feel the heat? Trends in Biochemical Sciences **37,** 118–125.

Mohammed A-R, Tarpley L. 2009. Impact of high nighttime temperature on respiration, membrane stability, antioxidant capacity, and yield of rice plants. Crop Science **49,** 313–322.

Mondal B, Singh A, Yadav A, Singh Tomar RS, Vinod Singh GP, Prabhu KV. 2017. QTL mapping for early ground cover in wheat (*Triticum aestivum* L.) under drought stress. Current Science **112,** 1266–1271.

Mooney HA, Di Castri F. 1973. Mediterranean type ecosystems: origin and structure. Berlin, Heidelberg: Springer-Verlag.

Morran S, Eini O, Pyvovarenko T, *et al*. 2011. Improvement of stress tolerance of wheat and barley by modulation of expression of DREB/CBF factors. Plant Biotechnology Journal **9,** 230–249.

Munns R, James RA, Xu B, *et al*. 2012. Wheat grain yield on saline soils is improved by an ancestral Na^+ transporter gene. Nature Biotechnology **30,** 360–364.

Neghliz H, Cochard H, Brunel N, Martre P. 2016. Ear rachis xylem occlusion and associated loss in hydraulic conductance coincide with the end of grain filling for wheat. Frontiers in Plant Science **7,** 920.

Nicotra AB, Atkin OK, Bonser SP, *et al*. 2010. Plant phenotypic plasticity in a changing climate. Trends in Plant Science **15,** 684–692.

Ogbonnaya FC, Rasheed A, Okechukwu EC, Jighly A, Makdis F, Wuletaw T, Hagras A, Uguru MI, Agbo CU. 2017. Genome-wide association study for agronomic and physiological traits in spring wheat evaluated in a range of heat prone environments. Theoretical and Applied Genetics **130,** 1819–1835.

Paliwal R, Röder MS, Kumar U, Srivastava JP, Joshi AK. 2012. QTL mapping of terminal heat tolerance in hexaploid wheat (*T. aestivum* L.). Theoretical and Applied Genetics **125,** 561–575.

Parent B, Bonneau J, Maphosa L, Kovalchuk A, Langridge P, Fleury D. 2017. Quantifying wheat sensitivities to environmental constraints to dissect Genotype × Environment interactions in the field. Plant Physiology **174,** 1669–1682.

Parent B, Shahinnia F, Maphosa L, Berger B, Rabie H, Chalmers K, Kovalchuk A, Langridge P, Fleury D. 2015. Combining field performance with controlled environment plant imaging to identify the genetic control of growth and transpiration underlying yield response to water-deficit stress in wheat. Journal of Experimental Botany **66,** 5481–5492.

Parent B, Tardieu F. 2012. Temperature responses of developmental processes have not been affected by breeding in different ecological areas for 17 crop species. New Phytologist **194,** 760–774.

Parent B, Tardieu F. 2014. Can current crop models be used in the phenotyping era for predicting the genetic variability of yield of plants subjected to drought or high temperature? Journal of Experimental Botany **65,** 6179–6189.

Passioura JB. 1977. Grain yield, harvest index, and water use of wheat. Journal of the Australian Institute of Agricultural Sciences **43,** 117–120.

Passioura JB. 1996. Drought and drought tolerance. Plant Growth Regulation **20,** 79–83.

Peleg Z, Fahima T, Abbo S, Krugman T, Nevo E, Yakir D, Saranga Y. 2005. Genetic diversity for drought resistance in wild emmer wheat and its ecogeographical associations. Plant, Cell & Environment **28,** 176–191.

Peleg Z, Fahima T, Krugman T, Abbo S, Yakir D, Korol AB, Saranga Y. 2009. Genomic dissection of drought resistance in durum wheat × wild emmer wheat recombinant inbreed line population. Plant, Cell & Environment **32,** 758–779.

Peng J, Richards DE, Hartley NM, *et al*. 1999. 'Green revolution' genes encode mutant gibberellin response modulators. Nature **400,** 256–261.

Perdomo JA, Capó-Bauçà S, Carmo-Silva E, Galmés J. 2017. Rubisco and Rubisco activase play an important role in the biochemical limitations of photosynthesis in rice, wheat, and maize under high temperature and water deficit. Frontiers in Plant Science **8,** 490.

Perdomo JA, Conesa MÀ, Medrano H, Ribas-Carbó M, Galmés J. 2015. Effects of long-term individual and combined water and temperature stress on the growth of rice, wheat and maize: relationship with morphological and physiological acclimation. Physiologia Plantarum **155,** 149–165.

Peterhansel C, Maurino VG. 2011. Photorespiration redesigned. Plant Physiology **155,** 49–55.

Pinto RS, Reynolds MP. 2015. Common genetic basis for canopy temperature depression under heat and drought stress associated with optimized root distribution in bread wheat. Theoretical and Applied Genetics **128,** 575–585.

Pinto RS, Reynolds MP, Mathews KL, McIntyre CL, Olivares-Villegas JJ, Chapman SC. 2010. Heat and drought adaptive QTL in a wheat population designed to minimize confounding agronomic effects. Theoretical and Applied Genetics **121,** 1001–1021.

Pradhan GP, Prasad PVV, Fritz AK, Kirkham MB, Gill BS. 2012. Effects of drought and high temperature stress on synthetic hexaploid wheat. Functional Plant Biology **39,** 190–198.

Prasad PVV, Pisipati SR, Momčilović I, Ristic Z. 2011. Independent and combined effects of high temperature and drought stress during grain filling on plant yield and chloroplast EF-Tu expression in spring wheat. Journal of Agronomy and Crop Science **197,** 430–441.

Price AH, Hendry GAF. 1991. Iron-catalysed oxygen radical formation and its possible contribution to drought damage in nine native grasses and three cereals. Plant, Cell & Environment **14,** 477–484.

Quarrie SA, Steed A, Calestani C, *et al*. 2005. A high-density genetic map of hexaploid wheat (*Triticum aestivum* L.) from the cross Chinese Spring × SQ1 and its use to compare QTLs for grain yield across a range of environments. Theoretical and Applied Genetics **110,** 865–880.

Rajaram S, van Ginkel M, Fischer RA. 1994. CIMMYT's wheat breeding mega-environments (ME). In: Proceedings of the 8th International Wheat Genetics Symposium, Beijing, 20–25 July 1993. Beijing: Institute of Genetics, Chinese Academy of Sciences, 1101–1106.

Rampino P, Mita G, Fasano P, Borrelli GM, Aprile A, Dalessandro G, De Bellis L, Perrotta C. 2012. Novel durum wheat genes up-regulated in response to a combination of heat and drought stress. Plant Physiology and Biochemistry **56,** 72–78.

Redondo-Gómez S. 2013. Abiotic and biotic stress tolerance in plants. In: **Rout GR, Das AB**, eds. Molecular stress physiology of plants. New Delhi: Springer India, 1–20.

Resco de Dios V, Loik ME, Smith R, Aspinwall MJ, Tissue DT. 2016. Genetic variation in circadian regulation of nocturnal stomatal conductance enhances carbon assimilation and growth. Plant, Cell & Environment **39,** 3–11.

Reynolds M, Foulkes MJ, Slafer GA, Berry P, Parry MA, Snape JW, Angus WJ. 2009. Raising yield potential in wheat. Journal of Experimental Botany **60,** 1899–1918.

Reynolds MP, Pellegrineschi A, Skovmand B. 2005. Sink-limitation to yield and biomass: a summary of some investigations in spring wheat. Annals of Applied Biology **146,** 39–49.

Reynolds MP, Pierre CS, Saad ASI, Vargas M, Condon AG. 2007. Evaluating potential genetic gains in wheat associated with stress-adaptive trait expression in elite genetic resources under drought and heat stress. Crop Science **47,** S172–S189.

Richards RA, Rawson HM, Johnson DA. 1986. Glaucousness in wheat: Its development and effect on water-use efficiency, gas exchange and photosynthetic tissue temperatures. Functional Plant Biology **13,** 465–473.

Rivero RM, Shulaev V, Blumwald E. 2009. Cytokinin-dependent photorespiration and the protection of photosynthesis during water deficit. Plant Physiology **150,** 1530–1540.

Rizhsky L, Liang H, Mittler R. 2002. The combined effect of drought stress and heat shock on gene expression in tobacco. Plant Physiology **130,** 1143–1151.

Rizhsky L, Liang H, Shuman J, Shulaev V, Davletova S, Mittler R. 2004. When defense pathways collide. The response of Arabidopsis to a combination of drought and heat stress. Plant Physiology **134,** 1683–1696.

Roche D. 2015. Stomatal conductance is essential for higher yield potential of C3 crops. Critical Reviews in Plant Sciences **34,** 429–453.

Sadok W. 2016. The circadian life of nocturnal water use: when late-night decisions help improve your day. Plant, Cell & Environment **39,** 1–2.

Sadras VO, Reynolds MP, de la Vega AJ, Petrie PR, Robinson R. 2009. Phenotypic plasticity of yield and phenology in wheat, sunflower and grapevine. Field Crops Research **110,** 242–250.

Sadras VO, Slafer GA. 2012. Environmental modulation of yield components in cereals: Heritabilities reveal a hierarchy of phenotypic plasticities. Field Crops Research **127,** 215–224.

Saini HS, Aspinall D. 1982. Abnormal sporogenesis in wheat (*Triticum aestivum* L.) induced by short periods of high temperature. Annals of Botany **49,** 835–846.

Saini HS, Lalonde S. 1997. Injuries to reproductive development under water stress, and their consequences for crop productivity. Journal of Crop Production **1,** 223–248.

Sairam RK, Saxena DC. 2000. Oxidative stress and antioxidants in wheat genotypes: possible mechanism of water stress tolerance. Journal of Agronomy and Crop Science **184,** 55–61.

Sairam RK, Srivastava GC, Saxena DC. 2000. Increased antioxidant activity under elevated temperatures: a mechanism of heat stress tolerance in wheat genotypes. Biologia Plantarum **43,** 245–251.

Salter PJ, Goode JE. 1967. Crop responses to water at different stages of growth. Farnham Royal, Bucks, England: Commonwealth Agricultural Bureaux.

Scharwies JD, Tyerman SD. 2017. Comparison of isohydric and anisohydric *Vitis vinifera* L. cultivars reveals a fine balance between hydraulic resistances, driving forces and transpiration in ripening berries. Functional Plant Biology **44,** 324–338.

Schauberger B, Archontoulis S, Arneth A, *et al*. 2017. Consistent negative response of US crops to high temperatures in observations and crop models. Nature Communications **8,** 13931.

Scheibe R, Dietz KJ. 2012. Reduction-oxidation network for flexible adjustment of cellular metabolism in photoautotrophic cells. Plant, Cell & Environment **35,** 202–216.

Schoppach R, Claverie E, Sadok W. 2014. Genotype-dependent influence of night-time vapour pressure deficit on night-time transpiration and daytime gas exchange in wheat. Functional Plant Biology **41,** 963–971.

Schoppach R, Sadok W. 2013. Transpiration sensitivities to evaporative demand and leaf areas vary with night and day warming regimes among wheat genotypes. Functional Plant Biology **40,** 708–718.

Schoppach R, Taylor JD, Majerus E, Claverie E, Baumann U, Suchecki R, Fleury D, Sadok W. 2016. High resolution mapping of traits related to whole-plant transpiration under increasing evaporative demand in wheat. Journal of Experimental Botany **67,** 2847–2860.

Sečenji M, Hideg É, Bebes A, Györgyey J. 2010. Transcriptional differences in gene families of the ascorbate–glutathione cycle in wheat during mild water deficit. Plant Cell Reports **29,** 37–50.

Shah NH, Paulsen GM. 2003. Interaction of drought and high temperature on photosynthesis and grain-filling of wheat. Plant and Soil **257,** 219–226.

Shahinnia F, Le Roy J, Laborde B, Sznajder B, Kalambettu P, Mahjourimajd S, Tilbrook J, Fleury D. 2016. Genetic association of stomatal traits and yield in wheat grown in low rainfall environments. BMC Plant Biology **16,** 150.

Sharma D, Singh R, Rane J, Gupta VK, Mamrutha HM, Tiwari R. 2016. Mapping quantitative trait loci associated with grain filling duration and grain number under terminal heat stress in bread wheat (*Triticum aestivum* L.). Plant Breeding **135,** 538–545.

Shiferaw B, Smale M, Braun H-J, Duveiller E, Reynolds M, Muricho G. 2013. Crops that feed the world 10. Past successes and future challenges to the role played by wheat in global food security. Food Security **5,** 291–317.

Shirdelmoghanloo H, Taylor JD, Lohraseb I, *et al*. 2016. A QTL on the short arm of wheat (*Triticum aestivum* L.) chromosome 3B affects the stability of grain weight in plants exposed to a brief heat shock early in grain filling. BMC Plant Biology **16,** 100.

Silva EN, Ferreira-Silva SL, Fontenele Ade V, Ribeiro RV, Viégas RA, Silveira JA. 2010. Photosynthetic changes and protective mechanisms against oxidative damage subjected to isolated and combined drought and heat stresses in *Jatropha curcas* plants. Journal of Plant Physiology **167,** 1157–1164.

Simmonds J, Scott P, Brinton J, Mestre TC, Bush M, Del Blanco A, Dubcovsky J, Uauy C. 2016. A splice acceptor site mutation in TaGW2-A1 increases thousand grain weight in tetraploid and hexaploid wheat through wider and longer grains. Theoretical and Applied Genetics **129,** 1099–1112.

Spielmeyer W, Hyles J, Joaquim P, Azanza F, Bonnett D, Ellis ME, Moore C, Richards RA. 2007. A QTL on chromosome 6A in bread wheat (*Triticum aestivum*) is associated with longer coleoptiles, greater seedling vigour and final plant height. Theoretical and Applied Genetics **115,** 59–66.

Stone P, Nicolas M. 1995. A survey of the effects of high temperature during grain filling on yield and quality of 75 wheat cultivars. Australian Journal of Agricultural Research **46,** 475–492.

Sun X, Cahill J, Van Hautegem T, *et al*. 2017. Altered expression of maize PLASTOCHRON1 enhances biomass and seed yield by extending cell division duration. Nature Communications **8,** 14752.

Suzuki N, Rivero RM, Shulaev V, Blumwald E, Mittler R. 2014. Abiotic and biotic stress combinations. New Phytologist **203,** 32–43.

Tahmasebi S, Heidari B, Pakniyat H, McIntyre CL. 2017. Mapping QTLs associated with agronomic and physiological traits under terminal drought and heat stress conditions in wheat (*Triticum aestivum* L.). Genome **60,** 26–45.

Talukder SK, Babar MA, Vijayalakshmi K, Poland J, Prasad PV, Bowden R, Fritz A. 2014. Mapping QTL for the traits associated with heat tolerance in wheat (*Triticum aestivum* L.). BMC Genetics **15,** 97.

Tardieu F, Parent B, Caldeira CF, Welcker C. 2014. Genetic and physiological controls of growth under water deficit. Plant Physiology **164,** 1628–1635.

Tester M, Langridge P. 2010. Breeding technologies to increase crop production in a changing world. Science **327,** 818–822.

Tilman D, Balzer C, Hill J, Befort BL. 2011. Global food demand and the sustainable intensification of agriculture. Proceedings of the National Academy of Sciences, USA **108,** 20260–20264.

Tixier A, Cochard H, Badel E, Dusotoit-Coucaud A, Jansen S, Herbette S. 2013. *Arabidopsis thaliana* as a model species for xylem hydraulics: does size matter? Journal of Experimental Botany **64,** 2295–2305.

Tricker PJ, Haefele SM, Okamoto M. 2016. The interaction of drought and nutrient stress in wheat. In: **Ahmad P**, ed. Water stress and crop plants: A sustainable approach. Chichester: John Wiley & Sons, Ltd, 695–710.

Tsai H, Howell T, Nitcher R, *et al*. 2011. Discovery of rare mutations in populations: TILLING by sequencing. Plant Physiology **156,** 1257–1268.

USDA. 2017. World agricultural production. Washington, DC, USA: United States Department of Agriculture Foreign Agricultural Service.

Vadez V, Kholova J, Medina S, Kakkera A, Anderberg H. 2014. Transpiration efficiency: new insights into an old story. Journal of Experimental Botany **65,** 6141–6153.

Verma V, Foulkes MJ, Worland AJ, Sylvester-Bradley R, Caligari PDS, Snape JW. 2004. Mapping quantitative trait loci for flag leaf senescence as a yield determinant in winter wheat under optimal and drought-stressed environments. Euphytica **135,** 255–263.

Vettakkorumakankav NN, Falk D, Saxena P, Fletcher RA. 1999. A crucial role for gibberellins in stress protection of plants. Plant and Cell Physiology **40,** 542–548.

Vijayalakshmi K, Fritz AK, Paulsen GM, Bai G, Pandravada S, Gill BS. 2010. Modeling and mapping QTL for senescence-related traits in winter wheat under high temperature. Molecular Breeding **26,** 163–175.

Voss I, Sunil B, Scheibe R, Raghavendra AS. 2013. Emerging concept for the role of photorespiration as an important part of abiotic stress response. Plant Biology **15,** 713–722.

Wang X, Cai J, Liu F, Dai T, Cao W, Wollenweber B, Jiang D. 2014*a*. Multiple heat priming enhances thermo-tolerance to a later high temperature stress via improving subcellular antioxidant activities in wheat seedlings. Plant Physiology and Biochemistry **74,** 185–192.

Wang Y, Chen L, Du Y, Yang Z, Condon AG, Hu Y-G. 2014*b*. Genetic effect of dwarfing gene *Rht13* compared with *Rht-D1b* on plant height and some agronomic traits in common wheat (*Triticum aestivum* L.). Field Crops Research **162,** 39–47.

Wardlaw I, Wrigley C. 1994. Heat tolerance in temperate cereals: an overview. Functional Plant Biology **21,** 695–703.

Weigand C. 2011. Wheat import projections towards 2050. Arlington, VA, USA: US Wheat Associates.

Weldearegay DF, Yan F, Jiang D, Liu F. 2012. Independent and combined effects of soil warming and drought stress during anthesis on seed set and grain yield in two spring wheat varieties. Journal of Agronomy and Crop Science **198,** 245–253.

Wheeler T. 2012. Agriculture: Wheat crops feel the heat. Nature Climate Change **2,** 152–153.

Xu Y-F, Li S-S, Li L-H, Ma F-F, Fu X-Y, Shi Z-L, Xu H-X, Ma P-T, An D-G. 2017. QTL mapping for yield and photosynthetic related traits under different water regimes in wheat. Molecular Breeding **37,** 34.

Xue GP, Sadat S, Drenth J, McIntyre CL. 2014. The heat shock factor family from *Triticum aestivum* in response to heat and other major abiotic stresses and their role in regulation of heat shock protein genes. Journal of Experimental Botany **65,** 539–557.

Yang DL, Jing RL, Chang XP, Li W. 2007. Identification of quantitative trait loci and environmental interactions for accumulation and remobilization of water-soluble carbohydrates in wheat (*Triticum aestivum* L.) stems. Genetics **176,** 571–584.

Zandalinas SI, Balfagón D, Arbona V, Gómez-Cadenas A. 2017. Modulation of antioxidant defense system is associated with combined drought and heat stress tolerance in *Citrus*. Frontiers in Plant Science **8,** 953.

Zandalinas SI, Mittler R, Balfagón D, Arbona V, Gómez-Cadenas A. 2018. Plant adaptations to the combination of drought and high temperatures. Physiologia Plantarum **162,** 2–12.

Zang X, Geng X, Wang F, *et al*. 2017. Overexpression of wheat ferritin gene *TaFER-5B* enhances tolerance to heat stress and other abiotic stresses associated with the ROS scavenging. BMC Plant Biology **17,** 14.

Zee S, O'brien T. 1970. A special type of tracheary element associated with "xylem discontinuity" in the floral axis of wheat. Australian Journal of Biological Sciences **23,** 783–792.

Zhang B, Li W, Chang X, Li R, Jing R. 2014. Effects of favorable alleles for water-soluble carbohydrates at grain filling on grain weight under drought and heat stresses in wheat. PLoS One **9,** e102917.

Zhang G, Zhang M, Zhao Z, Ren Y, Li Q, Wang W. 2017. Wheat TaPUB1 modulates plant drought stress resistance by improving antioxidant capability. Scientific Reports **7,** 7549.